Cretaceous to Quaternary Siliciclastic Sediments of the Tarfaya Basin, Marginal Atlantic, SW Morocco: Petrography, Geochemistry, Provenance, Climate and Weathering

Dissertation

zur Erlangung des Doktorgrades

der Mathematisch-Naturwissenschaftlichen Fakultät der Christian-Albrechts-Universität zu Kiel

Vorgelegt von

Sajid Ali

Kiel, 2012

Referent: Prof. Dr. Karl Stattegger

Koreferent: Prof. Dr. Martin Frank

Tag der mündlichen Prufung: 19.10.2012

Zum Druck genehmigt:

Der Dekan:

Erklärung

Hiermit versichere ich an Eides statt, dass ich diese Dissertation selbstständig und nur mit Hilfe der angegebenen Quellen und Hilfsmittel erstellt habe. Ferner versichere ich, dass der Inhalt dieses Dokuments weder in dieser, noch in veränderter Form einer weiteren Prüfungsbehörde vorliegt. Die Arbeit ist unter Einhaltung der Regeln guter wissenschaftlicher Praxis der Deutschen Forschungsgemeinschaft entstanden.

Kiel, August 2012

Sajid Ali

1

2

Contents

List of Figures

List of Tables

Acknowledgements

This Ph.D. thesis has been prepared and completed after three and half years doing research and studying at the Institute of Geosciences, Christian Albrecht University of Kiel, Germany. I would like to take this opportunity to thank those people and organizations that helped me to complete this work.

First of all I am deeply grateful to my advisor Prof. Dr. Karl Stattegger for his supervision and advise to solve many problems related to sedimentology, geochemistry, weathering in the source area and provenance studies as well as encouraging me to publish papers out of this PhD thesis. Prof. Karl is also generous to provide me funds for doing research, attending International and national conferences and short courses related to my current project and publishing articles. Further, I would like to thanks Prof. Wolfgang Kuhnt for his support in arrangement and guidance for fieldwork and to solving stratigraphic related problems. I would like to thanks Dr. Dieter Garbe-Schönberg for his contribution during geochemical data analysis and improving the quality of my writing. I also like to thank Prof. Martin Frank to allow me to work in his lab for Nd-Sr isotopic analysis and interpretation. Apart from that, my supervisors are very friendly and enthusiastic that I felt easily to be used with the European life.

I would like to thank RWE Dea for funding this project. In particular, Dr. Oliver Kluth, Dr. Torge Schumann and Dr. Haddou Jabour from ONHYM are acknowledged for cross-reading of various parts of the manuscript. I would also like to thank ONHYM for their support, organizing and accompanying the field campaign in March-April, 2009 and drilling in September-December, 2009. Dr. Peter Appel and Miss Ulrike Westernstroer, Institute of Geosciences, University of Kiel are thanked for their support in geochemical analytical work. I would like to thank my colleagues and friends, i.e., Dipl.-Geogr. Daniel Unverricht, Dipl.-Geol. Christoph Heinrich, Mohammad Aquit, Mohammad Faizan and Javed Iqbal, for their help, support.

Last but not least I thank my dear parents for their love, support, encouragement and standing by me during my Ph.D. studies. I would like to wish them always all the best and needed their love and support.

I would like to dedicate this thesis to my forever loving brother late Mohammad Ovaish Karni.

Abstract

This work on sediments of the Tarfaya basin comprises (for the first time) a samples collection from different outcrops and four newly drilled cores as well as recent sediments from wadis and dunes. The petrographical analysis of studied rocks provides information about rocks classification and is compared with major elements geochemical classification. Binary and ternary relationships of the major and trace elements are used to constrain depositional tectonic settings of the Tarfaya basin sediments. The radiogenic Nd-Sr isotopic studies reveal the provenance of the basin infill and its change with time. Finally, clay minerals analysis constrains the tectonic and climatic control on the weathering of the sediments in source area.

The petrographic studies of the Early Cretaceous and Miocene-Pliocene sandstones reveal variable mineralogical compositions including modern sediments. The Early Cretaceous sandstones are subarkosic in composition, while the Miocene-Pliocene sandstones as well as the recent sediments from wadis are generally carbonate-rich feldspathic or lithic arenites. However, recent sediment samples from dunes sediment are almost carbonate free. Their major element geochemistry reflects these findings.

The major elements relationships (SiO_2 % versus K_2O/Na_2O, Fe_2O_3*+MgO versus Al_2O_3/SiO_2 and $Fe2O_3$*+MgO versus TiO_2 %) indicate that the Tarfaya basin sediments since Early Cretaceous were deposited in tectonically passive margin setting. In addition, the trace elements relationships of La/Y-Sc/Cr and La-Th-Sc also support that the Tarfaya basin sediments were deposited in passive margin depositional setting. The heavy minerals, further, support the deposition of the sediments in tectonically stable passive margin settings.

The source rocks of the Tarfaya basin sediments are revealed by the hornblende and garnet grains geochemical analysis and trace elements geochemistry including rare earth elements (REE). The hornblende and garnets grains from Miocene-Pliocene and recent sediments suggest that the Tarfaya basin sediments are derived from the granitic rocks of the Reguibat shield, high grade metamorphic rocks of the Mauritanides and low grade metamorphosed or unmetamorphosed sedimentary rocks of the western Anti-Atlas. The trace element geological compositions and their ratios as well as REE distribution constrain composition of the source rocks. Low concentrations of Cr (<150ppm) and Ni (<100ppm) and their correlation suggest that the sediments of the Tarfaya basin are derived from felsic sources. This is supported by trace element ratios of La/Sc, Th/Sc, La/Co, Th/Co and Cr/Th that are similar to those of sediments derived from felsic source rocks. Moreover, chondrite-normalized

Abstract

REE patterns with light REE enrichment, a flat pattern of heavy REE and negative Eu anomalies can also be attributed to a felsic rock source for the Tarfaya basin sediments.

The similar Sm/Nd (0.18-0.20) ratios for all analyzed sediments in both coarse- and fine-grained siliclastics indicate that no significant fractionation of Sm and Nd occurred during the formation of the Tarfaya basin sediments due to depositional and post-depositional processes. The Nd isotope model ages (T_{DM}=2.1-2.2 Ga) of the Early Cretaceous sediments suggest that sediments were exclusively derived from the Eburnean terrane of West African Craton. On the other hand, Late Cretaceous to Miocene-Pliocene sediments show younger model ages (T_{DM}=1.7-1.9 Ga) indicating an origin from both the West African Craton and the western Anti Atlas. In contrast, the southernmost studied Sebkha Aridal section (Oligocene to Miocene-Pliocene) yields a provenance age (T_{DM}=2.5 Ga) indicating that these sediments are dominantly derived from the Archean terrane of West African Craton.

The clay minerals content from Late Cretaceous to recent sediments of the basin has been investigated to see the influence of the climatic and tectonic control on weathering in the source area. The clay mineral assemblages of the basin are variable in different stratigraphic units. Illite and chlorite which are indicating of physical weathering are abundantly distributed throughout all studied stratigraphic units which are derived from both sources of the Tarfaya basin sediments. The distribution of smectite is mainly associated with detrital origin which is formed under warm and less humid climatic conditions in the source area. The intensity of chemical weathering can be evaluated by the kaolinite abundance and ratios of kaolinite/illite. This is confirmed by the proxies of chemical index of alteration, Al_2O_3/Na_2O and Al_2O_3/TiO_2. During the Turonian and Santonian time the chemical weathering was more intense than that of Campanian. The Early Eocene to Miocene-Pliocene sediments indicate a low intensity of chemical weathering. In addition, corrensite in Campanian (Late Cretaceous) and Oligocene-Early Miocene sediments is associated with the diagenetic transformation of dioctahedral clay minerals under oxic conditions. The abundant palygorskite in the Early Eocene sediments indicates warm and dry climate conditions in a nearby exposed coastal area. However, palygorskite in the recent sediments clay mineral assemblages originated mainly from aeolian Saharan dust.

Zusammenfassung

Diese Arbeit beschäftigt sich mit Sedimenten aus dem Tarfaya Becken und beinhaltet die Bearbeitungon Sedimentproben aus verschiedenen Aufschlüssen, vier Bohrkernen und rezenten Wadi- und Dünensedimenten. Die petrographische Analyse erlaubt eine Klassifikation der Gesteine, welche mit einer geochemischen Klassifikation mittels der Hauptelemente verglichen wird. Binäre und ternäre Diagramme der Haupt und Spurenelemente werden genutzt, um die tektonische Position des Tarfaya Beckens seit der Unterkreide zu bestimmen. Die Nd-Sr Isotopen-Analytik erlaubt es, die Herkunft der Beckensedimente in ihrer zeitlichen Veränderung zu erfassen. Weiterhin zeigen Tonmineralanlysen den Einfluss von Tektonik und Klima auf die Verwitterung der Sedimente in den Herkunftsgebieten.

Die petrographischen Untersuchungen an Sandsteinen der Unterkreide, des Miozän-Pliozän und rezenter Sedimente zeigen deutlich variierende mineralogische Zusammensetzungen. Die Sandsteine der Unterkreide sind subarkosisch, während die Miozän-Pliozän Sandsteine und die rezenten Wadisedimente eher aus karbonatreichen feldspatreichen oder lithischen Areniten bestelen. Dagegen sind die rezenten Dünensande frei von Karbonaten. Ihre Hauptelementgeochemie bestätigt dies.

Die Hauptelement-Verhältnisse (SiO_2% vs. K_2O/Na_2O, Fe_2O_3*+MgO vs. Al_2O_3/SiO_2 and Fe_2O_3*+MgO vs. TiO2%) deuten darauf hin, dass die Sedimente des Tarfaya Beckens seit der frühen Kreidezeit an einem passiven Kontinentalrand abgelagert wurden. Zusätzlich unterstützen die Spurenelement-Verhältnisse von La/Y-Sc/Cr und La-Th-Sc diese Aussage zu den vorherrschenden Randbedingungen in dem Tarfaya Becken. Die Schwermineralanalyse untermauert die Annahme einer tektonisch stabilen und passiven Randlage.

Die Ausgangsgesteine der Tarfaya Beckensedimente können mit Hilfe der geochemischen Analyse von Hornblende und Granat und der Spurenelementgeochemie, inklusive der Seltenen Erdelemente (REE), identifiziert werden. Einzelkörner von Hornblende und Granat des Miozän-Pliozän und der rezenten Sedimente zeigen, dass die Tarfaya Beckensedimente als Ausgangsgesteine sowohl Granitgesteine aus dem Reguibat Schild haben, wie auch hochgradige methamorphe Gesteine der Mauretaniden und niedriggradig metamorphe, oder nicht metamorphe Sedimentgesteine des westlichen Anti-Atlas. Die Spurenelementzusammensetzung und die Verteilung der REE zeigen die geochemische Zusammensetzung der Ausgangsgesteine. Niedrige Konzentrationen von Cr (<150ppm) und Ni(<100ppm) und ihre Korrelation weisen darauf hin, dass die Sedimente des Tarfaya Beckens felsische Ausgangsgesteine besitzen. Diese

Aussage wird unterstützt durch die Elementverhältnisse von La/Sc, Th/Sc, La/Co, Th/Co and Cr/Th, da diese den Elementverhältnissen von Sedimenten mit felsischen Ausgangsgestein gleichen. Des weiteren deuten chondrit-normalisierte REE Verteilungen mit angereicherten leichten Seltenen Erdelementen flacher Verteilung der schweren Seltenen Erdelemente und negativen Eu Anomalien ebenfalls darauf hin, dass die Ausgangsgesteine der Tarfaya Beckensedimente felsisch sind.

Annähernd gleiche Sm/Nd-Verhältnisse (0.18-0.20) werden in allen analysierten Grob- und Feinklastika beobachtet, was darauf hin deutet, dass keine signifikante Fraktionierung von Sm und Nd, sowohl während der Ablagerung als auch nach der Ablagerung der Beckensedimente, stattgefunden hat.

Die Nd-Isotopen-Modellalter (T_{DM}=2.1-2.2 Ga) der Sedimente aus der Unterkreide lassen vermuten, dass diese vom eburneischen Terrane des Westafrikanischen Kratons stammen. Dagegen zeigen die Sedimente der Oberkreide bis Miozän-Pliozän jüngere Modellalter (T_{DM}=1.7-1.9 Ga), was auf den Westafrikanischen Kraton und den westlichen Anti-Atlas hindeutet. Im Gegensatz dazu zeigt die südlich gelegene Sebkha Aridal Sektion (Oligozän bis Miozän-Pliozän) durch das Modellalter (T_{DM}=2.5 Ga), dass die Sedimente hauptsächlich vom Archäischen Terrane des Westafrikanischen Kratons stammen.

Die Tonminerale von Sedimenten der späten Kreidezeit bis hin zu rezenten Sedimente des Beckens wurden untersucht, um den Einfluss des Klimas und der Tektonik auf die Verwitterung der Ausgangsgesteine zu bestimmen. Die Tonmineral-Zusammensetzungen der Beckensedimente variieren zwischen den stratigraphischen Einheiten. Illit und Chlorit, welche als Anzeiger für physikalische Verwitterung dienen, sind in allen untersuchten stratigraphischen Einheiten stark vertreten. Smektit wurde detritisch in das Tarfaya Becken eingebracht und weist auf warme und weniger feuchte Klimabedingungen im Liefergebiet hin. Die Intensität der chemischen Verwitterung wird durch das Vorhandensein von Kaolinit und dem Kaolinit/Illit-Verhältnis abgeleitet. Dies wird durch die Proxies Al_2O_3/Na_2O und Al_2O_3/TiO_2, die als chemischer Alterations-Index dienen, bestätigt. In der Oberkreide war während des Turons und des Santons die chemische Verwitterung deutlich stärker als im Campan. Die Sedimente aus dem frühen Eozän bis zum Miozän-Pliozän deuten auf eine geringe chemische Verwitterung hin. Zusätzlich wird Corrensit aus dem Campan und dem Oligozän bis frühen Miozän assoziiert mit der diagenetischen Transformation von Tonmineralen unter oxischen Bedingungen. Das Vorhandensein von Palygorskit in Sedimenten des frühen Eozän zeigen warme und trockene Klimabedingungen in einem nahegelegenen, freiliegenden Küstengebiet. Palygorskit in Tonmineralspektren von rezenten Sedimenten stammen hauptsächlich Von äolischem Sahara-Staub.

Chapter 1

Introduction

1.1 Previous work and motivation

The Tarfaya basin is the southernmost Atlantic marginal basin of Morocco. It extends over more than 1,000 km along the western margin of the Sahara (Hafid et al., 2008). The basin is limited by the Mauritanides to the south, the Reguibat Shield to the east and the Anti Atlas to the north and opens to the Atlantic Ocean in the west. In recent years, the basin has been primarily targeted for the study of fine-grained siliciclastics from the Upper Cretaceous to infer the intensity of anoxia, the magnitude and nature of the $\delta^{13}C$ excursion, the biotic effects on benthonic and planktonic foraminifera, the biostratigraphic records and paleo-environmental evolution by El Albani et al., 1999; Kuhnt et al., 1997, 2005, 2009; Kolonic et al., 2005; Mort et al., 2007, 2008; Keller et al., 2008, Gertsch et al., 2010, among others. The current project is a part of “Atlantic Margin Integrated Basin Analysis, Morocco” which includes petrography, geochemistry, provenance, climate and weathering related studies. The samples are collected from different section and newly drilled cores. The location of these sections and drilled cores are shown in Fig. 1.1.

The principal objectives of this project were to understand the reservoir and source rock distribution and sedimentary processes on the NW African shelf to connect the offshore seismic section with the onshore source area. Detection of temporal changes in sediment flux and sediment pathways in time should be achieved using sedimentological, climate and weathering of Lower Cretaceous to recent sediments combined with biostratigraphy and biofacies analysis of the onshore Tarfaya basin. Hence, the results of this project will help in ongoing and coming exploration campaigns. The project moreover serves as a case study for the entire NW African continental margin, the results of this study can subsequently be transferred to other locations on the NW African shelf awaiting exploration.

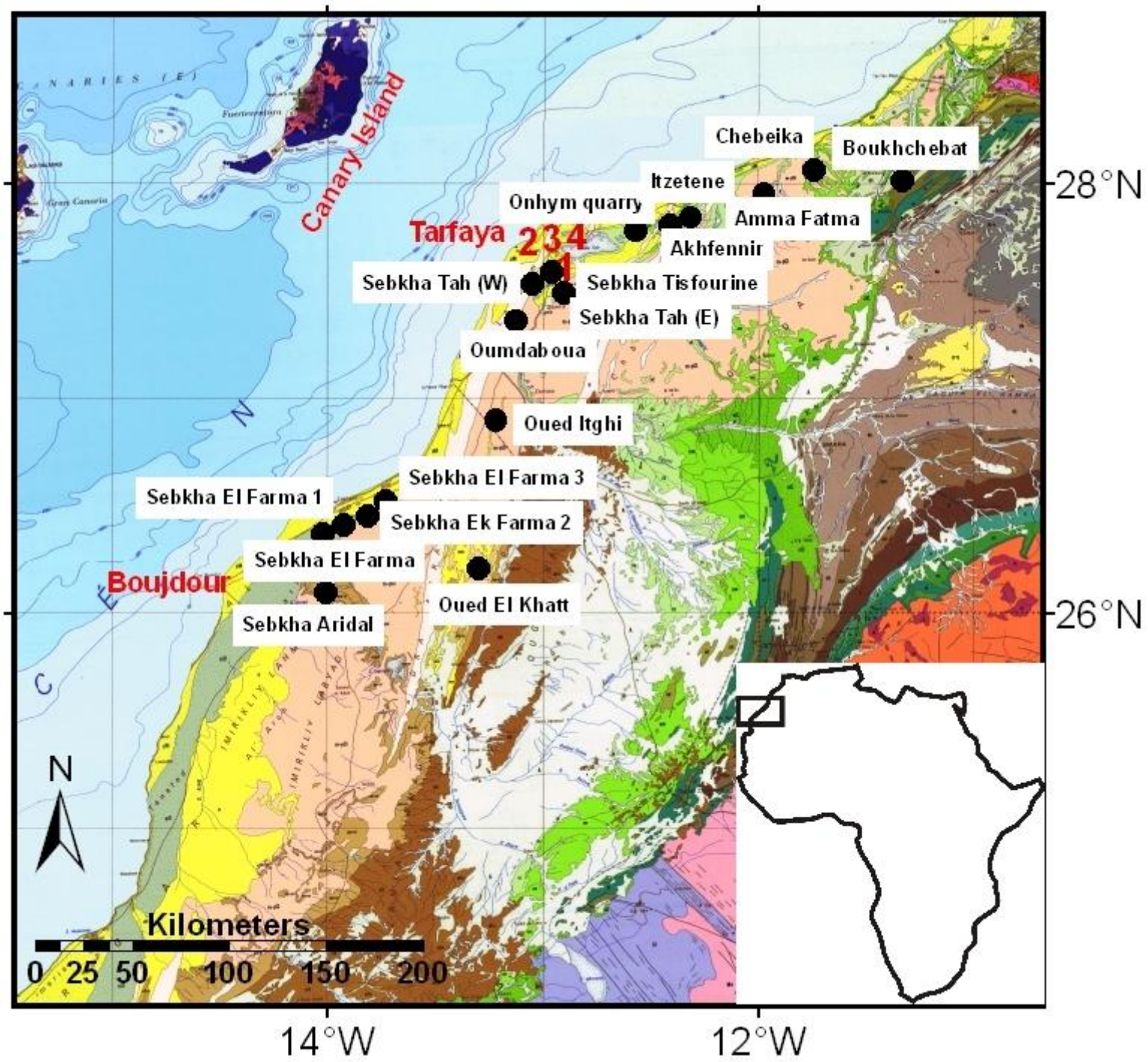

Fig. 1.1 Geological map of the Tarfaya basin including section location (Geological map of Morocco, Department of Energy and Mines, Morocco, 1985). 1, 2, 3 and 4 are the site of drilled cores.

1.2 Thesis overview

The main objective of this thesis is to obtain high resolution correlation of Cretaceous to recent siliciclastic rocks from key sections at the coastal cliffs between Boujdour and Oued Chebeika as well as from the upper sections of the four newly drilled cores. A high number of samples from these outcrop sections and newly drilled cores

were analyzed using thin sections, quartz types, heavy minerals, hornblende and garnet grain geochemistry, major and trace elements geochemical analysis including rare earth elements (REEs), radiogenic Nd-Sr isotopes and clay minerals. These parameters in combination provide detail information about petrography, depositional tectonic setting, provenance and its change with time and climatic and tectonic control on weathering in the source area. The thesis consists of 5 chapters. The contents of each chapter are described as following:

Chapter 1: Previous work and motivation, thesis overview and general geology of the study area.

Chapter 2: Methods overview and work flow

Chapter 3: Results

3.1 Petrography and geochemistry of Cretaceous to Quaternary siliciclastic rocks in the Tarfaya basin, marginal Atlantic, SW Morocco: implications for tectonic settings, weathering and provenance.

3.2 The provenance of Cretaceous to Quaternary siliciclastic rocks in the Tarfaya basin, marginal Atlantic, SW Morocco: evidence from trace element geochemistry and radiogenic Nd-St isotopes.

3.3 Climatic and Tectonic control on weathering from Upper Cretaceous to Quaternary in the Tarfaya basin, marginal Atlantic, SW Morocco: Clay mineralogical and geochemical investigations.

Chapter 4: General conclusions.

1.3 General geology of the study area

The Tarfaya basin is limited by the Anti-Atlas to the north, the Mauritanides to the south, the Reguibat Shield (West African Craton) in the east and open to the Atlantic Ocean in the West. The evolution of the basin is closely connected with the geological history of the African Craton and the opening of the Atlantic Ocean (Ranke et al., 1982), with development from a rift to a marginal basin. The basin is filled by Mesozoic and Cenozoic continental to shallow marine sediments overlying a basement of igneous and metamorphic rocks of Precambrian and/or Paleozoic age. The post-Triassic subsidence of the basin is related to the opening of the Atlantic Ocean (Wiedmann et al., 1982). Important is the activation of the Zemmour fault that separates the Anti-Atlas and the Tindouf basin to the east (Choubert et al., 1966). With the activation of the fault, steady subsidence of the Tarfaya basin commenced in the Triassic followed by stepwise subsidence in the Jurassic and the Cretaceous. A thick deltaic sequence, during the Early Cretaceous, accumulated during and after

a major global Valanginian regression (Vail et al., 1977). According to Ratschiller (1970), the shallow-marine from the Upper Cretaceous to the Eocene unconformably overlies the continental Lower Cretaceous formations. Late Oligocene to Early Miocene basin development shows an erosional hiatus because of the coincidence of a major regression with intensified slumping, canyon incision, and bottom water circulation (Arthur et al., 1979), with only little continental deposition taking place. After this long period of non-deposition or erosion, Miocene-Pliocene sediments unconformably overlay the Lower Cretaceous (Tan Tan Formation), Upper Cretaceous (NE part of the basin), Eocene and Oligocene (SW part of the basin) deposits. Following the Miocene-Pliocene, siliciclastic sediments once again started to be deposited both on- and off-shore with uplift events in the Atlas system (Frozen de Lamotte et al., 2009; Ruiz et al., 2010).

The location of the different sections and drilling cores are shown in Fig. 1.1, and the sample positions in the sections are shown in Fig. 3.1.2. In the present study, different sections were logged and investigated that contain rocks that are exposed in the Sebkhas and along the shoreline. These sections span a period from the Lower Cretaceous to recent time (SW and NE parts of the basin) along with four newly drilled cores. A 90-m-thick Lower Cretaceous Boukhchebat section, with outcrops in the NE part of the basin, was logged and sampled. This section consists of coarse sandstones (in the lower part) and sandstones intercalated with sandy marls and shales. The Upper Cretaceous section that is primarily exposed in the NE part of the basin consists of black shales and sandy marls intercalated with chert and nodular limestones or limestones. The Eocene deposits are mainly outcropped in the SW part of the basin and consist of black shales and sandy marls intercalated with cherts and limestones. The Oligo-Early Miocene sandy marls were sampled from the Sebkha Aridal section. The Miocene-Pliocene siliciclastic deposits consist of coarser or conglomeratic sandstones along with lumachelle in the lower part and sandstones intercalated with sandy marls and limestones all along the basin. Recent sediment samples were also collected from wadis and dunes.

Chapter 2

Methods

Several methods were used on collected samples from seventeen stratigraphic sections from the SW and NE parts of the Tarfaya basin, including four newly drilled cores. In order to obtain information about petrography, geochemistry, provenance, climate and weathering, a total of 400 samples were collected from these sections and upper sections of drilled cores ranging from Lower Cretaceous to Miocene-Pliocene. In addition, twenty recent sediment samples from wadis and dunes were also collected, including one sample from Pleistocene. These different methods are explained in detail in every subsection of *chapter 3.*

As far as work flow in the present study is concerned, the work started with the preparation of thin sections and heavy minerals separation and mounting to analysis petrography. The major element geochemical analysis of studied sediments was done in the Institute of Geosciences, University of Kiel. The preparation and analysis analytical work for analysis of trace elements was performed at the Institute of Geosciences, University of Kiel, Germany. A total of thirty seven trace elements were analyzed using inductively coupled plasma mass spectrometry (ICP-MS, Agilent 7500cs). Nd-Sr isotope measurements were carried out on a Multi-Collector ICP-MS (Nu Plasma), GEOMAR Kiel, Germany. In addition to petrography and geochemical analysis, the sample preparation and analysis for clay mineral content were performed at the State Key Laboratory of Marine Geology, Tongji University (China).

The general workflow that was adopted for the study of petrography, depositional tectonic settings, provenance and weathering in the source area and which are used in the following chapter is compiled in the flow chart in Fig. 2.1.

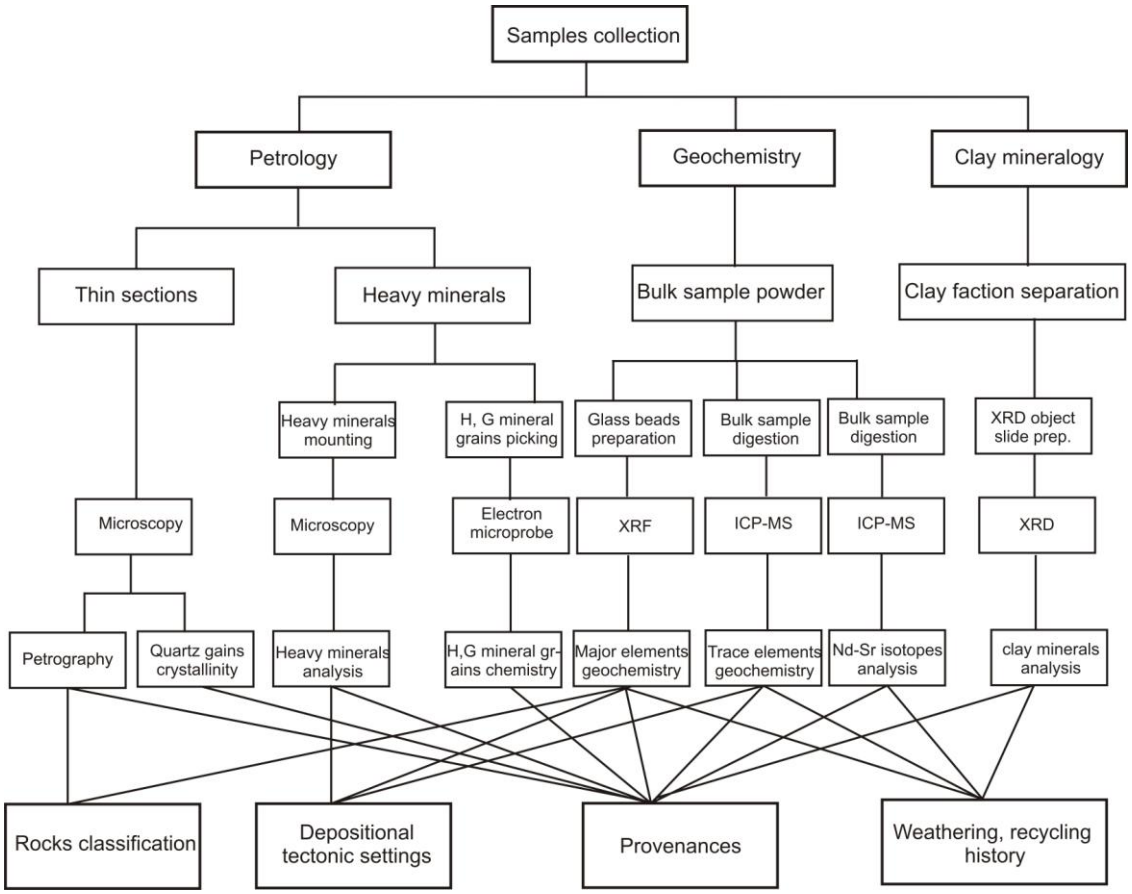

Fig. 2.1 Flow chart showing the workflow of the analytical program performed for the study.

Chapter 3 Results

Chapter 3 is subdivided into 3 parts according to 3 manuscripts which are in review, submitted and/or ready to be submitted.

3.1 Petrography and geochemistry of Cretaceous to Quaternary siliciclastic rocks in the Tarfaya basin, marginal Atlantic, SW Morocco: implications for tectonic settings, weathering and provenance[a]

Sajid Ali[1], Karl Stattegger[1], Dieter Garbe-Schönberg[1], Wolfgang Kuhnt[1], Oliver Kluth[2], Haddou Jabour[3]

[1]Institute of Geosciences, Christian-Albrechts-University, D-24118 Kiel, Germany

[2]RWE Dea AG, Hamburg, Germany

[3]ONHYM, Rabat, Morocco

Abstract

The petrography, heavy minerals, major element geochemical compositions and garnet and amphibole mineral chemistry of Lower Cretaceous to Miocene-Pliocene siliciclastic rocks, including recent sediments of the Tarfaya basin, SW Morocco, have been studied to reveal their depositional tectonic settings, weathering history and provenance. Compositional and mineral chemical data suggest that these rocks were derived from heterogeneous sources in the Reguibat Shield (West African Craton) including the Mauritanides and the western Anti-Atlas, which likely form the basement in this area. The Lower Cretaceous sandstones are subarkosic in composition, while the Miocene-Pliocene sandstones as well as the recent sediments from wadis and dunes are generally carbonate-rich feldspathic or lithic arenites. Their major element geochemistry reflects these findings. The siliciclastics are characterized by moderate SiO_2 contents and variable abundances of Al_2O_3, K_2O, Na_2O and ferromagnesian elements. Binary tectonic discrimination diagrams demonstrate that most samples can be characterized as passive continental marginal deposits. Al_2O_3/Na_2O and TiO_2/Na_2O ratios provide a good proxy for chemical index of alteration (CIA) and indicate intense chemical weathering during the Lower Cretaceous and a variable intensity of chemical weathering from Upper Cretaceous to recent time. Moreover, The Upper Cretaceous and Miocene-Pliocene weathered marls from weathering horizons also suggest variable intensity of chemical

weathering. Petrography, quartz undulosity and heavy mineral data suggest that siliciclastics of the Lower Cretaceous are primarily derived from the Reguibat Shield and the Mauritanides, SW of the basin. On the other hand, The Miocene-Pliocene and recent sediments suggest varied sources lie in the western Anti-Atlas (NE of the basin) and the Reguibat Shield, including the Mauritanides.

[a]This article is in review in International Journal of Earth Sciences.

3.1.1 Introduction

The Tarfaya basin is the southernmost Atlantic marginal basin of Morocco. It stretches over more than 1,000 km along the western margin of the Sahara (Hafid et al., 2008). The basin is limited by the Mauritanides to the south, the Reguibat Shield to the east and the Anti-Atlas to the north and opens to the Atlantic Ocean in the west. The evolution of the basin is closely connected to the geological history of the African Craton and the opening of the Atlantic Ocean (Ranke et al., 1982). In recent years, the basin has been primarily targeted for the study of fine-grained siliciclastics from the Upper Cretaceous to infer the intensity of anoxia, the magnitude and nature of the $\delta^{13}C$ excursion, the biotic effects on benthonic and planktonic foraminifera, the biostratigraphic records and paleo-environmental evolution by El Albani et al., 1999; Kuhnt et al., 1997, 2005, 2009; Kolonic et al., 2005; Mort et al., 2007, 2008; Keller et al., 2008 and Gertsch et al., 2010, among others. In the present study, coarse-gained siliciclastic were considered along with fine-grained siliciclastic for the first time to better understand the depositional tectonic settings, weathering history of the source area and provenance of the siliciclastics by integrating several analytical techniques.

Sandstone provenance studies are based on the assumptions that different tectonic settings contain specific compositional ranges (Dickinson and Suczek, 1979, Dickinson et al., 1983; Dickinson, 1985). Crook (1974) was the first to use the framework mineral composition to identify the tectonic settings of sandstones, and other researchers have since used this scheme with modifications (e.g., Dickinson and Suczek, 1979; Dickinson et al., 1883; Dickinson, 1985). Major element discrimination diagrams of Roser and Korsch (1986, 1988) and Bhatia (1983) further support the discrimination of different depositional tectonic settings of sedimentary basins. Al_2O_3/Na_2O and TiO_2/Na_2O ratios can serve as a proxy for the chemical index of alteration (CIA) because these ratios are directly related to plagioclase alteration (Roy et al., 2008). Heavy mineral analysis is a very effective tool for provenance discrimination (Morton, 1991). Chemical analysis of detrital mineral phases (amphiboles and garnets) serves to constrain source rock petrology and to emphasize the discrimination between different source areas (Morton, 1991; Mange and Morton, 2007). All of these approaches permit the discrimination of depositional tectonic settings, the weathering history of the source area and the provenance from the Lower Cretaceous to recent time.

3.1.2 Geological framework of the study area

The Tarfaya basin has developed from a rift to a marginal basin, which began to subside after the Late Paleozoic orogenic movements and a post-Hercynian

erosional phase of uplift. Rifting began in the Late Triassic and continued until Liassic times (Ranke et al., 1982). The Early to Middle Jurassic subsidence rates were small and the basin was filled by redbeds, evaporites, flood basalts and silty-sandy claystones in a continental to paralic environment. During the Late Jurassic, subsidence rates increased rapidly and the basin was filled by marine carbonates. The Lower Cretaceous deltaic clastics were deposited as the Tan-Tan deltaic formation with a 40 m/my subsidence rate. During the Upper Cretaceous to the Early Eocene, the subsidence rate was higher than the accumulation rate result in the deepening of the outer continental margin to its present depth and only carbonates were deposited. During most of the Neogene, the onshore area of the basin was exposed and eroded and there was little onshore sediment deposition. Since the Miocene-Pliocene, siliciclastic sediments again started to deposit both on and off shore with uplift events in the Anti-Atlas (Frizon de Lamotte et al. 2009; Ruiz et al., 2010).

The Tarfaya Atlantic marginal basin is filled by Mesozoic and Cenozoic continental to shallow marine sediments overlying a basement of Precambrian and/or Paleozoic age. The Triassic evaporites, redbeds, reddish sandstones, conglomerates and volcanic rocks overlie either metamorphic or folded rock sequences of the Mauritanides on a Hercynian unconformity or crystalline rocks of the Precambrian Reguibat Massif (Choubart et al., 1966; Auxini, 1969; Dillon and Sougy, 1974). The early Jurassic marine carbonates transgressed onto the Triassic rift sediments and/or evaporites. The Lower to Middle Jurassic silty sandstones, limestones, dolomitic limestones and dolomites are overlain by the Upper Jurassic neritic marly limestones and calcarenites, intercalated with marls, shales and sandstones. During the Early Cretaceous, a thick sequence of continental to marine-deltaic clastic sediments (Tan Tan Delta Formation) was deposited. This deltaic sequence accumulated during and after a major global Valanginian regression (Vail et al., 1977). The shallow-marine Upper Cretaceous to Early Eocene unconformably overlies the continental Lower Cretaceous formations. The Late Oligocene to Early Miocene basin development exhibits an erosional hiatus due to the coincidence of a major regression with intensified slumping, canyon incision, and bottom water circulation (Arthur et al., 1979), and only limited continental deposition occurred. This erosional event is also inferred by von Rad and Wissmann (1982) from geophysical and geological evidence. After this long period of non-deposition or erosion, the Miocene-Pliocene sediments unconformably overlie the Upper Cretaceous (NE part of the basin), Early Eocene and Oligocene (SW part of the basin) deposits.

The location of the different sections and drilled cores are shown in Fig. 3.1.1, and the sample positions in the sections are shown in Fig. 3.1.2a and b. in the present st-

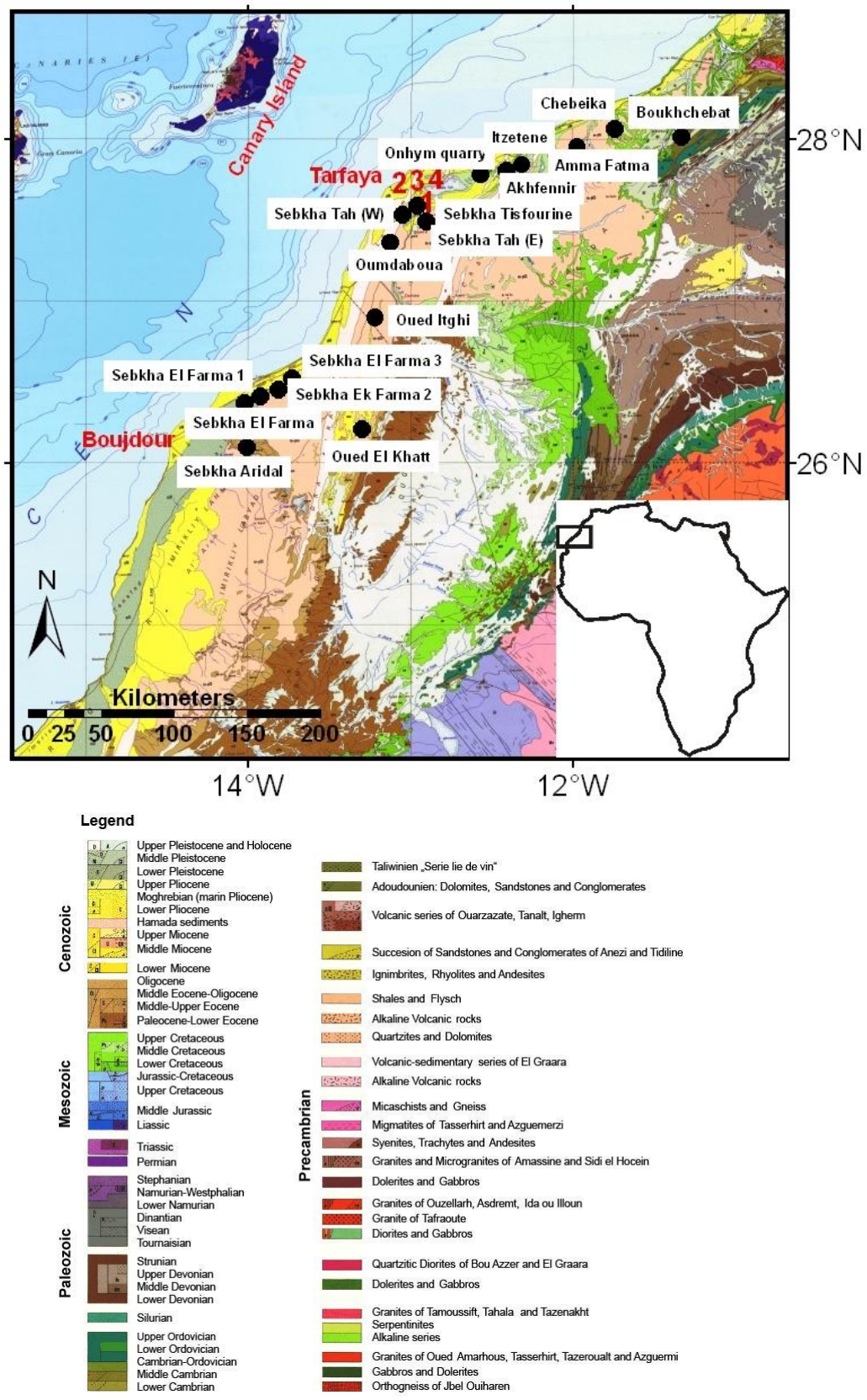

Fig. 3.1.1 Geological map of the Tarfaya basin including sections location (Geological map of Morocco, Department of Energy and Mines, Morocco, 1985). 1, 2, 3 and 4 are the sites of drilled cores.

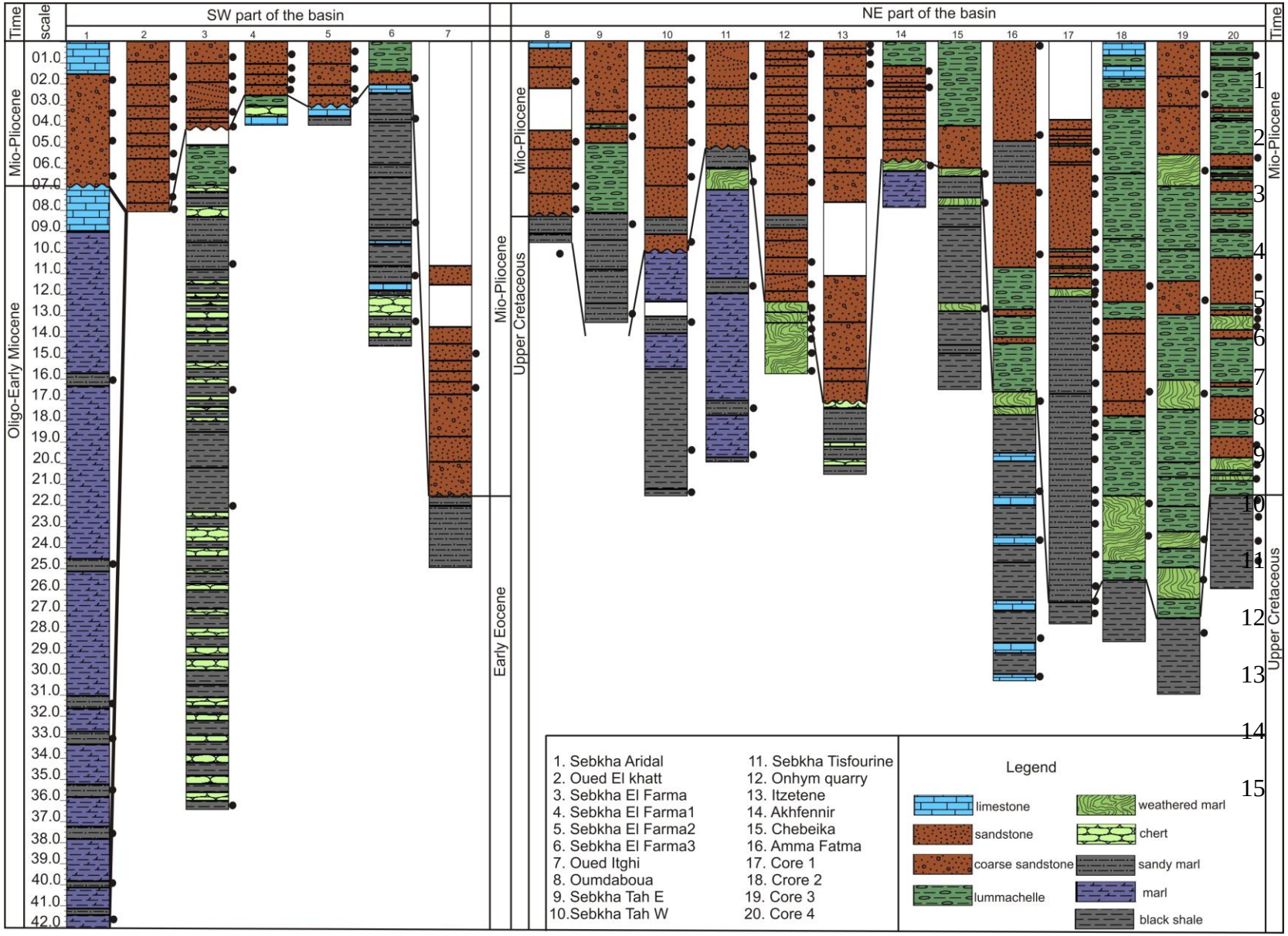

Fig. 3.1.2a Lithologic sec-tions of the Tarfaya basin from Upper Cretaceous to Mio-Pliocene. Black dots mark sample positions.

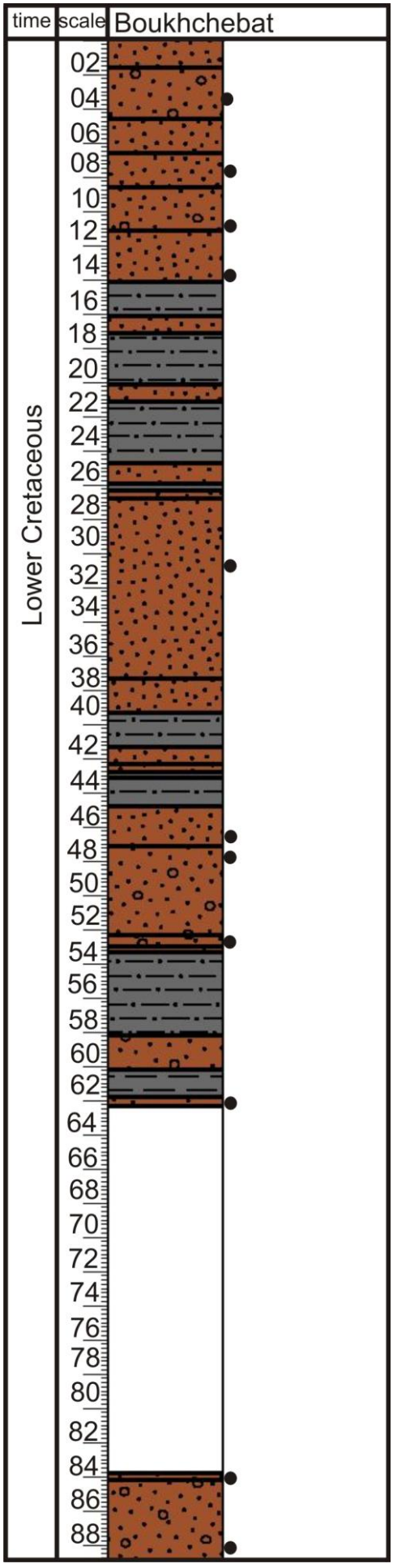

Fig. 3.1.2b. Lithologic section of the Lower Cretaceous Boukhchebat section. Black dots mark sample locations. Legend is same as Fig.3.1.2a

-udy, different sections were logged and investigated that contain rocks that are exposed in the Sebkhas and along the shoreline from the Lower Cretaceous to recent time (SW and NE parts of the basin) along with four new drilled cores. A 90-m-thick Lower Cretaceous Boukhchebat section, with outcrops in the NE part of the basin, was logged and sampled. This section consists of coarse sandstones (in the lower part) and sandstones intercalated with sandy marls and shales. The Upper Cretaceous section that is primarily exposed in the NE part of the basin consists of black shales and sandy marls intercalated with chert and nodular limestones or limestones. The Early Eocene deposits are mainly outcropped in the SW part of the basin and consist of black shales and sandy marls intercalated with cherts and limestones. The Oligocene-Early Miocene sandy marls were sampled from the Sebkha Aridal section. The Miocene-Pliocene siliciclastic deposits consist of coarser or conglomeratic sandstones along with lumachelle in the lower part and sandstones intercalated with sandy marls and limestones all along the basin. Recent sediments were also collected from wadis and dunes.

3.1.3 Materials and methods

Seventeen stratigraphic sections from the SW and NE parts of the Tarfaya basin, including four new drilled cores were examined. A total of 400 samples were collected from these sections and upper sections of drilled cores ranging from the Lower Cretaceous to Miocene-Pliocene. In addition, twenty recent sediment samples from wadis and dunes were also collected, including one sample from Pleistocene sediments at the margin of the river valley.

3.1.3.1 Sandstone petrography (light mineral analysis)

In total, 135 thin sections (perpendicular to bedding) were prepared. Thin sections of Pleistocene and recent sediments were also prepared by impregnating matrix-free sand with Specifix-40^{TM} resin. Only 101 mediums- to coarse-grained, thin sections were used for modal counting to minimize the effect of grain size on sandstone composition. Mineral assemblages were analyzed with a petrographic microscope. More than 300 points per slide were counted according to the Gazzi-Dickinson method (Dickinson 1970; Ingersoll et al. 1984; Zuffa 1985). The results of the point counting are presented in Table 3.1.1 with recalculated parameters according to Zuffa (1980, 1985, 1987), Folk (1974) and Dickinson et al. (1983).

3.1.3.2 Heavy mineral analysis

Eighty-five samples of sandstones, sandy marls and recent sediments, including one sample from the Pleistocene sand, were selected for heavy mineral analysis. Fresh sample material was crushed into small pieces (1 to 4 mm) after removing weathered rims whenever necessary. Disaggregation was performed in warm 10% HCL with repeated ultrasonic cleaning to remove clay mineral coatings, cement and/ or pseudo-matrix. The heavy minerals were separated from the total sand fraction with a sodium polytungstate solution (density 2.96 g/cm^3). Heavy mineral grain separates were embedded in Meltmount^{TM} 1.582 (Mange and Maurer, 1992). The 125-63-µm fraction was analyzed with a petrographic microscope. Percentages were calculated by counting more than 200 transparent detrital grains in each mount with the ribbon counting method (Morton, 1985; Mange and Maurer, 1992).

3.1.3.3 Mineral chemistry

Microprobe analysis was conducted on garnet and amphibole to identify the character of the source rocks. Seven sandstone samples from outcrops and drilled cores and three recent sediment samples were selected to handpick garnet and amphibole grains under the binocular microscope. Fifteen to twenty garnet and amphibole grains were individually selected from each heavy liquid, embedded in epoxy resin mounts, polished and coated with carbon to ensure conductivity for electron microprobe (EMP) analysis. The grains were then analyzed with a Jeol JXA 8900R microprobe analyzer with the wavelength-dispersive method, a 15-kV acceleration potential, and a beam current of 12 nA at the Institute of Geosciences, University of Kiel, Germany.

3.1.3.4 Major elements analysis

A total of 161 samples of sandstones, black shales, sandy marls and sands from the Lower Cretaceous to recent time were selected for major element geochemistry. The selected samples were broken into small pieces with a pestle. The pieces were washed, air-dried and homogenized before making powder using agate mills. Glass beads were prepared by fusing powdered sample with lithium tetraborate and measured with a PHILIPS 1480 XRF (X-ray fluorescence analyzer) at the Institute of Geosciences, University of Kiel, Germany. The analytical precision is greater than 3% for the analyzed elements. Accuracy was controlled by repetitive measurements of geostandards. The total loss on ignition (LOI) was determined after heating the samples for six hours at 950°C. The Sebkha samples with high Na_2O from Upper Cretaceous, Early Eocene, and Oligocene-Early Miocene and Upper Cretaceous weathered marls were corrected for seawater or brine salt. Hence, saltwater-bound Na_2O is corrected by subtracting Cl-bound Na_2O from the total Na_2O. The Cl

concentration was measured with 881 Compact Pro-Anion-MCS ion chromatograph at the Institute of Geography, University of Kiel, Germany.

3.1.4 Results

3.1.4.1 Sandstone petrography

The sandstones in the present study are composed of three main detrital constituents; quartz, feldspar and lithic fragments, together with prevailing intrabasinal carbonate and noncarbonate grains. Partly or completely altered or replaced feldspars and lithic grains were identified on the basis of remnant extinction and texture. Primary matrix and secondary cement were also estimated. Photomicrographs are shown in Fig. 3.1.3 and the results are shown in Table 3.1.1 and Fig. 3.1.4.

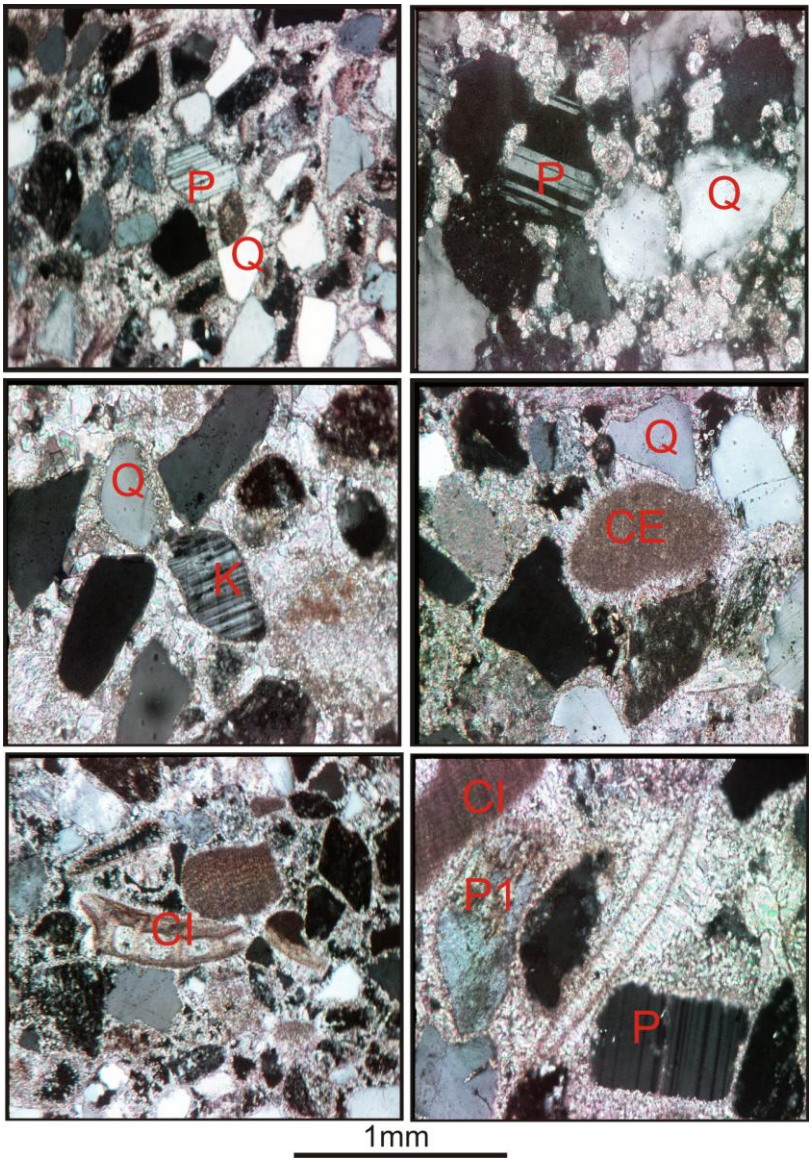

Fig. 3.1.3 Photomicrograph of the Tarfaya basin sandstones. Q= Quartz, P= Plagioclase, K= K-feldspar, C= carbonate extrabasinal, CI= Carbonate Intrabasinal, P1= Plagioclase alteration.

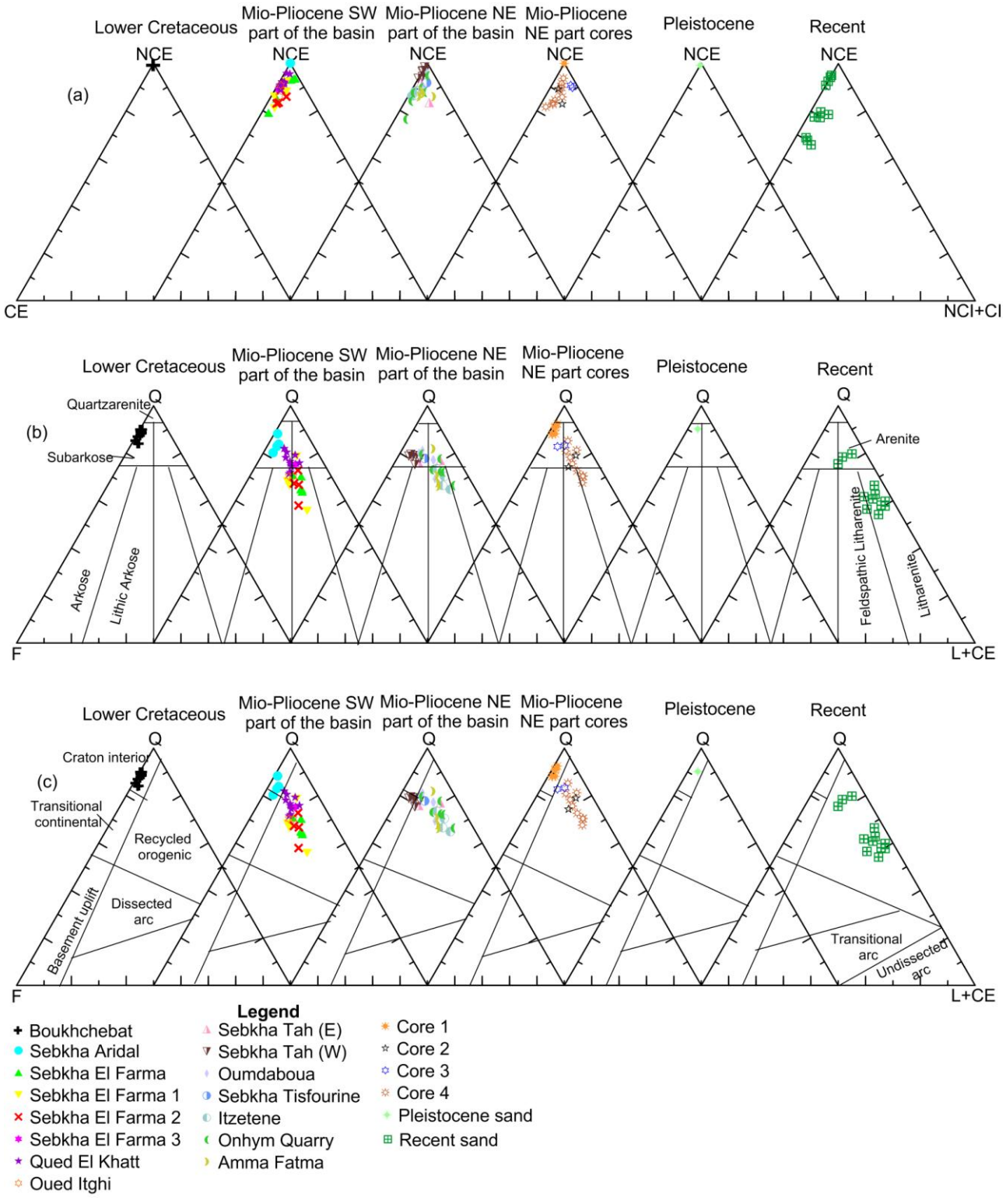

Fig. 3.1.4 Sandstone composition according to (1) NCE-CE-NCI+CI, Zuffa, 1980. (2) Q-F-L+CE, Folk. 1970, modification with inclusion of CE along with L pole. (3) Q-F-L, Dickinson et al. (1983).

Quartz (Q): Quartz is the most abundant grain type. Both monocrystalline (Q_m) and polycrystalline (Q_P) quartz occur in all of the studied samples. Q_m grains are generally angular to rounded. The Q_m grain content is higher than Q_p content. Q_p grains consist of three or more crystals. The Lower Cretaceous sandstones exhibit point to long contacts with some floating grains, while most of the Miocene-Pliocene sandstone grains are floating in carbonate groundmass. The total quartz (Q_m+Q_p) content is higher in the Lower Cretaceous (average 87.6 %) sandstones than in the Miocene-Pliocene sandstones in the SW part of the basin (average 72.4 %) and NE part of the basin (average 77.3 %). The Pleistocene and the recent sediments exhibit average quartz contents of 54.1 % to 90.2 % (Table 1). Chert is (microcrystalline Q_P) common.

According to Basu et al. (1975), comparing the undulosity of the monocrystalline quartz with the amount of polycrystalline quartz permits the differentiation of recent and ancient sands of either plutonic or low- and high-grade metamorphic origin. This scheme was successfully used by Abdel-Wahab, 1992; Anani, 1999; Etemad-Saeed et al., 2011; Ghosh et al., 2012, among others, to reconstruct the nature of the source area of sandstones and sands. The selected fifty sandstone and sand samples from the Lower Cretaceous and Miocene-Pliocene as well as recent sediment samples are used for undulosity and non-undulosity analysis. The results (Fig. 3.1.5) reveal that the Lower Cretaceous sandstone samples contain mostly monocrystalline quartz with non-undulatory quartz (78 to 86 %) and undulatory quartz (5 to 10 %).

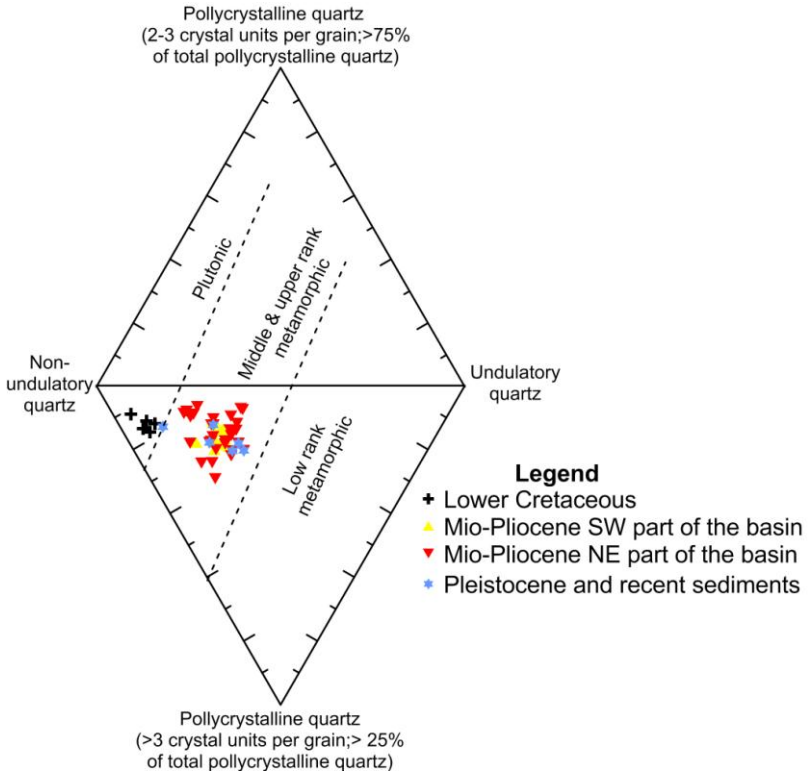

Fig. 3.1.5 Four variable plot of quartz populations in the selected sandstones and recent sediments (Lower Cretaceous to recent sands) from the Tarfaya basin after Basu et. al. (1985).

By contrast, the Miocene-Pliocene sandstone and recent sediment samples comprise monocrystalline and polycrystalline quartz grains in variable amounts. Further, the Miocene-Pliocene sandstones and recent sediment samples show that the monocrystalline quartz with non-undulatory quartz content varies upto 72 %; monocrystalline quartz with undulatory quartz varies upto 36 % and polycrystalline quartz ranges from 7 to 29 %. Hence, the Lower Cretaceous sandstones are mainly characterized by monocrystalline-non-undulatory quartz and Miocene-Pliocene and recent sediments by both, mono- and poly-crystalline quartz in variable frequency. The variation in the frequency of mono- and poly-crystalline quartz contents is point towards differential sources for the Lower Cretaceous and Miocene-Pliocene and recent sediments.

Feldspar (F): Both plagioclase and K-feldspar are present and are counted as total feldspar (F). In most of the studied samples, the proportions of plagioclase and K-feldspar are variable. Plagioclase grains are euhedral, compositionally zoned, and sub-angular, and most exhibit lamellar twinning. K-feldspar grains are subrounded to rounded and identified by the presence of their typical crossed-hatched twinning. The alteration or replacement of plagioclase grains is very low during the Lower Cretaceous but is significant during the Miocene-Pliocene and recent-time. K-feldspar content is higher in the Lower Cretaceous and drilled core-1 (Miocene-Pliocene) plagioclase. The frequencies of both plagioclase and K-feldspar vary in the Miocene-Pliocene sandstone and recent sediment samples.

Lithic fragments: Rock fragments formed from multiple mineral grains and are mostly fine to medium and occasionally coarse-grained, sub-rounded, rounded or angular. Metamorphic, sedimentary and extrabasinal carbonate (CE) rock fragments were identified as extrabasinal lithic fragments. Metamorphic rock fragments, which constitute 1.1 to 2.4 % of the total rock volume, are subangular to sub-rounded in shape. The sedimentary rock fragment abundance is variable, and recent sediment samples contain the highest frequency of sedimentary rock fragments. Extrabasinal carbonate rock fragments are quite common in the Miocene-Pliocene and recent sediments, including drilled cores-2, 3 and 4.

Carbonate and noncarbonate intrabasinal grains were also found. The identified intrabasinal non-carbonate (NCI) grains are glauconite and iron-oxides; intrabasinal carbonate (CI) grains include intraclasts, oolites, fossils and peloids. The Miocene-Pliocene sandstones and recent sediments exhibit variable proportions of NCI and CI

grains. These NCI and CI grains were not identified in the Lower Cretaceous section and drilled core-1 of the Miocene-Pliocene.

Matrix is very rare in all the studied samples and varies from 1.0 % to 2.0 %. It occurs as crushed lithic fragments, tiny quartz grains and pseudo-matrix including sericite. Sparite and micrite are common cement types. Quartz cement is also present in low proportion as quartz overgrowth in the Miocene-Pliocene sandstones. The overall cement proportion is variable and is as high as 40 %. The cement is low in concentration in the Lower Cretaceous sandstones (<10 %), but very high in the Miocene-Pliocene sandstones (30.0 % to 40.0 %).

3.1.4.2 Modal composition

The first-level classification of arenites by Zuffa (1980) containing extrabasinal non-carbonate grains (NCE), extrabasinal carbonate grains (CE), intrabasinal carbonate grains (CI) and intrabasinal non-carbonate grains (NCI), the second-level classification of Folk (1974) Quartz-Feldspar-Lithic fragments (QFL) triangular diagram (with the modification that CE grains are included in the L-pole) were used to classify the analyzed arenitic rocks and sands. This modification is useful for evaluating the influence of CE grains.

According to Zuffa's (1980) classification, all analyzed sandstones and sands are mainly carbonatic arenites (Fig.2.4a). There is no significant influence of NCI and CI grains on the total composition and only a slight influence of CE grains on Miocene-Pliocene sandstone and recent sediment samples.

The second-level classification of Folk's (1974) reveals differences among various stratigraphic units. The Lower Cretaceous sandstones ($Q_{88}F_{11}L+CE_1$) are classified as subarkose. The Miocene-Pliocene sandstones from the SW part ($Q_{72}F_{13}L+CE_{14}$) and NE part ($Q_{75}F_{11}L+CE_{14}$) belong to the subarkose, lithic arkose, litharenite and feldspathic litharenitic fields (Fig.2.4b). Drilled Core-1 ($Q_{90}F_8L+CE_2$) lies in the subarkose field and is similar to the Lower Cretaceous sandstones. The recent sediments ($Q_{58}F_7L+CE_{35}$) are classified as subarkose, arenite, litharenite or feldspathic litharenite (Fig. 4b). In addition, one sample from the Pleistocene sand ($Q_{90}F_6L+CE_4$) was also analyzed and lies in the subarkose field.

The QFL ternary diagram of Dickinson et al. (1983) was used to identify the possible source area of the detrital grains (Fig.2.4c). Extrabasinal carbonate (CE) grains were added with other lithic fragments. The Lower Cretaceous sandstones exclusively lie in the cratonic interior province field. The Miocene-Pliocene sandstones from both parts of the basin plot in the recycled orogenic province, with the exception of the Sebkha Aridal section, which lies in the Cratonic interior field or at the boundary with the recycled orogenic provenance. The sandstones in Drilled Cores-2, 3 and 4 fall in

the same field as the Miocene-Pliocene sandstones, but Core-1 sandstones cluster with the Lower Cretaceous sandstones. The recent sediment samples also lie in the recycled orogenic province field. The Pleistocene sand sample lies in the plutonic interior field.

3.1.4.3 Distribution of heavy minerals

The heavy mineral assemblages of the Tarfaya basin from the Lower Cretaceous sandstones, Oligocene-Early Miocene sandy marls, Miocene-Pliocene sandstones and recent sediment samples from wadis and dunes, including one Pleistocene sand sample, were studied, and modal counts were performed to infer possible provenance.

Nine different heavy minerals were found in the studied sandstones, sandy marls and sand samples, along with opaque minerals. These heavy minerals are zircon, tourmaline, rutile, garnet, hornblende, epidote, sphene, staurolite and apatite (Table 2.2). The dominant heavy mineral species are the stable minerals zircon, tourmaline, rutile (ZTR) and hornblende with variable amounts of garnet, sphene and epidote. Staurolite and apatite were also found in significant amounts. The heavy mineral concentration is shown in Table 3.1.2 and Fig. 3.1.6.

The Lower Cretaceous sandstone samples from the Boukhchebat section contain zircon, tourmaline, rutile, garnet and hornblende. Fine-grained heavy minerals are subrounded to rounded, while coarser-grained sand-size heavy minerals are angular to subangular in shape. The transparent grains content is higher than opaque mineral grains. Together, zircon, tourmaline and rutile constitute > 90 % of the bulk, while garnet and hornblende are 3.5 % and 5.5 %, respectively.

The heavy mineral assemblages of the Oligocene-Early Miocene sandy marls from the Sebkha Aridal section contain zircon, tourmaline, rutile, garnet, hornblende, apatite, epidote and staurolite. Most of the heavy mineral grains are fine to medium sized and subrounded to rounded in shape. The opaque grains content is higher than transparent mineral grains. Together, zircon, tourmaline and rutile constitute approximately 64 % of the bulk, while hornblende comprises 24 %. Few grains of epidote, staurolite and apatite were also found.

The heavy minerals of the Miocene-Pliocene, seven sections from the SW part of the basin as well as seven sections from NE part of the basin consist of zircon, tourmaline, rutile, hornblende, garnet, epidote, sphene, staurolite and apatite. Most of these heavy mineral grains are angular to subangular and medium sand sized. Zircon, tourmaline and rutile constitute 48 % and 52 % in the SW and NE parts of the basin, respectively. The garnet and hornblende concentration is variable in all of the studied sections. Epidote, sphene and staurolite were present in significant

proportions in almost all of the studied samples, and traces of apatite grains were found in some samples.

The heavy minerals of the Pleistocene and recent sediments from wadis and dunes consist of zircon, tourmaline, rutile, garnet, hornblende, epidote and sphene. Most of the heavy minerals are fine to medium sand sized and angular to subangular or rounded to subrounded in all sand samples. Garnet percentages vary from 4 % to 10 %. Epidote and sphene are present in minor amounts. The Pleistocene sand sample contains 77 % ZTR.

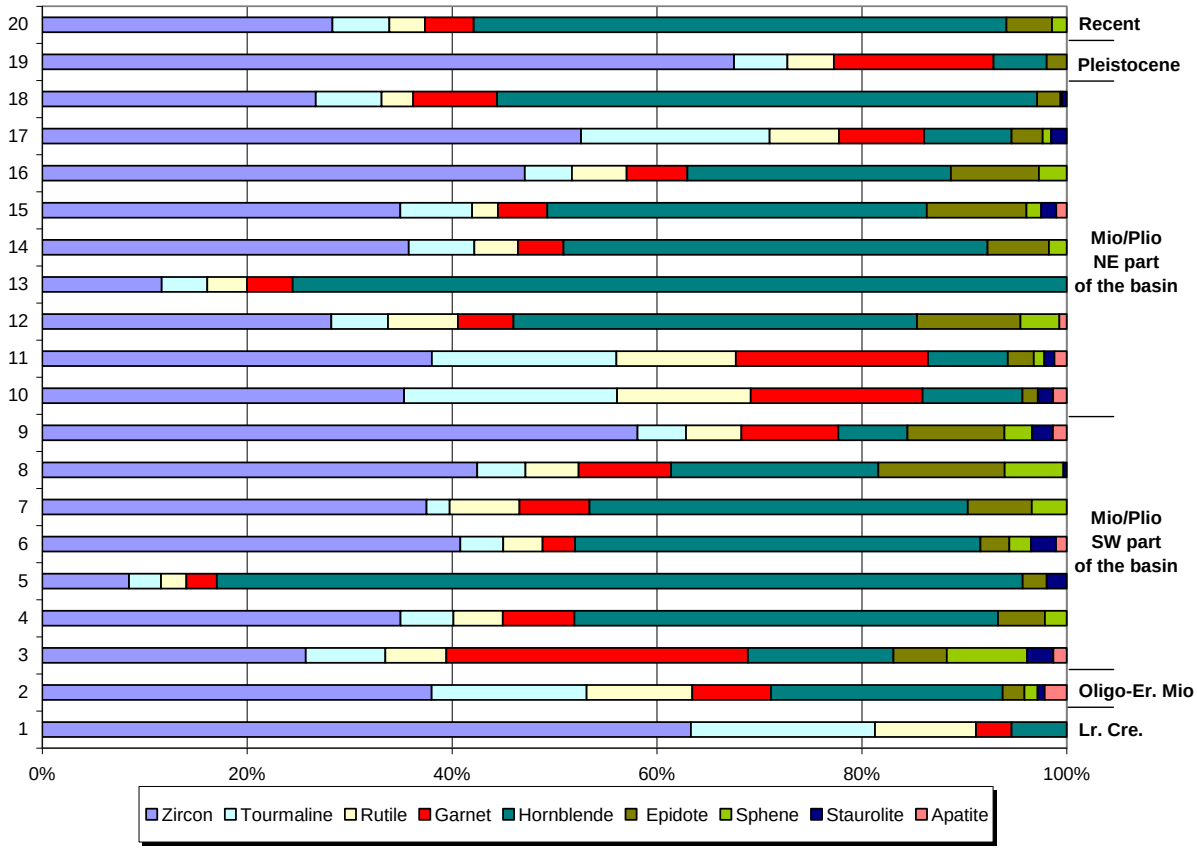

Fig. 3.1.6 Average heavy mineral composition of different sections and stratigraphic divisions.1-Boukhchebat (n=09), 2&3-Sebkha Aridal, (n=05), (n=04) , 4-Sebkha El Farma (n=02), 5-Sebkha El Farma1 (n=04), 6-Sebkha El Farma2 (n=02), 7-Sebkha El Farma3 (n=01), 8-Oued El Khatt (n=05), 9-Oued itghi (n=01), 10-Sebkha Tah-E (n=02), 11-Sebkha Tah-W (n=06), 12-Oumdaboua (n=06), 13-Sebkha Tisfourine (n=01), 14-Itzetene (n=03), 15-Onhym quarry (n=03), 16-Amma Fatma (n=04), 17-Core-1 (n=07), 18-Core-4 (n=09), 19-Pleistocene sand (n=01), 20-Recent sediments (n=11).

3.1.4.4 Mineral chemistry

Microprobe analysis rapidly and effectively confirms optical mineral identification, permits the identification of composite grains consisting of microcrystalline or cryptocrystalline aggregates of material unidentifiable by optical methods and provides information on the geochemistry of mineral grains (Morton, 1991). The chemical variability of mineral phases is most useful because it can be used to discriminate between different source rocks and their petrology (von Eynatten and Gaupp, 1999). Hornblende and garnet mineral grain (Miocene-Pliocene and recent sediment samples) chemistry was used in the present study and the data are plotted in Fig. 3.1.7a and b and Fig. 3.1.8a and b.

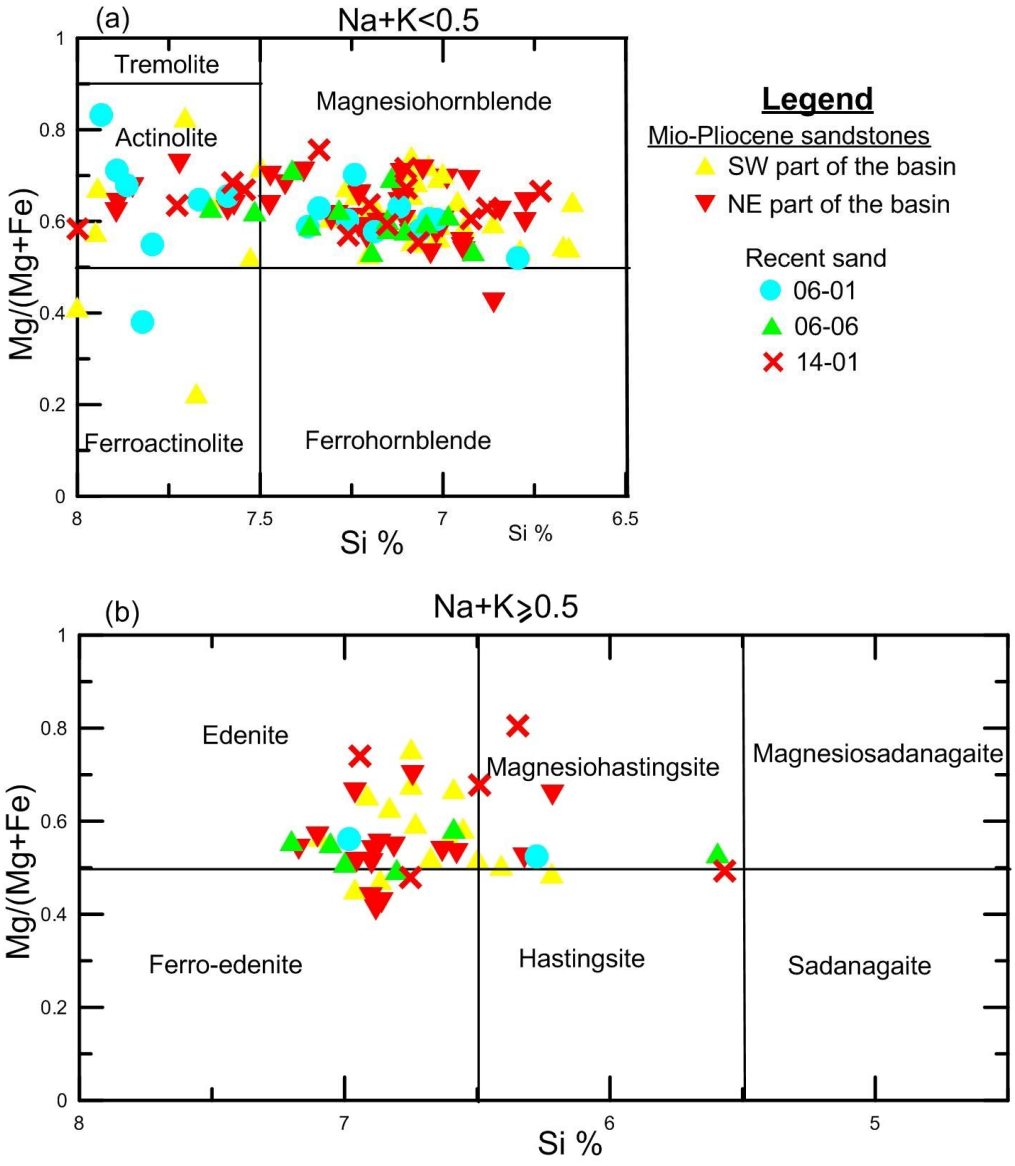

Fig. 3.1.7 Chemical classification of the studied amphiboles: (A) lower Na+K; (B) higher Na+K (after Leake et al., 1997).

3.1.4.4a Detrital amphibole

Amphiboles are good indicators of provenance because of their presence in different rock types. Chemical analyses of single-grain amphiboles distinguish different potential source rocks (Morton, 1991, Mange and Morton, 2007). The analyzed amphiboles are characterized by variable FeO (7.1-31.4 %), higher MgO (4.9-20.7 %), variable CaO (0.4-22.1 %), and lower Na_2O (0.05-3.1 %). According to the classification of Leake et al. (1997), all amphiboles in the present study are calcic amphiboles. These calcic amphiboles are further divided into two groups depending on the Na+K value (greater or less than 0.5 atoms per formula (apfu)) in the A site of their classification (Fig. 3.1.7a). The first group (Fig. 3.1.7a) consists of mainly edenite with some grains of ferroedenite, magnesiohastingsite and hastingsite. The second group (Fig. 3.1.7b) mainly comprises actinolite and magnesio-hornblende with few grains of ferroactinolite and ferrohornblende. Tremolite is not present.

Edenite and hastingsite are common varieties of hornblende because the hornblende series is variable in chemistry (Hurlbut and Klein, 1993). Actinolite is a characteristic mineral of very-low- to low-grade greenschist metamorphic facies. Generally, hornblende is an important constituent of both igneous and metamorphic rocks (Deer et al., 1992).

3.1.4.4b Detrital garnet

Garnet group minerals are generally found in metamorphic rocks (Mange and Maurer 1992) but are also present in some acidic rocks such as granites, pegmatites, and acid volcanic rocks (Deer et al., 1992). Because garnets are resistant to abrasion and to chemical solution under slightly basic conditions, they occur frequently in detrital sediments (Deer et al. 1992); hence, their geochemistry is useful for provenance analyses (Morton, 1991, Morton et al., 2004).

The garnet assemblages of the Tarfaya basin sediments are highly variable and reveal changes among the studied Miocene-Pliocene sandstone and recent sediment samples. Three main populations (Fig. 3.1.8a and b) can be identified in the ternary diagram with the end members pyrope (Mg), almandine (Fe) + spessartine (Mn) and grossular + andradite + uvarovite (Ca) (Morton, 1985; Morton et al., 2004).

According to Morton (1985) and Morton et al. (2004), garnets are classified into four types based on the percentages of pyrope, almandine, spessartine and grossular in the triangular diagram in Fig. 3.1.8a and b.

(1) Type A garnets are typically of low grossular (< 10 %), high pyrope (20 to 40 %), and generally low spessartine content (<5 %). The studied garnets contain grossular, pyrope and spessartine in variable amounts, which lie in the A field of the triangular diagram. These correspond to high-grade metamorphic rocks and/or orthopyroxene charnockites (Sabeen et al., 2002).

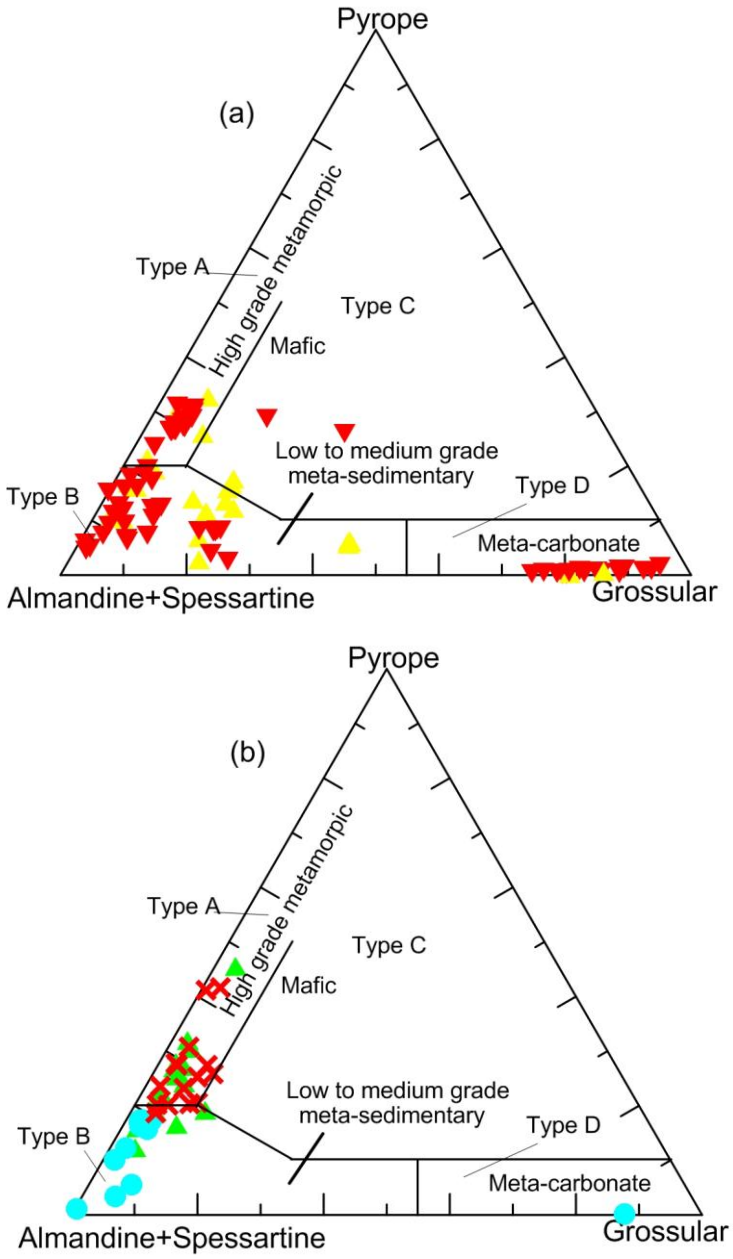

Fig. 3.1.8 Ternary diagram illustrating the classification of the studied garnets after Morton et al. (2003). (a) Mio-Pliocene sanstone garnets classification, (a) Recent sand garnets classification. Legend is same as in Fig. 3.1.7a and b.

(2) Type B garnets have high almandine, low pyrope, low to moderate grossular and variable spessartine contents. The studied garnet also contains low pyrope, moderate grossular and variable spessartine and falls in field B of the triangular diagram. These garnet types are typically derived from low- to medium-grade meta-sedimentary rocks, whereas garnet from granitic and aplitic igneous origin exhibits

almandine + spessartine contents > 90 % (Deer et al., 1992; Morton, 1985; Morton et al., 2004).

(3) Garnets with higher pyrope and lower almandine-spessartine and grossular contents fall in field C of the ternary diagram. These garnets correspond to mafic source rocks (Morton et al., 2004) and are not present in the studied sediments, with very few exceptions.

(4) Type D garnets have high grossular contents. Some of the studied garnets contain very high grossular concentrations (up to 93 %). These are derived from meta-carbonatic rocks.

Accordingly, the garnets from the Miocene-Pliocene sandstones indicate that they have been derived from high-grade metamorphic and low- to medium-grade meta-sedimentary and/or meta-carbonatic rocks with no contribution from mafic rocks. The garnets from the NE part (sample #06-01) and the SW part (sample #14-01) of the basin cluster separately (Fig.2.8b), indicating low- to medium-grade metasedimentary and high-grade metamorphic source rocks, respectively. Sample #06-06 is distributed between the medium- and high-grade metamorphic fields.

3.1.4.5 Geochemistry (major elements)

The whole rock chemical composition for 10 major elements, including LOI, for the selected sandstones, sandy marls, black shales and sands is given in Table 3.1.3. The elemental distribution is compared with the upper continental crust (UCC, Taylor and McLennan, 1985).

The SiO_2 content is variable from the Lower Cretaceous to recent sediments. It is comparatively higher during the Lower Cretaceous but decreases toward the top within the Boukhchebat-Section, with the exception of samples #27-24 and #27-25 because of the high CaO content. Sandy marls exhibit higher SiO_2 content than black shales during the Upper Cretaceous and Early Eocene. The Miocene-Pliocene sandstones exhibit a variable concentration of SiO_2 % in both parts of the basin along with recent sediment samples. One sand sample from the Pleistocene deposit exhibits 85 % SiO_2.

Al_2O_3, Na_2O, K_2O, FeO and MgO are variable and lower than UCC (Taylor and McLennan, 1985). The Al_2O_3 content is much lower than UCC in almost all samples, with the exception of #07-02 and #07-05 from recent finer grained sediment samples. Some samples of black shales and sandy marls from the Upper Cretaceous, Early Eocene and Oligocene-Early Miocene deposits exhibit higher Na_2O contents. One sample from the Lower Cretaceous and some samples from Recent Time have higher concentrations of K_2O compared to UCC (Taylor and McLennan, 1985). The

Al_2O_3/K_2O ratio is greater than 0.3 in all but a few samples (~0.2) (Table 3.1.3), indicating that most of the K_2O is present in K-feldspar (Armstrong-Altrin et al., 2004). CaO and LOI contents are vary widely in the siliciclastic sediments. Most of the samples are enriched in CaO relative to UCC (Taylor and McLennan, 1985). The higher values of CaO in all studied samples are likely due to the presence of carbonates as a major component of most samples. Recent sediment samples also have higher CaO content due to the presence of carbonate rock fragments, as identified by polarizing microscopy.

The major elements can be used to chemically classify siliciclastic rocks. The SiO_2/Al_2O_3 ratio reflects the abundance of quartz as well as clay and feldspar content (Potter 1978), and the Fe_2O_3/K_2O ratio improves the classification and can also be used to measure mineral stability (Herron, 1988) because ferro-magnesian minerals tend to be among the least-stable minerals during weathering and diagenesis.

SiO_2/Al_2O_3 and Fe_2O_3/K_2O parameters are used to draw a classification diagram according to Herron (1988) [Fig. 3.1.9].

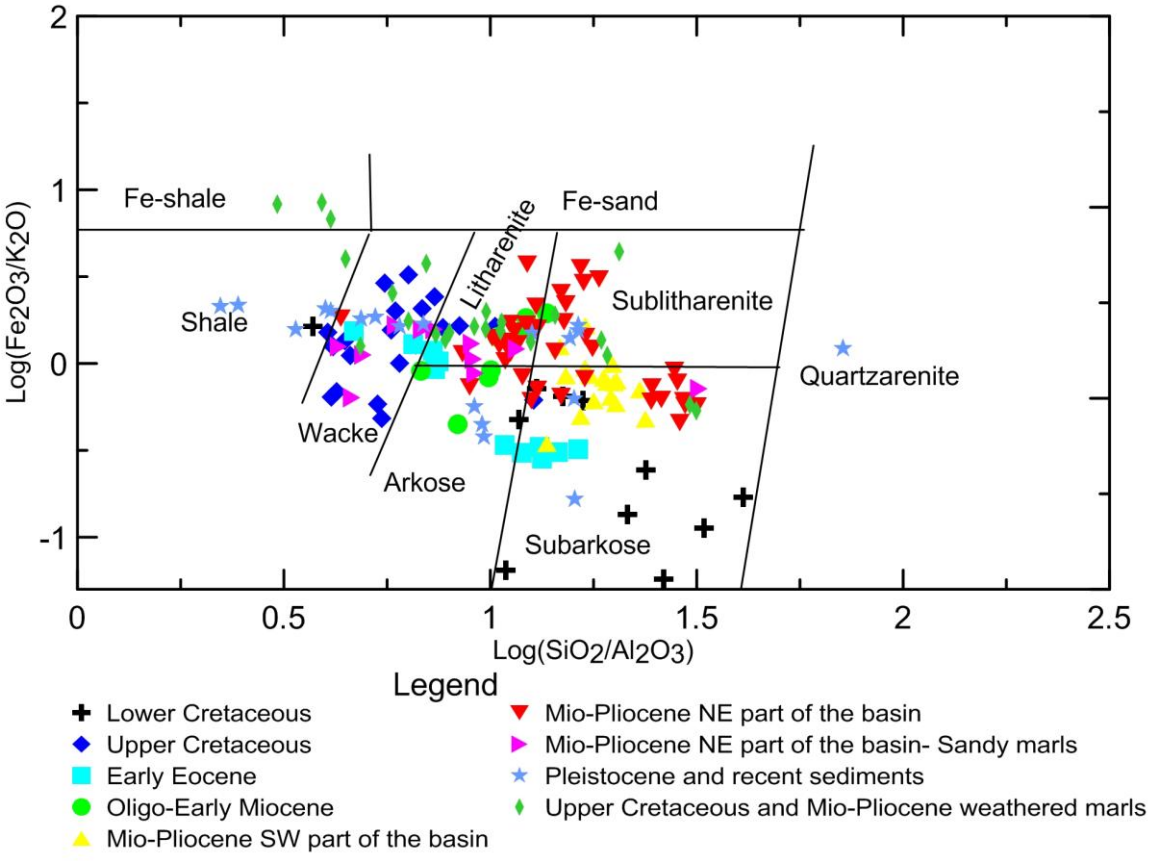

Fig. 3.1.9 Plot of Tarfaya basin sandstones, sandy marls, black shales and recent sediment samples on the geochemical classification diagram after Herron (1988).

In this Herron (1988) diagram, the Lower Cretaceous sandstones fall in the subarkose field, and one sandy marl sample, #27-25, lies in the wacke field. The

Upper Cretaceous black shales cluster more closely than sandy marls and also lie in the field for greywacke. The Early Eocene sandy marls are sandier than the Upper Cretaceous sandy marls and fall in the subarkose or arkose fields. Black shales are more or less similar to the Upper Cretaceous black shales and lie in the same field. The Oligocene-Early Miocene sandy marls lie in the litharenite or arkose field. The Miocene-Pliocene sandstones from the SW part of the basin lie in the sublitharenite and subarkose fields, while those from the NE part are more scattered and fall in the litharenite, sublitharenite and subarkose fields, with the exception of sample #20-42, which lies in the wacke field. The recent finer-grained sediment samples fall in the wacke or shale field, and coarser grained sediment samples are more scatter.

3.1.5 Discussion

3.1.5.1 Tectonic setting

The major elements compositions of sedimentary rocks have been used to decipher the ancient tectonic settings of the depositional environment (Maynard et al., 1982; Bhatia, 1983, Bhatia and Crook ,1986; Roser and Korsch, 1986, 1988).

The studied samples have high concentrations of CaO and LOI. The major element data were recalculated to 100 % by discarding CaO and LOI due to their high concentration, as suggested by Roser and Korsch (1986, 1988) and used by Armstrong Altrin et al. (2004), before plotting in Fig. 3.1.10 a and b. Most of the sandstone and recent sediment samples from the Lower Cretaceous and Miocene-Pliocene to recent time lie in the “passive margin” field. The Upper Cretaceous to Oligocene-Early Miocene black shale and sandy marl samples are mostly plotted in the passive margin field, with the exception of a few samples that lie in the active margin field. These active margin plotted samples may be the result of low SiO_2 concentrations and lower K_2O/Na_2O ratio.

The discrimination diagrams described by Bhatia (1983) were also used to infer tectonic settings (Fig. 3.1.10c, d, e and f). Again, most of the studied sandstone and recent sediment samples from the Lower Cretaceous and Miocene-Pliocene to recent time are plotted in the passive margin field. Some of these samples exhibit slightly higher values of either Fe_2O_3+MgO or Al_2O_3/SiO_2. These higher values are due to secondary MgO, which is largely derived from dolomite (von Eynatten, 2003) and high Al_2O_3 or low SiO_2 concentrations. The Upper Cretaceous to Early Eocene black shale, sandy marl and some recent sediment samples plots are more scattered, including Oligocene-Early Miocene sandy marls because these discrimination diagrams are preliminarily prepared for coarse-grained siliciclastic sediments.

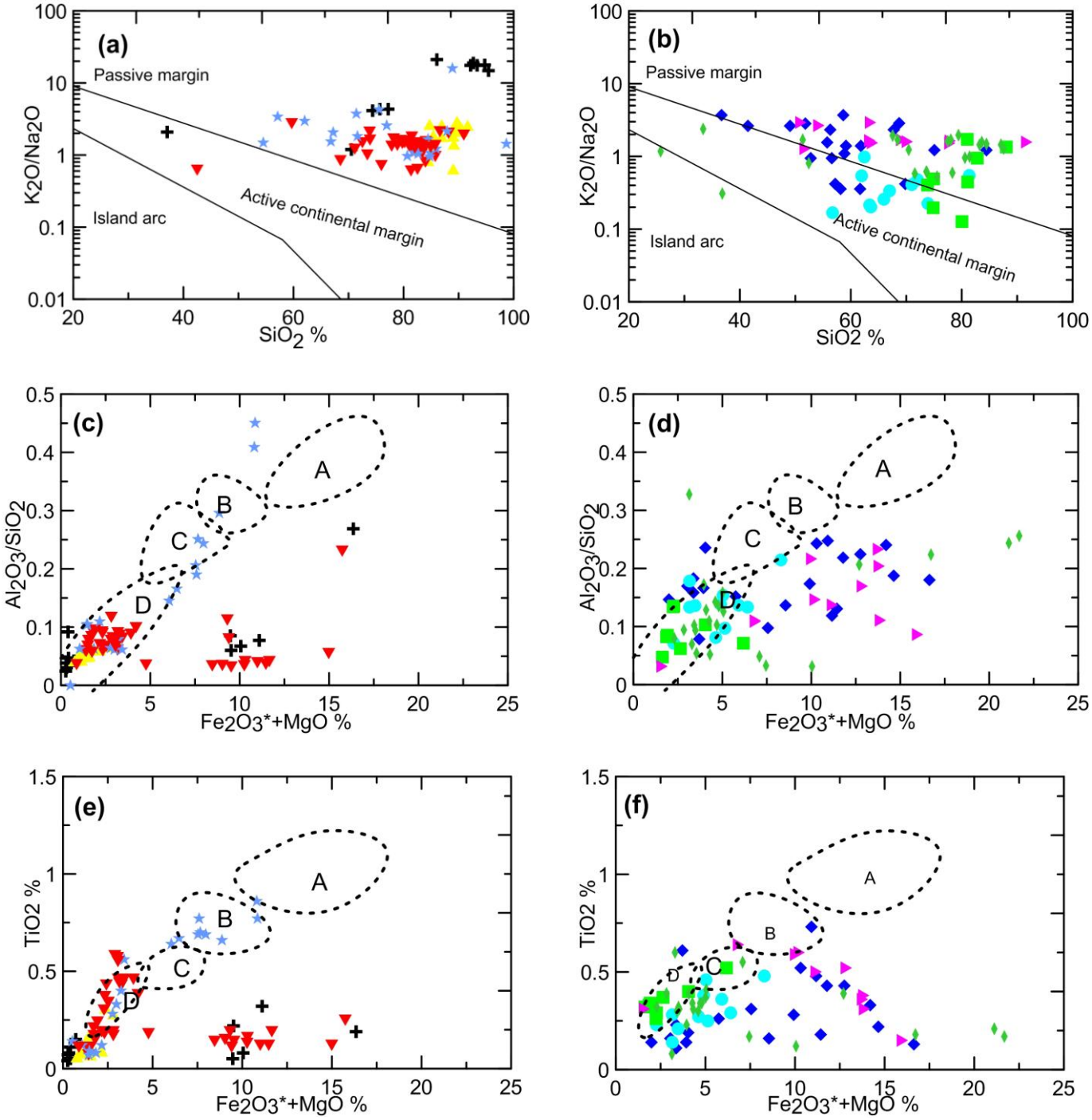

Fig. 3.1.10. Plots of the major element composition of the sand and sandstones, sandy marls and mudstones from the Tarfaya basin on the tectonic-setting discrimination diagrams of Roser and Korsch (1988): a&b, Bhatia (1983): c,d, e &f. A: Oceanic Island Arc, B Continental Island Arc, C: Active Continental Margin, D: Passive Margin. Legend is same as in Fig. 3.1.9.

In addition, a right-triangle diagram of Nechaev and Isphording (1993) was used to plot heavy minerals (Fig. 3.1.11) for comparison with the tectonic settings

discrimination diagrams of the major element data. These authors divided heavy minerals into three groups,

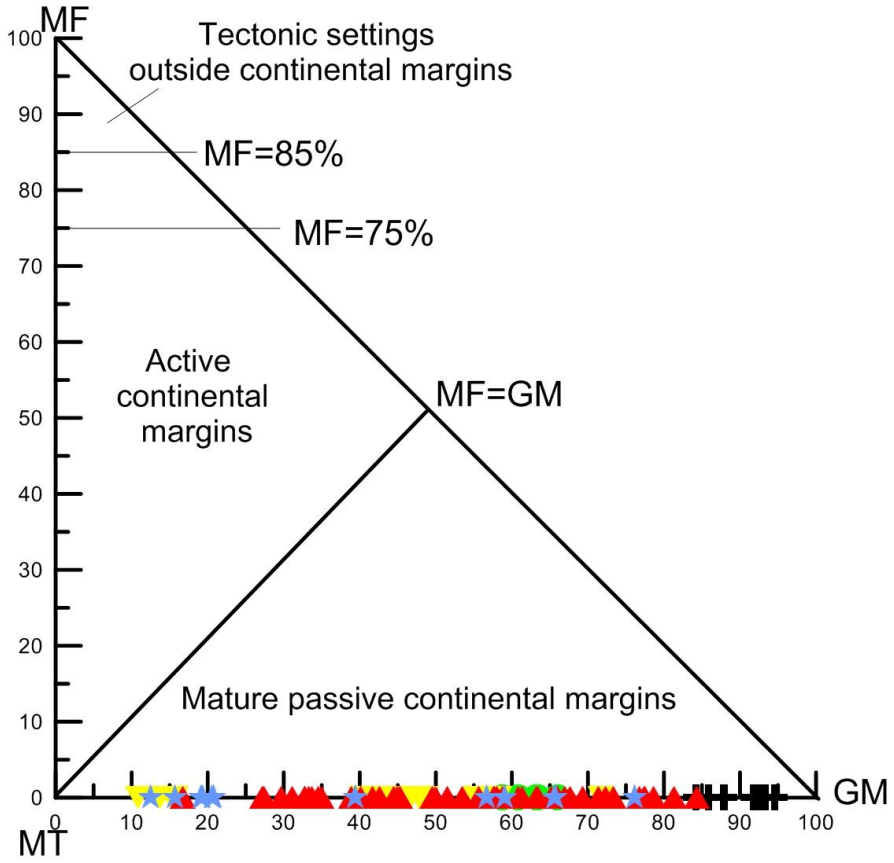

Fig. 3.1.11. Interrelationship of the MF-MT-GM suits in the Tarfaya basin sedimentary rocks. MF= total content of olivine, iddingsite, all pyroxenes, and green-brown hornblende; MT= total content of pale-colored and blue-green amphiboles, epidote (group) and garnet; GM= total content of zircon, tourmaline, staurolite, monazite, andalusite, silimanite, and kyanite. Legend is same as in Fig. 3.1.9.

i.e., (MF= total content of olivine, iddingsite, all pyroxenes, and green-brown hornblende), (MT= total content of pale-colored and blue-green amphiboles) and (GM= total content of zircon, tourmaline, staurolite, monazite, andalusite, silimanite, and kyanite) [Fig.2.11]. All of the studied samples from the Lower Cretaceous and the Miocene-Pliocene, including recent sediment as well as Pleistocene samples, plot on the MT-GM line, indicating mature passive continental margin setting.

Hence, the discrimination diagrams proposed by Roser and Korsch (1986, 1988) are more useful than those of Bhatia (1983) to discriminate depositional tectonic settings that are indicative of passive margin depositional setting of the studied siliciclastics and these findings are supported by heavy-mineral counts. These findings are in agreement with the tectonic history of the Tarfaya basin, which was driven by the

evolution of the passive NW African Atlantic margin since Cretaceous (Ranke et al., 1982; Michard et al., 2008).

3.1.5.2 Weathering history

A good measure of the degree of chemical weathering can be obtained by calculating the chemical index of alteration (CIA=100*[Al_2O_3/ (Al_2O_3+CaO+K_2O+Na_2O)]) proposed by Nesbitt and Young (1982), where Al_2O_3, CaO*, K_2O and Na_2O are in chemical proportion. CaO* represents Ca in silicate-bearing minerals. There is no direct method to distinguish and quantify the contents of CaO belonging to the silicate fraction and non-silicate fraction. However, in the present study, we used the method reported by McLennan (1993) to calculate CaO* (CaO*=CaO-10/3*P2O5, see detail in McLennan, 1993). In the proposed CIA index, Al_2O_3 is used as the immobile component and CaO*, K_2O and Na_2O are the mobile components because they are readily leached during weathering. High CIA values imply increasing removal of K_2O, CaO and Na_2O relative to the more stable Al_2O_3, and consequently, the CIA values reflect the intensity of weathering. CIA values ranging from 50 to 60 indicate nearly absent or low chemical alteration, whereas CIA values close to 100 indicate intense chemical weathering (Nesbitt and Young, 1982; McLennan, 1993; Fedo et al., 1995; Liang et al., 2009; Conceptian et al., 2012).

The CIA values (Table 3.1.3) for the Tarfaya basin vary in the coarse-grained sediments from 55 to 65 (Lower Cretaceous), 40 to 50 (Miocene-Pliocene from both parts of the basin) and, in the finer grained sediments, from 25 to 55 (Upper Cretaceous), 20 to 45 (Early Eocene) and 30 to 50 (Oligocene-Early Miocene-Pliocene). Petrographic data demonstrate that K-feldspar dominates over plagioclase, which may result from intense weathering and/or recycling during the Lower Cretaceous (Armstrong Altrin et al., 2004); hence, the CIA values are not consistent with the petrographic data. Furthermore, for other stratigraphic units, the CIA values do not reveal significant chemical weathering, which may be due to the high proportion of non-silicate carbonate, which may distort the CIA values. Because the CIA index is not representative of weathering in the studied samples, we used the ratios of Al_2O_3/Na_2O and TiO_2/Na_2O, which indicate the increasing proportion of kaolinite to primary plagioclase with increased chemical weathering (Roy et al., 2008). The highest Al_2O_3/Na_2O and TiO_2/Na_2O ratios (Table 3.1.3) were found in the Lower Cretaceous sandstones, indicating more intense chemical weathering during this time. The lower part of the Boukhchebat section (Lower Cretaceous) indicates more intensely weathered sediments compared to the upper part. Al_2O_3/Na_2O and TiO_2/Na_2O ratios of the Upper Cretaceous and the Early Eocene, including the Oligocene-Early Miocene (fine-grained sediments), exhibit variable weathering of

lower intensity than that of the Lower Cretaceous. There is a variation in Al_2O_3/Na_2O and TiO_2/Na_2O ratios may be due to the differential intensity of weathering during Upper Cretaceous, as reported by El Albani et al. (2009), based on clay mineral analysis of the Upper Cretaceous fine-grained sediments of the Tarfaya basin. The Miocene-Pliocene sediments exhibit Al_2O_3/Na_2O and TiO_2/Na_2O ratios that are more or less similar in both parts of the basin imply a similar distribution of intensely weathered sediments. The recent fine grained sediments have higher ratios than the coarse-grained sediments, which may be because fine-grained rocks represent more intense chemical weathering than coarse-grained rocks (McLennan et al., 1980; Faundez et al., 2002; Conception et al., 2012). In addition, the intensity of weathering in twenty-six weathered marl samples from different Upper Cretaceous weathering horizons within sections including the Miocene-Pliocene (drilled cores) were evaluated because they were exposed until the beginning of the Miocene-Pliocene and during the Miocene-Pliocene because of folding and uplifting of the Atlas Mountains (von Rad and Wissmann, 1982; Frozen de Lamotte et al., 2009; Ruiz et al., 2010). It was found that these horizons also underwent a moderate degree of chemical weathering.

3.1.5.3 Provenance over time

Lower Cretaceous: According to Dickinson's (1983) provenance discrimination scheme of the QFL triangular diagram, the Lower Cretaceous sandstones are derived from the cratonic interior settings, namely the West African Craton (Fig. 3.1.12). These cratonic sandstones indicate intensively weathered granitic and gneissic source rocks with higher K-feldspar content than that of plagioclase. In addition, quartz undulosity was useful for discriminating plutonic and metamorphic quartz (Basu et al., 1975). The high percentages of undulose quartz (always more than 78 %) in the Lower Cretaceous sandstones support plutonic derived sediments during this time.

Heavy minerals were also considered to infer probable provenance as these are good indicators (Morton et al., 1992; Morton and Hallsworth, 1994; Morton et al., 2004; Nechaev and Isphording, 1993). In the Lower Cretaceous sequence of the Tarfaya Atlantic marginal basin, zircon, tourmaline and rutile (ZTR) are the main heavy minerals, accounting for more than 90 %, with minor amounts of garnet and hornblende. These stable ZTR minerals are derived from granite or granitic gneiss of the Reguibat Shield (West African Craton, Fig. 3.1.12). Garnet and hornblende are probably derived from metamorphic rocks of the Mauritanides. Hence, the heavy mineral data are in agreement with petrographic and quartz undulosity which signify a cratonic provenance.

Upper Cretaceous to Oligocene-Early Miocene: Only fine-grained rocks, black shales and sandy marls were found and sampled from the Upper Cretaceous to Early Eocene, including the Oligocene-Early Miocene,

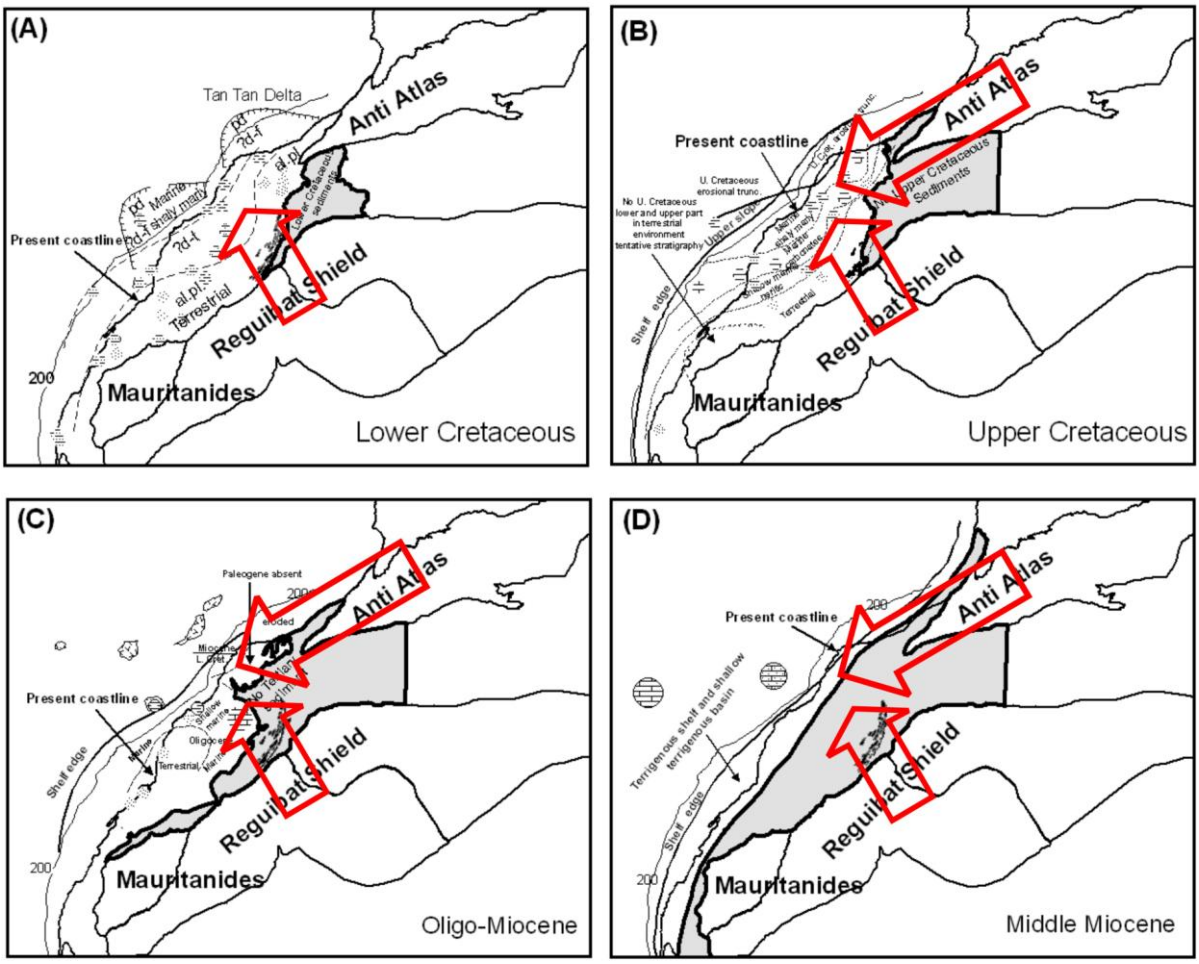

Fig. 3.1.12 Paleogeographic evolution of the Tarfaya basin (modified from Ranke et al., 1982): (A) Early Cretaceous, (B) Late Cretaceous, (C) Oligo-Miocene, (D) Middle Miocene. Present coastline and -200 m contour for comparison. Land-based part of the Tarfaya basin in grey and red arrow showing direction of sedimentation.

Oligocene-Early Miocene sandy marls were used to extract heavy minerals. ZTR was higher on average, possibly derived from the Reguibat Shield. Garnet, hornblende, epidote and sphene indicate the source as the metamorphic Mauritanides. Apatite grains are not indicative of a particular provenance and hence tectonic setting.

Miocene-Pliocene to recent: The Miocene-Pliocene sandstones and recent sediments are carbonate-rich arenites deposited in the shallow marine environment of the Atlantic passive margin. Three different approaches were used to infer the provenance of the Miocene-Pliocene siliciclastic sediments.

The first approach used the petrographic and QFL detrital modes of sandstones and sands. Medium- and coarse-sand-sized detrital quartz grains are derived from the

weathering of granites (Basu et al., 1975; Pettijohn et al., 1987; Datta, 2005), whereas fine-sand-sized grains are the product of breakage and chipping of large quartz grains (Dickinson, 1970). The polycrystalline quartz grains were most likely derived from a metamorphic source (Blatt, 1967). Additionally, rounded and well-rounded quartz grains are derived from a recycled sedimentary source (Basu et al., 1975; Pettijohn et al., 1987). Detrital K-feldspar grains were mainly derived from granite and gneiss (Datta, 2005), whereas plagioclase feldspar grains were derived from low-grade metamorphic rocks. Sedimentary rock fragments are the main rock fragments, including extrabasinal carbonate grains, indicating a sedimentary recycled source. The metamorphic rock fragments are, in minor quantity, derived from metamorphic rocks (Fig. 3.1.12). This points towards recycled orogenic and/or cratonic sources, which lie in the western Anti-Atlas and/or Reguibat Shield, including the Mauritanides (Fig. 3.1.12).

A second approach used heavy mineral analysis. The ZTR frequency is similar in the sandstones of the SW and NE parts of the basin, including recent sediments. The ZTR are derived from granite or granitic gneiss of the Reguibat shield and the Mauritanides. Garnet is present in variable amounts in both parts of the basin and hornblende was found as a dominant heavy mineral in both parts. These findings indicate that these heavy minerals are derived from low- and/or medium-grade metamorphosed pelitic rocks of the western Anti-Atlas and metamorphosed rocks of the Reguibat Shield and the Mauritanides (Fig. 3.1.12). Staurolite and apatite were also present in some samples, indicating that the sediments were derived from metamorphic rocks.

Finally, the third approach for the provenance analysis demonstrated that hornblende and garnet mineral chemistry are useful tools to discriminate between provenance rocks. In general, both amphiboles and garnets reveal that possible sources are low- to high-grade metamorphic rocks, which are derived from the Reguibat shield, including the Mauritanides and the western Anti-Atlas (Fig. 3.1.12). Further, the Miocene-Pliocene garnets from the SW and NE parts of the basin mainly contain Type B garnets with less dominance of Type A and Type D garnets. The Type D garnets were mainly found in the NE part of the basin with minor exceptions. Garnets from the Reguibat Shield and Mauritanides are dominated by Type A garnets, suggesting a high-grade metamorphic source, whereas garnets from the western Anti-Atlas are dominated by Type B and Type D garnets, indicating a low- to medium-grade metasedimentary and metacarbonate source.

In addition, three sand samples from recent sediments were also useful for discriminating source rocks. Sample # 06-01 lies in the NE part of the basin, Oued Draa, in which sediments are derived mainly from the western Anti-Atlas, contains

type B garnets, whereas sample # 14-01 from the SW part of the basin, Oued L' Craa, in which sediments are derived from the Mauritanides and or the Reguibat Shield, contains Type A garnets. Sample # 06-06 is from the middle part of the basin, Oued Chebeika, in which sediments are derived from the Reguibat Shield and the western Anti-Atlas, contains Type A and Type B garnets, indicating a mixed source. The hornblende and garnet minerals were derived from metamorphic and meta-sedimentary rocks. Calcic amphiboles are the main type of amphiboles derived from low- to medium-grade metamorphic sources.

In summary, petrographic and heavy mineral data indicate that, during the Lower Cretaceous, the main source was SW of the basin (West African Craton). According to Hafid et al. (2008) and Frizon de Lamotte et al. (2009), the Uplift began in the Atlas system as early as the Late Cretaceous due to convergence between the African and Eurasian plates, and sedimentation began from the western Anti-Atlas to the basin. Although, the fine-grained siliciclastics from the Upper Cretaceous to Oligocene-Early Miocene were not useful for determining provenance due to limitations of significance of provenance. However, Miocene-Pliocene siliciclastics support mixed sources from the Reguibat Shield and the Mauritanides in the SW of the basin and the western Anti-Atlas in the NE of the basin.

3.1.6 Summary and conclusions

The Lower Cretaceous to recent sediments of the Tarfaya basin from SW Morocco are carbonate-rich arenites. During the Lower Cretaceous, the Reguibat Shield and metamorphosed Mauritanides were the dominant sources of these sediments. During the Miocene-Pliocene, sediments were derived from mixed sources, which lie in the SW and NE of the basin, i.e., the Reguibat shield and metamorphic Mauritanides and the western Anti-Atlas, respectively.

The petrographic data for the studied area suggest that the Lower Cretaceous sandstones are subarkosic in composition, while the Miocene-Pliocene sandstones and the recent sediments are carbonate-rich feldspathic or lithic arenites. The geochemical classification of these siliciclastics is in agreement with petrographic findings.

Different discrimination diagrams of tectonic settings based on major element geochemical compositions suggest that the Lower Cretaceous to recent sediments were deposited at the tectonically stable passive Atlantic continental margin of NW Africa. These findings are also supported by a tectonic settings discrimination diagram of heavy mineral data.

Al_2O_3/Na_2O and TiO_2/Na_2O ratios are useful in the present study to constrain the intensity of weathering. The chemical weathering was higher during the Lower

Cretaceous. The weathering was lower and variable since Upper Cretaceous to Miocene-Pliocene and recent time, including weathered marls (Upper Cretaceous and Miocene-Pliocene).

Petrographic, quartz undulosity and heavy mineral data suggest that the Lower Cretaceous siliciclastics were mainly derived from the Reguibat Shield and Mauritanides sources (West African Craton). The Miocene-Pliocene siliciclastics indicate a mixed source from the Reguibat Shield, the Mauritanides and the western Anti-Atlas. These Miocene-Pliocene sources are also supported by amphibole and garnet mineral chemistry. Hence, the West African Craton was the main source of siliciclastics until the beginning of the Upper Cretaceous. The contribution of siliciclastics from the western Anti-Atlas possibly began during the Upper Cretaceous, but fine-grained siliciclastics do not provide clear evidence of these mixed sources. However, the Miocene-Pliocene rocks and recent sediments confirm mixed sources, both the West African Craton and western Anti-Atlas.

3.1.7 Acknowledgements

We thank RWE Dea for funding this project. We also thank ONHYM for supporting, organizing and accompanying the field campaign in March-April, 2009 and drilling in September-December, 2009. Dr. Peter Appel, Institute of Geosciences, University of Kiel, is thanked for his support in the geochemical analytical work.

Chapter 3 Results

3.2 The provenance of Cretaceous to Quaternary siliciclastic rocks in the Tarfaya basin, marginal Atlantic, SW Morocco: evidence from trace element geochemistry and radiogenic Nd-Sr isotopes[a]

Sajid Ali[1], Karl Stattegger[1], Dieter Garbe-Schönberg[1], Martin Frank[2], Steffanie Kraft[2], Wolfgang Kuhnt[1]

[1]Institute of Geosciences, Christian-Albrechts-University, D-24118 Kiel, Germany

[2] GEOMAR | Helmholtz-Zentrum für Ozeanforschung, Wischhofstrasse 1-3 Kiel, Germany

Abstract

We present trace element geochemical compositions including rare earth elements (REE) and radiogenic Nd-Sr isotope analyses of Lower Cretaceous to Miocene-Pliocene and recent siliciclastic sediments of the Tarfaya basin, SW Morocco, in order to identify depositional tectonic settings, source rocks composition and sediment provenance. The analyzed data suggest that the sediments originate from heterogeneous source areas in the Reguibat Shield (West African Craton) and from the Mauritanides, as well as the western Anti-Atlas, which probably form the basement in this area. The La/Y-Sc/Cr binary and La-Th-Sc ternary relationships suggest that the Tarfaya basin sediments were deposited in passive margin depositional settings. Low concentrations of Cr (<150ppm) and Ni (<100ppm) and their correlation suggest that the sediments of the Tarfaya basin are derived from felsic sources. This is supported by trace element ratios of La/Sc, Th/Sc, Cr/Th and Th/Co that are similar to those of sediments derived from felsic source rocks. Moreover, chondrite-normalized REE patterns with light rare earth elements (LREE) enrichment, a flat pattern of heavy rare earth elements (HREE), and negative Eu anomalies can also be attributed to a felsic rock source for the Tarfaya basin sediments.

The similar Sm/Nd (0.18-0.20) ratios for all analyzed sediments in both coarse- and fine-grained siliclastics indicate that no significant fractionation of Sm and Nd occurred during the formation of the Tarfaya basin sediments due to depositional and post-depositional processes. Low $^{143}Nd/^{144}Nd$ ($\varepsilon Nd(0)$ =-10.6 to -25.5) and high

$^{87}Sr/^{86}Sr$ (0.714 to 0.846) ratios suggest a predominance of old upper crustal sources. The Nd isotope model ages (T_{DM}=2.1-2.2 Ga) of the Lower Cretaceous sediments suggest that sediments were exclusively derived from the Eburnean terrane (West African Craton). On the other hand, Upper Cretaceous to Miocene-Pliocene sediments show younger model ages (T_{DM}=1.7-1.9 Ga) indicating an origin from both the West African Craton and the western Anti-Atlas. In contrast, the southernmost studied Sebkha Aridal section (Oligocene to Miocene-Pliocene) yields a provenance age (T_{DM}=2.5 Ga) indicating that these sediments are dominantly derived from the Archean terrane (West African Craton).

[a]This article is submitted in Journal of Geochemistry, Geophysics, Geosystems.

3.2.1 Introduction

Siliciclastic sedimentary rocks contain important information about changes in the supply of material from different sources, and geochemical analyses have proven to be a powerful tool for studying the signature of tectonic settings, the composition of the source area, and the provenance of the sediments (Wronkiewicz and Condie, 1987; McLennan, 1989; Taylor and McLennan, 1985; McLennan and Taylor, 1991; McLennan et al., 1993; Roddaz et al., 2011). However, the chemical composition of sedimentary rocks can be modified by chemical weathering and sorting processes during transport, sedimentation and post-depositional diagenesis (Nesbitt et al, 1980; Nesbitt and Young, 1982; Middleburg, 1988; Nesbitt et al., 1996). Nevertheless, the distribution of selected immobile trace elements, such as Zr, Hf, Sc, Y, Cr, Th and Co and the rare earth elements (REE), can be used to discriminate the tectonic settings and provenance of these rocks (Taylor and McLennan, 1985; Bhatia and Crook, 1986; McLennan, 1989; Zimmermann and Bahlburg, 2003; Amstrong-Altrin et al., 2004). Further, Sm-Nd isotope model ages of the sedimentary rocks are more useful for distinguishing between various sources and their average crustal residence ages (e.g., McCulloch and Wasserburg, 1978; O'Nions et al., 1983; McLennan et al., 1990; McDaniel, 1994; Zimmermann and Bahlburg, 2003; Wade et al., 2005; Xie et al., 2012). Hence, these studies performed in combination are important for constraining tectonic settings and source area characteristics of sedimentary rocks.

No provenance studies have, so far, been based on the geochemistry and Nd-Sr isotopes of the Tarfaya basin sediments, Morocco. Earlier studies in the Tarfaya basin were based on fine-grained sediments from the Upper Cretaceous and were focused on the understanding of the intensity of anoxia, the magnitude and nature of the $\delta^{13}C$ excursion, the biotic effects on benthonic and planktonic foraminifera, biostratigraphic records and paleo-environmental evolution (e.g. El Albani et al., 1999; Kuhnt et al., 1997, 2005, 2009; Kolonic et al., 2005; Mort et al., 2007, 2008; Keller et al., 2008 and Gertsch et al., 2010). In the present study, we present results obtained from the Lower Cretaceous to recent siliciclastic rocks from key sections of the coastal cliffs and sebkhas between Boujdour and Oued Chebeika and the upper sections of four newly drilled cores. We use trace element geochemistry including studies of rare-earth elements (REE) and Nd-Sr isotopes in order to decipher tectonic settings, source rock composition and changes in provenance with time.

3.2.2 Geological background

The evolution of the Tarfaya basin has been closely connected with the geological history of the African Craton and the opening of the Atlantic Ocean (Ranke et al.,

1982), with development from a rift to a marginal basin. The basin is filled by Mesozoic and Cenozoic continental to shallow marine sediments overlying a basement of Precambrian and/or Paleozoic age. According to Choubart et al. (1966), Auxini (1969), and Dillon and Sougy (1974), Triassic evaporites, redbeds, reddish sandstone, conglomerates and volcanic rocks overlie either metamorphic or folded rock sequences of the Mauritanides (ages 3.04-2.83 Ga) or crystalline rocks of the Precambrian Reguibat Massif. The Early Jurassic marine carbonates transgressed onto the Triassic rift sediments and/or evaporate. Silty sandstone, limestone, dolomitic limestones, and dolomites of Lower to Middle Jurassic are overlain by Upper Jurassic neritic marly limestone and calcarenites, intercalated with marls, shales and sandstones. A thick deltaic sequence, during the Early Cretaceous, accumulated during and after a major global Valanginian regression (Vail et al., 1977). According to Ratschiller (1970), the shallow-marine from the Upper Cretaceous to the Early Eocene unconformably overlies the continental Lower Cretaceous formations. Late Oligocene to Early Miocene basin development shows an erosional hiatus because of the coincidence of a major regression with intensified slumping, canyon incision, and bottom water circulation (Arthur et al., 1979), with only little continental deposition taking place. After this long period of non-deposition or erosion, Miocene-Pliocene sediments unconformably overlay the Lower Cretaceous (Tan Tan formation), Upper Cretaceous (NE part of the basin), Early Eocene and Oligocene (SW part of the basin) deposits. Following the Miocene-Pliocene, siliciclastic sediments once again started to be deposited both on- and off-shore with uplift events in the Anti-Atlas (de Lamotte et al., 2009; Ruiz et al., 2010).

In the present study, various sections, cropping out in the Sebkhas and along the shoreline from the Lower Cretaceous to recent time (SW and NE parts of the basin) have been logged and investigated together with four newly drilled cores. The location of the various sections and drilled cores are shown in Fig. 3.1.1 and sample positions within sections are given in Fig. 3.1.2a and b. The Lower Cretaceous Boukhchebat section crops out in the NE part of the basin consisting of coarse sandstones intercalated with sandy marls and shales. The Upper Cretaceous rocks mainly exposed in the NE part of the basin consist of black shales and sandy marls intercalated with chert and nodular limestone or just limestone. The Early Eocene deposits occur in the SW part of the basin and consist of black shales and sandy marls intercalated with cherts and limestones. The Oligocene-Early Miocene sandy marls have been sampled from the Sebkha Aridal section. The Miocene-Pliocene siliciclastic deposits consist of coarse or conglomeratic sandstones together with lumachelle in the lower part and sandstones intercalated with sandy marls and

limestones. Recently deposited sand samples have also been collected from various wadis and dunes.

3.2.2.1 Potential source areas surrounding the Tarfaya basin

The Tarfaya basin is located at the margin of the western Atlantic and has been filled by sediments of the Reguibat Shield (West African Craton, WAC) including the Mauritanides and the western Anti-Atlas (Michard et al., 2008). The WAC basement exposed in the Reguibat shield consists of two contrasting deformational ages in crustal domains, namely a western Archean terrane and an eastern Eburnean terrane. According to Lahondere et al. (2003), the western Archean terrane is dated 3.04-2.83 Ga from the presence of intrusive granitoids, whereas rocks of the eastern Eburnean terrane are younger than those of the western terrane, i.e., 2.12-2.06 Ga (Schofield et al., 2006; Schofield and Gillespie, 2007). The western Anti-Atlas consists of sediments that are mainly derived from various Precambrian inliers and or West African Craton. According to de Lamotte et al. (2009) and Ruiz et al. (2010), sedimentation to the Tarfaya basin from the western Anti-Atlas started during the middle-Late Upper Cretaceous as a consequence of uplifting and erosion attributable to the convergence of the African and Eurasian plates. In addition, Sehrt et al. (2011) have also suggested that the Tarfaya basin is filled by mixed provenance sources based on apatite fission track ages (AFT) and zircon (U-Th-Sm)/He dating (ZHe).). The Lower Cretaceous rocks are characterized by older ages (2.04±0.04 to 2.87±0.04 Ga) indicating sources from the West African craton while Upper Cretaceous and younger sediments show a considerable admixture of younger ages (1.72±0.12 to 1.85±.14 Ga) derived from the western Anti-Atlas.

The petrography, major elements geochemistry and heavy mineral and mineral chemistry (hornblende, garnet) of the siliciclastics of the Tarfaya basin indicate a passive margin depositional setting and differential sources for the Lower Cretaceous and the Miocene-Pliocene sediments (Chapter 3.1). The petrographic and heavy mineral data are indicative of cratonic source for the Lower Cretaceous sediments of the Tarfaya basin. On the other hand, Miocene-Pliocene sediments of the basin indicate that the sediments are derived from mixed sources. The hornblende and garnet geochemistry further suggest that the Miocene-Pliocene sediments are derived from high-grade metamorphosed Mauritanides and low-grade metamorphosed western Anti-Atlas source rocks. However, the fine-grained sediments from the Upper Cretaceous to the Early Eocene provide limited information about provenance. The trace element geochemical compositions including REE and radiogenic Nd-Sr isotopic data obtained in the present study

provide new and independent information to constrain the depositional tectonic settings, source rock composition and provenance of the Tarfaya basin sediments.

3.2.3 Materials and Methods

In total, 110 samples from 16 stratigraphic sections from SW and NE parts of the Tarfaya basin and four newly drill cores as well as recent sediment samples from wadis were selected for trace element analysis. Furthermore, 40 selected samples were also used for Nd-Sr isotopes analysis. The locations of the selected samples in sections and drill cores are shown in Fig. 3.1.1 and 3.1.2.

The samples were carefully cleaned for geochemical analysis after removing weathered coatings and veined surfaces. These samples were broken into small pieces of about 4 mm in size by a pestle. These small pieces were air-dried and powdered to <200 mesh by using an agate mill.

After crushing, pulverization and homogenization of the solids, 150 mg powder of each sample was first dissolved in dilute HNO_3 in Teflon vials to remove excess carbonate before commencement of the digestion process. In the second step, a mixture of concentrated sub-boiled HNO_3-HCl-Hf (3:1:4) was used for first-step dissolution overnight at 160°C. After evaporation of the resulting digest solution nearly to dryness, a pressure bomb step was used for the complete dissolution of the heavy minerals. Concentrated HNO_3 and HF (1:4) were added and the bombs (Parr bombs) were heated for 4 days at 160°C. In the final step, perchloric acid was added and then evaporated nearly to dryness. The residue was re-dissolved in dilute HNO_3 (1:4) and made up to a final volume of 50 ml. This analytical work was performed at the Institute of Geosciences, University of Kiel, Germany. A total of thirty seven trace elements were analyzed using inductively coupled plasma mass spectrometry (ICP-MS, Agilent 7500cs). Details of sample preparation techniques and calibration strategies are given by Garbe-Schönberg (1993). The accuracy and precision of the method was monitored with control samples and duplicates and by running USGS international rock standards G-2, BHVO-2, and AC-E. The error of replicate analyses is better than 5% for all analyzed trace elements

Nd-Sr isotope measurements were carried out on a Multi-Collector ICP-MS (Nu Plasma), GEOMAR Kiel, Germany. For isotope analysis, 150 mg powder of each sample was first dissolved in dilute HNO_3 in PFA (perfluoralkoxy, Savillex TM) vials to remove excess carbonate before initiation of the digestion process. In the second step, samples were completely digested by using a mixture of concentrated HF-HNO_3-$HCLO_4$. The separation and purification of Nd and Sr from the totally digested samples followed previously published procedures for Nd (Barrat et al., 1996; Cohen

et al.; 1988; Le Fevre and Pin, 2005) and Sr (Bayon et al., 2002; Horwitz et al., 1992). $^{143}Nd/^{144}Nd$ ratios were mass-bias-corrected to $^{146}Nd/^{144}Nd=0.7219$ and were then normalized to the accepted value of the JNdi-1 standard of 0.512115 (Tanaka et al., 2000). Repeated measurements of the JNdi-1 standard over a period of several months gave a long-term reproducibility of ±0.35 (2σ). Procedural Nd blanks were ≤25 pg. Measured Sr isotope ratios were interference (^{86}K, ^{87}Rb) and mass bias corrected (using $^{86}Sr/^{87}Sr= 0.1194$, Steiger and Jäger, 1977), $^{86}Sr/^{87}Sr$ results were normalized to that of NIST NBS987 = 0.710245, which was measured between samples. The 2σ external reproducibility during the measurements for this study was ±0.00004. Procedural Sr blanks were less than 0.7 ng.

3.2.4 Results

3.2.4.1 Major elements

All the studied siliciclastics from the Lower Cretaceous to recent (Table 3.1) have a wide range of SiO_2 (5.9-84.5%, average 43.1%), Al_2O_3 (1.3-20.9, average 4.7%), TiO_2 (0.07-0.86, average 0.33%), Fe_2O_3+MgO (0.3-21.7, average 6.2%), K_2O (0.2-3.7%, average 1.4) and Na_2O (0.1-6.9, average1.2%). The significant enrichment of CaO (up to 59.7%) and LOI (up to 43.8%) is related to the high carbonate content. The petrographic data from the Lower Cretaceous, Miocene-Pliocene and recent sediments also support the high carbonate content of the studied siliciclastics (Ali et al., in review). A marked negative correlation has been noted between SiO_2-CaO (r=-0.83) and SiO_2-LOI (r=-0.94) as a consequence of a “closed data set” (i.e., the sum of all components is always 100%). The highly significant correlation, however, provides some evidence that both the detrital and the matrix carbonates in the sediments are of primary rather than secondary origin, because the influence of secondary carbonate could result in SiO_2-CaO scatter (Feng and Kerrich 1990; Gu 1994). The SiO_2/Al_2O_3 and K_2O/Na_2O ratios are highly variable and range from 2.2 to 32.0 (average12.4) and 0.13 to17.6 (2.1), respectively.

3.2.4.2 Trace elements

Trace element composition including REE of coarse-grained (sandstones and sands) and fine-grained rocks (black shales and sandy marls) from the Lower Cretaceous to recent in the Tarfaya basin are given in Table 3.2.1. In addition, one carbonate sample from Upper Cretaceous and one from Miocene-Pliocene lumachelle have also been analyzed to check the comparative trace element concentration and variation in these samples. All trace element data have been normalized to average Upper Continental Crust (UCC, Taylor and McLennan, 1985; McLennan, 2001) and

compared with Post-Archean Australian shale (PAAS, Taylor and McLennan, 1985) in Fig. 3.2.1. In the spider diagrams, UCC-normalized trace elements are arranged in order of increasing atomic number. The concentration of trace elements is variable and most of the elements have a lower abundance than that of UCC (Fig. 3.2.1).

3.2.4.2a Large-ion lithophile elements (LILE, Rb, Cs, Ba, Sr), Th, U

The concentration of LILE in the analyzed samples is variable (Table 1). Most of the analyzed samples from various stratigraphic units are moderately to strongly depleted in LILE (Table 3.2.1 and Fig. 3.2.1) when compared with UCC and PAAS. The alkali element Rb is highly variable and ranges from 11 to 133 ppm, with Cs varying from 0.88 to 3.0 ppm. The average abundance of Ba (402 ppm) is higher in the Lower Cretaceous sandstone samples than in other analyzed samples. The Sr concentration, on average, in fine-grained siliclastics from the Upper Cretaceous and the Early Eocene is 508 ppm and 402 ppm, respectively, and relevant values for the recent sediments (414 ppm) are higher than those of other siliciclastic rocks in other stratigraphic units. When Sr is correlated with CaO content, we have found that the Sr content in fine-grained siliciclastics is highly correlated, with Sr-CaO (r=0.91), but is only weakly correlated in coarse-grained siliclastics (r=0.21). Hence, the higher correlation between Sr and CaO in fine-grained siliciclastics indicates their contribution mainly from sea water/marine carbonate in equal proportion.

The positive correlations between K-Rb (r=0.94), K-Cs (r= 0.81) and K-Ba (r=0.51) provide evidence that K-bearing clay minerals (illite, muscovite and biotite) primarily control the abundance of these elements (McLennan et al., 1983; Feng and Kerrich, 1990). All studied samples show high positive correlations between Al_2O_3-Rb (0.90), Al_2O_3-Cs (r=0.96) and Al_2O_3-Ba (r=0.39) further supporting the idea that the distribution of these elements is controlled by phyllosilicates (Bauluz et al., 2000).

The Th concentration is low when compared with those of other trace elements and with UCC. Uranium is highly variable (0.4 ppm to 28 ppm) and the highest value was found in black shale sample #C1-35 (110 ppm, Table 3.2.1). In general, fine-grained siliciclastics are enriched in U, but coarse-grained siliciclastics are depleted as compared with UCC. The poor correlation between Th-U (r=0.17) indicates different redox geochemical behavior. The Th/U ratios are found to be much lower than UCC in all studied samples (Table 3.2.1). This may be attributable both to the lower concentration of Th and/or the higher concentration of U.

3.2.4.2b High field strength elements (HFSE, Zr, Hf, Y, Nb, Ta)

HFSE are preferentially partitioned into melts during crystallization and anatexis (Feng and Kerrich, 1990), and as a result, these elements are enriched in felsic

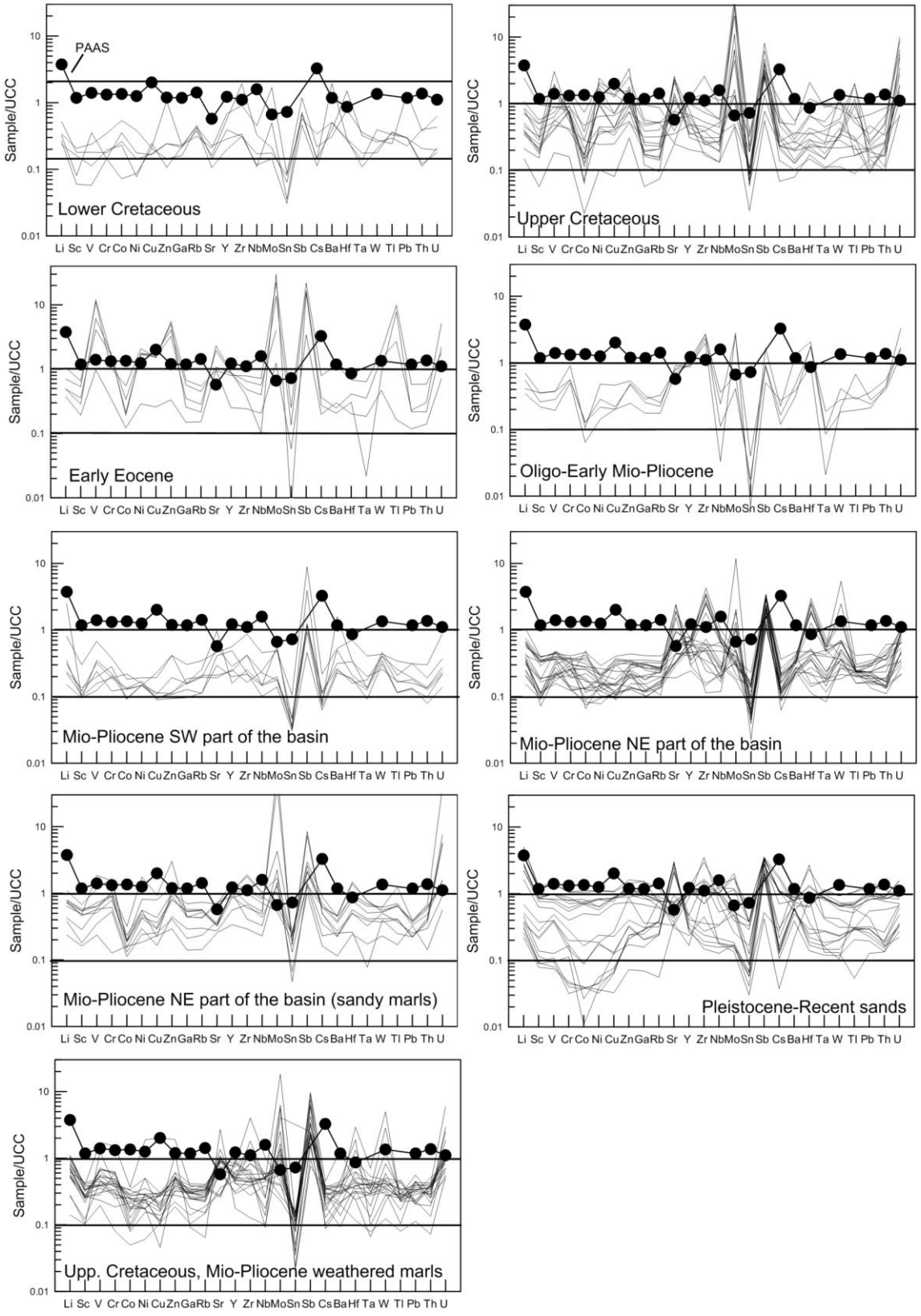

Fig. 3.2.1 Trace element concentration of the siliciclastic samples from Lower Cretaceous to recent in the Tarfaya basin normalized to the composition of average UCC (Taylor and McLennan, 1986; McLennan, 2006).

rather than mafic rocks. Because of their immobile characteristics, these elements are considered as a good provenance indicator, together with REE (Taylor and McLennan, 1985).

The average concentration of HFSE is depleted when compared with UCC and PAAS, except for some elements in a few samples (Fig. 3.2.1). Zr and Hf are variably concentrated in the diverse stratigraphic units and are highly enriched in the Oligocene-Early Miocene sandy marls and Miocene-Pliocene (NE part of the basin) sandstone samples. These Oligocene-Early Miocene and Miocene-Pliocene stratigraphic units show average concentrations of Zr of 460 ppm and 253 ppm and of Hf of 9.4 ppm and 5.6 ppm, respectively. The Y abundance is higher in the sandy marls of Miocene-Pliocene stratigraphic unit (Core 1). The average concentrations of Ta and Nb are higher in the recent sediments at 8.0 ppm and 0.56 ppm, respectively.

The high correlation between Zr-Hf (r=0.99) highlights their similar behavior throughout the stratigraphic units of the Tarfaya basin sediments. The Zr/Hf ratio in all the analyzed siliciclastics ranges from 24 to 51 (average 40), excluding two samples having higher ratios 70 (sample #16-10) and 82 (sample # C1-09), and implies that these elements are controlled by zircon. The average Zr/Hf ratios in siliciclastic rocks of different stratigraphic units are higher when compared with UCC (32.8, Taylor and McLennan, 1985), indicating that these higher ratios are possibly the result of recycling in the source area/s.

In addition, Zr is positively correlated with Zr-Yb (r=0.59). The less significant correlation of heavy rare earth elements as a group (∑HREE, r=0.30) reflects that not all the HREEs are controlled by Zr abundance.

3.2.4.2c Transition metal trace elements (TTE, Cr, V, Co, Ni, Sc)

The first-row transition metals Cr, V, Co, Ni and Sc generally behave similarly as highly compatible elements during magmatic fractionation processes, being enriched in mafic to ultramafic rocks. However, during weathering, they might be mutually fractionated (Feng and Kerrich, 1990).

The average abundance of the transition trace elements is variable and lower than in UCC. The fine-grained siliciclastics from the Upper Cretaceous and the Early Eocene are more concentrated in Cr, V and Ni, being higher than in UCC. This may be attributable to enrichment together with the organic matter and the formation of secondary minerals. Co and Sc show variable abundance and higher values are found in recent sediments from wadis than in sediments from dunes in which they occur as a minor proportion (Table 3.2.1).

The most significant correlations exist between K-Sc (r=0.76), K-Co (r=0.49), Al_2O_3-Sc (r=0.94) and Al_2O_3-Co (r=0.81) suggesting that they are controlled by weathering

and concentrated in the phyllosilicates. Cr, V and Ni are more scattered and less correlated with K_2O and Al_2O_3 indicating that varied factors control the distribution of these elements. Furthermore, the Cr, V and Ni elemental concentration is higher in the fine-grained siliciclastics, especially in black shales, indicating that their higher concentration is attributable to organic matter. These elements are evidently enriched under anoxic conditions. These anoxic conditions are already discussed by Kuhnt et al. (1997, 2005 and 2009). On the other hand, no evidence has been found of a contribution of these elements from ultramafic source rocks as all other elements distribution and their ratios indicate the felsic composition of the source rocks.

3.2.4.2d Rare earth elements (REE)

The concentration of REE is given, separately, in Table 3.2.2, and chondrite-normalized REE patterns are shown in Fig. 3.2.2 together with the comparative pattern of PAAS. All analyzed coarse- and fine-grained siliciclastics from the Lower Cretaceous to the recent time have variable concentrations. Moreover, we have found that these elements are less abundant when compared with UCC and PAAS because of high carbonate contents (Taylor and McLennan, 1985). The highest variation is seen when comparing sands from wadis (average 150 ppm) with sands from dunes (average 37 ppm). This variation in average concentration is because of grain size effect. In general, chondrite-normalized REE patterns for the various stratigraphic units appear similar (Fig. 3.2.2) and are characterized by high LREE/HREE ratios, an almost flat HREE pattern and pronounced but variable Eu anomaly. There is no significant difference in the REE pattern among all analyzed samples of the different stratigraphic units (Fig. 3.2.2). Most patterns are similar to PAAS indicating their derivation from post-Archean upper continental crust (Taylor and McLennan, 1985). Their variation in absolute concentration reflects mostly the variation in the grain size. However, systematic variations are present in the distribution of HREE (Dy to Lu).

The analyzed samples have Eu/Eu* values lying within the range of 0.60-0.81 except in samples # 27-28 (0.92, Lower Cretaceous), 17-37(0.84, Early Eocene) and 06-06 (0.91, recent sediments). This range of Eu/Eu* anomaly is exclusively indicative of felsic composition in the source area/s. The La/Sm (indicating LREE slope), Gd/Yb (HREE slope) and La/Yb (LREE-HREE slope) ratios are present in the range of to and to respectively. The Y/Ho ratios vary from 1.8 to 3.3 with an average of 2.4, which is close to that of UCC. However, most of the fine-grained siliclastics show a slightly higher ratio of Y/Ho than is found in UCC, indicating a contribution of these elements from marine carbonate (Bau et al., 1995; Bau, 1999).

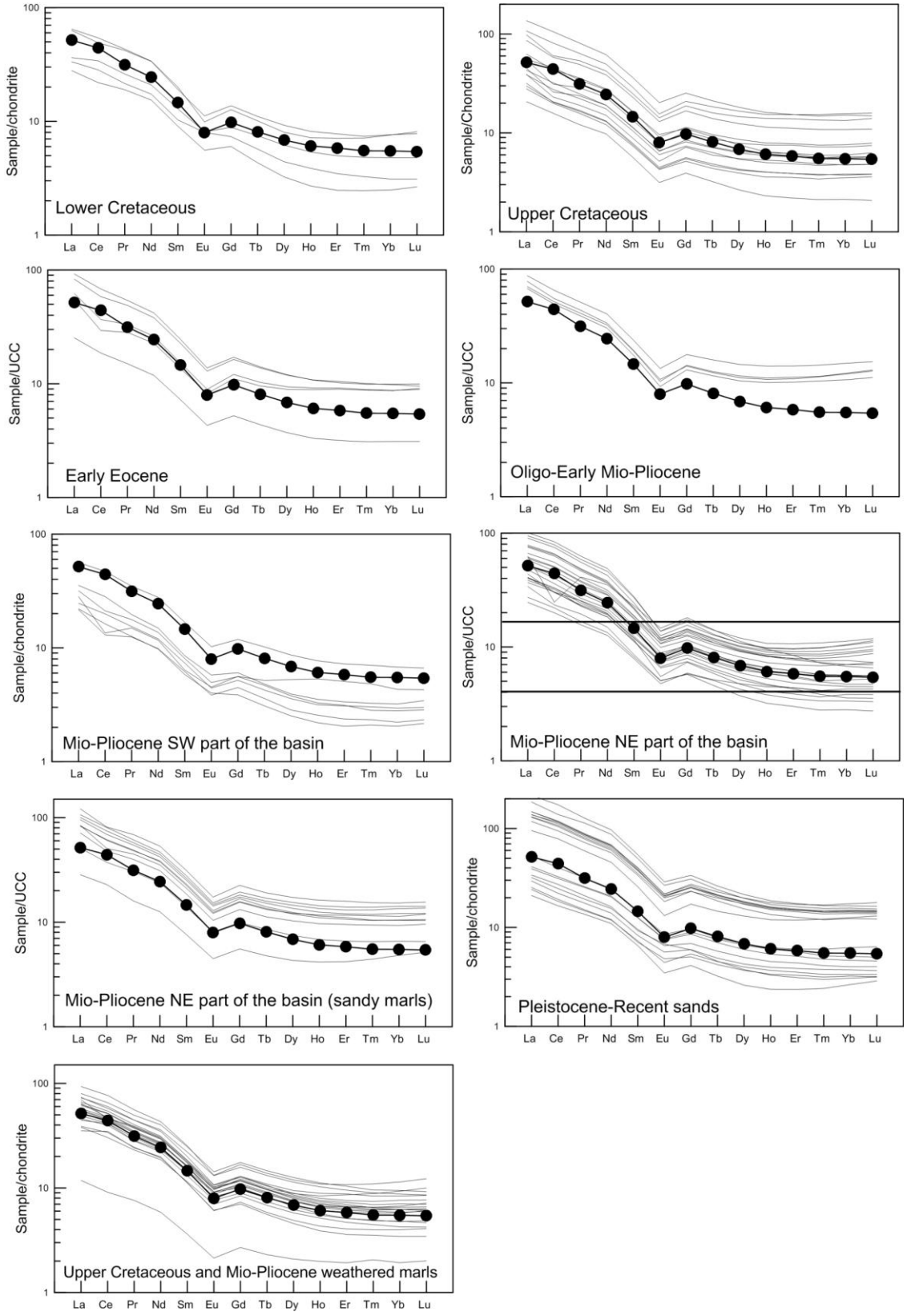

Fig. 3.2.2 Chondrite normalized REEs patterns of the siliciclastic samples from Lower Cretaceous to recent in the Tarfaya basin.

In addition, a weak positive correlation between Zr-HREE (r=0.42) indicates that HREE fractionation is only in part controlled by the occurrence of zircon; this is further supported by a weak negative correlation of Zr-$(Gd/Yb)_N$ (r=-0.41) (where the subscript 'N' refers to chondrite-normalized abundances) correlation. Zircon is typically enriched in HREE resulting in values <1 for $(Gd/Yb)_N$. This is in contrast to the average HREE distribution in UCC rocks having $(Gd/Yb)_N$ >1. Both LREE and HREE show a high positive correlation with LREE-Al_2O_3 (r=0.88) and HREE-Al_2O_3 (r=0.80) and with LREE-TiO_2 (r=0.90) and HREE-TiO_2(r=0.87) but a weak correlation with LREE-P_2O_5(r=0.12) and HREE-P_2O_5 (r=0.0.26). All these correlations indicate the variable influence of alumosilicates such as phyllosilicates and zircon, but no control of phosphate minerals, which are highly enriched in REE.

3.2.4.3 Sm-Nd isotopes

The data for the $^{143}Nd/^{144}Nd$ isotopic composition of 40 samples are given in Table 3.2.3 and the calculated provenance ages (T_{DM}) against the various stratigraphic units are illustrated in Fig. 3.2.7. Although Sm (0.87 to 8.3ppm) and Nd (4.6 to 45ppm) values are lower than UCC and PAAS, $^{147}Sm/^{144}Nd$ ratios in the sediments (0.1081 to 0.1244) are equivalent or slightly higher than typical terrigenous sediments (0.105 to 0.115; Taylor and McLennan, 1985). One carbonate sample showing the lowest concentration for both Sm (0.13ppm) and Nd (0.72ppm), however the ratio, Sm/Nd=0.18, is still consistent with terrigenous sediments.

A total of four analyzed sandstone samples of the Lower Cretaceous from the Boukhchebat section show ranges in $\varepsilon_{Nd}(0)$ values from -15.7 to -19.2 and have an average value of -17.1, $^{147}Sm/^{144}Nd$ ratios of 0.1080, T_{CHUR} ages of 2.0 Ga, T_{DM} ages 2.2 of Ga (Table 3.2.3).

Eight fine-grained samples from the Upper Cretaceous exhibit $\varepsilon_{Nd}(0)$ values in the range between -14.1 to -15.0 (average 14.6) and similar provenance (T_{DM}) ages (1.8 to 1.9, average 1.8 Ga). Further, three fine-grained Early Eocene samples also have similar $\varepsilon_{Nd}(0)$ values in the range -14.4 to -14.7 (average -14.3) and, hence, have model ages equivalent to those from the Upper Cretaceous sediments. In addition, one carbonate sample shows a more radiogenic $\varepsilon_{Nd}(0)$ value (-12.0) and a slighty younger T_{DM} age (1.6 Ga) compared with other fine-grained samples.

Because of their similarity, the Nd isotope data of Oligocene-Early Miocene (lower Part) and Miocene-Pliocene (upper part) in the Sebkha Aridal section are discussed together. Two sandy marl samples from the lower part of the section (Oligocene-Early Miocene) and one sandstone sample from the upper part of this section (Miocene-Pliocene) yielded the most negative $\varepsilon_{Nd}(0)$ values ranging from -23.1 to -25.6 with an average of -24.2. These samples have $^{147}Sm/^{144}Nd$ ratios ranging from

0.108 to 0.117 (average = 0.113). The slight variability observed in the $^{147}Sm/^{144}Nd$ ratios is possibly attributable to grain-size effects (McLennan et al., 1993, Meyer et al., 2011). The T_{DM} ages calculated from these samples are the oldest among all the studied siliciclastics, ranging from 2.5 Ga to 2.6 Ga (average 2.5 Ga).

Sandstone samples of the Miocene-Pliocene from both parts of the basin show a range of $\varepsilon_{Nd}(0)$ from -12.1 to -13.0 (average -12.6) in the SW part and -12.6 to -17.6 (average -14.8) in the NE part of the basin. However, the average T_{DM} ages at nearly 1.8Ga are similar in both parts of the basin. One sample from drill core-4 (sample #C4-03) yielded a more positive $\varepsilon_{Nd}(0)$ value of -9.8 and, hence, a younger T_{DM} age of 1.5 Ga, which is possibly due to a contribution from other younger source areas.

Four samples of recently deposited sands from wadis provide variable $\varepsilon_{Nd}(0)$ values ranging from -13.9 to -19.3 (average -16.3). The T_{DM} ages consequently range from 1.7 to 2.2 Ga. The southernmost sample (# 14-01) exhibits the oldest T_{DM} age (2.2) among the four recent sediment samples. In addition, one Pleistocene sand sample has an $\varepsilon_{Nd}(0)$ value of -10.6, which is again more positive compared with the other sand samples and yields a younger provenance age of 1.5 Ga.

In order to determine the direct effect of weathering processes on the obtained Nd-isotope compositions, three samples, one Upper Cretaceous weathered marl sample from the Onhym quarry and two Miocene-Pliocene weathered marl samples from drilled cores), have been analyzed. The weathered marls exhibit $\varepsilon_{Nd}(0)$ values ranging from -13.0 to -13.7 (average −13.4), a similar $^{147}Sm/^{144}Nd$ ratio (0.20), T_{CHUR} ages from 1.3 to 1.4 Ga (1.4 Ga on average) and T_{DM} ages varying from 1.7 to 1.8 Ga (1.8 Ga on average). The T_{CHUR} and T_{DM} ages obtained from weathered marls are compatible with the Upper Cretaceous and Miocene-Pliocene provenance ages implying that weathering process did not significantly alter the Nd isotope compositions and hence the model ages.

3.2.4.4 Rb-Sr isotopes

Fourty samples from various stratigraphic units were also analyzed for their radiogenic Sr isotope composition (Table 3.2.4). The Lower Cretaceous sandstone samples show higher $^{86}Sr/^{87}Sr$ values, ranging from 0.8027 to 0.8461, than the other younger sediments. In the Upper Cretaceous stratigraphic unit more variable, but less radiogenic $^{86}Sr/^{87}Sr$ ratios have been found including those of the Upper Cretaceous (average 0.7285), Early Eocene (0.7268), Oligocene-Early Miocene and Miocene-Pliocene (0.7309, Sebkha Aridal section), Miocene-Pliocene SW part of the basin (0.7369), NE part of the basin (0.0.7316) recent and Pleistocene sediments (0.7289) and weathered marls (0.7327). The calculated $^{86}Sr/^{87}Sr$ compositions at stratigraphic age (I_{Sr}) are also highly variable ranging from 0.7976 to 0.8398 during

the Lower Cretaceous and 0.7140 to 0.7523 from the Upper Cretaceous to the recent time.

According to McLennan et al. (1993) $f^{Sm/Nd}$ is the fractional deviation of the $^{147}Sm/^{144}Nd$ from that in chondritic meteorites ($f^{Sm/Nd}$= ($^{147}Sm/^{144}Nd$sample/ ($^{147}Sm/^{144}Nd$) chondrite-1) and monitors the general extent of differentiation. The studied sediments of the Tarfaya basin show a narrow range of $f^{Sm/Nd}$ from -0.35 to -0.45 (Table 3.2.3). A poor correlation also exists between the $^{144}Sm/^{147}Nd$ ratios and $\varepsilon_{Nd}(0)$ values (r=0.41). The narrow range of Sm/Nd fractionation and poor correlation indicate that no resetting of Sm-Nd compositions occurred during sedimentary and post-sedimentary processes (McLennan et al., 1993; Bock et al., 1994; McDaniel, 1994; Xie et al., 2012). On the other hand, the $^{87}Rb/^{86}Sr$ ratios show a large variation range from 0.010 to 3.65, possibly resulting from grain size sorting and Rb-Sr redistribution in the studied siliciclastics during the post-sedimentary processes (Xie et al., 2012). Therefore, the provenance reconstructions based on the Sm-Nd isotope system are considered more reliable and, thus, are used here to place constraints on the provenance of the Tarfaya basin sediments.

3.2.5 Discussion

3.2.5.1 Tectonic setting

Geochemistry (major and trace elements) of sedimentary rocks has been extensively used to discriminate tectonic settings of sedimentary basins (Bhatia, 1983; 1984 and 1985; Roser and Korsch, 1986 and 1988; McLennan and Taylor, 1991). Further, Bhatia and Crook (1986) have also used immobile trace elements in wackes to discriminate between different tectonic settings. However, these criteria must be used with caution, as sometimes sediments are transported from their tectonic setting of origin into a sedimentary basin in a different tectonic environment (McLennan et al., 1990).

The La/Y versus Sc/Cr binary diagram (Fig. 3.2.3a), in general, suggests passive continental margin settings for the studied samples, as most of the data (both coarse- and fine-grained sediments) plot to the field D for “Passive Margins” or around it. These ratios (La/Y=1.0-1.5 and Sc/Cr<0.2) are also almost within the range of the passive marginal depositional settings of Bhatia and Crook (1986). Furthermore, the La-Th-Sc triangular diagram (Fig. 3.2.3b) also suggests a continental marginal depositional setting. In the Th-Sc-Zr/10 diagram (Fig. 3.2.3c), the data are more scattered and have been found to differentiate less significantly between active and passive continental margin settings. This may be mainly attributable to the variation in concentration of Zr (Ghosh and Sarkar, 2010) and the relatively low Th concentrat-

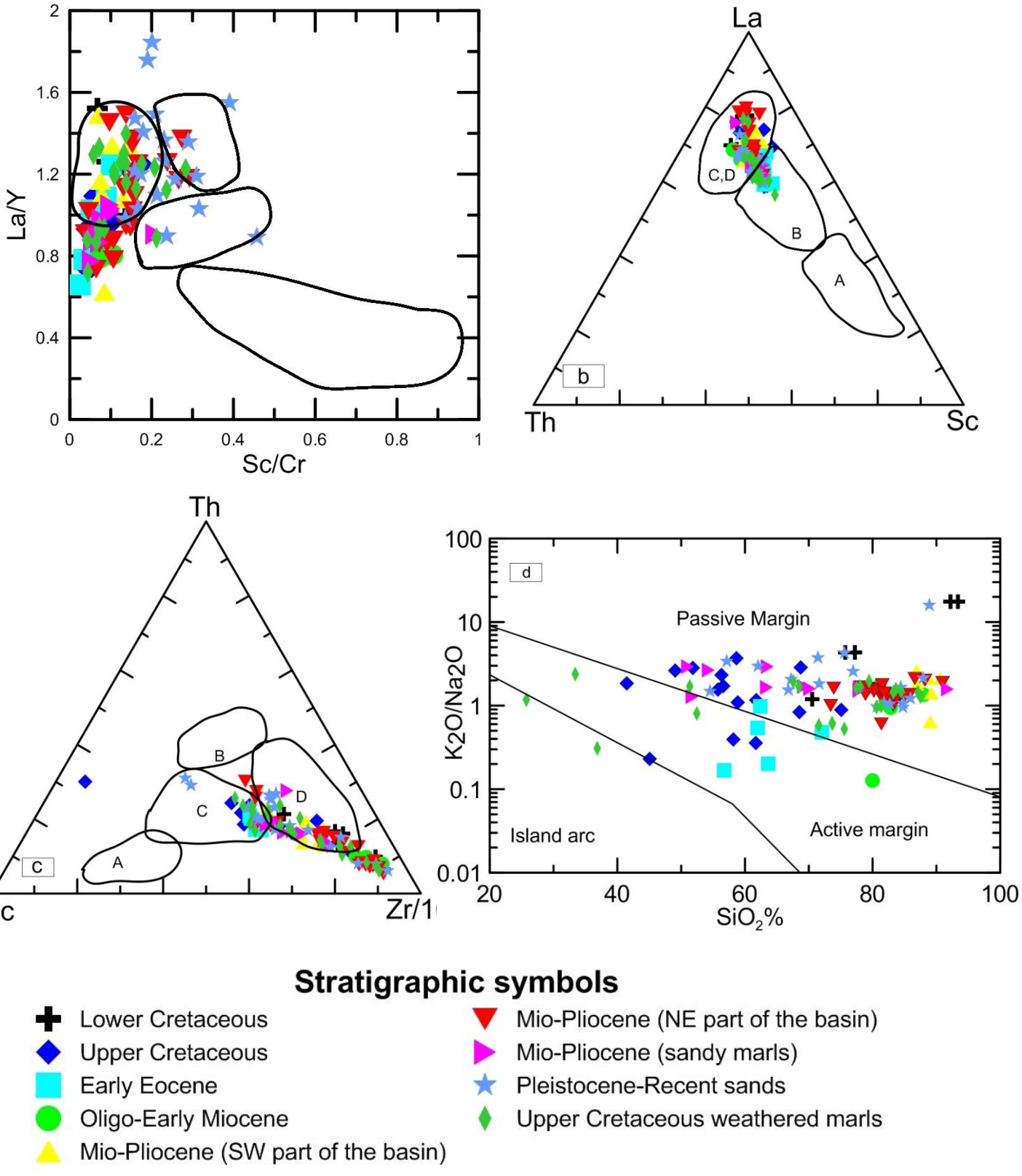

Fig. 3.2.3 Plots of the major and trace element composition of the sands and sandstones, sandy marls and mudstones from the Tarfaya basin on the tectonic-setting discrimination diagrams of Bhatia (1983): a, b & c; Roser and Korsch (1988): d. A: Oceanic Island Arc, B Continental Island Arc, C: Active Continental Margin, D: Passive Margin.

-ion. In Roser and Korsch's (1986) binary diagram based on K_2O/Na_2O versus SiO_2% (Fig. 3.2.3d; plotted for reference), coarse-grained siliciclastics from the Lower Cretaceous, the Miocene-Pliocene and the recent sediments lie within the passive margin deposition field. The fine-grained sediments from the Upper Cretaceous, Early Eocene, and Oligocene-Early Miocene are also indicative of passive margin depositional settings, except some black shale samples that plot to the active margin field because of the low SiO_2 or higher Na_2O concentrations and, hence, the fine-grained black shales have been found to be less significant. Thus, trace elements are more useful, in the present study, for discriminating tectonic settings of fine-grained siliclastics as compared to major elements. In conclusion, the various diagrams of tectonic settings indicate that the studied sediments of Tarfaya basin were deposited in a passive margin depositional setting.

3.2.5.2 Source rock composition

The abundance of Cr and Ni in siliciclastics can be considered as a proxy in provenance studies. A high content of Cr and Ni is predominantly found in sediments derived from ultramafic rocks, whereas a low concentration of Cr and Ni indicates a felsic provenance (Wrafter and Graham, 1989; Graver et al., 1996; Amstrong-Altrin et al., 2004). Graver et al. (1996) have shown that elevated Cr and Ni abundances (Cr>150 and Ni>100) and a high correlation coefficient between these two elements (r=0.90) are indicative of ultramafic rocks in the source region. The Cr and Ni concentrations in most of the studied samples are relatively low, with a less significant correlation coefficient (r=0.60) and variable Cr/Ni ratios. Hence, these low Cr and Ni concentrations, low Cr/Ni ratios, and poor correlation between Cr and Ni from both coarse- and fine-grained rocks do not indicate any signature of the mafic or ultramafic rocks in the source region. Furthermore, a binary diagram of Cr/V versus Y/Ni ratios has also been used to discriminate the source area (Hiscott, 1984; McLennan et al., 1993). The Cr/V ratios are the index of the enrichment of Cr over the other ferromagnesian trace elements, whereas Y/Ni monitors the general level of ferromagnesian trace elements (Ni) compared with a proxy for HREE (Y). The mafic to ultramafic sources tend to have higher Cr/V and lower Y/Ni ratios. The samples in the present study have an extremely low Cr/V ratio and a variable abundance of Y/Ni (Fig. 3.2.4) exhibiting a predominantly felsic lithology of the source area. Hence, these low Cr/V and variable Y/Ni ratios preclude any presence of the ophiolitic component in the source region.

The ratios between relatively immobile trace elements such as La/Sc, Th/Sc, Cr/Th and Th/Co are considered as good indicators of source rocks (Taylor and McLennan 1985; Cullers, 1994 and 2000; Cullers and Podkovyrov, 2000; Wronkiewicz and Con-

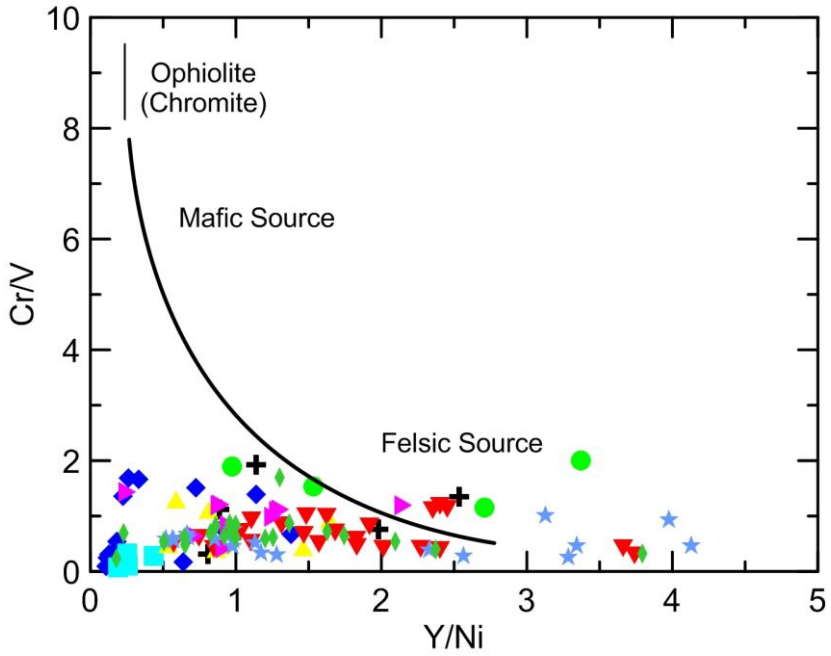

Fig. 3.2.4 Provenance plot using relations of Cr/V versus Y/Ni (after Hiscott, 1984). Curve model between granite and ultramafic end members. Ultramafic rocks have very low Y/Ni and high Cr/V ratios. Arrow indicates the direction of the mafic-ultramafic source end-end members. Symbols as in Fig. 3.2.3.

-die, 1990). In the present study, these ratios are compared with those of sediments derived from felsic and mafic rocks and also with UCC (Table 3.2.5). The comparisons show that the majority of our data are within the range of felsic source rocks and lower than UCC. According to Armstrong-Altrin et al. (2004), La/Sc and Th/Sc ratios of sediments derived from felsic rocks are always higher than those of sediments derived from mafic rocks. Ratios for our samples clearly indicate felsic sources, although some of the samples have slightly lower values of Th/Sc, although ratios are still much higher than those of mafic rocks. Most of the coarse-grained siliclastics have Cr/Th ratios close to those of UCC (Cr/Th=7.76, McLennan, 2006).The Th/Co ratios of the studied samples also lie within the range of felsic source and extremely close to UCC (Table 3.2.5).

The REE pattern of the source can be preserved in sedimentary rocks (Taylor and McLennan 1985). Felsic rocks contain higher LREE/HREE ratios and negative Eu anomalies, whereas mafic rocks generally contain lower LREE/HREE ratios and no or positive Eu anomalies (Cullers and Graf, 1983; Cullers, 1994). Hence, the REE patterns help to distinguish between felsic and mafic source rock lithologies of sedimentary rocks. The studied samples of the Tarfaya basin have high LREE/HREE ratios and moderately negative Eu anomalies. The chondrite-normalized samples show REE patterns similar to that of PAAS, with LREE enrichment, an almost flat

HREE and negative Eu anomalies. This suggests a contribution of sediments from felsic source rocks to the Tarfaya basin. Further, Eu/Eu* ratios are considered as being more sensitive to provenance signature (McLennan et al., 1993; Cullers, 2000). The Th/Sc ratio is used as an indicator of chemical differentiation and, hence, infers compositional heterogeneity of the sources (Cox et al., 1995; Hassan et al., 1999). The Zr/Sc ratio is used as an index of sediment recycling in the source region (McLennan et al. 1993). Further, Th/Sc ratios higher than 0.8, if coupled with higher values of Zr/Sc, probably indicate input from mature and/or recycled sources. All the studied samples, when plotted into the Th/Sc versus Zr/Sc binary diagram (Fig. 3.2.5) show a positive slope and display higher values of both ratios. The Th/Sc ratio has a narrow range (Table 3.2.1), whereas the Zr/Sc ratio exhibits a wide range. No particular trend is present along the line of mineral fraction and therefore, no indicat-

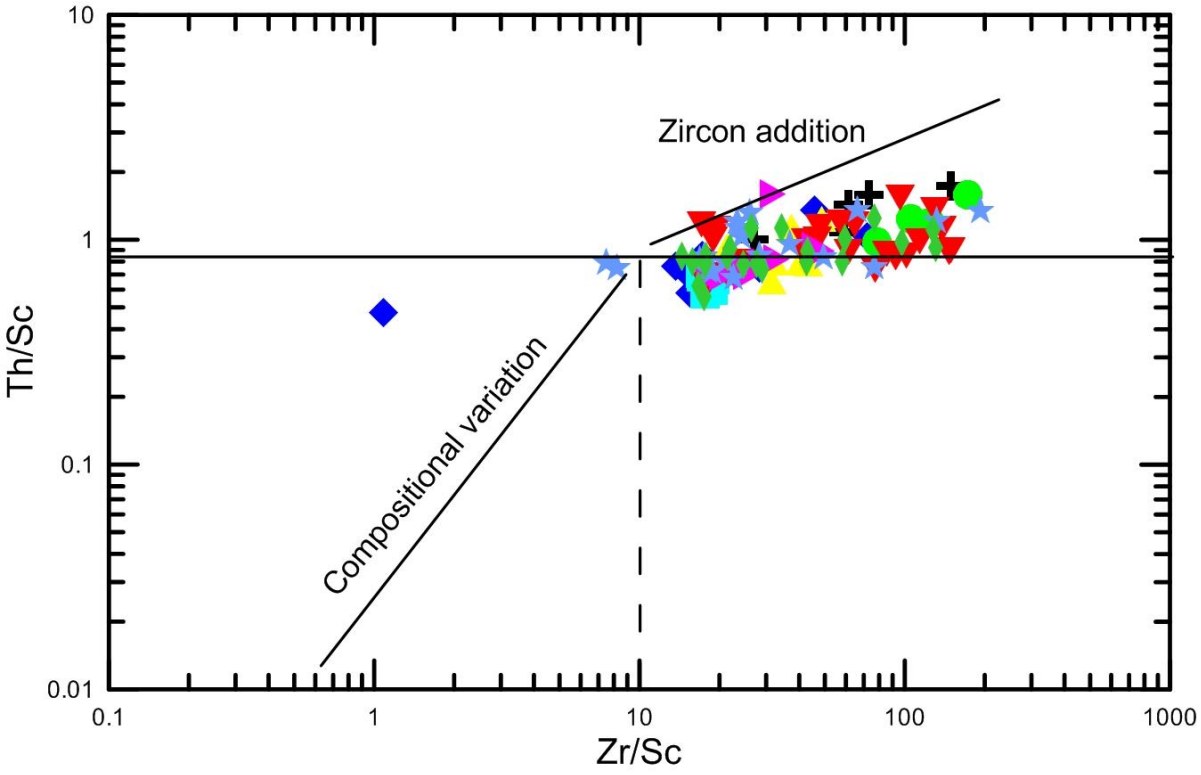

Fig. 3.2.5. Th/Sc versus Zr/Sc plot (after McLennan et al., 1993) of Tarfaya basin sediments. Explanation for both the compositional variation trend line and the zircon addition trend line can be found in the text. Symbols as in Fig. 3.2.3.

-ion of a mafic source. The absence of mafic sources is also indicated by generally high Th/Sc, >0.85. A particular trend is shown by Zr/Sc and indicates recycling or sediment sorting in the source region. Hence, from the Th/Sc versus Zr/Sc ratios, we can conclude that source areas have undergone recycling before sediment transport, together with an increasing addition of zircon mineral.

In summary, the low concentration of Cr and Ni, the ratios of La/Sc, Th/Sc, Cr/Th, Th/Co and the REE distribution patterns of the Tarfaya basin sediments indicate that these sediments are derived from felsic source rocks. In addition, the Zr/Sc distribution pattern and Zr/Hf ratios are is clearly indicative of recycling in the source area. However, these geochemical results are unable to trace whether the sediments are derived from single or varied source areas. Hence, Nd-Sr isotopic results are discussed in the next section in order to determine whether the studied sediments indicate the same provenance or mixed provenances from the Lower Cretaceous to recent time.

3.2.5.3 Provenance of the Tarfaya basin sediments

The analyzed samples of the Tarfaya basin from the Lower Cretaceous to recent show a large range of $\varepsilon_{Nd}(0)$ values (Table 3.2.3). A clear difference exists in the εNd(0) values between the Lower Cretaceous and the other sediments, with younger stratigraphic units and the most negative values occurring in the southernmost Sebkha Aridal section ($\varepsilon_{Nd}(0)$=-25.6). Hence, the calculated depleted mantle model ages (T_{DM}) of these sediments show variation in provenance ages because of variation in the source area. Previous findings indicate that during the Lower Cretaceous, sediments originated from the WAC and that the contribution of sediments from the western Anti-Atlas to the Tarfaya basin only started during the Upper Cretaceous (Fig. 3.2.12, Chapter 3.1).

The Nd and Sr isotopic compositions of the studied samples are compared in (Fig. 3.2.6) and exhibit three distinct groups. The first group consists of the samples from the Lower Cretaceous sediments characterized by T_{DM}= 2.1±0.05Ga provenance age and by higher Sr-isotopic ratios (0.8250). The second group comprises the Upper Cretaceous to Miocene-Pliocene samples and is characterized by T_{DM}= 1.8±0.02Ga provenance age and by variable Sr-isotopic ratios in the range from 0.7140 to 0.7523. On the other hand, the third group, which consists of sediments from the Sebkha Aridal section, is characterized by T_{DM}= 2.5±0.0Ga, older provenance ages, and more or less similar Sr-isotopic ratios (0.7190±0.002) to that of the second group. The recent sediment samples show an affinity with these groups as three recent sediment samples cluster along with the Upper Cretaceous to Miocene-Pliocene sediment samples (second group) and one sample corresponds to the Lower Cretaceous (first group), being similar in value on the Y-axis, but because of the low $^{86}Sr/^{87}Sr$ isotopic ratio on the X-axis, lying close to the Y-axis. The Upper Cretaceous carbonate and the Pleistocene sand samples are scattered because of the lower values of $\varepsilon_{Nd}(0)$. These different groups suggest that sediments originated from distinct source areas.

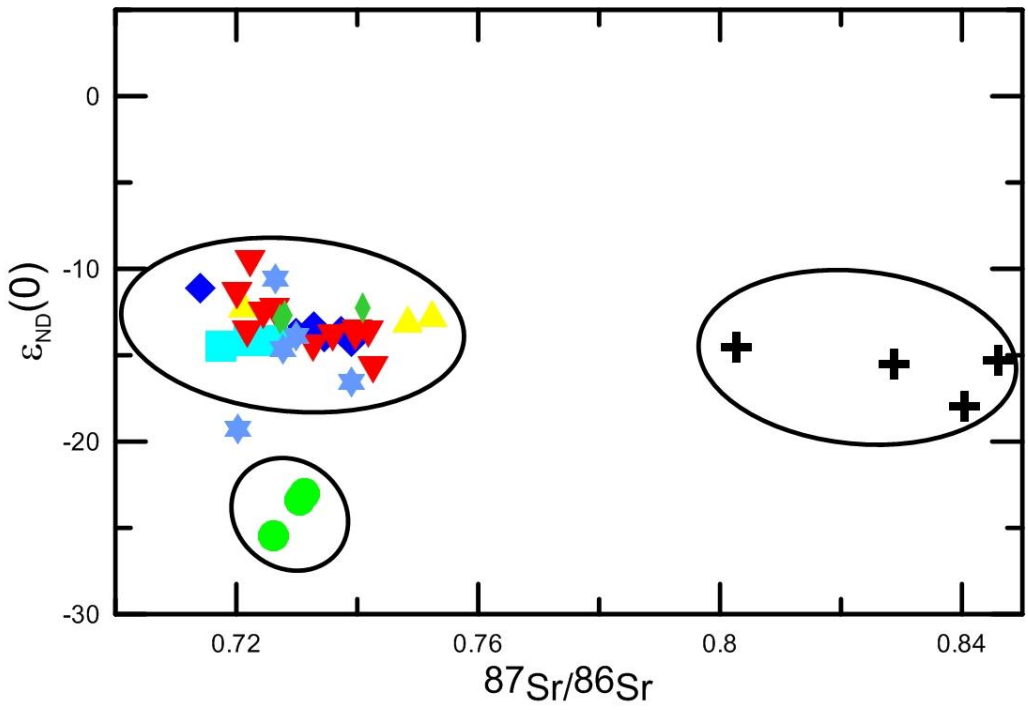

Fig. 3.2.6 ε_{Nd} (0) versus $^{87}Sr/^{86}Sr$ plots for Tarfaya basin sediments. Symbols as in Fig. 3.2.3.

Modern sediments provenance: One can directly constrain provenance from these data providing that no change in the isotopic composition of the source area occurred as a consequence of unroofing processes (Mearns et al., 1989). Four modern river-transported sediment samples, which originated from the WAC and the western Anti-Atlas, have been used for this purpose. One sand sample (sample # 14-01) has a provenance age of 2.2 Ga (Table 3.2.3, Fig. 3.2.7) and contains sediments that are derived from the Eburnean terrane (WAC) and have an age similar to the proveance ages (2.12-2.06 Ga) obtained by Schofield et al. (2006) and Schofield and Gillespie (2007). This indicates that no change has occurred in the gross isotopic composition in the WAC source areas between the Lower Cretaceous until the present day because of unroofing processes in the Eburnean terrane. On the other hand, two samples whose sediments are derived from the western Anti-Atlas suggest a provenance age (1.7 Ga) for the western Anti-Atlas source area (the western Anti-Atlas sediments that were deposited during the Paleozoic were derived from the Precambrian inliers and or WAC). Finally, a fourth sample whose sediments are possibly derived from both the WAC and the western Anti-Atlas source areas suggest a 1.9 Ga proveance age for these mixed source-derived sediments. The mixed provenance ages of the Atlantic Ocean younger sediments were also found in the range from 1.7 to 1.9 Ga by Cole et al. (2009) and Meyer et al. (2011).

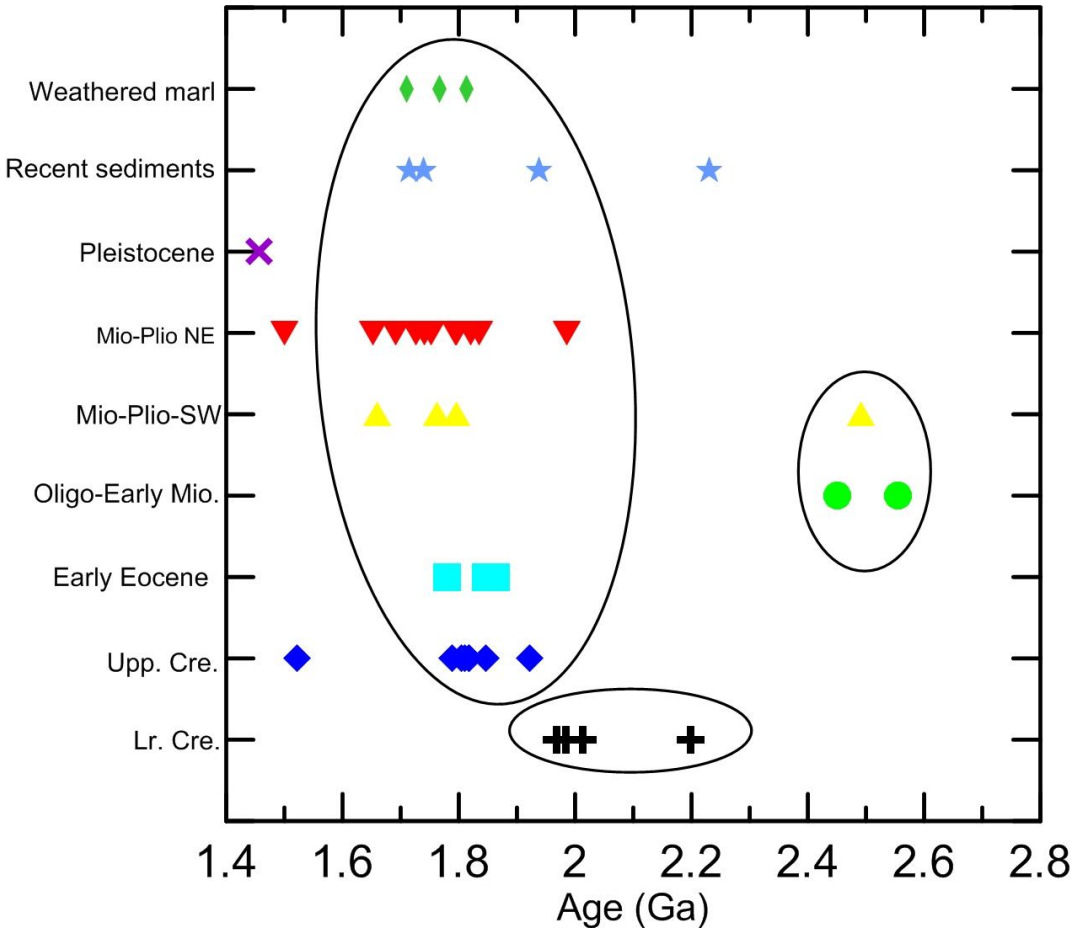

Fig. 3.2.7 Stratigraphic versus provenance age plots of the Tarfaya Basin sediments.

Lower Cretaceous sediment provenance: The Lower Cretaceous sediments have similar $\varepsilon_{Nd}(0)$ values and higher $^{87}Sr/^{86}Sr$ ratios than those of the modern West African Craton river sand. The higher $^{87}Sr/^{86}Sr$ ratios might be attributable to a post-depositional diagenesis process. The calculated provenance ages (average 2.2 Ga) in the Boukhchebat section are comparable with the Eburnean terrane indicating that the source is in the northern part of the Reguibat Shield (WAC). Sehrt et al. (2011) also indicate that the Reguibat Shield was the main source for the Lower Cretaceous sediment based on zircon (U-Th-Sm)/He dating (ZHe). The homogeneously negative Nd isotope values and restricted Sm/Nd ratios indicate their passive margin depositional tectonic setting, old provenance and long sedimentary recycling (Zhang et al., 2007). In addition, the petrographic data and SiO_2/Al_2O_3 ratios support Cratonic and recycled source areas for these sediments (Chapter 3.1).

Upper Cretaceous to Miocene-Pliocene sediment provenance: The Lower to Upper Cretaceous transition is marked by a shift toward more positive $\varepsilon_{Nd}(0)$ values

and a decrease in $^{87}Sr/^{86}Sr$ ratios. This shift may be attributable to the sediments starting to originate from the western Anti-Atlas as a consequence of uplifting and erosion attributable to the convergence of the African and Eurasian plates as mentioned earlier. The Upper Cretaceous to Early Eocene fine-grained and Miocene-Pliocene coarse-grainded sediments (from both the SW and NE parts of the Tarfaya basin) produce a narrow range of provenance ages of 1.7 to 1.8 Ga (average 1.8 Ga) and 1.6 to 1.8 Ga (average 1.8 Ga), respectively. The similarity in the $\varepsilon_{Nd}(0)$ values during the Miocene-Pliocene from both parts of the Tarfaya basin indicates the same source areas for Miocene-Pliocene sediments, and hence, these sediments demonstrate similar provenance ages (1.8Ga) being younger than those of the Lower Cretaceous. These provenance age groups signify the first contribution from the western Anti-Atlas source areas to the Tarfaya basin. Further, three samples from the Sebkha Aridal section (south most section in the present study) of the Tarfaya basin show the most negative $\varepsilon_{Nd}(0)$ values and hence the oldest provenance ages (T_{DM}=2.5±0.0Ga). These provenance ages are higher than Eburnean (2.12-2.06Ga) and lower than the Archean terrane (3.04-2.83Ga) indicating that these provenance ages were produced by a mixing of detritus from both these terranes.

3.2.6 Conclusions

The geochemical and Nd-Sr isotopic analysis of the siliciclastic sediments from Lower Cretaceous to recent indicate that the Tarfaya basin sediments have been deposited in a passive marginal tectonic settings, the sediments of which are derived from the heterogeneous source areas of felsic composition. These source areas are in the Eburnean and Archean terrane (WAC) along with the Mauritanides and the western Anti-Atlas.

The La-Th-Sc and La/Y versus Sc/Cr diagrams mostly indicate a passive margin tectonic setting for both coarse- and fine-grained siliciclastics. Nevertheless, La-Th-Zr/10 fails to distinguish between active and passive continental margin settings, possibly because of the wide variation of Zr concentrations in the studied sediments. Furthermore, the K_2O/Na_2O versus SiO_2% relationship for the coarse-grained siliciclastics indicates a passive margin tectonic setting. However, the fine-grained sediments show more scatter for this same relationship.

The low concentrations of Cr and Ni and the trace elements, as well as ratios of La/Sc, Th/Sc, Cr/Th and Th/Co of the Tarfaya basin sediments indicate that these sediments are derived from source rocks of acidic composition. In addition, similarity of REE patterns to that of PAAS, a light rare earth elements (LREE) enrichment, flat heavy rare earth elements (HREE), and negative Eu anomalies support the felsic source for the Tarfaya basin sediments. Moreover, a binary plot of Th/Sc and Zr/Sc

as well as Zr/Hf ratios show considerable enrichment of zircon, a finding that indicates recycling in the source area.

The uniform Sm/Nd ratios of coarse- and fine-grained sediments from Lower Cretaceous to recent in the Tarfaya basin show that no noticeable fractionation occurred during deposition or diagenesis and, hence, the lack of any isotopic compositional modification. The recent sediment samples from wadis and dunes have been found useful to direct constrain provenance. One sample indicates a similar provenance age to that of the Eburnean terrane (2.12-2.06 Ga) that was also found in the Lower Cretaceous sediments, imply that no modification took place in provenance age from the Lower Cretaceous to the recent due to unroofing. Two samples give a provenance age of 1.7 Ga for the sediments derived from the western Anti-Atlas and the other one sample gives 1.9 Ga for the mixed provenance. Further, the Nd isotopic data indicates that the Lower Cretaceous sediments are exclusively derived from the Eburnean terrane of the West African Craton. Since the Upper Cretaceous, the sediments show source areas from the West African Craton and the western Anti-Atlas. The contribution of sediments from western Anti-Atlas is associated with the tectonic activity in the Anti-Atlas. Finally, the southernmost Sebkha Aridal section shows the predominance of Archean terrane derived sediments from WAC.

3.2.7 Acknowledgements

We thank RWE Dea for funding this project. We also thank ONHYM for supporting, organizing and accompanying the field campaign in March-April, 2009 and drilling in September-December, 2009. We would like to thank Claudia Ehlert from IFM-GEOMAR for support of the ICP-MS measurements.

Chapter 3 Results

3.3 Climatic and tectonic control on weathering from Upper Cretaceous to Quaternary in the Tarfaya basin, marginal Atlantic, SW Morocco: evidence from clay mineralogy and geochemistry[a]

Sajid Ali[1], Karl Stattegger[1], Zhifei Liu[2], Wolfgang Kuhnt[1]

[1]Institute of Geosciences, Christian-Albrechts-University, D-24118 Kiel, Germany

[2] State Key Laboratory of Marine Geology, Tongji University, Shanghai 200092, China

Abstract

Clay mineral contents from Upper Cretaceous to modern sediments in the Tarfaya basin have been investigated by using X-ray diffraction method. The basin is filled by sediments that were derived from plutonic rocks from the Reguibat Shield (West African Craton) and Paleozoic sedimentary and/or low grade metamorphosed rocks (carbonates and sandstones) of the western Anti-Atlas. The clay mineral assemblages of the Tarfaya basin sediments vary through different stratigraphic units. Illite and chlorite, which are formed by physical weathering, are derived from rocks of the West African Craton and western Anti-Atlas. The higher concentration of smectite throughout the stratigraphic units is of detrital origin, mainly indicative of warm and semi-arid climatic conditions in the source area. The higher abundance of kaolinite, higher ratios of kaolinite/illite, and high Al_2O_3/Na_2O and TiO_2/Na_2O ratios in the Turonian and Santonian sediments suggest intense chemical weathering of the soil in the source area. The presence of corrensite in Campanian (Upper Cretaceous) and Oligocene-Early Miocene sediments is associated with the diagenetic transformation of other clay minerals under oxic/anoxic conditions. Abundant palygorskite in the Early Eocene sediments indicates warm and dry climate conditions in the nearby coastal area. The higher abundance of illite and smectite throughout the basin during the Miocene-Pliocene suggests physical weathering in the source area, which is also associated with large-scale tectonic activities. The marls from Miocene-Pliocene weathered horizons show more intense chemical weathering as compared with Upper Cretaceous marls and hence more humid climatic conditions. Moreover, the Th/Sc and Zr/Sc binary relationships and higher

Zr/Hf ratio show a considerable enrichment of zircon, which indicates recycling in the source area.

[a]To be submitted to Clays and Clay Minerals.

3.3.1. Introduction

Clay minerals are an important and widely distributed component in types of sediments. Their vertical distributions have been interpreted in terms of contemporaneous palaeoclimatic changes prevailing in continental source areas (Petschick et al., 1996; Gingele et al., 2001; Liu et al., 2010). The clay mineral concentration is widely controlled by climate, tectonics and lithology of the source region. Kaolinite is chiefly used to monitor the intensity of chemical weathering in the source region. Other clay mineral indices are also important for climate tracing. For example, the illite chemical index can be used to reflect the strength of physical erosion or hydrolysis (Gingele et al. 2001; Boulay et al., 2005; Liu et al., 2007), and illite crystallinity is often used as a source region tracer of the sediments (Petschick et al., 1996; Liu et al., 2007). The Al_2O_3/Na_2O and TiO_2/Na_2O ratios can serve as proxies for the chemical index of alteration (CIA) because these ratios are directly related to the plagioclase alteration (Roy et al., 2008). Hence, these elemental ratios together with kaolinite abundance can better understand weathering in the source area.

Earlier studies in the Tarfaya basin were based on fine-grained sediments from the Upper Cretaceous and were focused on an understanding of the intensity of anoxia, the magnitude and nature of the $\delta^{13}C$ excursion, the biotic effects on benthic and planktonic foraminifera, biostratigraphic records, and paleo-environmental evolution (e.g. El Albani et al., 1999; Kuhnt et al., 1997, 2005, 2009; Kolonic et al., 2005; Mort et al., 2007, 2008; Keller et al., 2008; Gertsch et al., 2010). Further, clay mineral studies in the Upper Cretaceous sediments were done by El Albani et al. (1999) and in the Early Eocene sediments from the offshore Atlantic Ocean sediments by Robert and Chamley (1991). We present results obtained from the Upper Cretaceous to recent siliciclastic rocks from key sections of the coastal cliffs and sebkhas between Boujdour and Oued Chebeika and the upper sections of four newly drilled cores. We use clay mineralogy compared with geochemical data in order to evaluate climatic and tectonic control on weathering and erosion processes in the source region and weathered horizons in the Tarfaya basin.

3.3.2 Geological background

The Tarfaya basin is limited by the Anti-Atlas to the north, the Mauritanides to the south, the Reguibat Shield (West African Craton) in the east and is open to the Atlantic Ocean in the west. The evolution of the basin is closely connected with the geological history of the African Craton and the opening of the Atlantic Ocean (Ranke et al., 1982), with development from a rift to a marginal basin. The basin is filled by

Mesozoic and Cenozoic continental to shallow marine sediments overlying a basement of igneous and metamorphic rocks of Precambrian and/or Paleozoic age. The post-Triassic subsidence of the basin is related to the opening of the Atlantic Ocean (Wiedmann et al., 1982). The importance is the activation of the Zemmour fault, which separates the Anti-Atlas and the Tindouf basin to the east (Choubert et al., 1966). With the activation of the fault, a steady subsidence of the Tarfaya basin commenced in the Triassic followed by a stepwise subsidence in the Jurassic and the Cretaceous. A thick deltaic sequence, during the Early Cretaceous, accumulated during and after a major global Valanginian regression (Vail et al., 1977). According to Ratschiller (1970), the shallow-marine sediments from the Upper Cretaceous to the Early Eocene unconformably overlay the continental Lower Cretaceous formations. Late Oligocene to Early Miocene basin development shows an erosional hiatus, because of the coincidence of a major regression with intensified slumping, canyon incision, and bottom water circulation (Arthur et al., 1979), with only little continental deposition taking place. After this long period of non-deposition or erosion, Miocene-Pliocene sediments unconformably overlay the Lower Cretaceous (Tan Tan Formation), Upper Cretaceous (NE part of the basin), Early Eocene and Oligocene-Early Miocene (SW part of the basin) deposits. Miocene-Pliocene siliciclastic sediments once again started to be deposited both on- and off-shore associated with uplift events in the Anti-Atlas producing several hiatuses and weathered horizons of sediments (Frozen de Lamotte et al., 2009; Ruiz et al., 2010).

In the present study, samples were collected from various sections (Upper Cretaceous to recent time) that cropped out in the Sebkhas and along the shoreline in the Tarfaya basin; these samples have been logged and investigated together with four newly drilled cores. The location of the various sections and drilled cores are shown in Fig. 3.1.1 and the sample positions within sections are given in Fig. 3.3.1. The Upper Cretaceous rocks mainly exposed in the NE part of the basin consist of black shales and sandy marls intercalated with chert and nodular limestone or just pure limestone. The Early Eocene deposits occur in the SW part of the basin and consist of black shales and sandy marls intercalated with cherts and limestones. The Oligocene-Early Miocene sandy marls have been sampled from the Sebkha Aridal section. The Miocene-Pliocene siliciclastic deposits consist of coarse or conglomeratic sandstones together with lumachelle in the lower part and sandstones intercalated with sandy marls and limestones. Recently deposited sediment samples have also been collected from various wadis. Weathered marl samples from the Upper Cretaceous and Miocene-Pliocene weathering horizons have also been collected to direct constraint weathering history.

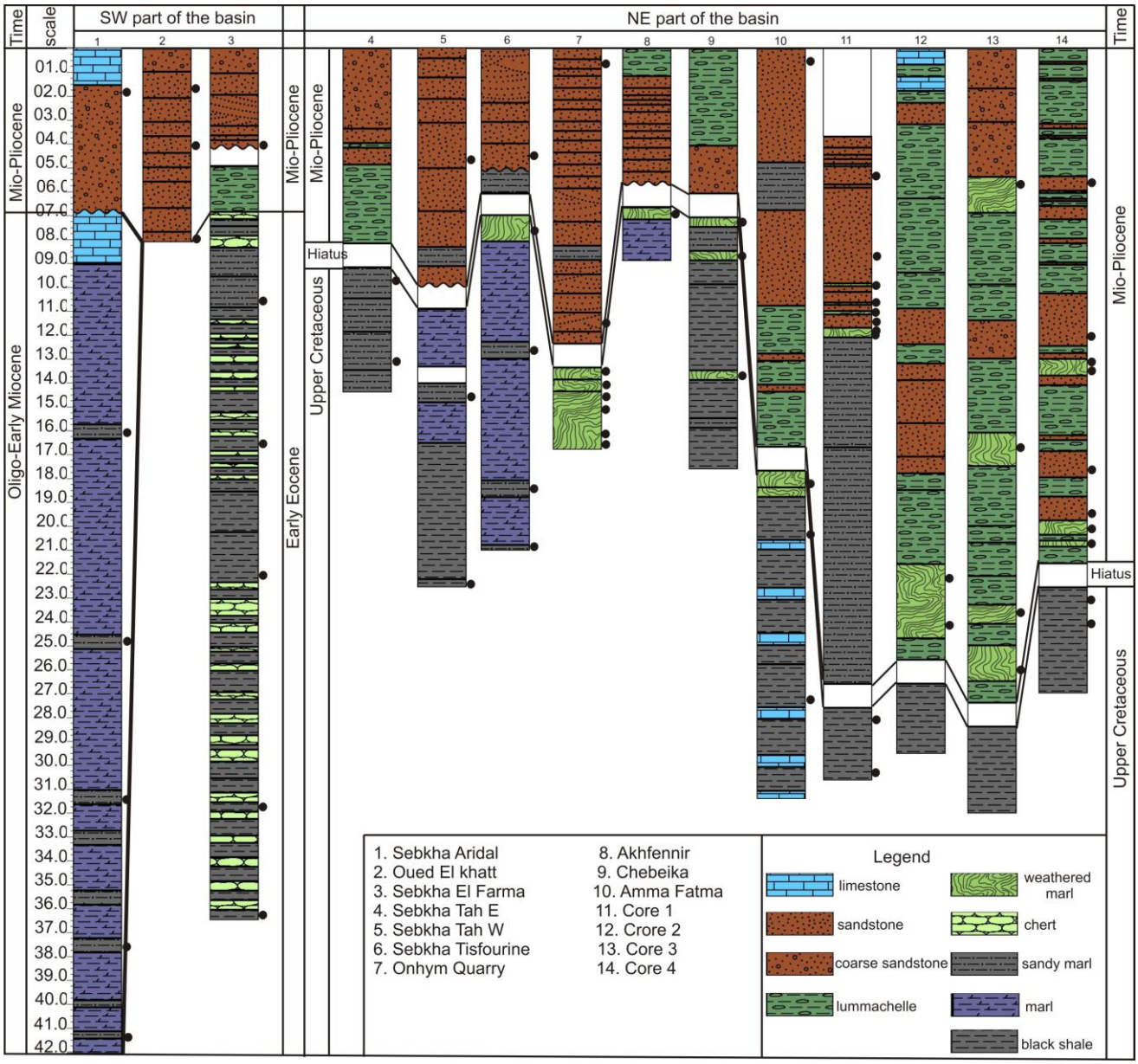

Fig. 3.3.1 Lithologic sections of the Tarfaya basin from Upper Cretaceous to Mio-Pliocene. Black dots mark sample positions.

3.3.3 Materials and methods

Clay mineral analysis was carried out on a total of 71 samples comprising black shales, sandy marls, sandstones, and recent sediments as well. These samples were selected from sixteen outcrop sections and four newly drilled cores, representing different stratigraphic units (Upper Cretaceous to recent) in the Tarfaya basin. Prior to the clay fraction (<2 um) separation, the samples were treated for removing the carbonate contents (using hydrochloric acid). Following the Stokes' Law, the clay fractions (<2 um) were separated from the stabilized suspension and oriented clay slides were prepared by smearing the clay suspension onto glass slides. The

analyses were conducted using a PANalytical X'Pert PRO diffractometer with CuKα radiation and Ni filter, under a voltage of 45 kV and an intensity of 40 mA. The XRD runs following ethylene-glycol salvation for 24 h, and heating at 490°C for 2 h. The sample preparation and analysis were performed at the State Key Laboratory of Marine Geology, Tongji University (China).

The relative contents of each clay mineral species were estimated mainly according to the position of the (001) series of the basal reflections on the XRD diagrams, i.e. smectite (001) at 17 Å, illite (001) at 10 Å , kaolinite (001) and chlorite (002) at 7 Å . Kaolinite and chlorite were discriminated according to the relative proportions given by a ratio of the 3.57 Å and 3.54 Å peak areas. Corrensite, palygorskite, and sepiolite are also identified at 14 Å, 10.46 Å, and 11.9 Å, respectively. The illite chemistry index and illite crystallinity have been calculated from the X-ray diffractograms. Illite chemistry index refers to a ratio of the 5 Å and 10 Å peak areas (Esquevin, 1969). Illite crystallinity was obtained from the half height width of the 10 Å peak (Chamley, 1989). These two parameters are usually used to track source regions and transport paths.

3.3.4 Results

The proportion of the clay minerals and their distribution in the different stratigraphic intervals are shown in Table 4.1 and are plotted in a pie chart and ternary diagram in Figs. 3.3.2 and 3.3.3, respectively. The measured clay minerals include chlorite, illite, smectite, kaolinite, palygorskite, sepiolite and corrensite in variable proportions. Their proportions are variable between the different stratigraphic intervals and within the stratigraphic units.

The clay minerals for the Upper Cretaceous sediments are highly variable within each sub-stratigraphic unit; for Santonian (smectite (20-74%), illite (13-50%), kaolinite (10-18%)), for Turonian (smectite (1-37%, illite (35-47%), kaolinite (10-51%)), and for Turonian, the distribution of clay minerals is variable both in the outcrop section (smectite 0%, illite 15-42%, kaolinite 0-1% and corrensite 58-84%) and in the drilled core (smectite 36-38%, illite 52-55%, kaolinite 5%) [Table 3.3.1]. The distribution of clay minerals from the Upper Cretaceous sediments is in agreement with those obtained by El Albani et al. (1999). However, corrensite has not been considered by the El Albani group. The illite chemistry index ranges from 0.21 to 0.50, and the illite crystallinity ranges from 0.26 to 0.68°$\Delta 2\theta$, with an average value of 0.39°$\Delta 2\theta$ (Table 3.3.1).

In the Early Eocene sediments, palygorskite (22-71%) is the most dominant clay mineral with an average of 43% followed by smectite (0-42%), illite (9-33%), corrensite (2-19%) and kaolinite (0-5%). The illite chemistry index varies between

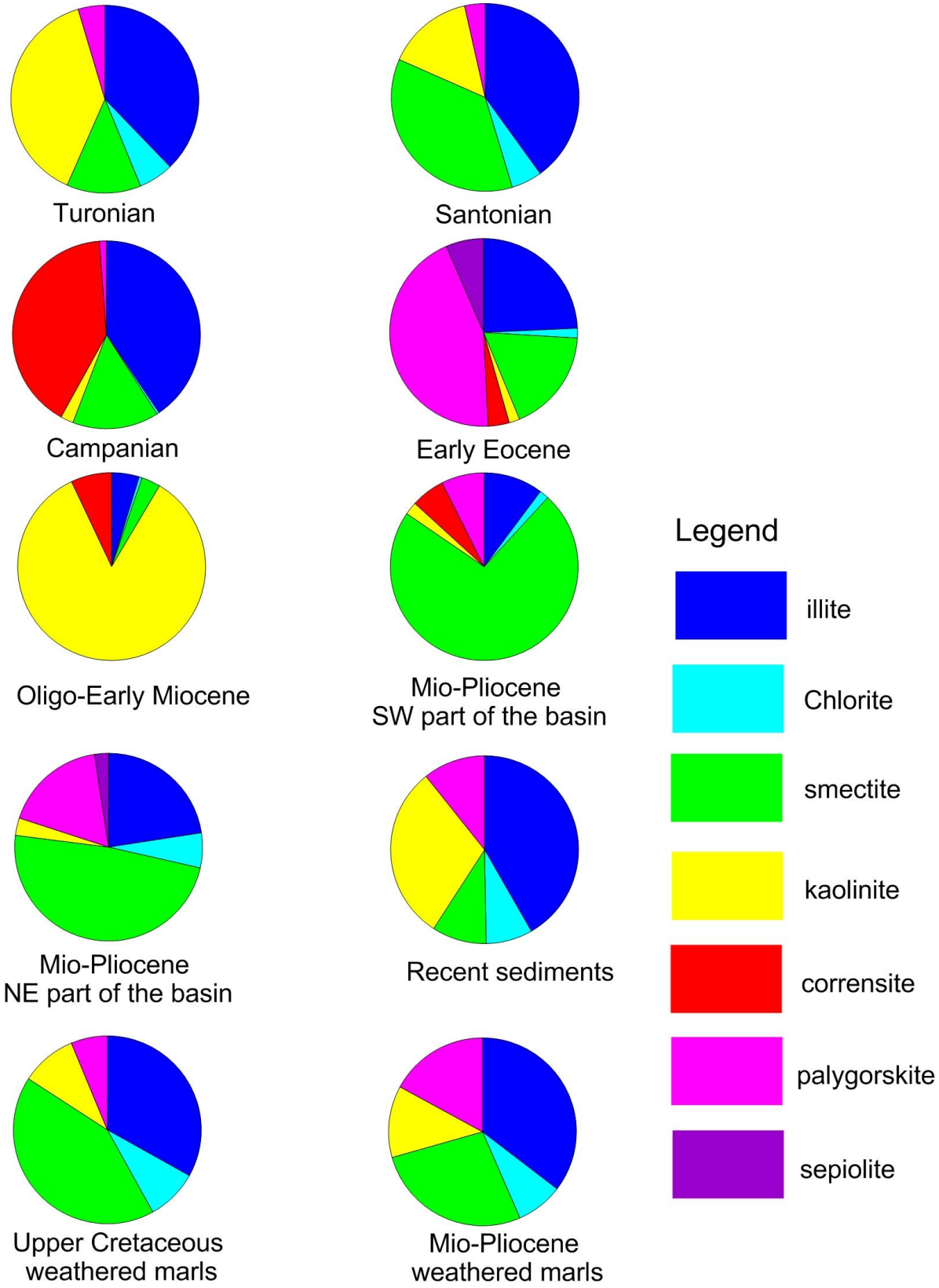

Fig. 3.3.2 The distribution of average clay minerals of Tarfaya basin sediments from Upper Cretaceous to recent. Weathered Upper Cretaceous and Miocene-Pliocene marls are shown separately in the two lowermost diagrams.

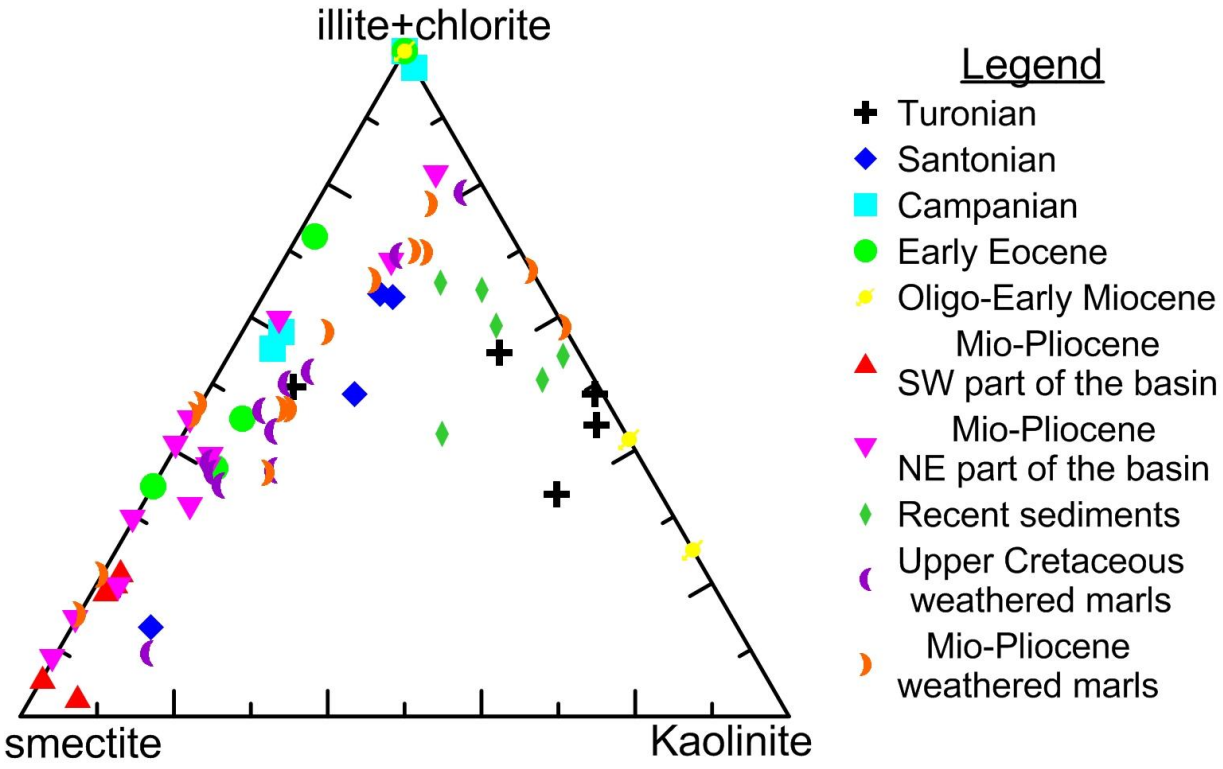

Fig. 3.3.3 Comparison of clay mineral assemblages of Tarfaya basin sediments from Upper Cretaceous to recent.

0.24 and 0.40, and the illite crystallinity is between 0.22 and 0.43 Δ2θ, with an average value of 0.30°Δ2θ (Table 4.1).

Samples from the Oligocene-Early Miocene sediments have extremely high concentration of corrensite (73-92%), with an average of 84%, the other clay minerals include smectite, illite and kaolinite occurring in minor proportions.

The clay minerals in the SW and NE part of the basin sediments from the Miocene-Pliocene are variably distributed. The NE part of the basin is characterized by more abundant primary minerals, i.e., illite (8-40%) and chlorite (0-22%) and variable abundant secondary mineral, i.e., smectite (2-88%); palygorskite content varies from 0 to 58%. On the other hand, the SW part of the basin is characterized by more abundant secondary smectite mineral (50-80%), with an average of 73%, and less abundant illite (2-20%), chlorite (0-6%) and palygorskite (3-15%). The illite chemistry index varies between 0.22 and 0.44, and the illite crystallinity is between 0.13 and 0.42°Δ2θ, with an average of 0.27°Δ2θ (Table 3.3.1).

The clay mineral fractions in the Upper Cretaceous and Miocene-Pliocene weathered marls show the following distribution variability. The Upper Cretaceous weathered marls include smectite (3-67%), illite (18-55%), chlorite (0-15%), kaolinite (5-16%), and palygorskite (1-12%). The clay minerals in the Miocene-Pliocene weathered

marls comprise smectite (0-72%), illite (13-52%), and kaolinite (0-42%). Chlorite and palygorskite are also present in minor proportions. The illite chemistry index varies between 0.17 and 0.43, and the illite crystallinity is between 0.14 and 0.50°Δ2θ, with an average of 0.25°Δ2θ (Table 3.3.1).

The clay mineral present in the recent sediments are smectite, illite, kaolinite, chlorite, and palygorskite. Illite (32-50%) is the most dominant clay mineral with an average of 42%; kaolinite (19-38%) is the second with an average of 30%, with smectite (2-22%), chlorite (7-11%) and palygorskite (7-14%) being present as less dominant clay minerals in recent sediments. The illite chemistry index varies between 0.31 and 0.42, and the illite crystallinity is between 0.23 and 0.63°Δ2θ, with an average of 0.39°Δ2θ (Table 3.3.1).

3.3.5 Discussion

3.3.5.1 Origin of clay minerals in the Tarfaya basin sediments

Illite and chlorite are considered as detrital primary clay minerals. Illite reflects decreased hydrolytic processes in continental weathering and increased direct rock erosion under cold and/or arid climatic conditions. Chlorite is a characteristic mineral for low-grade chlorite-bearing metamorphic rocks. It is also found in sedimentary rocks and may be retained in repeated erosion cycles (Hong et al., 2007). It has an origin similar to that of illite under physical weathering conditions that allow chlorite to survive and even be concentrated in the erosion cycle (Madhavaraju et al., 2002; Hong et al., 2007). The illite concentration in the studied samples is relatively higher than that of other clay minerals that are present, except in the Oligocene-Early Miocene sandy marls and Miocene-Pliocene sandstones from the SW part of the basin. In the Tarfaya basin sediments, illite might have been derived from the physical erosion of granitic and metamorphic rocks of the Reguibat Shield (WAC) and sedimentary rocks of the western Anti-Atlas. The low illite concentration in the studied samples is associated with the higher concentration of the clay minerals. Further, the weathered marls of the drilled core-1 from the Miocene-Pliocene also show a relatively low illite concentration, which is also associated with higher abundances of smectite and palygorskite. The chlorite abundances are low and variable in the different stratigraphic units. The source of chlorite is mainly associated with low-grade metamorphosed and sedimentary rocks of the western Anti-Atlas.

Smectite can form frequently during chemical weathering in warm temperatures, but it principally develops at climatic conditions between warm-humid and cold-dry and requires less water percolation than that needed for kaolinite formation (Chamley, 1989; Gibson et al., 2000; Suresh et al., 2004; Liu et al., 2007). According to Deconinck and Chamley (1995), three possible main processes lead to smectite and

smectite mineral formation: (1) reworking of exposed soils and sediments under a warm and less humid climate, (2) early digenetic authigenesis and (3) submarine weathering or alteration of volcanic material. The Tarfaya basin sediments are derived from sources of felsic composition from the Reguibat Shield (WAC) and western Anti-Atlas Chapter 2 and Chapter 3), and therefore, a volcanogenic origin of smectite can be excluded because of the absence of volcanic material. In addition, the volcanogenic origin of the high smectite presence in marine sediments of Atlantic origin has also been rejected by Chamley et al. (1990) because of the rarity of volcanic debris and of specific volcanic clay mineral shapes and chemistry in common marine sediments. Therefore, the higher concentration of smectite in the studied Tarfaya basin sediments is mainly the result of the reworking and transport from exposed soils and sediments under warm and semi-arid climate in the source area. Diagenetic smectitization is less documented and could not be confirmed.

Kaolinite forms during the warm and wet weathering of acidic igneous and metamorphic rocks or their detrital products (Hong et al., 2007). The occurrence of kaolinite is associated with the intensity of chemical weathering under tropical conditions (Hallamnet al., 1991) during which abundant rainfall favors ionic transformation and pedogenic development (Millot, 1970; Chamley, 1989). The granitic rocks and/or metamorphosed rocks of the Reguibat Shield (WAC) and sedimentary rocks from the western Anti-Atlas or their detrital products produce a significant amount of kaolinite in recent clay mineral assemblages. The variation in the kaolinite concentration within the different stratigraphic units is mainly attributable to the variation in the intensity of chemical weathering in the source region.

Results show that palygorskite is abundant in Early Eocene and Miocene-Pliocene (drilled core-1) sediments of the Tarfaya basin, but less abundance in recent sediments. Low contents of palygorskite have also been found in the Oligocene-Early Miocene and Miocene-Pliocene sediments. However, palygorskite is absent or present only as traces in the Upper Cretaceous. Palygorskite has also not been identified in the Upper Cretaceous sediments of the Tarfaya basin by El Albani et al. (1999). The occurrence of palygorskite in the present studied sediments is mainly associated with detrital origin which is formed under dry and arid/semi-arid conditions as those recognized in Late Cenozoic and later sediments from many locations of the NE Atlantic, Mediterranean and Indian basins, where fibrous clays including palygorskite and sepiolite are commonly transported by river discharge, turbidity currents or winds (Robert et al., 1984; Tomadin et al., 1984; Chamley, 1989; Debrabant et al., 1993). The higher abundance of Palygorskite in Early Eocene sediments is associated with massive dryness and evaporation in coastal areas from low- and middle- latitudes during this time (Robert and Chamley, 1991). However, an

increase in palygorskite and decrease in smectite in drilled core-1 weathered sediments (Miocene-Pliocene) may be the result of an *in situ* transformation of smectite into palygorskite which also attribute to the location of core-1 being further landward. Furthermore, palygorskite abundance in the recent sediments is mainly associated with the eolian transport of Sahara desert dust.

Corrensite is a 1:1 regular interstratification of trioctahedral chlorite and trioctahedral smectite. The occurrence of corrensite is very abundant in Campanian (Upper Cretaceous) and Oligo-Early Miocene sediments, indicating a very special provenance information or local diagenesis condition, because it is not a common interstratified clay mineral. As far as corrensite occurrence is concerned, it can occur as a product of the hydrothermal alteration of various types of igneous rocks (Meunier et al., 1988; Shaun et al., 1990; Bettison-Varra and Mackinon, 1997; Schmidt and Robinson, 1997) or is related to the diagenesis of volcanoclastic sedimentary materials (Almon et al., 1976; Chang et al., 1986; Jiang and Peacor, 1994a, 1994b). However, corrensite and chlorite can also form by the replacement of biotite (Jiang and Peacor, 1994a, 1994b; Li et al., 1998) and amphibole (Meunier et al., 1988) or by the reaction between detrital dioctahedral clay mineral assemblages and Mg-rich carbonate during burial diagenesis (Hutcheon et al., 1980; Hillier, 1993). Furthermore, according to Barrenechea et al. (2000), the transformation into corrensite and corrensite+chlorite clay minerals is related to redox conditions. The occurrence of corrensite+chlorite appears to be related to reducing conditions, i.e., in mudstones of high organic content, and the presence of corrensite alone is apparently favored by oxic conditions. The studied samples show a higher content of corrensite alone in the Campanian (Upper Cretaceous) and Oligocene-Early Miocene sediments suggesting strongly their digenetic transformation under oxic conditions. Further, one black shale sample from the Early Eocene also contains corrensite, together with some chlorite, which might have been formed under reducing conditions.

The illite chemistry index and illite crystallinity can be used as indicators of the intensity of chemical weathering; if no significant diagenesis or reworking of the illite clay mineral has occurred. According to Esquevin (1969) ratios of illite chemistry index higher than 0.5 are found in Al-rich illite, which is formed by intense chemical weathering; on the other hand, ratios lower than 0.5 represent Fe-Mg-rich illite, which is characteristic of weak chemical weathering conditions. Lower values of illite crystallinity represent higher crystallinity, which are characteristic of weak hydrolysis in source area (Chamley, 1989; Krumm and Buggisch, 1991) and vice versa when the values are higher. The results obtained in the present study show low and variable illite chemistry index and illite crystallinity; no correlation has been found with

kaolinite abundance, and thus the hypothesis, in the present study, of strong chemical weathering is not supported.

3.3.5.2 Geochemical interpretation

The intensity and duration of weathering in the siliclastics sediments is associated with the relationships between alkali and alkaline earth elements (Nesbitt and Young, 1982). Since the upper crust contains a considerable amount of feldspar (Nesbitt and Young, 1982), the dominant process during chemical weathering and soil formation is the degradation of feldspars from source rocks to secondary clay minerals. These chemical signatures are ultimately transferred to sedimentary records and supply a useful means for monitoring the intensity of chemical weathering. The chemical index of alteration (CIA) has been proposed by Nesbitt and Young (1982) in order to estimate the intensity of chemical weathering in the source region of siliciclastic rocks. In the present study, this index was not found to be particularly useful in the interpretation of the intensity of chemical weathering (Chapter 2). However, the Al_2O_3/Na_2O and TiO_2/Na_2O ratios can be used directly as markers for intensity of chemical weathering (Roy et al., 2008).

The geochemical results (Al_2O_3/Na_2O, TiO_2/Na_2O and K_2O/Na_2O ratios) together with the kaolinite clay mineral abundance show the variable influence of chemical weathering from the Upper Cretaceous to recent time. The higher ratios of Al_2O_3/Na_2O and TiO_2/Na_2O are found associated with the increase in kaolinite content and kaolinite/illite ratio in the various stratigraphic units. However, the K_2O/Na_2O ratio is variable and less comparable with the kaolinite content and kaolinite/illite ratios and hence is not useful for monitoring the intensity of weathering. On the other hand, the Al_2O_3/Na_2O and TiO_2/Na_2O ratios, kaolinite content, and kaolinite/illite ratio can be used to monitor the intensity of chemical weathering in the different stratigraphic units of the Tarfaya basin sediments. Their values are high in the Turonian, Santonian and recent sediments and extremely low in the Campanian, Early Eocene, Oligocene-Early Miocene, and Miocene-Pliocene sediments. These results suggest that chemical weathering was intense during Turonian, Santonian, and recent time, but negligible during Campanian, Early Eocene, Oligocene-Early Miocene, and Miocene-Pliocene times. Further, a difference has been found in the values of these parameters in the weathered marls at the top of Upper Cretaceous and within Miocene-Pliocene sediment successions. Hence, these parameters suggest that Miocene-Pliocene weathered marls did indeed form under more intense chemical weathering as compared to the Upper Cretaceous weathered marls.

The Th/U ratio reflects, together with the increasing abundance of the kaolinite, the intensity of the chemical weathering in the source region, with the highest value

occurring in the more deeply weathered rocks (McLennan et al., 1993). The results obtained from the Th/U ratio are low and incomparable with the kaolinite abundance. This low ratio of Th/U and non-correlation with kaolinite abundance might be attributable to differences in oxidation state, and therefore the Th/U ratio does not reflect the intensity of chemical weathering In the source area of Tarfaya basin sediments (Bauluz et al., 2000).

The maturity of the Tarfaya basin sediments can be monitored in terms of the variation in SiO_2/Al_2O_3 ratios. The ratios increase because of an increase of quartz as compared with less resistant components such as feldspar and lithic fragments during transport and recycling. The SiO_2/Al_2O_3 elements ratio is about 3 in basic rocks (basalt and Gabbros), about 5 in acidic rocks (granite and rhyolites) [LeMaitre, 1976; Roser et al., 1996], and 4.44 in the Upper Continental Crust (UCC, Taylor and McLennan, 1985). Ratios of more than 5 suggest sedimentary maturation in sedimentary rocks (Roser et al., 1996). The values of SiO_2/Al_2O3 are variable in the different stratigraphic units (Table 3.3.1). The results of the studied samples indicate the higher maturity of the Tarfaya basin sediments, except for the Upper Cretaceous black shales. However, their values are higher than the Post Archean Australian shales (PAAS, Taylor and McLennan, 1985) suggesting that the Upper Cretaceous shales are more mature than the PAAS.

The recycling influence can be recognized on the Th/Sc versus Zr/Sc binary plot (Fig. 3.3.4) in which the Th/Sc ratio is used as an indicator of chemical differentiation (Cox et al., 1995; Hassan et al., 1999) and the Zr/Sc ratio is used as an index of sediment recycling in the source region (McLennan et al., 1993).

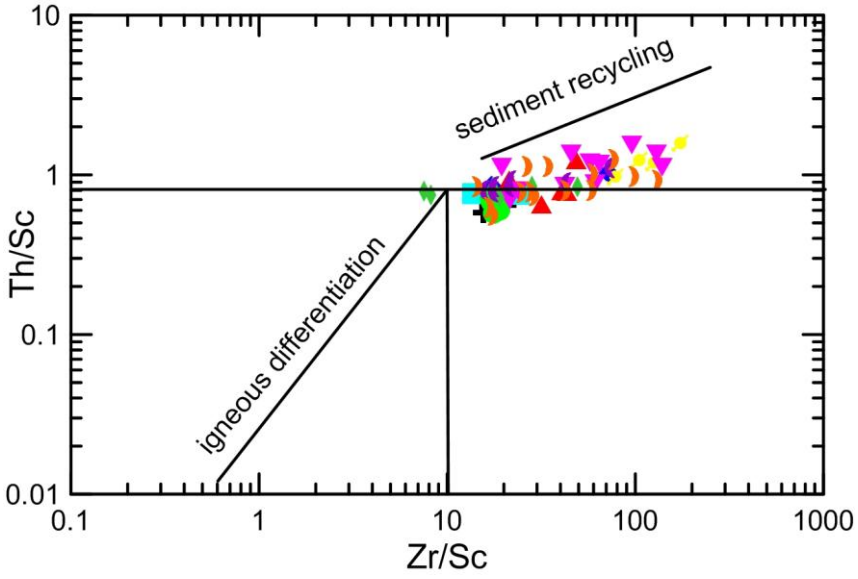

Fig. 3.3.4 Th/Sc versus Zr/Sc plot (after McLennan et al., 1993). Samples depart from the compositional trend indicating zircon addition suggestive of recycling effect in the source area. The legend is same as in Fig. 3.3.3.

Zr is referred to the physically and chemically ultra-stable mineral zircon that can indicate the effect of recycling in the source area. In the binary plot, all the studied samples demonstrate a linearly increasing compositional trend toward a higer ratio of Zr/Sc. These results suggest that the increase in the zircon concentration in the source area has undergone recycling before the transport of sediments to the Tarfaya basin. In addition, the Zr/Hf ratios can also be used to monitor the recycling in the source area. The results show that average Zr/Hf ratios in the studied samples of the various stratigraphic units in the Tarfaya basin are higher (24.3-82.0, average 41.7) when compared with UCC (32.8, Taylor and McLennan, 1985), indicating that these higher ratios are possibly the result of recycling in the source area.

3.3.5.3 Climatic and tectonic control on weathering

As we know, the clay mineral concentration is widely controlled by climate, tectonics and lithology of the source region. As far as the lithology of Tarfaya basin sediments is concerned, the source rocks of the Tarfaya basin sediments are characterized by granitic and metamorphosed rocks (Mauritanides) of the Reguibat shield (West African Craton) in the SW of the basin and by sedimentary (sandstones and carbonates) and low-grade metamorphosed rocks of the western Anti-Atlas in the NE of the basin. The Tarfaya basin sediments have been derived from the acidic rocks of these two source areas since the Upper Cretaceous, and hence, there is no change in lithology. The sedimentation rate to the Tarfaya basin is highly controlled by tectonic activities in the Atlas system which are occurred fistly in Upper Cretaceous (early Alpine orogeny) and secondly large-scale tectonic activities in Miocene-Pliocene. On the other hand, The West African Craton has acted as a cratonic source area since 1700 Ma (Michard et al., 2008). Therefore, the variation in clay mineral abundance is mainly controlled by changes in climate and tectonic activity in the western Anti-Atlas. The higher concentrations of illite and kaolinite in the Turonian and Santonian are associated with the tectonic activity that occurred in the Atlas system at that time (Frizon de Lamotte et al., 2009). The high abundance of kaolinite together with the higher ratios of kaolinite/illite, Al_2O_3/Na_2O and TiO_2/Na_2O (Fig. 3.3.6) indicates intense chemical weathering of the soil in the source area during Turonian and Santonian times. These findings are similar to that of El Albani et al. (1999). The extremely high content of corrensite in Campanian reflects the digenetic alteration of smectite into corrensite under oxic conditions. A higher concentration of palygorskite is found in Early Eocene sediments and is associated with the weathering of the nearby coastal area under warm and dry conditions. Higher corrensite contents, which are also attributed to the diagenetic alteration of

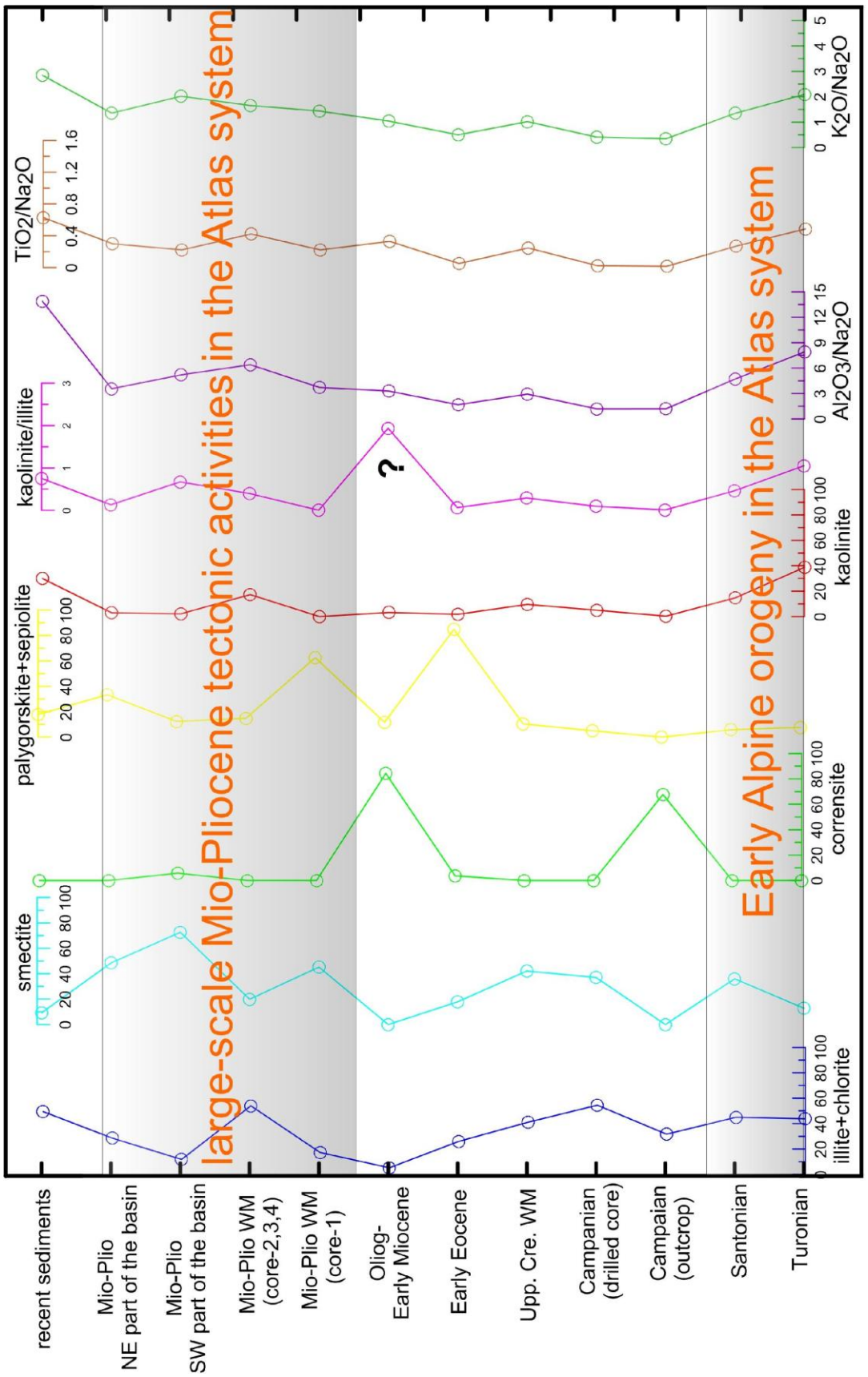

Fig.6. Average clay mineral assemblages from Late Cretaceous to recent time including Upper Cretaceous and Mio-Pliocene weathered marls, compared with geochemical data. ?=high uncertainty in kaolinite/illite ratio due to very high corrensite content. WM=weathered marl.

smectite under oxic conditions, occurred again in the Oligocene-Early Miocene sediments. According to Ruiz et al. (2010), large-scale uplift took place in the western Anti-Atlas during the Middle Miocene-Pliocene and is associated with a high denudation rate. The Miocene-Pliocene coarse-grained sediments are widely distributed throughout the Tarfaya basin. The clay minerals are mainly dominated by illite and smectite; traces of chlorite indicate their detrital derivation and dominant physical erosion of the sediments under dry climatic conditions. The higher concentration of kaolinite and the higher ratios of kaolinite/illite, Al_2O_3/Na_2O and TiO_2/Na_2O in modern river sediments suggest warm and more humid climatic conditions in the river drainage basins. Palygorskite in recent sediments reflects its derivation from Sahara desert soil, which formed under arid conditions.

The weathered marls from the Upper Cretaceous and the Miocene-Pliocene weathering horizons indicate a differential *in situ* climatic influence on the weathering of these sediments. Illite and chlorite are variable within Upper Cretaceous and Miocene-Pliocene weathered marls (Fig. 3.3.6). However, their average abundance in the Upper Cretaceous and Miocene-Pliocene are more or less similar and hence indicate similar climatic conditions during this time. On the other hand, the average abundance of smectite and kaolinite are significantly variable, and a higher concentration of smectite and low Kaolinite are associated with the Upper Cretaceous weathered marls, whereas a higher abundance of kaolinite and low smectite are associated with the Miocene-Pliocene sediments. These higher concentrations in the Upper Cretaceous weathered marls indicate dry and less-humid climatic conditions and less-intense chemical weathering than those for the weathered marls of the Miocene-Pliocene. In addition, drilled core-1 samples (Miocene-Pliocene) show an extremely high concentration of palygorskite. This suggests weathered marl formation in the drilled core-1 samples formation indicate dry climatic conditions, which might be attributable to the core-1 location further landward.

3.3.6 Conclusions

The clay mineralogy of the Tarfaya basin sediments from the Upper Cretaceous to recent time has been examined with the aim of identifying the climatic and tectonic controls on weathering since the Upper Cretaceous, as the sediment sources are unchanged. The clay minerals in the Tarfaya basin sediments predominantly consist of illite, chlorite, smectite, kaolinite, palygorskite, sepiolite and corrensite. The clay mineral abundances are variable in the different stratigraphic units indicating variable climatic and tectonic control on the weathering and erosion of sediments.

The higher transportation of clay minerals is associated with the tectonic events that first occurred during the beginning of the Upper Cretaceous and secondly in Miocene-Pliocene. The climatic conditions constrain the intensity of chemical weathering of the rocks in the source area. The higher abundance of smectite and kaolinite during the Turonian and Santonian are associated with the first tectonic event in the Atlas system and the formation of kaolinite under warm and humid climatic conditions. The second event, which occurred during the Miocene-Pliocene, is mainly associated with the transportation of smectite and illite in high abundance and with the extremely low kaolinite content, which is associated with warm and semi-arid climatic conditions during this time. Highly abundant corrensite during the Campanian and Oligocene-Early Miocene indicate its diagenetic alteration from smectite under oxic conditions. An extremely high concentration of palygorskite occurred during the Early Eocene indicating dry conditions in the nearby coastal areas. The higer abundance of kaolinite and the high kaolinite/illite ratios together with the higher Al_2O_3/Na_2O and TiO_2/Na_2O ratios suggest warm and more humid climatic conditions in the river drainage basins. The presence of palygorskite in the recent river sediments shows its aeolian derivation from the Sahara desert.

The weathered horizons from the Upper Cretaceous and Miocene-Pliocene have undergone a variable intensity of chemical weathering and hence reveal the different climatic conditions occurring during that time. The Miocene-Pliocene weathered marls were formed under more intense chemical weathering conditions as compared with the Upper Cretaceous weathered marls. However, in drilled core-1 (Miocene-Pliocene), weathered marl formation seems to be associated with dry climatic conditions; this might be attributable to the location of core-1 being further landward.

The higher ratio of SiO_2/Al_2O_3 suggests that the Tarfaya basin sediments are chemically mature. An increase in the Zr/Sc ratio reflects the increase in zircon concentration suggests that the source area has undergone recycling before the transport of sediments to the Tarfaya basin. Moreover, the higher Zr/Hf ratio also supports recycling in the source area.

3.3.7 Acknowledgements

We thank RWE Dea for funding this project. We also thank ONHYM for supporting, organizing and accompanying the field campaign in March-April, 2009 and drilling in September-December, 2009. We would like to thank colleagues at “State Key Laboratory of Marine Geology, Tongji University (China)” for measurement of clay minerals and instructions to improve manuscript.

Chapter 4

General Conclusions

This study is part of the project “Atlantic Margin Intergraded Basin Analysis, Morocco”. The main focus was to investigate rock types, tectonic settings, provenances and climatic and tectonic control on weathering in the source area as well as recycling in the source region from Early Cretaceous to recent time. The general conclusions are given in the following paragraphs…

For the petrographic studies, medium- and coarse-grained sandstones were selected from the Early Cretaceous and Miocene-Pliocene as well as recent sediment samples from river wadis and dunes. These clastic sediments indicate variable mineralogical compositions. Early Cretaceous sandstones contain more K-feldspar than that of Miocene-Pliocene and recent sediments. On the basis of major elements geochemistry, the analyzed siliciclastics are characterized by moderate SiO_2 contents and variable abundances of Al_2O_3, K_2O, Na_2O and ferromagnesian elements. Early Cretaceous sandstones, based on petrographic classification, are classified as subarkosic in composition, while Miocene-Pliocene sandstones and recent sediments are generally carbonate-rich feldspathic or lithic arenites. However, sandstone samples of the Sebkha Aridal section (SW part of the basin) and drilled cores-1 from the Miocene-Pliocene are similar in composition to that of the Early Cretaceous sandstones. The classification of coarse-grained siliciclastics based on major elements geochemistry supports the petrographic findings. Further, the fine-grained siliciclastics also show large range of SiO_2/Al_2O_3.

Binary tectonic discrimination diagrams based on major elements distribution i.e. SiO_2% versus K_2O/Na_2O, Fe_2O_3*+MgO versus Al_2O_3/SiO_2 and $Fe2O_3$*+MgO versus TiO_2% suggest that the Early Cretaceous to recent sediments in the Tarfaya basin were deposited at the tectonically stable passive Atlantic continental margin of NW Africa. In addition, trace elements based on Ti/Zr-La/Sc binary and La-Th-Sc ternary relationships also suggest that the Tarfaya basin sediments were deposited in passive margin depositional settings. Heavy minerals, further, support the deposition of the basin sediments in tectonically stable passive margin setting.

The source rocks of the Tarfaya basin sediments are revealed by the analysis of the heavy minerals, especially hornblende and garnet grains geochemical analysis and trace elements geochemistry including rare earth elements (REE). Hornblende and

garnets grains from Miocene-Pliocene and recent sediments suggest that the Tarfaya basin sediments are derived from the granitic rocks of the Reguibat shield, high grade metamorphic rocks of the Mauritanides, low grade metamorphosed or unmetamorphosed sedimentary rocks of the western Anti-Atlas. Trace elements composition and their ratios as well as REE distribution constrain the composition of the source rocks. Low concentrations of Cr (<150ppm) and Ni (<100ppm) and their correlation suggest that the sediments of the Tarfaya basin are derived from felsic sources. This is supported by trace element ratios of La/Sc, Th/Sc, La/Co, Th/Co and Cr/Th that are similar to those of sediments derived from felsic source rocks. Moreover, chondrite-normalized REE patterns with light REE enrichment, a flat pattern of heavy REE and negative Eu anomalies can also be attributed to a felsic rock source for the Tarfaya basin sediments.

The West African Craton in the SW of the Tarfaya basin and western Anti-Atlas in the NE, principally supply sediments to the Tarfaya basin. The West African Craton is containing two different age terrains: (1) the older Archean terrain (3.04-2.83 Ga), and (2) the younger Eburnean terrain (2.12-2.06 Ga) and metamorphosed Mauritanides. On the other hand, the western Anti-Atlas is containing predominantly Paleozoic sedimentary cover of which sediments are derived from Precambrian inliers and/or West African Craton. This western Anti-Atlas sedimentary cover was affected by low grade metamorphism during Atlas system tectonics (Veriscan orogeny).

The calculated provenance ages in the Early Cretaceous Boukhchebat section of 2.2 Ga in average are comparable with the Eburnean terrane indicating that the source is in the northern part of the West African Craton (Fig. 4.1A). The homogeneously negative Nd isotope values and restricted Sm/Nd ratios also indicate their passive margin depositional tectonic setting, old provenance and long sedimentary recycling. In addition, the petrographic data and SiO_2/Al_2O_3 ratios support cratonic and recycled source areas for Early Cretaceous sediments. The Early to Late Cretaceous transition in provenance is marked by a shift toward more positive $\varepsilon_{Nd}(0)$ values and a decrease in $^{87}Sr/^{86}Sr$ ratios. This shift is attributed to an initial sediment supply from the western Anti-Atlas as a consequence of uplifting and erosion due to the convergence of the African and Eurasian plates triggering compressional tectonics in the Atlas system. The Late Cretaceous to Early Eocene fine-grained and Miocene-Pliocene coarse-grainded sediments (from both the SW and NE parts of the Tarfaya basin) produce a narrow range of provenance ages of 1.7 to 1.8 Ga (average 1.8 Ga) and 1.6 to 1.8 Ga (average 1.8 Ga), respectively. The similarity in the $\varepsilon_{Nd}(0)$ values during the Miocene-Pliocene from both parts of the Tarfaya basin indicates the same source areas for Miocene-Pliocene sediments, and hence, these sediments

demonstrate similar provenance ages (1.8Ga) being younger than those of the Early Cretaceous sediments. These provenance age groups signify the first contribution of sediments from the western provenance ages of 1.7 to 1.8 Ga (average 1.8 Ga) and

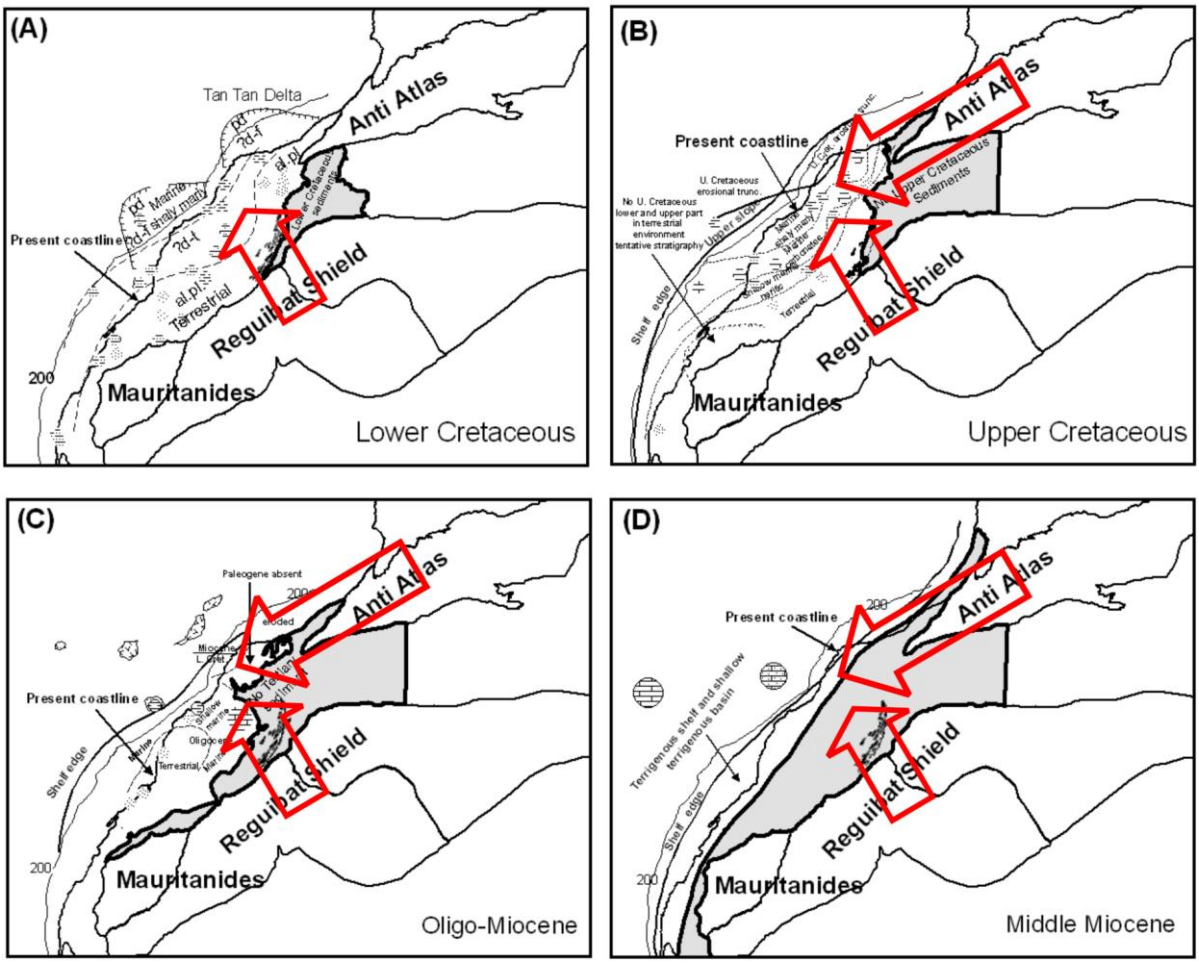

Fig.4.1 Paleogeographic evolution of the Tarfaya basin (modified from Ranke, 1982): (A) Early Cretaceous, (B) Late Cretaceous, (C) Oligo-Miocene, (D) Middle Miocene. Present coastline and -200 m contour for comparison. Land-based part of the Tarfaya basin in grey and red arrow showing direction of sedimentation.

1.6 to 1.8 Ga (average 1.8 Ga), respectively. The similarity in the $\varepsilon_{Nd}(0)$ values during the Miocene-Pliocene from both parts of the Tarfaya basin indicates the same source areas for Miocene-Pliocene sediments, and hence, these sediments demonstrate similar provenance ages (1.8Ga) being younger than those of the Early Cretaceous sediments. These provenance age groups signify the first contribution of sediments from the western Anti-Atlas source areas to the Tarfaya basin during the Late Cretaceous (Fig. 4.1B). There is no change in provenance ages record due to intense tectonic activity in the western Anti-Atlas which occurred during Middle Miocene-Pliocene time as there is similarity in provenance ages since Late Cretaceous (Fig. 4.1B, C and D). Further, three samples from the Sebkha Aridal section (south most section in the present study) of the Tarfaya basin show the most

negative $\varepsilon_{Nd}(0)$ values and hence the oldest provenance ages (average 2.5 Ga). These provenance ages are higher than Eburnean (2.12-2.06Ga) and lower than the Archean terrane (3.04-2.83Ga) indicating that these provenance ages were produced by a mixing of detritus from both these terranes. In addition, provenance ages from recent river sediments which are derived from West African Craton and western Anti-Atlas directly constrain provenance of these recent sediments. One samples from "Oued El Craa" of which sediments are directly derived from West African Craton suggest provenance ages of 2.2 Ga which are similar to Eburnean terrain (2.12-2.06 Ga). This indicates that no change has occurred in the gross isotopic composition in the West African Craton source areas between the Early Cretaceous until the present day because of unroofing processes in the Eburnean terrane. Two other samples from "Oued Draa and Seguit El Hamra" samples whose sediments are derived from the western Anti-Atlas suggest a provenance age 1.7 Ga for the western Anti-Atlas source area. Finally, a fourth sample whose sediments are possibly derived from both the West African Craton and the western Anti-Atlas source areas suggest a 1.9 Ga provenance age for these mixed source-derived sediments.

.The clay mineralogy of Tarfaya basin sediments from Late Cretaceous to recent times was examined, with the aim to identify the climatic and tectonic control on weathering since the sediments sources remained unchanged during this whole time period. Clay minerals in the Tarfaya basin sediments predominantly consist of illite, chlorite, smectite, kaolinite, palygorskite, sepiolite and corrensite. Clay mineral abundances are variable in different stratigraphic units indicating variable climatic and tectonic control on weathering and erosion of sediments.

Periodical higher abundances of specific clay minerals are associated with the tectonic events which occurred firstly in the beginning of the Late Cretaceous and secondly the Middle Miocene-Pliocene. The climatic conditions constrain intensity of chemical weathering of rocks in the source area. Higher abundance of smectite and kaolinite during the Turonian and Santonian are associated with first tectonic event in the Atlas system and formation of kaolinite under warm and humid climatic conditions. The second event which occurred during Miocene-Pliocene is mainly associated with the transport of smectite and illite in high abundance and very low kaolinite content which is associated with warm and semi-arid climatic conditions during this time. Highly abundant corrensite during Campanian and Oligocene-Early Miocene indicate its diagenetic alteration from smectite under oxic conditions. Very high concentration of palygorskite occurs during Early Eocene which indicates dry conditions near by coastal areas. The higer abundance of kaolinite and kaolinite/illite ratios along with higher Al_2O_3/Na_2O and TiO_2/Na_2O suggest warn and more humid

climatic conditions in the river drainage basins. The presence of palygorskite in the recent river sediments shows its aeolian derivation from the Sahara desert.

References

Abdel-Wahab AA (1992) Provenance of Gebel El-Zeit sandstones, gulf of Suez, Egypt. Sedimentary Geolgy 75:241–255.

Almon WR, Fullerton LB, Davies DK (1976) Pore space reduction in Cretaceous sandstones through chemical precipitation of clay minerals. Journal of Sedimentary Petrology 46:89-96.

Anani C (1999) Sandstone petrology and provenance of the Neoproterozoic Voltaian Group in the southeastern Voltaian Basin, Ghana. Sedimentary Geology 128:83–98.

Armstrong-Altrin JS, Lee YI, Verma SP, Ramasamy S (2004) Geochemistry of Sandstones from the Upper Miocene Kudankulam Formation, Southern India: Implications for Provenance, Weathering, and Tectonic Setting. Journal of Sedimentary Research 74:285–297.

Arthur MA, von Rad U, Cornford C, McCoy FC, Sarnthein M (1979) Evolution and Sedimentary history of the Cape Bojador continental margin, Northwestern Africa. In: Ryan WBF, von Rad U, et al. Init Reps DSDP 47 (1): 773-816.

AUXINI (Departamento de Investigaciones Petroliferas de AUXINI 1969) Correlacion estratigraphica de los sondeos perforados en el Sahara espanol. Bol Geol Minero, Madrid 83:235-251.

Barrat JA, Keller F, Amossé J, Taylor RN, Nesbitt RW, Hirata T (1996) determination of rare earth elements in sixteen silicate reference samples by icp-ms after tm addition and ion exchange separation. Geostandards Newsletter 20:133–139.

Basu A, Young SW, Suttner LJ, James WC, Mack GH (1975) Re-evaluation of the use of undulatory extinction and polycrystallinity in detrital quartz for provenance interpretation. Journal of Sediment Petrology 45:873-882.

Bau M (1999) Scavenging of dissolved yttrium and rare earths by precipitating iron oxyhydroxide: experimental evidence for Ce oxidation, Y-Ho fractionation, and lanthanide tetrad effect. Geochimica et Cosmochimica Acta 63:67-77.

Bau M, Dulski P, Moller P (1995) Yttrium and holmium in South Pacific seawater: vertical distribution and possible fractionation mechanisms. chem Erde-Geochemistry 55:1-15.

References

Bauluz B, Mayayo MJ, Fernandez-Nieto C, Gonzalez Lopez JM (2000) Geochemistry of Precambrian and Paleozoic siliciclastic rocks from the Iberian Range (NE Spain): implications for source-area weathering, sorting, provenance, and tectonic setting. Chemical Geology 168:135–150.

Bayon G, German CR, Boella RM, Milton JA, Taylor RN, Nesbitt RW (2002) An improved method for extracting marine sediment fractions and its application to Sr and Nd isotopic analysis. Chemical Geology 187:179–199.

Berrenchea JF, Rodas M, Frey M, Alonso-Azcarate J, Mas JR (2000) Chlorite, corrensite and chlorite-mica in Late Jurassic fluvio-Lacustraine sediments of the Cameros basin of northeastern Spain. Clay and Clay Minerals 48:256-265.

Bettison-Varga L, Mackinnon IDR (1997) The role of randomly mixed-layered chlorite/smectite in the transformation of smectite to chlorite. Clays and clay minerals 45:506-516.

Bhatia MR (1983) Plate tectonics and geochemical composition of sandstones. Journal of Geology 91:611–627.

Bhatia MR (1984) Composition and classification of Paleozoic flysch mudrocks of eastern Australia: Implications in provenance and tectonic setting interpretation. Sedimentary Geology 41:249–268.

Bhatia MR (1985) Rare earth element geochemistry of Australian Paleozoic graywackes and mudrocks: Provenance and tectonic control. Sedimentary Geology 45:97–113.

Bhatia MR, Crook KAW (1986) Trace element characteristics of graywackes and tectonic setting discrimination of sedimentary basins. Contribution to Mineralogy and Petrology 92:181–193.

Blatt H (1967) Original characteristics of quartz grains. Journal of Sediment Petrology 37: 401-424.

Bock B, McLennan SM, Hanson GN (1994) Rare earth element redistribution and its effects on the neodymium isotope system in the austin Glen Member of the Normanskill Formation, New York, USA. Geochimica et Cosmochimica Acta, 58:5245–5253.

Boulay S, Colin C, Trentesaux A, Frank N, Liu Z (2005) Sediment sources and East Asian monsoon intensity over the last 450 ky. Mineralogical and geochemical investigations on South China Sea sediments. Palaeogeography, Palaeoclimatology, Palaeoecology 288:260-277.

Chamley H (1989) Clay Sedimentology, Springer-Verlag, Heidelberg, Germany, pp 623.

Chamley H, Deconinck JF, Millot G (1990) Sur l'abondance des mineraux smectitiques dans les sediments marins communs deposes lors des periodes de haut niveau marin du Jurassique superieur au Paleogene. Comptes Rendus Academic science 311:1529-1536.

Chang HK, Mackenzie FT, Schoonmaker J (1986) Comparisions between the diagenesis of dioctahedral and trioctahedral smectite, Brazilian offshore basins. Clays and clay minerals 34:407-423.

Choubert G, FaureMuret A, Hottinger L (1966) Apercu geologique du bassin cotier de Tarfaya. Notes et Mem Serv Geol Maroc (I):7-106.

Cohen AS, O'Nions RK, Siegenthaler R, Griffin WL (1988) Chronology of the pressure-temperature history recorded by a granulite terrain. Contributions to Mineralogy and Petrology 98:303–311.

Cole JM, Goldstein SL, de Menocal PB, Hemming SR, Grousset FE (2009) Contrasting compositions of Saharan dust in the eastern Atlantic Ocean during the last deglaciation and African Humid Period. Earth and Planetary Science Letters 278:257–266.

Conceptian RAB, Dimalanta CB, Yumul GP, Faustino-Eslava DV, Queano KL, Tamayo RA, Imai A (2012) Petrography, geochemistry, and tectonics of a rifted fragment of Mainland Asia: evidence for the Lasala Formation, Mindoro Island, Philippines. International Journal of Earth Sciences 101:273-290.

Cox R, Lowe DR, Cullers RL (1995) The influence of sediment recycling and basement composition on evolution of mudrock chemistry in the southwestern United States. Geochimica et Cosmochimica Acta 59:2919–2940.

Crook KAW (1974) Lithogenesis and geotectonics: the significance of compositional cariations in flysch arenites (graywackes), In: Dott, RH, Shaver, RH (eds)

Modern and Ancient Geosynclinal Sedimentation. Society for Sedimentary Geology Special Publication 19:304-310.

Cullers RL (1994) The controls on the major and trace element variation of shales, siltstones, and sandstones of Pennsylvanian-Permian age from uplifted continental blocks in Colorado to platform sediment in Kansas, USA. Geochimica et Cosmochimica Acta 58:4955–4972.

Cullers RL (2000) The geochemistry of shales, siltstones and sandstones of Pennsylvanian–Permian age, Colorado, USA: implications for provenance and metamorphic studies. Lithos 51:181–203.

Cullers RL, Graf J (1983) Rare earth elements in igneous rocks of the continental crust: intermediate and silicic rocks, or petrogenesis. *Rare-Earth Geochemistry*, Elsevier, Amsterdam, 275-312.

Cullers RL, Podkovyrov VN (2000) Geochemistry of the Mesoproterozoic Lakhanda shales in southeastern Yakutia, Russia: implications for mineralogical and provenance control, and recycling. Precambrian Research 104:77–93.

Datta B (2005) Provenance, tectonics and palaeoclimate of Proterozoic Chandarpur sandstones, Chattisgarh Basin: a petrographic view. Journal of Earth System Sciences 114:227-245.

Debrabant P, Fagel N, Chamley H, Bout V, Caulet JP (1993) Neogene to Quaternary caly mineral fluxes in the Central Indian basin. Paleogeograhy Paleoclimatology Paleoecology 103:117-131.

Deconinck JF, Chamley H (1995) Diversity of smectite origins in Late Cretaceous sediments: example of chalks from northern France. Clay Minerals 30:365-379.

Deer WA, Howie RA, Zussman J (1992) An introduction to the Rock-Forming Minerals (eds) Longman Scientific & Technical, Hong Kong.

Dickinson WR (1970) Interpreting detrital modes of greywacke and arkose. Journal of Sediment Petrology 40:695-707.

Dickinson WR (1985) Interpreting provenance relation from detrital modes of sandstones, in Zuffa GG (eds) Provenance of arenites: NATO ASI series, C 148, D. Reidel Publishing Company, Dordrecht, pp 333-363.

Dickinson WR, Suczek CA (1979) Plate tectonics and sandstone compositions. American Association of Petroleum Geology Bulletin 63:2164-2182.

Dickinson WR, Beard LS, Brakenridge GR, Rejavec JL, Ferguson RC, Inman KF, Kneep FA, Linberg FA, Ryberg PT (1983) Provenance of North American Phanerozoic sandstones in relation to tectonic setting. Geological Society of American Bulletin 94:222–235.

Depaolo DJ (1980), Sources of Continental Crust: Neodymium Isotope Evidence from the Sierra Nevada and Peninsular Ranges. Science 209:684–687.

DePaolo DJ (1981) Neodymium isotopes in the Colorado Front Range and crust–mantle evolution in the Proterozoic. Nature 291:193–196.

Dillon RS, Sougy JHA (1974) Geology of West Africa and canary and Cape Verde Island. In: Nairn AEM, Stehli FG (eds) The ocean basins and margins, 2. The North Atlantic: New York (Plenum Press): 315-390.

El Albani A, Kuhnt W, , Luderer F, Herbin JP, Caron M (1999) Palaeoenvironmental Evolution of the Late Cretaceous Sequence in the Tarfaya Basin (southwest of Morocco). Journal of Geological Society London Special Publication 153:223–240.

Esquevin J (1969) Influence de la composition chimique des illites surcristallinite. Bulletin Central Research Rau SNPA 3:147-153.

Etemad-Saeed N, Hosseini-Barzi M, Armstrong-Altrin JS (2011) Petrography and geochemistry of clastic sedimentary rocks as evidences for provenance of the Lower Cambrian Lalun Formation, Posht-e-badam block, Central Iran. Journal of African Earth Sciences 61:142–159.

Faundez V, Herve F, Lacassie JP (2002) Provenance and depositional setting of pre-Late Jurassic turbidite complexes in Patagonia, Chile. New Zealand Journal of Geology and Geophysics 45:411-425.

Fedo CM, Nesbitt HW, Young GM (1995) Unravelling the effects of potassium metasomatism in sedimentary rocks and paleosols, with implications for paleoweathering conditions and provenance. Geology 23:921-924.

Feng R, Kerrich R (1990) Geochemistry of fine-grained clastic sediments in the Archean Abitibi greenstone belt, Canada: Implications for provenance and tectonic setting. Geochimica et Cosmochimica Acta 54:1061–1081.

Le Fèvre B, Pin C (2005), A straightforward separation scheme for concomitant Lu–Hf and Sm–Nd isotope ratio and isotope dilution analysis. Analytica Chimica Acta 543:209–221.

Folk RL (1974) Petrology of Sedimentary Rocks: Austin TX, Hemphill Press, second edition, pp 182.

Frizon de Lamotte D, Leturmy P, Missenard Y, Khomsi S, Ruiz G, Saddiqi O, Guillocheau F, Michard A (2009) Mesozoic and Cenozoic vertical movements in the Atlas system (Algeria, Morocco, Tunisia): an overview. Tectonophysics 475:9–28.

Garbe-Schönberg C-D (1993) simultaneous determination of thirty-seven trace elements in twenty-eight international rock standards by ICP-MS. Geostandards Newsletter 17: 81–97.

Garver JI, Royce PR, Smick TA (1996) Chromium and Nickel in Shale of the Taconic Foreland; a Case Study for the Provenance of Fine-Grained Sediments with an Ultramafic Source. Journal of Sedimentary Research 66:100–106.

Gertsch B, Adatte T, Keller G, Tantawy AAAM, Berner Z, Mort HP, Fleitmann D (2010) Middle and late Cenomanian oceanic anoxic events in shallow and deeper shelf environments of western Morocco. Sedimentology 57:1430–1462.

Ghosh S, Sarkar S (2010) Geochemistry of Permo-Triassic mudstone of the Satpura Gondwana basin, central India. Clues for provenance. Chemical Geology 277:78–100.

Ghosh S, Sarkar S, Ghosh P (2012) Petrography and major element geochemistry of the Permo-Triassic sandstones, central India: Implications for provenance in an intracratonic pull-apart basin. Journal of Asian Earth Sciences 43:207–240.

Gibson TG, Bybell LM, Mason DB (2000) Stratigraphic and climatic implications of clay minerals changes around the Paleocene-Eocene boundary of the northeastern US margin. Sedimentary Geology 134:65-92.

Gingele FX, De Deckker P, Hillenbrand C-D (2001) Clay mineral distribution in surface sediments between Indonesia and NW Australia-source and transport by ocean currents. Marine Geology 179:135-146.

Gu X (1994) Geochemical characteristics of the Triassic Tethys-turbidites in northwestern Sichuan, China: Implications for provenance and interpretation of the tectonic setting. Geochimica et Cosmochimica Acta 58:4615–4631.

Hafid M, Tari G, Bouhadioui D, El Moussaid I, Echarfaoui H, A it Salem A, Nahim M, Dakki M (2008) Atlantic basins. In: A Michard, O Saddique, A Chalouan, D Frizon de Lamotte (eds), The Atlas System, Continental Evolution: The Geology of Morocco. Springer, Heidelberg, pp 303-328.

Hallam A, Grose JA, Ruffel AH (1991) Paleoclimatic significance of changes in clay mineralogy across the Jurassic-Cretaceous boundary in England and France. Palaeogeography Palaeoclimatology Palaeoecology 81:173-187.

Hassan S, Ishiga H, Roser BP, Dozen K, Naka T (1999) Geochemistry of Permian–Triassic shales in the Salt Range, Pakistan: implications for provenance and tectonism at the Gondwana margin. Chemical Geology 158:293–314.

Herron MM (1988) Geochemical classification of terrigenous sands and shales from core or log data. Journal of Sediment Petrology 58:820–829.

Hillier S (1993) Origin, diagenesis and mineralogy of chlorite minerals in Devonian lacustrine mudrocks, Orcadian Basin, Scotland. Clays and clay minerals 41:240-259.

Hiscott RN (1984) Ophiolitic Source Rocks for Taconic-Age Flysch: Trace-Element Evidence. Geological Society of America Bulletin 95:1261–1267.

Hong H, Li Z, Xue H, Zhu Y, Zhang K, Xiang S (2007) Oligocene clay mineralogy of the Linxia basin: evidence of palaeoclimatic evolution subsequent to the initial-stage uplift of the Tibetan plateau. Clays and Clay Minerals 55:492-505.

Horwitz EP, Chiarizia R, Dietz ML (1992) A novel strontium-selective extraction chromatographic resin, Solvent Extraction and Ion Exchange 10:313–336.

Hurlbut CS, Klein C (1993). Dana's Manual of Mineralogy (19th eds) John Willey and Sons, New York, pp 681.

Hutcheon I, Oldershaw A, Ghent ED (1980) Diagenesis of Cretaceous sandstones of the Kootenay Formation at Elk Valley (Southeast British Columbia) and Mt. Allan (Southwest Alberta). Geochimica et Cosmochimica Acta 44:1425-1435.

Ingersoll RV, Bullard TF, Ford RL, Grimm JP, Pickle JD, Sares SW (1984) The effect of grain size on detrital modes: a test of the Gazzi–Dickinson point-counting method. Journal of Sediment Petrology 54:03– 116.

Jiang WT, Peacor DR (1994a) Formation of corrensite, chlorite and chlorite-mica stacks by replacement of detrital biotite in low-grade pelitic rocks. Journal of Metamorphic Geology 12:867-884.

Jiangn WT, Peacor DR (1994b) Prograde transition of corrensite and chlorite in low-grade pelitic rocks from the Gaspe Peninsula, Quebec. Clays and clay minerals 42: 497-517.

Keller G, Adatte T, Berner Z, Chellai EH, Stüben D (2008) Oceanic events and biotic effects of the Cenomanian-Turonian anoxic event, Tarfaya Basin, Morocco. Cretaceous Research 29:976–994.

Kolonic S, Wagner T, Forster A, Damsté JSS, Walsworth-Bell B, Erba E , Turgeon S, Brumsack HJ, Chellai EH, Tsikos H, Kuhnt W, Kuypers MMM (2005) Black shale deposition on the northwest African Shelf during the Cenomanian/Turonian oceanic anoxic event: Climate coupling and global organic carbon burial. Paleoceanography 20:17.

Krumm S, Buggisch W (1991) Sample preparation effects on illite crystallinity measurements: Grain size gradation and particle orientation. Journal of Metamorphic Petrology 9:671-677.

Kuhnt W, Holbourn A, Gale A, Chellai EH, Kennedy WJ (2009) Cenomanian Sequence Stratigraphy and Sea-Level Fluctuations in the Tarfaya Basin (SW Morocco). Geological Society of American Bulletin 121:1695–1710.

Kuhnt W, Luderer F, Nederbragt S, Thurow J, Wagner T (2005) Orbital-scale record of the late Cenomanian–Turonian oceanic anoxic event (OAE-2) in the Tarfaya Basin (Morocco). International Journal of Earth Sciences 94:147–159.

Kuhnt W, Nederbragt A, Leine L (1997) Cyclicity of Cenomanian-Turonian organic-carbon-rich sediments in the Tarfaya Atlantic Coastal Basin (Morocco). Cretaceous Research 18:587–601.

Lahondere D, Thieblemont D et al. (2003) Notice explicative des cartes geologiques a 1/200.000 et 1/500.000 du nord dela Mauritanie, DMG, Ministere Mines Industrie, Nouakchott.

Leake BE, Woolley AR, Arps CES, Birch WD, Gilbert MC, Grice JD, Hawthorne FC, Kato A, Kisch HJ, Krivovichev VG, Linthout K, Laird J, Mandaring JA, Maresch WV, Nickel EH, Rock NMS, Schumacher JC, Smith DC, Stephenson NCN, Ungaretti L, Whittaker EJW, Youzhi G (1997) Nomenclature of amphiboles: report of the subcommittee on amphiboles of the International Mineralogical Association, comission on new minerals and mineral names. Canadian Mineralogist 35:pp 219±246.

Le Maitre RW (1976) The chemical variability of some common igneous rocks. Journal of Petrology 17:589-637.

Li G, Peacor DR, Essene EJ (1998) The formation of sulfides during alteration of biotite to chlorite-corrensite. Clays and clay minerals 46:649-657.

Liang M, Guo Z, Kahmann AJ, Oldfield F (2009) Geochemical characteristics of the Miocene eolian deposits in China: their provenance and climate implications. Geochemistry Geophysics Geosystems 10. doi:10.1029/2008GC002331.

Liu Z, Colin C, Huang W, Le Phone K, Tong S, Chen Z, Trentesaux A (2007) Climatc and tectonic controls on weathering in south China and Indochina Peninsula: Clay mineralogical and geochemical investigations from the Pearl, Red, and Mekong drainage basins. Gechemistry Geophysics Geosystems 8, Q05005, doi:10.1029/2006GC001490.

Liu J, Muhong C, Zhong C, Wen Y (2010) Clay mineral distribution in surface sediments of the South China Sea and its significance for in sediment sources and transport. Chinese Journal of Oceanology and Limnology 28:407-415.

Madhavaraju J, Ramasamy S, Ruffell A, Mohan SP (2002) Clay mineralogy of the Late Cretaceous and early Tertiary successions of the Cauvery basin (southeastern India): implications for sediment source and palaeoclimates at the K/T boundary. Cretaceous Research 23:153-163.

Mange MA, Maurer HFW (1992) Heavy minerals in colour. Chapman and Hall, London, pp147.

Mange MA, Morton AC (2007) Geochemistry of heavy minerals. In: Mange MA, Wright DK (eds) Heavy Minerals In Use. Developments in Sedimentology 58: pp 345-391.

Maynard JB, Valloni R, Yu H (1982) Composition of modern deep sea sands from arc-related basins. Journal of Geological Society London Specical Publication 10:551-561.

McCulloch MT, Wasserburg GJ (1978) Sm-Nd and Rb-Sr Chronology of Continental Crust Formation. Science 200:1003–1011.

McDaniel DK, Hemming SR, McLennan SM, Hanson GN (1994) Resetting of neodymium isotopes and redistribution of REEs during sedimentary processes: The Early Proterozoic Chelmsford Formation, Sudbury Basin, Ontario, Canada. Geochimica et Cosmochimica Acta 58:931–941.

McLennan SM (1989) Rare Earth Elements in Sedimentary Rocks; Influence of Provenance and Sedimentary Processes. Reviews in Mineralogy and Geochemistry 21:169–200.

McLennan SM (1993) Weathering and global denudation. Journal of Geology 101:295-303.

McLennan SM (2001) Relationships between the trace element composition of sedimentary rocks and upper continental crust: Geochemistry Geophysics Geosystems 2, 24 , doi: 2001 10.1029/2000GC000109.

McLennan SM, Nance WB, Taylor SR (1980) Rare earth element-thorium correlations in sedimentary rocks, and the composition of the continental crust. Geochimica et Cosmochimica Acta 44:1833-1839.

McLennan SM, Taylor SR (1991) Sedimentary Rocks and Crustal Evolution: Tectonic Setting and Secular Trends. The Journal of Geology 99:1–21.

McLennan SM, Taylor SR, Eriksson KA (1983) Geochemistry of Archean shales from the Pilbara Supergroup, Western Australia. Geochimica et Cosmochimica Acta 47:1211–1222.

McLennan SM, Taylor SR, , McDaniel DK, Hanson GN (1993) Geochemical approaches to sedimentation, provenance and tectonics, in Processing Controlling the Composition of Clastic Sediments, edited by M.J. Johnson and A. Basu, Special Publication Geological Society of America 284:21-40.

McLennan SM, Taylor SR, McCulloch TM, Maynard JB (1990) Geochemical and Nd-Sr isotopic composition of deep-sea turbidites: Crustal evolution and plate tectonic associations. Geochimica et Cosmochimica Acta 54:2015–2050.

Mearns EW, Knarud R, Ræstad N, Stanley KO, Stockbridge CP (1989) Samarium-Neodymium Isotope Stratigraphy of the Lunde and Statfjord Formations of Snorre Oil Field, Northern North Sea. Journal of the Geological Society 146:217–228.

Meyer I, Davies GR, Stut JBW (2011), Grain size control on Sr-Nd isotope provenance studies and impact on paleoclimate reconstructions: An example from deep-sea sediments offshore NW Africa: Geochemistry Geophysics Geosystems 12, 14 ., doi: 201110.1029/2010GC003355.

Meunier A, Clement JI, Bouchet A, Beaufort D (1988) Chlorite-calcite and corrensite-dolomite crystallization during two superimposed events of hydrothermal alteration in the “Les Cretes” granite, Vosgues, France. Canadian Mineralogist 26:413-426.

Michard A, Sadiqi O, Chalouan A, Frizon de Lamotte D (2008) Continental Evolution: The Geology of Morocco. Springer-Verlag, Berlin, pp 424.

Middelburg JJ, van der Weijden CH, Woittiez JRW (1988) Chemical processes affecting the mobility of major, minor and trace elements during weathering of granitic rocks. Chemical Geology 68:253–273.

Millot G (1970) Geology of Clays. Springer-Verlag, Berlin, pp 499.

Mort HP, Adatte T, Föllmi KB, Keller G, Steinmann P, Matera V, Berner Z, Stüben D (2007) Phosphorus and the Roles of Productivity and Nutrient Recycling During Oceanic Anoxic Event 2. Geology 35:483–486.

Mort HP, Adatte T, Keller G, Bartels D, Föllmi KB, Steinmann P, Berner Z, Chellai EH (2008) Organic carbon deposition and phosphorus accumulation during Oceanic Anoxic Event 2 in Tarfaya, Morocco. Cretaceous Research 29:1008–1023.

Morton AC (1985) Heavy minerals in provenance studies. In: Zuffa, GG (ed) Provenance of arenites: NATO ASI series, C 148, D. Reidel Publishing Company, Dordrecht, pp 249-227.

Morton AC (1991) Geochemical studies of detrital heavy minerals and their application to provenance research. In: Morton AC, Todd SP, Haughton PDW (eds) Developments in Sedimentary Provenance studies. Geological Society of London Special Publication 57:31-45

Morton AC, Davies JR, Waters RA (1992) Heavy minerals as a guide to the turbidite provenaces in the Lower Paleozoic South Welsh Basin: a pilot study. Geological Magazine 129:573-580.

Morton AC, Hallsworth C (1994) Identifying provenance-specific features of detrital heavy mineral assemblages in sandstones. Sedimentary Geology 90:241-256

Morton AC, Hallsworth C, Chalton B (2004) Garnet compositions in Scottish and Norwegian basement terrains: a framework for interpretation of North Sea sandstone provenance. Marine and Petroleum Geology 21:399-410.

Nechaev VP, Isphording WC (1993) Heavy mineral assemblages of continental margins as indicators of tectonic settings environments. Journal of Sedimentary Petrology 63:1110–1117.

Nesbitt HW, Markovics G, price RC (1980) Chemical processes affecting alkalis and alkaline earths during continental weathering. Geochimica et Cosmochimica Acta 44:1659–1666.

Nesbitt HW, Young YM (1982) Early Proterozoic climates and plate motions inferred from major element chemistry of lutites. Nature 299:715–717.

Nesbitt HW, Young GM, McLennan SM, Keays RR (1996) Effects of Chemical Weathering and Sorting on the Petrogenesis of Siliciclastic Sediments, with Implications for Provenance Studies. The Journal of Geology 104:525–542.

O'Nions RK, Hamilton PJ, Hooker PJ (1983) A Nd isotope investigation of sediments related to crustal development in the British Isles. Earth and Planetary Science Letters 63:229–240.

Petschick R, Kuhn G, Gingele F (1996) Clay mineral distribution in surface sediments of the South Atlantic: sources, transport and relation to oceanography. Marine Geology 130:203-229.

Pettijohn FJ, Potter PE, Siever R (1987) Sand and sandstones. Springer-Verlag. New York, pp 553.

Ratschiller LK (1970) Lithostratigraphy of the northern Spanish Sahara. Memorie Museo Tridentino Sci Trento 18:1-18.

Ranke U, von Rad U, Wissmann G (1982) Stratigraphy, facies, and tectonic development of on- and offshore Aaiun–Tarfaya Basin-a review. In: von Rad U, Hinz-K, Sarnthein M, Seibold E (eds) Geology of the North West African Continental Margin. Springer-Verlag, pp 86–104.

Robert C, Chamley H (1991) Development of Early Eocene warm Climates as inferred from clay mineral variations in oceanic sediments. Palaeogeography Palaeoclimatology Palaeoecology 89:315-331.

Robert C, Gauthier A, Chamley H (1984) Origine autochtone et allochtone des argiles recentes de haute altitude en Corse. Geol. Medit 11:243-253.

Roddaz M, Said A, Guillot S, Antoine PO, Montel J-M, Martin F, Darrozes J (2011) Provenance of Cenozoic Sedimentary Rocks from the Sulaiman Fold and Thrust Belt, Pakistan: Implications for the Palaeogeography of the Indus Drainage System. Journal of the Geological Society 168:499–516.

Roser BP, Cooper RA, Nathan S, Tulloch AJ (1996) Reconnaissance sandstone geochemistry, provenance and tectonic settings of the Lower Paleozoic terraines of the West Coast and Nelson, New Zealand. New Zealand Journal of Geology Geophysics 39:1-16.

Roser BP, Korsch RJ (1986) Determination of tectonic setting of sandstone–mudstone suites using SiO2 content and K2O/Na2O ratio. Journal of Geology 94:635–650.

Roser BP, Korsch RJ (1988) Provenance signatures of sandstone–mudstone suites determined using discrimination function analysis of major-element data. Chemical Geology 67:119–139.

Roy PD, Caballaeroa M, Lozanoc R, Smykatz-Klossd W (2008) Geochemistry of late quaternary sediments from teccomulco lake, central Mexico: implicaitions to chemical weathering and provenance. Chemie der Erde 68:383-393.

Ruiz G, Sebti S, Negro F, Saddiqi O, Frizon de Lamotte D, Stockli D, Foeken J, Stuart F, Barbarand J, Schaer JP (2010) From central Atlantic continental rift to Neogene uplift – western Anti-Atlas (Morocco). Terra Nova 23:35–41.

Sabeen HM, Ramanujam N, Morton AC (2002) The provenance of garnet: Constraints provided by studies of coastal sediments from southern India. Sedimentary Geology 152: 279-287.

Schofield DI, Gillespie MR (2007) A tectonic interpretation of “Eburnean terrane” outliers in the Reguibat Shield, Mauritania. Journal of African Earth Sciences 49:179–186.

Schofield DI, Horstwood MSA, Pitfield PEJ, Crowley QG, Wilkinson AF, Sidaty HCO (2006) Timing and Kinematics of Eburnean Tectonics in the Central Reguibat Shield, Mauritania. Journal of the Geological Society 163:549–560.

Schmidt S Th, Robinson D (1997) Metamorphic grade and porosity and permeability controls on mafic phyllosilicates distributions in a regional zeolite to greenschist facies transition of the North Shore Volcanic Group, Minnesota. Geological Society of America Bulletin 109:683-697.

Shaun YH, Peacor DR, Essene EJ (1990) Corrensite and mixed-layer chlorite/corrensite in metabasalt from northern Taiwan: TEM/AEM, EMPA, XRD, and optical studies. Contribution to Mineralogy and Petrology 105:123-142.

Steiger RH, Jäger E (1977) Subcommission on geochronology: Convention on the use of decay constants in geo- and cosmochronology. Earth and Planetary Science Letters 36:359–362.

Suresh N, Ghosh SK, Kumar R, Sangode SJ (2004) Clay mineral distribution patterns in Late Neogene fluvial sediments of the Subathu sub-basin, central sector of Himalayan foreland basin: implications for provenance and climate. Sedimentary Geology 163:256-278.

Tanaka T, Togashi S, Kamioka H, Amakawa H, Kagami H, Hamamoto T, Yuhara M, Orihashi Y, Yoneda S, Shimizu H, Kunimaru T, Takahashi K, Yanagi T, Nakano T et al. (2000) JNdi-1: a neodymium isotopic reference in consistency with LaJolla neodymium. Chemical Geology 168:279–281.

Taylor SR, McLennan SM (1985) The Continental Crust: Its Composition and Evolution. Blackwell, Oxford, pp 312.

Tomadin L, Lenaz R, Landuzzi V, Mazzucotelli A, Vannuci R (1984) On wind-blown dusts over the central Mediterranean. Oceanologica Acta 7:13-24.

Vail PR, MItchum Jr RM, Thompson III S (1977) Global cycles of relative changes of sea level. In: Vail PR et al. (eds) Seismic Stratigraphy and global changes of sea level. American Association of Petroleum Geology Memoir 26: 83-98.

von Eynatten H (2003) Petrography and chemistry of sandstones from the Swiss Molasse Basin: an archive of the Oligocene to Miocene evolution of the central Alps. Sedimentology 50:703-724.

von Eynatten H, Gaupp R (1999) Provenance of Cretaceous synorogenic sandstones in the eastern Alps: constraints from framework petrography, heavy mineral analysis and mineral chemistry. Sedimentary Geology 124:81-111.

von Rad U, Wissmann G (1982) Cretaceous-Cenozoic History of the West Saharan Continental Margin (NW Africa). In: von Rad U, Hinz k, Sarnthein M, Seibold E (eds) Geology of the North West African Continental Margin. Springer-Verlag, pp 106–131.

Wade BP, Hand M, Barovich KM (2005) Nd isotopic and geochemical constraints on provenance of sedimentary rocks in the eastern Officer Basin, Australia: implications for the duration of the intracratonic Petermann Orogeny. Journal of the Geological Society 162:513–530.

Wiedmann J, Butt A, Einsele G (1978) Cretaceous stratigraphy, environment and subsidence history at the Moroccan continental margin. In: von Rad, U., Hinz, K., Sarnthein, M. and Seibold, E. (ed.) Geology of the Northern African Continental Margin. Springer 366-395.

Wrafter' JP, Graham JR (1989) Short Paper: Ophiolitic Detritus in the Ordovician Sediments of South Mayo, Ireland. Journal of the Geological Society 146:213–215.

Wronkiewicz DJ, Condie KC (1990) Geochemistry and mineralogy of sediments from the Ventersdorp and Transvaal Supergroups, South Africa: Cratonic evolution during the early Proterozoic. Geochimica et Cosmochimica Acta 54:343–354.

Wronkiewicz DJ, Condie KC (1987) Geochemistry of Archean shales from the Witwatersrand Supergroup, South Africa: Source-area weathering and provenance. Geochimica et Cosmochimica Acta 51:2401–2416.

Xie S , Wu Y, Gao S, Liu X, Zhou L, Zhao L, Hu Z (2012) Sr–Nd isotopic and geochemical constraints on provenance of late Paleozoic to early cretaceous

sedimentary rocks in the Western Hills of Beijing, North China: Implications for the uplift of the northern North China Craton. Sedimentary Geology 245–246:17–28.

Zhang KJ, Zhang YX, Li B, Zhong LF (2007) Nd isotopes of siliciclastic rocks from Tibet, western China: Constraints on provenance and pre-Cenozoic tectonic evolution. Earth and Planetary Science Letters 256: 604–616.

Zimmermann U, Bahlburg H (2003) Provenance analysis and tectonic setting of the Ordovician clastic deposits in the southern Puna Basin, NW Argentina. Sedimentology 50:1079–1104.

Zuffa GG (1980) Hybrid arenites: their composition and classification. Journal of Sediment Petrology 50:21–29.

Zuffa GG (1985) Optical analysis of arenites: Influence of methodology on compositional results. In: Zuffa GG (ed) Provenance of arenites: NATO Advance study series 148:165-189.

Zuffa GG (1987) Unravelling hinterland and offshore paleo-geography from deep water arenites. In: Leggett JK, Zuffa GG (eds) Marine Clastic Sedimentology, Model and Case Studies (Volume in Memory of C Tarquin Teale): London, Grahan & Trotman, pp 39-61.

Appendix

Table 3.1.1. Modal gross composition of analyzed Lower Cretaceous and Mio-Pliocene sandstones and recent sediments

			in %										NCE+CE+CI+NCI %			QFL %		
Sections	Stratigraphic age	Sa. no.	Qm	Qp	Ch	P	K	Ls	LM	CE	CI	NCI	NCE	CE	CI+NCI	Q(Qm+Qp)	F	L+CE
Boukhchebat	Lower Cretaceous	27--02	75.9	5.5	2.6	2.1	11.3	0.0	2.6	0.0	0.0	0.0	100.0	0.0	0.0	84.0	13.4	2.6
"	"	27--03	85.1	1.9	2.5	1.9	7.6	0.0	1.0	0.0	0.0	0.0	100.0	0.0	0.0	89.5	9.5	1.0
"	"	27--04	84.5	2.4	2.1	1.5	8.8	0.0	0.6	0.0	0.0	0.0	100.0	0.0	0.0	89.1	10.3	0.6
"	"	27--05	82.1	3.1	2.5	1.3	9.7	0.0	1.3	0.0	0.0	0.0	100.0	0.0	0.0	87.7	11.0	1.3
"	"	27--08	76.4	6.3	1.4	2.4	11.4	0.0	2.2	0.0	0.0	0.0	100.0	0.0	0.0	84.0	13.9	2.2
"	"	27--11	80.9	5.4	2.1	2.7	7.5	0.0	1.5	0.0	0.0	0.0	100.0	0.0	0.0	88.4	10.1	1.5
"	"	27--12	81.8	5.0	1.9	1.9	8.5	0.0	0.9	0.0	0.0	0.0	100.0	0.0	0.0	88.7	10.4	0.9
"	"	27--13	83.3	2.9	2.3	1.4	8.9	0.0	1.1	0.0	0.0	0.0	100.0	0.0	0.0	88.5	10.3	1.1
"	"	27--14	75.3	4.2	5.8	2.5	11.7	0.0	0.6	0.0	0.0	0.0	100.0	0.0	0.0	85.3	14.2	0.6
"	"	27--15	76.5	3.8	6.7	2.0	10.4	0.0	0.6	0.0	0.0	0.0	100.0	0.0	0.0	87.0	12.5	0.6
"	"	27--24	85.1	2.4	2.4	2.1	7.9	0.0	0.0	0.0	0.0	0.0	100.0	0.0	0.0	90.0	10.0	0.0
"	"	27--26	84.1	2.7	3.0	1.8	7.3	0.0	0.9	0.0	0.0	0.0	100.0	0.0	0.0	89.9	9.1	0.9
"	"	27--27	78.9	7.1	2.6	1.5	8.3	0.0	1.5	0.0	0.0	0.0	100.0	0.0	0.0	88.7	9.8	1.5
"	"	27--28	76.9	7.3	3.1	2.1	9.1	0.0	1.4	0.0	0.0	0.0	100.0	0.0	0.0	87.4	11.2	1.4
Sebkha Aridal	Mio-Pliocene	16--18	71.4	5.8	5.8	2.1	11.2	0.0	3.6	0.0	0.0	0.0	100.0	0.0	0.0	83.0	13.4	3.6
"	SW part of basin	16--19	72.5	5.4	2.2	2.6	13.7	0.0	3.5	0.0	0.0	0.0	100.0	0.0	0.0	80.2	16.3	3.5
"	"	16--20	74.6	4.1	5.0	3.5	8.8	0.0	3.8	0.0	0.0	0.0	100.0	0.0	0.0	83.8	12.4	3.8
"	"	16--21	83.2	2.2	2.8	2.5	8.1	0.0	1.2	0.0	0.0	0.0	100.0	0.0	0.0	88.2	10.6	1.2
Sebkha El Farma	"	17--32	58.0	1.5	2.7	9.2	4.2	2.7	0.7	18.4	1.0	1.5	79.1	18.4	2.5	63.8	13.8	22.4
"	"	17--35	52.1	2.0	9.0	10.1	3.1	7.3	1.4	12.4	0.0	2.5	85.1	12.4	2.5	64.7	13.6	21.7
"	"	17--36	62.3	2.1	3.2	5.8	4.8	14.3	0.5	3.2	1.3	2.4	93.1	3.2	3.7	70.2	11.0	18.7
"	"	17--37	52.1	5.2	4.3	6.2	6.9	16.4	2.4	1.4	1.7	3.3	93.6	1.4	5.0	64.9	13.8	21.3
"	"	17--38	55.4	8.9	3.4	5.8	7.4	9.1	3.6	1.9	1.4	3.1	93.5	1.9	4.6	70.9	13.8	15.3
Sebkha El Farma1	"	18--03	70.0	2.8	3.8	5.0	3.2	4.4	3.2	5.0	0.0	2.5	92.4	5.0	2.5	78.6	8.4	12.9
"	"	18--05	57.0	3.4	6.9	15.0	1.9	0.9	0.9	12.8	0.0	1.2	86.0	12.8	1.2	68.1	17.0	14.8
"	"	18--07	43.5	2.5	7.6	15.0	0.6	10.5	1.4	15.3	1.1	2.5	81.1	15.3	3.7	55.7	16.1	28.2
"	"	18--08	50.2	6.8	6.4	8.7	7.7	6.4	1.9	7.4	3.2	1.3	88.1	7.4	4.5	66.3	17.2	16.5
Sebkha El Farma2	"	18--25	48.8	0.8	6.0	13.8	3.5	8.9	1.6	12.5	2.4	1.6	83.5	12.5	4.1	57.9	18.1	24.0
"	"	18--26	54.1	5.6	6.2	12.4	2.4	5.6	2.6	9.1	1.2	0.9	88.8	9.1	2.1	67.3	15.0	17.7
"	"	18--27	52.3	3.8	8.2	12.5	0.5	4.4	1.4	13.4	1.1	2.5	83.1	13.4	3.5	66.7	13.6	19.8
"	"	18--28	58.2	4.7	5.8	4.1	6.1	4.7	2.3	8.5	3.5	2.0	86.0	8.5	5.6	72.8	10.8	16.4

Sebkha El Farma3	"	18--40	61.9	1.7	10.7	9.0	1.3	2.7	1.7	9.7	0.0	1.3	89.0	9.7	1.3	75.3	10.5	14.2
Oued El Khatt	"	19--02	56.1	9.8	7.3	7.5	4.7	2.0	4.2	6.7	0.0	1.7	91.6	6.7	1.7	74.4	12.5	13.1
"	"	19--03	58.8	4.5	7.2	9.6	4.2	1.2	3.3	9.3	0.0	2.1	88.7	9.3	2.1	72.0	14.0	14.0
"	"	19--06	57.1	7.3	6.2	8.4	6.2	1.6	3.2	8.9	0.0	1.1	90.0	8.9	1.1	71.4	14.7	13.9
"	"	19--07	70.2	5.2	4.8	8.3	2.8	2.8	1.4	2.4	0.0	2.1	95.5	2.4	2.1	82.0	11.3	6.7
"	"	19--08	66.7	7.7	5.4	6.3	4.8	1.7	3.1	3.4	0.0	0.9	95.7	3.4	0.9	80.5	11.2	8.3
"	"	19--12	63.3	8.5	6.6	5.7	2.8	2.2	2.8	7.0	0.0	0.9	92.1	7.0	0.9	79.2	8.6	12.1
"	"	19--14	64.6	3.4	7.1	7.7	4.0	2.8	2.5	6.2	0.0	1.8	92.0	6.2	1.8	76.5	11.9	11.6
Oued Itghi	"	21--10	55.9	6.1	7.5	8.9	6.3	2.0	4.0	8.1	0.0	1.2	90.8	8.1	1.2	70.3	15.5	14.3
"	"	21--11	57.0	4.5	6.5	8.1	5.3	2.2	2.2	11.0	1.1	2.0	86.0	11.0	3.1	70.1	13.9	15.9
Sebkha Tah (E)	Mio-Pliocene	20--07	65.0	2.5	7.1	9.0	5.9	0.6	1.7	6.5	0.0	1.7	91.8	6.5	1.7	75.9	15.2	8.9
"	NE part of basin	20--09	62.0	3.1	4.8	1.7	4.5	5.4	1.7	7.6	5.9	3.1	83.3	7.6	9.1	76.9	6.9	16.2
Sebkha Tah (W)	"	20--23	72.2	1.8	3.9	8.1	5.7	0.6	1.2	6.6	0.0	0.0	93.4	6.6	0.0	77.8	13.8	8.4
"	"	20--26	67.8	3.2	3.2	7.4	9.4	0.9	2.1	4.7	0.0	1.2	94.1	4.7	1.2	75.2	17.0	7.8
"	"	20--27	70.4	2.6	6.0	8.3	6.3	0.9	1.7	3.7	0.0	0.0	96.3	3.7	0.0	79.0	14.7	6.3
"	"	20--28	70.8	2.5	5.1	9.0	7.3	0.0	2.0	3.4	0.0	0.0	96.6	3.4	0.0	78.4	16.3	5.3
"	"	20--29	71.0	2.1	6.3	8.8	7.6	1.2	1.2	1.8	0.0	0.0	98.2	1.8	0.0	79.5	16.3	4.2
"	"	20--30	69.6	2.3	6.1	6.7	10.5	0.6	0.9	2.3	0.0	0.9	96.8	2.3	0.9	78.8	17.4	3.8
Oumdaboua	"	20--36	66.9	7.2	5.6	6.4	4.5	1.3	4.0	2.1	1.1	0.8	96.0	2.1	1.9	81.3	11.1	7.6
"	"	20--37	63.5	8.0	5.6	7.6	4.9	2.1	1.4	3.1	1.0	2.8	93.1	3.1	3.8	80.1	13.0	6.9
"	"	20--39	56.2	4.8	5.5	7.8	4.4	8.0	3.0	6.4	1.8	2.1	89.7	6.4	3.9	69.2	12.6	18.1
"	"	20--40	64.2	3.5	5.9	4.9	3.8	3.5	2.1	7.6	2.1	2.4	87.8	7.6	4.5	77.1	9.1	13.8
"	"	20--42	63.7	3.0	8.0	6.0	3.0	3.0	1.3	8.7	0.7	2.7	88.0	8.7	3.3	77.2	9.3	13.4
Sebkha Tisfourine	"	23--15	60.3	6.7	7.7	6.5	5.1	2.6	2.8	4.4	1.6	2.3	91.6	4.4	3.9	77.8	12.1	10.1
Itzetene	"	23--29	48.4	4.9	10.7	5.5	3.6	10.1	2.9	12.7	0.0	1.3	86.0	12.7	1.3	64.8	9.2	26.0
"	"	23--30	49.5	5.2	10.7	6.4	4.6	8.9	2.4	10.7	0.0	1.5	87.8	10.7	1.5	66.5	11.2	22.4
"	"	23--31	54.1	4.8	9.9	5.5	3.1	6.5	2.4	11.6	0.7	1.4	86.3	11.6	2.1	70.3	8.7	21.0
"	"	23--32	58.3	6.3	7.3	6.0	3.7	5.0	1.7	9.7	0.7	1.3	88.3	9.7	2.0	73.5	9.9	16.7
Onhym Quarry	"	24--09	65.9	4.0	7.4	7.4	4.6	2.9	2.3	2.6	0.6	2.3	94.6	2.6	2.9	79.6	12.4	8.0
"	"	24--10	56.5	3.2	4.0	4.0	3.2	3.2	2.2	19.8	0.0	4.0	76.3	19.8	4.0	66.3	7.5	26.2
"	"	24--12	60.8	5.4	4.7	7.6	3.9	4.9	2.2	7.6	1.7	1.2	89.5	7.6	2.9	73.0	11.9	15.2
"	"	24--13	64.5	3.3	5.8	3.6	2.8	5.8	1.9	7.2	3.3	1.9	87.6	7.2	5.2	77.6	6.7	15.7
"	"	24--15	56.5	4.9	9.1	4.2	3.9	4.2	1.1	14.0	0.7	1.4	83.9	14.0	2.1	72.0	8.2	19.7
"	"	24--16	59.2	4.2	8.0	6.1	3.1	5.0	1.9	11.5	0.0	1.1	87.4	11.5	1.1	72.2	9.3	18.5
Amma Fatma	"	26--30	53.6	4.6	6.8	7.7	4.3	7.1	1.7	10.3	0.0	4.0	85.8	10.3	4.0	67.7	12.5	19.9
"	"	26--31	50.4	4.2	8.4	7.6	4.7	10.0	1.8	8.1	1.8	2.9	87.1	8.1	4.7	66.1	12.9	20.9
"	"	26--33	54.5	4.2	9.5	7.1	3.9	7.7	1.2	8.3	1.2	2.4	88.1	8.3	3.6	70.7	11.4	17.9

"	"	26--34	69.3	0.7	4.1	1.5	4.9	5.2	0.0	4.9	6.7	2.6	85.8	4.9	9.4	81.8	7.0	11.2
Core-1	"	C1--01	84.3	4.5	2.6	2.2	5.1	0.0	1.3	0.0	0.0	0.0	100.0	0.0	0.0	91.3	7.4	1.3
"	"	C1--02	85.5	3.5	3.5	1.6	4.7	0.0	1.3	0.0	0.0	0.0	100.0	0.0	0.0	92.4	6.3	1.3
"	"	C1-03	80.0	5.1	2.9	1.7	8.6	0.0	1.7	0.0	0.0	0.0	100.0	0.0	0.0	88.0	10.3	1.7
"	"	C1--04	82.5	3.6	4.8	1.5	6.3	0.0	1.2	0.0	0.0	0.0	100.0	0.0	0.0	91.0	7.8	1.2
"	"	C1--05	81.1	2.5	4.5	2.0	7.3	0.0	2.5	0.0	0.0	0.0	100.0	0.0	0.0	88.2	9.3	2.5
"	"	C1--08	84.9	2.0	3.8	2.3	5.8	0.0	1.2	0.0	0.0	0.0	100.0	0.0	0.0	90.7	8.1	1.2
Core-2	"	C2--01	69.6	2.1	4.8	3.7	2.4	6.1	0.5	7.7	2.1	1.1	89.2	7.7	3.2	79.0	6.3	14.8
"	"	C2--02	61.6	2.7	4.2	8.1	2.4	3.9	0.0	9.3	5.1	2.7	82.9	9.3	7.8	74.3	11.4	14.3
Core-3	"	C3--01	66.1	3.5	7.0	5.1	2.4	5.6	0.0	2.2	5.6	2.4	89.8	2.2	8.1	83.3	8.2	8.5
"	"	C3--03	61.2	6.7	9.0	6.5	3.9	3.4	0.0	2.2	5.3	1.7	90.7	2.2	7.0	82.8	11.2	6.0
Core-4	"	C4--01	58.1	2.4	4.3	6.5	2.8	7.6	1.7	12.5	3.2	0.9	83.4	12.5	4.1	67.6	9.7	22.7
"	"	C4--02	61.9	2.2	4.6	5.1	2.7	4.6	0.7	15.9	1.4	1.0	81.7	15.9	2.4	70.4	7.9	21.7
"	"	C4--03	61.9	1.9	3.3	5.7	2.1	7.3	0.5	12.8	3.1	1.4	82.7	12.8	4.5	70.3	8.2	21.5
"	"	C4--05	65.4	1.8	2.3	5.8	2.8	5.6	1.0	11.1	2.3	2.0	84.6	11.1	4.3	72.6	9.0	18.5
"	"	C4--07	73.1	1.1	3.4	6.0	2.6	2.9	0.9	6.0	2.3	1.7	90.0	6.0	4.0	80.9	9.0	10.1
"	"	C4--08	78.8	1.3	2.8	4.4	1.6	3.1	1.9	3.4	2.2	0.6	93.8	3.4	2.8	85.2	6.1	8.7
"	"	C4--11	69.8	1.4	4.6	6.0	2.5	5.4	1.9	5.2	1.6	1.6	91.6	5.2	3.3	78.3	8.7	13.0
"	"	C4--13	65.9	1.4	3.5	6.5	2.2	5.7	0.5	7.9	3.5	2.7	85.8	7.9	6.3	75.6	9.3	15.1
"	"	C4--14	71.5	0.9	5.5	3.5	1.2	4.9	0.9	7.6	1.7	2.3	88.4	7.6	4.1	81.2	4.8	13.9
Seguit El Hamra	Pleistocene	07--04	84.9	3.6	1.7	1.7	4.5	0.6	2.2	0.8	0.0	0.0	99.2	0.8	0.0	90.2	6.2	3.6
Oued Draa	Recent Sediments	06--01	51.7	2.0	8.9	3.7	1.5	23.3	1.5	7.4	0.0	0.0	92.6	7.4	0.0	62.6	5.2	32.2
Oued Draa	"	06--03	51.1	2.7	6.0	2.0	1.0	26.8	1.2	9.2	0.0	0.0	90.8	9.2	0.0	59.8	3.0	37.2
Tan-Tan River	"	06--04	67.0	4.2	7.2	6.6	2.7	4.2	2.4	5.7	0.0	0.0	94.3	5.7	0.0	78.4	9.3	12.3
Tan-Tan River	"	06--05	71.6	3.0	5.1	3.6	1.5	8.5	0.9	5.7	0.0	0.0	94.3	5.7	0.0	79.8	5.1	15.1
Oued Chebeika	"	06--06	67.3	5.5	2.6	7.0	5.2	4.4	2.9	5.0	0.0	0.0	95.0	5.0	0.0	75.5	12.2	12.2
Cap Jubi	"	08--02	44.2	2.3	4.9	4.9	2.8	5.4	3.1	27.4	4.9	0.0	67.7	27.4	4.9	54.1	8.2	37.8
Oued Akhfennir	"	09--01	47.9	2.2	5.3	2.9	1.0	7.5	1.9	27.4	3.9	0.0	68.8	27.4	3.9	57.7	4.0	38.3
Oued Akhfennir	"	09--02	46.9	2.7	4.2	3.5	1.5	6.0	1.0	27.0	7.2	0.0	65.8	27.0	7.2	58.0	5.3	36.6
Ouel El Craa	"	14--01	56.4	5.1	3.3	2.4	1.1	7.0	2.2	20.1	2.4	0.0	77.5	20.1	2.4	66.4	3.6	30.0
Laayoune Plage	"	15--10	45.8	3.4	7.1	1.7	4.7	13.8	2.0	14.3	7.1	0.0	78.6	14.3	7.1	60.7	6.9	32.4
Tarfaya E beach	"	18--03a	42.8	3.7	7.2	2.6	8.1	11.2	1.5	18.0	4.8	0.0	77.2	18.0	4.8	56.5	11.3	32.3
Tarfaya E beach	"	18--04a	48.1	4.5	6.8	3.8	5.6	9.4	1.4	16.7	3.8	0.0	79.6	16.7	3.8	61.7	9.8	28.5

Qm=monocrystalline quartz
Qp=polycrystalline quartz
Ch=chert
P=plagioclase
K=k-feldspar
Ls=sedimentary lithic fragments
LM=metamorphic lithic fragments
CE=extrabasinal carbonate
NCI=intrabasinal non-carbonate
NCE= extrabasinal non-carbonate
CI= intrabasinal carbonate

Table 3.1.2. Heavy mineral data of analyzed Lower Cretaceous and Mio-Pliocene sandstones and recent sediments

Sections	Stratigraphic age	Sa. no.	Zircon	Tourmaline	Rutile	Garnet	hornblende	Epidote	Staurolite	Sphene	Apatite
Boukhchebat	Lower cretaceous	27--02	67.9	17.9	8.0	3.1	3.1	0.0	0.0	0.0	0.0
"	"	27--05	66.1	17.6	8.8	3.5	4.0	0.0	0.0	0.0	0.0
"	"	27--08	69.0	19.4	6.5	2.8	2.3	0.0	0.0	0.0	0.0
"	"	27--11	65.3	15.7	13.2	2.1	3.7	0.0	0.0	0.0	0.0
"	"	27--12	59.3	18.1	11.9	2.3	8.5	0.0	0.0	0.0	0.0
"	"	27--13	70.1	11.8	7.0	4.3	7.0	0.0	0.0	0.0	0.0
"	"	27--24	51.7	25.6	8.1	4.7	9.9	0.0	0.0	0.0	0.0
"	"	27--26	57.2	16.8	13.9	5.2	6.9	0.0	0.0	0.0	0.0
"	"	27--28	63.2	19.0	11.3	3.5	3.0	0.0	0.0	0.0	0.0
Sebkha Aridal	Oligo-Early Miocene	16--02	41.9	12.1	4.8	6.5	19.4	5.6	0.0	6.5	3.2
"	"	16--05	48.0	6.4	17.6	8.8	19.2	0.0	0.0	0.0	0.0
"	"	16--07	22.5	30.6	8.8	5.6	24.4	5.0	1.3	0.0	1.9
"	"	16--10	34.8	14.1	8.7	13.0	22.8	0.0	2.2	0.0	4.3
"	"	16--14	42.9	12.3	11.7	4.5	27.3	0.0	0.0	0.0	1.3
Sebkha	Mio-Pliocene	16--18	27.8	7.9	5.3	31.8	16.6	4.6	0.0	6.0	0.0
Aridal	SW part of basin	16--19	27.6	7.5	6.9	30.5	12.1	3.4	3.4	7.5	1.1
"	"	16--20	25.9	6.3	5.2	28.2	13.8	6.3	4.0	9.2	1.1
"	"	16--21	21.6	9.4	6.5	27.3	14.4	6.5	2.9	8.6	2.9
Sebkha El Farma	"	17--32	35.3	5.1	3.8	7.1	41.7	5.1	0.0	1.9	0.0
"	"	17--37	34.7	5.2	5.8	6.9	41.0	4.0	0.0	2.3	0.0
Sebkha El Farma1	"	18--03	9.3	2.1	2.1	3.6	78.8	2.1	2.1	0.0	0.0
"	"	18--05	7.9	2.6	3.1	3.1	81.7	1.6	0.0	0.0	0.0
"	"	18--07	8.5	3.7	2.1	2.1	77.7	2.7	3.2	0.0	0.0
"	"	18--08	8.2	4.1	2.6	3.1	76.5	3.1	2.6	0.0	0.0
Sebkha El Farma2	"	18--26	35.2	4.8	4.8	2.8	43.4	2.8	2.8	1.4	2.1
"	"	18--28	46.4	3.6	2.9	3.6	35.7	2.9	2.1	2.9	0.0
Sebkha El Farma 3	"	18--40	37.5	2.3	6.8	6.8	36.9	6.3	0.0	3.4	0.0
Oued El Khatt	"	19--06	40.9	8.6	1.1	8.6	19.9	11.3	1.6	8.1	0.0
"	"	19--07	37.9	5.5	3.7	9.6	22.8	13.2	0.0	7.3	0.0
"	"	19--08	47.7	4.7	4.1	6.7	17.1	13.5	0.0	6.2	0.0
"	"	19--12	38.2	3.1	10.7	9.2	22.1	13.7	0.0	3.1	0.0
"	"	19--14	47.7	1.7	6.4	11.0	19.2	9.9	0.0	4.1	0.0
Oued Itghi	"	21--11	58.1	4.7	5.4	9.5	6.8	9.5	2.0	2.7	1.4
Sebkha Tah (E)	Mio-Pliocene	20--07	33.3	24.7	10.7	12.7	14.0	2.0	0.0	0.0	2.7

"	NE part of basin	20--09	37.3	16.9	15.4	20.9	5.5	1.0	3.0	0.0	0.0
Sebkha Tah (W)	"	20--23	32.3	19.0	12.8	20.0	10.8	1.5	0.0	2.1	1.5
"	"	20--26	42.6	16.6	11.2	19.5	5.3	2.4	2.4	0.0	0.0
"	"	20--27	27.2	23.6	10.5	21.5	8.9	6.8	0.0	0.0	1.6
"	"	20--28	48.6	13.0	8.2	15.1	7.5	2.1	0.0	2.7	2.7
"	"	20--29	41.9	16.3	11.9	18.1	5.6	0.0	3.8	1.3	1.3
"	"	20--30	35.6	19.6	15.3	18.4	8.6	2.5	0.0	0.0	0.0
Oumdaboua	"	20--34	38.5	5.2	5.9	3.0	29.6	11.9	0.0	3.0	3.0
"	"	20--36	20.6	2.7	9.0	8.1	43.0	10.8	0.0	4.5	1.3
"	"	20--37	23.0	5.9	8.6	5.3	43.4	9.2	0.0	4.6	0.0
"	"	20--38	40.5	5.9	4.9	5.9	28.1	9.7	0.0	4.9	0.0
"	"	20--40	15.3	8.9	7.6	5.7	51.0	8.3	0.0	3.2	0.0
"	"	20--42	31.3	4.6	5.0	4.6	41.2	10.7	0.0	2.7	0.0
Sebkha Tisfourine	"	23--15	11.7	4.4	3.9	4.4	75.6	0.0	0.0	0.0	0.0
Itzetene	"	23--29	35.3	6.9	2.9	5.2	40.5	6.9	0.0	2.3	0.0
"	"	23--30	36.2	5.6	5.1	3.4	42.4	5.6	0.0	1.7	0.0
"	"	23--31	35.9	6.6	4.8	4.8	41.3	5.4	0.0	1.2	0.0
Onhym Quarry	"	24--09	34.4	11.3	3.3	5.3	32.5	9.9	2.0	0.0	1.3
"	"	24--13	36.3	5.7	1.9	5.1	38.9	8.3	1.3	2.5	0.0
"	"	24--16	34.1	4.0	2.3	4.0	39.9	11.0	1.2	1.7	1.7
Amma Fatma	"	26--30	44.8	3.8	11.5	4.4	26.8	7.7	0.0	1.1	0.0
"	"	26--31	52.5	2.5	1.9	2.5	32.3	5.7	0.0	2.5	0.0
"	"	26--33	39.6	9.6	3.2	9.6	19.3	13.9	0.0	4.8	0.0
"	"	26--34	51.5	2.4	4.8	7.2	24.6	7.2	0.0	2.4	0.0
Core 1	"	C1--01	51.5	18.4	6.6	8.2	8.7	4.1	1.5	1.0	0.0
"	"	C1--02	53.9	16.6	6.2	6.2	9.3	4.1	2.1	1.6	0.0
"	"	C1--03	50.5	19.0	6.5	9.8	9.8	2.2	2.2	0.0	0.0
"	"	C1--04	54.2	19.0	4.5	8.9	8.4	3.9	0.0	1.1	0.0
"	"	C1--05	51.4	20.5	7.6	8.1	7.0	2.2	3.2	0.0	0.0
"	"	C1--06	53.0	23.8	7.0	8.1	6.5	0.0	1.6	0.0	0.0
"	"	C1--08	53.7	11.6	8.9	8.9	10.0	4.7	0.0	2.1	0.0
Core 4	"	C4--01	24.9	5.2	3.5	8.1	56.6	1.7	0.0	0.0	0.0
"	"	C4--02	24.4	4.2	2.4	10.1	55.4	2.4	0.0	1.2	0.0
"	"	C4--03	32.3	6.9	3.2	8.5	47.1	0.0	2.1	0.0	0.0
"	"	C4--05	30.4	7.9	2.1	6.8	49.2	2.6	1.0	0.0	0.0
"	"	C4--07	25.9	5.9	2.9	5.9	55.9	3.5	0.0	0.0	0.0
"	"	C4--08	27.1	5.0	2.2	9.4	51.9	4.4	0.0	0.0	0.0

"	"	C4--11	25.6	8.3	3.0	7.7	54.2	1.2	0.0	0.0	0.0
"	"	C4--13	26.7	5.6	3.6	6.7	53.8	2.6	1.0	0.0	0.0
"	"	C4--14	23.2	8.8	5.0	10.5	50.3	2.2	0.0	0.0	0.0
Seguit El Hamra	Pleistocene	07--04	54.2	5.9	5.9	5.2	21.6	4.6	0.0	2.6	0.0
Oued Draa	Recent Sediments	06--01	13.5	4.5	5.1	4.5	64.0	6.7	0.0	1.7	0.0
Oued Draa	"	06--03	16.1	3.3	2.2	3.3	66.1	5.6	0.0	3.3	0.0
Tan-Tan River	"	06--04	29.0	7.0	4.5	2.5	48.5	4.5	0.0	4.0	0.0
Tan-Tan River	"	06--05	13.8	5.7	4.6	6.3	62.1	6.3	0.0	1.1	0.0
Oued Chebeika	"	06--06	49.1	12.4	4.3	10.6	13.7	8.1	0.0	1.9	0.0
Oued Akhfennir	"	09--01	50.5	6.6	3.3	1.6	34.6	3.3	0.0	0.0	0.0
Oued Akhfennir	"	09--02	50.0	4.6	2.6	3.6	34.0	4.1	0.0	1.0	0.0
Ouel El Craa	"	14--01	67.5	5.2	4.5	15.6	5.2	1.9	0.0	0.0	0.0
Laayoune Plage	"	15--10	15.8	3.0	1.8	6.1	70.9	2.4	0.0	0.0	0.0
Tarfaya E beach	"	18--03a	10.9	4.6	1.7	4.6	76.6	1.7	0.0	0.0	0.0
Tarfaya E beach	"	18--04a	8.8	3.3	2.2	3.9	80.1	1.7	0.0	0.0	0.0

Table 3.1.3. Major element compositions of the sandstones, black shales, sandy marls, weathered marls and sands from Lower Cretaceous to recent

Sections	Stratigraphic age	Rock type	Sa. no.	SiO_2%	Al_2O_3%	TiO_2%	MgO%	Fe_2O_3%	CaO%	P_2O_5%	Na_2O%	K_2O%	MnO%	LOI%	Total	Na_2O*%	SiO_2/Al_2O_3	K_2O/Al_2O_3	Al_2O_3/Na_2O	TiO_2/Na_2O	CIA
Boukhchebat	Lower cretaceous	sandstone	27--02	67.81	3.15	0.11	0.16	0.26	14.87	0.02	0.11	1.93	0.02	12.06	100.55		21.53	0.61	28.64	1.00	56
"	"	sandstone	27--05	89.01	3.74	0.15	0.17	0.55	0.34	0.02	0.12	2.26	UD	5.00	101.44		23.80	0.60	31.17	1.25	57
"	"	sandstone	27--08	60.59	5.55	0.05	0.18	0.23	16.65	0.02	0.17	3.57	0.06	10.66	97.79		10.92	0.64	32.65	0.29	56
"	"	sandstone	27--12	67.28	2.56	0.07	0.19	0.10	15.24	0.02	0.10	1.75	UD	14.50	101.85		26.28	0.68	25.60	0.70	53
"	"	sandstone	27--13	68.98	1.68	0.04	0.07	0.20	14.37	0.03	0.08	1.18	0.02	16.00	102.68		41.06	0.70	21.00	0.50	52
"	"	sandstone	27--14	90.47	2.75	0.08	0.12	0.20	0.38	0.01	0.10	1.77	UD	6.00	101.92		32.90	0.64	27.50	0.80	55
"	"	sandstone	27--21	43.24	3.34	0.32	9.88	1.22	15.43	0.11	1.43	1.70	0.06	22.50	99.30	0.16	12.95	0.51	2.63	0.25	36
"	"	sandy marl	27--25	12.84	3.45	0.19	14.49	1.86	27.97	0.03	0.55	1.14	0.08	35.50	98.15		3.72	0.33	6.27	0.35	53
"	"	sandstone	27--26	51.42	3.07	0.22	8.41	1.11	13.95	0.04	0.42	1.81	0.08	21.39	101.98		16.75	0.59	7.31	0.52	48
"	"	sandstone	27--27	48.13	4.10	0.05	8.39	1.08	13.70	0.03	0.55	2.28	0.08	23.00	101.44		11.74	0.56	7.45	0.09	49
"	"	sandstone	27--28	49.07	3.28	0.08	8.92	1.14	14.49	0.02	0.41	1.77	0.12	22.50	101.94		14.96	0.54	8.00	0.20	50
Sebkha Tah E	Upper Cretaceous	sandy marl	20--02	47.14	11.67	0.73	6.36	4.56	7.73	0.19	2.60	3.01	0.03	18.00	102.15	0.25	4.04	0.26	4.97	0.31	51
"	"	sandy marl	20--05	47.02	4.58	0.31	5.22	2.34	17.75	0.12	1.60	1.43	0.02	21.50	101.96	0.10	10.27	0.31	3.05	0.21	41
Sebkha Tah W	"	sandy marl	20--13	30.54	6.86	0.43	10.13	2.62	18.30	0.29	1.13	1.93	0.02	29.50	101.89	0.14	4.45	0.28	6.93	0.43	56
"	"	black shale	20--16	36.37	8.84	0.52	8.68	1.63	15.33	1.07	1.83	2.54	0.02	25.50	102.44	0.22	4.11	0.29	5.49	0.32	52
		sandy marl	20-19	75.86	5.95	0.61	2.58	1.13	3.18	0.34	1.51	1.84	UD	8.50	101.61	0.11	12.75	0.31	4.25	0.44	47
"	"	sandy marl	20--22	47.59	5.65	0.48	8.54	2.63	12.54	0.37	1.27	1.60	0.02	18.00	98.76	0.10	8.42	0.28	4.83	0.41	50
Sebkha Tisfourine	"	sandy marl	23--03	12.67	2.28	0.13	15.01	1.62	26.92	0.37	1.89	0.56	0.02	38.50	100.04	0.21	5.56	0.25	1.36	0.08	27
"	"	sandy marl	23--04	14.48	2.65	0.23	2.86	0.51	41.42	0.39	2.70	1.06	0.01	35.82	102.27	0.32	5.46	0.40	1.11	0.10	23
"	"	sandy marl	23--07	16.27	2.38	0.14	0.83	1.16	37.60	0.29	2.39	0.56	UD	40.89	102.67	0.26	6.84	0.24	1.12	0.07	24
		sandy marl	23-11	13.76	2.58	0.22	14.03	0.61	28.16	0.34	0.57	1.05	0.01	41.58	102.98		5.33	0.41	4.53	0.39	46
Akhfennir		black shale	24--17	11.81	2.78	0.19	2.95	1.09	40.17	0.28	1.68	1.58	0.01	35.50	98.20	0.45	4.25	0.57	2.26	0.15	33
		carbonate	26-14	1.05	UD	0.02	0.79	0.11	56.81	0.04	0.26	0.06	UD	42.86	102.22		-	-	-	0.08	-
Amma fatma	"	black shale	26--17	29.65	6.48	0.43	9.25	2.54	18.03	0.99	0.99	2.29	0.02	29.95	100.75		4.58	0.35	6.55	0.43	53
"	"	black shale	26--23	21.68	5.21	0.33	12.01	2.19	23.17	0.35	0.67	1.75	0.02	34.09	101.58		4.16	0.34	7.78	0.49	56
Core-1	"	black shale	C1--27	11.63	1.93	0.14	3.19	0.74	38.91	0.18	1.77	0.74	0.01	39.80	99.20		6.03	0.38	1.09	0.08	25
"	"	black shale	C1--28	21.42	3.25	0.26	4.43	1.31	30.84	0.16	2.86	1.02	0.02	35.68	101.36	0.32	6.59	0.31	1.28	0.10	26
Core-3	"	black shale	C3--07	21.56	3.74	0.28	8.60	1.32	35.61	0.14	0.23	0.85	0.02	28.60	101.13		5.76	0.23	16.26	1.22	69
Core-4	"	black shale	C4--17	8.35	1.32	0.11	2.27	1.10	43.67	0.37	0.31	0.34	0.01	43.84	101.85		6.33	0.26	4.26	0.35	49
"	"	black shale	C4--18	14.90	2.03	0.16	7.34	1.21	34.27	0.25	0.32	0.50	0.02	40.18	101.29		7.34	0.25	6.34	0.50	56
"	"	black shale	C4--20	15.57	2.03	0.18	10.62	0.82	29.84	0.11	0.18	0.51	0.02	38.79	98.76		7.67	0.25	11.28	1.00	64
"	"	black shale	C4--25	13.79	2.34	0.16	2.12	0.92	43.08	0.10	0.16	0.46	0.01	37.77	101.07		5.89	0.20	14.63	1.00	70
Sebkha El Farma	Early Eocene	black shale	17--01	47.88	6.59	0.38	2.51	2.40	11.58	0.40	4.23	2.03	0.02	20.50	98.75	0.59	7.27	0.31	1.81	0.10	32
"	"	black shale	17--07	19.92	2.71	0.21	2.45	1.02	27.54	1.11	6.59	1.10	0.01	38.00	100.88	0.77	7.35	0.41	0.47	0.04	12
"	"	black shale	17--09	38.40	5.91	0.46	2.70	2.34	17.12	0.25	5.42	1.82	0.02	23.86	98.52	0.43	6.50	0.31	1.18	0.09	24
"	"	black shale	17--16	28.46	3.80	0.28	1.79	1.37	24.10	1.08	6.63	1.33	UD	33.83	102.89	0.71	7.49	0.35	0.64	0.05	15
"	"	black shale	17--20	36.88	7.90	0.48	5.20	3.09	14.95	0.19	3.74	2.02	0.02	24.39	99.16	0.38	4.67	0.26	2.35	0.14	37
"	"	sandy marl	17--24	10.51	1.87	0.14	2.28	0.88	46.54	0.08	0.54	0.53	0.01	35.29	98.76		5.62	0.28	3.46	0.26	44
"	"	sandy marl	17--28	27.91	2.71	0.25	3.79	1.35	33.36	0.10	2.27	0.92	0.02	26.37	99.14	0.21	10.30	0.34	1.32	0.12	26

Sebkha Aridal	Oligo-	sandy marl	16--02	40.00	3.41	0.34	1.08	0.84	29.87	0.72	0.97	0.92	0.02	23.00	101.32		11.73	0.27	3.52	0.35	45
"	Early Miocene	sandy marl	16--03	23.70	3.17	0.26	1.18	1.06	39.24	0.70	1.44	0.58	0.02	30.65	102.11		7.48	0.18	2.23	0.18	37
"	"	sandy marl	16--04	53.34	5.48	0.40	2.12	1.93	13.21	1.94	5.02	0.99	UD	16.00	100.56	1.00	9.73	0.18	1.36	0.10	28
"	"	sandy marl	16--05	39.61	3.27	0.33	1.10	0.77	28.10	0.71	2.10	0.93	0.02	23.50	100.57	0.14	12.11	0.28	1.67	0.17	30
"	"	sandy marl	16--06	25.99	3.51	0.29	1.18	1.10	37.28	0.44	1.43	0.70	0.03	27.86	99.90	0.20	7.40	0.20	2.85	0.24	42
"	"	sandy marl	16--07	62.20	3.85	0.37	1.39	1.25	6.89	0.85	6.94	0.88	UD	16.42	101.15	0.78	16.16	0.23	0.63	0.06	15
"	"	sandy marl	16--10	46.12	2.17	0.32	0.96	0.67	28.00	0.84	0.55	0.74	0.03	20.90	101.39		21.25	0.34	3.95	0.58	45
"	"	sandy marl	16--14	60.80	4.34	0.52	5.52	0.66	10.93	0.83	0.86	1.48	0.04	15.84	102.00		14.01	0.34	5.05	0.60	49
"	Mio-Pliocene	sandstone	16--18	38.60	1.97	0.08	0.93	0.34	32.80	0.07	0.83	0.53	UD	23.15	99.33		19.59	0.27	2.37	0.10	37
"	SW part of basin	sandstone	16--21	43.09	2.42	0.10	0.57	0.53	28.02	0.04	0.62	0.87	0.10	24.50	100.99		17.81	0.36	3.90	0.16	45
Sebkha El Farma	"	sandstone	17--32	65.84	4.32	0.28	1.51	1.29	12.74	0.10	0.84	1.52	0.02	13.00	101.52		15.24	0.35	5.14	0.33	49
"	"	sandstone	17--37	40.21	2.43	0.09	1.55	0.60	29.52	0.06	0.92	1.21	UD	22.00	98.66		16.55	0.50	2.64	0.10	36
Sebkha El Farma2	"	sandstone	18--26	38.51	2.81	0.07	1.07	0.47	30.40	0.07	0.72	1.36	UD	24.50	100.08		13.70	0.48	3.90	0.10	42
Sebkha El Farma 3	"	sandstone	18-40	45.26	3.07	0.31	1.02	1.36	26.21	0.15	1.31	1.09	0.02	22.39	102.30		14.74	0.36	2.34	0.24	36
Oued El Khatt	"	sandstone	19--02	18.19	1.07	0.10	0.63	0.74	45.87	0.09	0.17	0.45	0.02	33.33	100.69		17.00	0.42	6.29	0.59	51
"	"	sandstone	19--03	49.40	2.48	0.12	0.57	0.82	25.85	0.06	0.44	1.06	UD	20.50	101.35		19.92	0.43	5.64	0.27	49
"	"	sandstone	19--06	42.84	1.86	0.09	0.53	0.60	30.49	0.11	0.40	0.85	UD	22.89	100.70		23.03	0.46	4.65	0.23	45
"	"	sandstone	19--07	40.62	2.12	0.13	0.60	0.71	31.29	0.03	0.50	0.91	UD	24.50	101.44		19.16	0.43	4.24	0.26	45
"	"	sandstone	19--08	57.85	2.86	0.17	0.50	0.95	20.16	0.03	0.48	1.20	UD	17.00	101.26		20.23	0.42	5.96	0.35	50
"	"	sandstone	19--09	42.09	2.24	0.13	0.46	0.75	31.13	0.02	0.31	0.91	UD	20.30	98.39		18.79	0.41	7.23	0.42	53
"	"	sandstone	19--10	40.81	2.34	0.13	0.62	0.76	31.15	0.02	0.42	0.89	UD	22.84	100.03		17.44	0.38	5.57	0.31	50
"	"	sandstone	19--12	21.72	1.28	0.08	0.72	0.47	44.51	0.03	0.19	0.50	UD	29.56	99.10		16.97	0.39	6.74	0.42	52
"	"	sandstone	19--13	19.06	1.37	0.13	0.92	0.55	46.07	0.11	0.25	0.45	UD	31.86	100.84		13.91	0.33	5.48	0.52	51
"	"	sandstone	19--14	67.64	3.49	0.15	1.65	1.10	13.53	0.14	1.07	1.34	0.01	9.55	99.72		19.38	0.38	3.26	0.14	41
Oued Itghi	"	sandstone	21--10	50.58	2.13	0.06	0.24	0.53	26.67	0.09	0.43	1.11	0.02	17.82	99.73		23.75	0.52	4.95	0.14	45
"	"	sandstone	21--11	45.68	2.27	0.09	0.37	0.64	29.48	0.08	0.46	1.09	UD	22.77	102.97		20.12	0.48	4.93	0.20	46
Sebkha Tah E	Mio-Pliocene	sandstone	20--07	35.21	3.24	0.15	0.81	0.98	34.76	0.03	0.93	0.95	0.01	23.38	100.49		10.87	0.29	3.48	0.16	44
Sebkha Tah W	NE part of basin	sandstone	20--23	73.86	2.57	0.18	4.29	0.47	7.56	0.86	0.51	1.03	UD	10.05	101.44		28.74	0.40	5.04	0.35	48
"	"	sandstone	20--27	46.95	1.91	0.16	9.70	0.60	15.62	0.49	1.15	0.82	0.02	24.12	101.59		24.58	0.43	1.66	0.14	29
"	"	sandstone	20--28	50.72	1.60	0.14	9.13	0.40	16.60	0.72	0.44	0.70	0.01	21.50	102.01		31.70	0.44	3.64	0.32	42
"	"	sandstone	20--29	35.97	1.29	0.12	10.93	0.54	22.04	0.61	0.49	0.59	0.02	29.00	101.65		27.88	0.46	2.63	0.24	36
"	"	sandstone	20--30	26.59	1.45	0.12	13.15	1.84	24.70	0.56	0.22	0.60	0.02	32.18	101.47		18.34	0.41	6.59	0.55	51
Oumdaboua	"	sandstone	20--37	40.13	2.80	0.19	0.94	1.22	30.86	0.11	1.31	1.04	0.03	21.61	100.30		14.33	0.37	2.14	0.15	34
"	"	sandstone	20--40	25.80	1.74	0.34	1.02	1.51	41.10	0.06	0.52	0.59	0.02	29.15	101.96		14.83	0.34	3.35	0.65	43
"	"	sandstone	20--42	19.37	1.49	0.17	1.90	0.91	43.35	0.04	0.43	0.57	0.01	32.00	100.33		13.00	0.38	3.47	0.40	42
Sebkha Tah W	"	sandstone	23--13	32.37	1.32	0.19	11.32	0.34	22.08	0.45	0.67	0.56	UD	31.82	101.19		24.52	0.42	1.97	0.28	32
"	"	sandstone	23--15	44.38	3.53	0.11	8.37	1.03	17.64	0.17	0.81	1.68	0.02	23.00	100.82		12.57	0.48	4.36	0.14	44
Itzetene	"	sandstone	23--29	29.46	1.74	0.11	0.76	0.62	39.02	0.10	0.80	0.76	UD	27.50	100.99		16.93	0.44	2.18	0.14	33
"	"	sandstone	23--30	27.60	1.81	0.43	1.04	1.37	39.34	0.12	0.57	0.62	0.02	27.50	100.54		15.25	0.34	3.18	0.75	42
"	"	sandstone	23--31	36.12	3.44	0.24	0.60	1.32	33.61	0.04	0.70	1.04	0.02	24.62	101.82		10.50	0.30	4.91	0.34	50
"	"	sandstone	23--32	40.28	3.10	0.11	0.53	1.01	29.11	0.10	1.25	1.42	0.01	25.38	102.40		12.99	0.46	2.48	0.09	35
Onhym Quarry	"	sandstone	24--09	40.23	3.68	0.30	0.72	1.58	28.53	0.04	1.01	1.18	0.01	22.00	99.35		10.93	0.32	3.64	0.30	44

"	"	sandstone	24--15	21.03	1.25	0.37	0.79	1.55	42.63	0.06	0.39	0.53	0.02	32.00	100.76	16.82	0.42	3.21	0.95	40
"	"	sandstone	24--16	42.26	2.85	0.11	0.64	0.87	29.02	0.07	0.64	1.35	0.01	24.00	101.95	14.83	0.47	4.45	0.17	44
Akhfennir	"	sandstone	24--21	17.18	3.96	0.25	13.54	2.20	22.86	0.07	1.97	1.21	0.04	39.50	102.85	4.34	0.31	2.01	0.13	34
"	"	sandstone	24--23	47.89	5.38	0.19	7.93	1.38	13.45	0.07	1.27	1.88	0.03	21.39	100.93	8.90	0.35	4.24	0.15	46
Amma fatma	"	sandstone	26--30	32.29	2.88	0.18	1.08	1.24	33.83	0.09	0.84	1.08	0.02	26.63	100.26	11.21	0.38	3.43	0.21	42
"	"	sandstone	26--31	17.83	1.05	0.07	0.76	0.66	46.06	0.07	0.30	0.46	0.01	34.33	101.60	16.98	0.44	3.50	0.23	41
"	"	sandstone	26--33	24.53	1.48	0.44	1.10	2.06	39.23	0.13	0.40	0.58	0.03	30.81	100.90	16.57	0.39	3.70	1.10	43
"	"	sandstone	26--34	17.70	1.44	0.46	1.55	1.86	42.80	0.07	0.50	0.50	0.02	32.83	99.86	12.29	0.35	2.88	0.92	40
Core-1	"	sandstone	C1--01	37.81	1.33	0.11	0.38	0.50	35.06	0.45	0.34	0.64	0.01	26.32	102.98	28.43	0.48	3.91	0.32	42
"	"	sandstone	C1--03	48.07	1.60	0.13	9.80	0.46	17.22	0.23	0.45	0.75	0.01	24.05	102.81	30.04	0.47	3.56	0.29	41
"	"	sandstone	C1--04	39.78	1.53	0.12	10.57	0.43	19.91	0.27	0.43	0.69	0.01	27.59	101.38	26.00	0.45	3.56	0.28	41
"	"	sandstone	C1--05	53.29	1.80	0.14	7.99	0.47	14.59	0.68	0.52	0.82	0.01	20.26	100.60	29.61	0.46	3.46	0.27	41
"	"	sandstone	C1--08	52.49	1.78	0.15	8.56	0.47	14.94	0.69	0.52	0.77	0.02	21.05	101.49	29.49	0.43	3.42	0.29	41
Core-2	"	sandstone	C2--01	54.23	4.65	0.43	1.33	1.93	20.43	0.12	2.47	1.48	0.03	14.30	101.51	11.66	0.32	1.88	0.17	32
"	"	sandstone	C2--02	57.79	5.05	0.46	1.62	2.30	17.23	0.24	1.15	1.50	0.03	14.90	102.38	11.44	0.30	4.39	0.40	48
Core-3	"	sandstone	C3--01	49.96	4.09	0.58	1.00	1.90	24.12	0.21	1.08	1.13	0.03	17.10	101.35	12.22	0.28	3.79	0.54	46
"	"	sandstone	C3--03	37.81	4.41	0.19	1.11	1.70	32.30	0.11	1.09	1.49	0.02	20.30	100.62	8.57	0.34	4.05	0.17	46
Core-4	"	sandstone	C4--01	29.50	1.67	0.17	0.85	0.88	37.94	0.05	0.53	0.72	0.01	29.98	102.41	17.66	0.43	3.15	0.32	40
"	"	sandstone	C4--03	37.26	3.11	0.21	0.75	0.96	32.02	0.14	0.93	1.15	0.02	25.15	101.82	11.98	0.37	3.34	0.23	42
"	"	sandstone	C4--05	40.50	3.14	0.57	0.79	2.25	29.25	0.21	0.84	1.05	0.03	22.95	101.75	12.90	0.33	3.74	0.68	45
"	"	sandstone	C4--07	52.42	3.48	0.55	1.09	1.97	20.63	0.14	0.88	1.13	0.03	18.04	100.48	15.06	0.32	3.95	0.63	46
"	"	sandstone	C4--08	48.72	3.86	0.46	1.14	1.94	23.01	0.16	0.89	1.21	0.03	18.96	100.48	12.62	0.31	4.34	0.52	48
"	"	sandstone	C4--13	59.69	5.91	0.38	1.68	2.51	14.71	0.26	1.01	1.79	0.03	13.11	101.16	10.10	0.30	5.85	0.38	53
"	"	sandstone	C4--14	44.66	4.02	0.45	1.08	2.11	25.36	0.11	0.88	1.24	0.03	20.80	100.86	11.11	0.31	4.57	0.51	49
Core-1	"	sandy marl	C1--11	20.48	1.77	0.15	15.30	0.68	25.35	0.18	0.44	0.56	0.04	36.96	101.94	11.57	0.32	4.02	0.34	46
"	"	sandy marl	C1--16	34.96	3.88	0.31	12.44	1.44	19.06	0.33	0.67	1.11	0.02	28.76	103.04	9.01	0.29	5.79	0.46	53
"	"	sandy marl	C1--18	42.74	7.26	0.52	9.70	3.16	13.84	0.31	1.24	1.91	0.02	22.77	103.53	5.89	0.26	5.85	0.42	54
"	"	sandy marl	C1--19	48.40	6.63	0.50	8.33	2.85	12.01	0.38	1.07	1.82	0.02	19.27	101.36	7.30	0.27	6.20	0.47	55
"	"	sandy marl	C1--20	52.15	7.65	0.60	7.02	3.20	9.78	0.38	1.28	2.04	0.02	16.58	100.80	6.82	0.27	5.98	0.47	54
"	"	sandy marl	C1--21	64.35	7.09	0.64	4.67	2.17	6.25	0.38	1.25	2.04	0.01	11.02	99.96	9.08	0.29	5.67	0.51	53
"	"	sandy marl	C1--22	63.49	6.92	0.64	5.11	1.74	7.26	0.34	1.31	1.99	0.01	12.29	101.22	9.17	0.29	5.28	0.49	52
"	"	sandy marl	C1--23	84.46	2.64	0.31	0.93	0.67	3.29	1.55	0.60	0.94	UD	2.87	98.32	31.99	0.36	4.40	0.52	47
"	"	sandy marl	C1--24	27.47	5.60	0.38	11.77	2.05	22.16	0.86	0.69	1.83	0.02	29.80	102.74	4.91	0.33	8.12	0.55	57
"	"	sandy marl	C1--25	42.61	9.23	0.59	8.16	1.87	14.08	0.66	1.00	2.94	0.02	20.80	102.09	4.62	0.32	9.23	0.59	59
"	"	sandy marl	C1--26	23.56	5.49	0.36	11.45	2.32	22.72	0.51	0.63	1.85	0.02	31.33	100.37	4.29	0.34	8.71	0.57	57
Seguit El Hamra	Pleistocene	sand	07--04	85.69	UD	0.14	0.25	0.28	6.77	0.05	0.16	0.23	0.01	5.63	100.04				0.88	
Oued Draa	Recent Sediments	sand+silt	06--01	67.59	11.21	0.67	2.06	4.42	4.22	0.12	0.63	2.70	0.05	6.91	100.72	6.03	0.24	17.79	1.06	69
"	"	silt	06--02	61.65	11.71	0.77	2.59	5.00	5.59	0.13	1.48	2.70	0.06	9.11	100.95	5.26	0.23	7.91	0.52	60
"	"	silt+sand	06--03	61.53	12.66	0.69	2.55	4.98	5.74	0.14	0.74	2.76	0.07	8.67	100.67	4.86	0.22	17.11	0.93	70
Tan-Tan River	"	sand	06--04	82.23	5.03	0.56	0.94	2.48	3.04	0.06	0.70	1.49	0.03	3.41	100.09	16.35	0.30	7.19	0.80	56
Tan-Tan River	"	sand+silt	06--05	65.15	9.47	0.64	2.21	3.84	6.98	0.13	0.89	2.27	0.05	9.36	101.13	6.88	0.24	10.64	0.72	64
Oued Chebeika	"	sand	06--06	81.88	5.11	0.12	0.44	0.61	3.86	0.05	0.23	3.67	0.01	3.63	99.71	16.02	0.72	22.22	0.52	52

Oued Chebeika	"	mud	06--07	45.19	13.37	0.66	3.61	5.25	12.53	0.23	1.13	3.35	0.07	16.10	101.61		3.38	0.25	11.83	0.58	65
Seguit El Hamra	"	mud	07--01	52.07	12.68	0.69	3.10	4.86	10.56	0.43	1.17	2.42	0.07	13.10	101.28		4.11	0.19	10.84	0.59	66
Seguit El Hamra	"	mud	07--02	46.49	20.93	0.77	3.34	7.52	3.66	0.25	1.37	3.51	0.09	12.73	100.80		2.22	0.17	15.28	0.56	72
Seguit El Hamra	"	silt+sand	07--03	51.98	13.04	0.70	2.71	4.95	10.27	0.39	1.57	2.40	0.06	11.86	100.08		3.99	0.18	8.31	0.45	63
Seguit El Hamra	"	mud	07--05	47.81	19.54	0.86	3.54	7.27	5.62	0.26	0.99	3.34	0.08	11.56	101.03		2.45	0.17	19.74	0.87	74
Cap Jubi	"	sand	08--02	42.88	2.69	0.08	1.05	0.79	28.82	0.13	1.03	1.26	0.01	23.47	102.37		15.94	0.47	2.61	0.08	36
Oued Akhfennir	"	sand	09--01	49.12	3.01	0.33	1.16	1.82	24.28	0.09	1.23	1.18	0.02	20.05	102.43		16.32	0.39	2.45	0.27	36
Oued Akhfennir	"	sand	09--02	47.74	3.06	0.28	1.11	1.66	24.80	0.10	1.12	1.19	0.02	20.59	101.79		15.60	0.39	2.73	0.25	38
Ouel El Craa	"	sand	14--01	56.83	4.51	0.40	1.20	2.03	18.49	0.14	0.82	1.36	0.02	15.48	101.41		12.60	0.30	5.50	0.49	52
Laayoune Plage	"	sand	15--10	47.17	5.16	0.12	1.12	1.04	23.46	0.11	1.91	1.84	0.01	19.38	101.48		9.14	0.36	2.70	0.06	38
Tarfaya E beach	"	sand	18--03a	44.12	4.57	0.07	0.72	0.71	26.34	0.10	1.75	1.88	0.01	20.95	101.38		9.65	0.41	2.61	0.04	37
Tarfaya E beach	"	sand	18--04a	50.23	5.25	0.09	0.66	0.82	22.45	0.10	1.77	1.84	0.01	18.33	101.68		9.57	0.35	2.97	0.05	40
Sebkha Tisfurine	Upper Cretaceous	WM	23--01	24.93	5.15	0.39	10.45	2.25	22.73	0.36	2.22	1.79	0.02	30.58	101.08	0.25	4.84	0.35	2.61	0.20	38
Onhym Quarry	"	WM	24--02	33.28	5.26	0.37	2.37	2.64	28.72	0.56	1.22	1.50	0.03	24.75	100.81	0.07	6.33	0.29	4.57	0.32	49
"	"	WM	24--03	42.53	5.35	0.41	2.62	2.44	21.64	0.17	2.62	1.61	0.03	23.33	102.86	0.28	7.95	0.30	2.29	0.18	36
"	"	WM	24--04	36.82	4.74	0.39	2.13	1.95	26.32	0.15	2.34	1.42	0.03	23.88	100.26	0.24	7.77	0.30	2.26	0.19	36
"	"	WM	24--05	34.91	4.73	0.34	2.70	2.10	26.45	0.12	2.45	1.42	0.03	26.00	101.34	0.24	7.38	0.30	2.14	0.15	35
"	"	WM	24--06	41.08	4.22	0.34	2.59	2.11	23.54	0.14	2.52	1.33	0.03	22.61	100.60	0.24	9.73	0.32	1.85	0.15	32
"	"	WM	24--07	39.56	3.71	0.32	1.38	2.11	27.05	0.16	2.04	1.22	0.02	21.72	99.39	0.17	10.66	0.33	1.98	0.17	33
"	"	WM	24--18	13.89	3.11	0.18	13.57	3.16	25.02	0.42	2.55	0.79	0.01	39.13	101.96	0.28	4.47	0.25	1.37	0.08	27
Chebeica	"	WM	26--04	87.46	4.01	0.75	0.38	1.64	0.23	0.04	0.79	2.21	0.01	1.50	99.69		21.81	0.55	5.08	0.95	45
"	"	WM	26--08	53.31	2.60	0.55	1.87	5.22	17.91	0.06	1.25	1.19	0.09	14.85	100.00	0.14	20.50	0.46	2.34	0.50	34
"	"	WM	26--09	51.49	11.98	0.70	3.78	5.15	5.56	0.13	3.57	3.79	0.03	13.93	100.20	0.99	4.30	0.32	4.64	0.27	49
Amma fatma	"	WM	26--25	50.31	4.60	0.70	1.90	5.25	18.50	0.06	1.25	1.29	0.09	66.14	100.15	0.10	10.94	0.28	4.00	0.61	47
Core-1	Mio-Pliocene	WM	C1--06	45.77	1.45	0.12	9.68	0.37	17.34	0.52	0.43	0.69	0.01	24.50	100.91		31.57	0.48	3.37	0.28	40
"	"	WM	C1--07	58.43	1.92	0.17	6.96	0.49	12.02	0.78	0.59	0.85	0.01	17.21	99.46		30.43	0.44	3.25	0.29	40
"	"	WM	C1--09	80.95	4.22	0.31	2.75	1.56	3.34	0.77	0.97	1.40	UD	5.58	101.91		19.18	0.33	4.35	0.32	47
"	"	WM	C1--10	82.44	4.44	0.31	1.58	1.97	1.60	0.84	1.14	1.45	UD	3.24	99.08		18.57	0.33	3.89	0.27	45
Core-2	"	WM	C2--03	8.86	2.27	0.17	16.52	5.16	33.36	0.27	0.52	0.61	0.04	34.30	102.14		3.90	0.27	4.37	0.33	49
"	"	WM	C2--04	13.11	3.19	0.21	14.68	6.43	30.48	0.27	0.40	0.95	0.03	32.30	102.16		4.11	0.30	7.98	0.53	58
Core-3	"	WM	C3--02	42.04	3.97	0.39	1.12	1.71	29.57	0.17	1.12	1.11	0.02	20.80	102.13		10.59	0.28	3.54	0.35	45
"	"	WM	C3--04	48.47	5.30	0.34	1.55	2.72	21.34	0.12	0.85	1.67	0.02	17.30	99.79		9.15	0.32	6.24	0.40	53
"	"	WM	C3--05	33.77	3.46	0.30	1.17	2.24	33.73	0.51	0.67	1.13	0.02	24.20	101.31		9.76	0.33	5.16	0.45	50
"	"	WM	C3--06	5.89	1.93	0.08	1.31	1.82	59.71	0.07	0.13	0.22	0.02	28.50	99.87		3.05	0.11	14.85	0.62	74
Core-4	"	WM	C4--09	52.75	3.67	0.60	1.12	2.18	20.55	0.17	0.78	1.15	0.03	17.09	100.22		14.37	0.31	4.71	0.77	49
"	"	WM	C4--10	40.75	3.25	0.32	0.85	1.45	28.27	0.29	0.69	1.09	0.02	23.18	100.25		12.54	0.34	4.71	0.46	48
"	"	WM	C4--15	20.72	3.57	0.23	1.30	2.66	40.05	0.58	0.54	1.05	0.02	31.46	102.28		5.80	0.29	6.61	0.43	55
"	"	WM	C4--16	21.93	3.13	0.30	1.19	3.42	39.11	0.58	0.54	0.91	0.03	30.78	102.00		7.01	0.29	5.80	0.56	53
"			UCC	64.93	14.63	0.52	2.24	3.97	4.12	0.15	3.46	3.10	0.07	6.00	99.90		4.44	0.21	4.23	0.15	50

Na_2O*%= Cl- bound Na_2O from seawater or brine salt
CIA=chemical index of alteraton
WM=weathered marl
UD= under detection limit
UCC=upper continental crust
LOI=loss on ignition

Table 3.2.1 Major and trace element compositions of the Tarfaya basin sediments from Lower Cretaceous to recent

Stratigraphic age	Lower cretaceous					Upper Cretaceous									
Sections	Boukhchebat					Sebkha Tah E		Sebkha Tah W		Sebkha Tisfourine		Amma fatma		Core-1	
Rock type	S	S	S	S	S	SM	SM	SM	SM	SM	SM	carbonate	BS	BS	BS
Sa. no.	27--02	27--12	27--21	27--26	27--28	20--02	20--05	20--13	20-19	23--04	23-11	26-14	26--23	C1--27	C1--28
SiO_2	67.81	67.28	43.24	51.42	49.07	47.14	47.02	30.54	75.86	14.48	13.76	1.05	21.68	11.63	21.42
Al_2O_3	3.15	2.56	3.34	3.07	3.28	11.67	4.58	6.86	5.95	2.65	2.58	UD	5.21	1.93	3.25
TiO_2	0.11	0.07	0.32	0.22	0.08	0.73	0.31	0.43	0.61	0.23	0.22	0.02	0.33	0.14	0.26
MgO	0.16	0.19	9.88	8.41	8.92	6.36	5.22	10.13	2.58	2.86	14.03	0.79	12.01	3.19	4.43
Fe_2O_3	0.26	0.10	1.22	1.11	1.14	4.56	2.34	2.62	1.13	0.51	0.61	0.11	2.19	0.74	1.31
CaO	14.87	15.24	15.43	13.95	14.49	7.73	17.75	18.30	3.18	41.42	28.16	56.81	23.17	38.91	30.84
P_2O_5	0.02	0.02	0.11	0.04	0.02	0.19	0.12	0.29	0.34	0.39	0.34	0.04	0.35	0.18	0.16
Na_2O	0.11	0.10	1.43	0.42	0.41	2.60	1.60	1.13	1.51	2.70	0.57	0.26	0.67	1.77	2.86
K_2O	1.93	1.75	1.70	1.81	1.77	3.01	1.43	1.93	1.84	1.06	1.05	0.06	1.75	0.74	1.02
MnO	0.02	UD	0.06	0.08	0.12	0.03	0.02	0.02	UD	0.01	0.01	UD	0.02	0.01	0.02
LOI	12.06	14.50	22.50	21.39	22.50	18.00	21.50	29.50	8.50	35.82	41.58	42.86	34.09	39.80	35.68
Total	100.55	101.85	99.30	101.98	101.94	102.15	101.96	101.89	101.61	102.27	102.98	102.22	101.58	99.20	101.36
Na_2O^*			0.16			0.25	0.10	0.14	0.11	0.32					0.32
SiO_2/Al_2O_3	21.53	26.28	12.95	16.75	14.96	4.04	10.27	4.45	12.75	5.46	5.33		4.16	6.03	6.59
K_2O/Na_2O	17.55	17.50	1.34	4.31	4.32	1.28	0.95	1.95	1.31	0.45	1.84	0.23	2.61	0.42	0.40
Li	4.70	5.27	6.81	10.47	6.42	48.23	16.49	21.52	13.93	7.58	6.84	0.60	10.20	14.77	17.28
Sc	2.18	0.81	2.81	2.44	1.09	13.18	4.24	7.76	6.80	3.34	2.96	0.35	3.84	5.49	6.86
V	12.02	6.18	25.54	19.31	37.92	95.45	51.39	78.97	97.02	44.58	43.05	56.96	197.86	57.09	67.69
Cr	16.14	11.92	28.60	14.65	12.01	74.44	35.07	133.33	64.86	62.02	65.04	5.10	62.60	77.33	112.85
Co	3.92	1.23	9.16	4.44	6.03	7.96	4.74	12.64	3.61	2.51	1.19	0.60	2.54	4.83	6.48
Ni	3.40	3.82	16.89	6.23	7.76	28.54	10.75	84.07	19.21	15.41	19.87	10.27	75.61	66.88	90.78
Cu	6.16	5.13	5.22	4.30	4.13	16.71	6.23	31.16	8.39	10.34	11.08	1.17	17.87	34.70	39.83
Zn	7.60	10.23	75.36	17.25	17.21	66.97	36.79	179.34	53.21	38.71	53.79	52.98	127.67	68.28	107.89
Ga	3.67	2.73	3.90	3.63	3.87	16.40	5.35	9.65	7.93	3.21	3.38	0.30	4.06	6.59	8.62
Rb	51.08	46.27	35.18	42.13	48.08	97.60	35.67	57.98	58.20	23.39	23.28	1.51	25.81	45.17	59.13
Sr	50.33	37.20	72.84	56.63	78.87	137.40	123.84	208.66	89.11	826.89	205.87	424.76	398.80	265.41	274.89
Y	8.62	4.35	14.96	12.34	6.27	25.91	10.64	22.05	26.47	17.60	14.41	1.12	9.73	15.13	30.29
Zr	59.14	59.42	172.51	365.06	64.48	265.40	73.05	140.20	488.60	45.78	50.56	0.38	58.75	101.33	166.15
Nb	2.05	1.40	5.39	3.93	1.31	13.49	6.32	6.99	11.64	3.33	3.21	0.23	3.71	5.29	6.98
Mo	0.26	0.22	2.54	0.31	0.75	2.00	1.19	31.41	1.52	6.77	2.00	2.44	2.44	44.59	58.94
Sn	0.44	0.17	0.47	0.35	0.20	1.76	0.59	1.25	1.03	0.34	0.47	0.10	0.47	1.98	1.04
Sb	0.11	0.09	0.24	0.13	0.14	0.62	0.52	1.62	0.47	0.15	0.27	0.10	0.93	0.75	1.25
Cs	1.56	0.52	0.99	0.67	0.64	5.20	1.24	2.95	2.40	1.07	1.06	0.09	1.42	2.20	2.61
Ba	280.51	276.95	171.50	212.55	1067.98	303.39	201.98	158.95	267.08	107.63	70.50	143.21	77.48	139.68	184.01
La	8.60	6.63	14.89	15.32	7.91	32.35	13.13	20.45	25.48	13.04	10.69	1.15	9.19	14.87	23.30
Hf	1.66	1.56	4.54	8.73	1.67	6.85	2.03	3.71	12.06	1.32	1.44	0.10	1.64	2.50	3.99
Ta	0.18	0.14	0.36	0.32	0.11	0.95	0.39	0.54	0.88	0.22	0.22	0.02	0.25	0.34	0.45
W	0.35	0.78	0.55	0.51	0.40	1.67	1.08	2.11	2.09	0.85	0.43	0.16	2.52	0.61	1.18
Tl	0.27	0.25	0.18	0.22	0.26	0.45	0.20	0.49	0.39	0.24	0.18	0.22	0.12	0.70	1.47
Pb	5.00	5.08	23.62	3.82	5.07	11.67	7.92	4.30	5.98	1.66	1.56	0.31	3.42	3.91	4.71
Th	2.19	1.29	4.01	4.24	1.18	9.19	3.60	5.42	6.99	2.54	2.33	0.17	2.69	3.94	5.18
U	0.55	0.50	1.76	1.20	0.59	2.96	1.79	17.96	3.63	13.62	5.35	0.74	9.79	24.25	28.02
La/Sc	3.94	8.15	5.29	6.27	7.23	2.46	3.10	2.64	3.75	3.90	3.61	3.30	2.39	2.71	3.40
Th/Sc	1.00	1.58	1.42	1.74	1.08	0.70	0.85	0.70	1.03	0.76	0.79	0.48	0.70	0.72	0.76
Cr/Th	7.37	9.26	7.14	3.45	10.15	8.10	9.74	24.58	9.28	24.42	27.95	30.86	23.25	19.62	21.79
Th/Co	0.56	1.05	0.44	0.96	0.20	1.15	0.76	0.43	1.93	1.01	1.96	0.28	1.06	0.82	0.80
Zr/Hf	35.59	38.08	38.01	41.83	38.69	38.75	36.04	37.76	40.50	34.57	35.16	3.71	35.87	40.60	41.65
La/Y	1.00	1.52	1.00	1.24	1.26	1.25	1.23	0.93	0.96	0.74	0.74	1.03	0.94	0.98	0.77
Sc/Cr	0.14	0.07	0.10	0.17	0.09	0.18	0.12	0.06	0.10	0.05	0.05	0.07	0.06	0.07	0.06
Cr/Ni	4.75	3.12	1.69	2.35	1.55	2.61	3.26	1.59	3.38	4.02	3.27	0.50	0.83	1.16	1.24
Cr/V	1.34	1.93	1.12	0.76	0.32	0.78	0.68	1.69	0.67	1.39	1.51	0.09	0.32	1.35	1.67
Y/Ni	2.53	1.14	0.89	1.98	0.81	0.91	0.99	0.26	1.38	1.14	0.73	0.11	0.13	0.23	0.33
Zr/Sc	27.11	73.12	61.30	149.45	58.89	20.14	17.25	18.07	71.89	13.71	17.07	1.08	15.31	18.46	24.23
La/Co	2.20	5.39	1.63	3.45	1.31	4.06	2.77	1.62	7.05	5.19	8.99	1.91	3.62	3.08	3.60

Upper Cretaceous					Early Eocene					Oligo-Early Miocene			
Core-3	Core-4				Sebkha El Farma					Sebkha Aridal			
BS	BS	BS	BS	BS	BS	BS	BS	BS	SM	SM	SM	SM	SM
C3--07	C4--17	C4--18	C4--20	C4--25	17--01	17--07	17--16	17--20	17--24	16--02	16--07	16--10	16--14
21.56	8.35	14.90	15.57	13.79	47.88	19.92	28.46	36.88	10.51	40.00	62.20	46.12	60.80
3.74	1.32	2.03	2.03	2.34	6.59	2.71	3.80	7.90	1.87	3.41	3.85	2.17	4.34
0.28	0.11	0.16	0.18	0.16	0.38	0.21	0.28	0.48	0.14	0.34	0.37	0.32	0.52
8.60	2.27	7.34	10.62	2.12	2.51	2.45	1.79	5.20	2.28	1.08	1.39	0.96	5.52
1.32	1.10	1.21	0.82	0.92	2.40	1.02	1.37	3.09	0.88	0.84	1.25	0.67	0.66
35.61	43.67	34.27	29.84	43.08	11.58	27.54	24.10	14.95	46.54	29.87	6.89	28.00	10.93
0.14	0.37	0.25	0.11	0.10	0.40	1.11	1.08	0.19	0.08	0.72	0.85	0.84	0.83
0.23	0.31	0.32	0.18	0.16	4.23	6.59	6.63	3.74	0.54	0.97	6.94	0.55	0.86
0.85	0.34	0.50	0.51	0.46	2.03	1.10	1.33	2.02	0.53	0.92	0.88	0.74	1.48
0.02	0.01	0.02	0.02	0.01	0.02	0.01	UD	0.02	0.01	0.02	UD	0.03	0.04
28.60	43.84	40.18	38.79	37.77	20.50	38.00	33.83	24.39	35.29	23.00	16.42	20.90	15.84
101.13	101.85	101.29	98.76	101.07	98.75	100.88	102.89	99.16	98.76	101.32	101.15	101.39	102.00
					0.59	0.77	0.71	0.38			0.78		
5.76	6.33	7.34	7.67	5.89	7.27	7.35	7.49	4.67	5.62	11.73	16.16	21.25	14.01
3.70	1.10	1.56	2.83	2.88	0.56	0.19	0.22	0.60	0.98	0.95	0.14	1.35	1.72
9.10	4.22	7.34	8.23	7.66	14.04	9.73	9.83	21.24	7.51	11.04	14.05	6.90	8.20
4.34	2.08	2.43	2.61	2.78	7.27	3.90	4.85	8.85	2.62	3.54	4.78	2.97	4.82
324.26	210.72	166.85	61.45	170.86	1282.25	656.70	437.95	1185.82	104.45	30.25	39.82	20.77	40.19
55.98	52.90	61.04	33.03	45.97	139.30	149.09	141.90	87.53	29.40	46.35	75.53	41.66	46.37
2.21	1.08	1.93	2.87	2.94	5.76	3.27	3.57	9.37	2.08	2.16	1.81	1.09	2.20
16.83	106.78	47.79	41.74	44.13	74.59	78.82	74.82	91.66	12.70	12.51	21.03	6.27	9.53
9.45	33.08	17.67	10.82	10.92	44.00	38.43	38.89	37.59	6.48	5.48	11.55	5.04	5.04
65.00	238.49	115.71	105.29	81.67	289.78	358.16	231.57	390.74	23.68	33.22	38.21	17.54	34.96
4.52	2.06	2.78	2.89	3.02	9.66	4.37	5.94	11.45	2.55	4.29	5.46	2.97	4.88
28.07	10.70	15.88	18.04	16.79	50.11	24.21	31.75	61.15	17.07	24.93	28.38	19.66	36.57
730.09	798.81	499.29	446.07	907.06	376.67	806.80	683.56	332.59	339.52	317.50	276.60	244.77	278.84
10.77	12.53	8.11	7.64	6.84	19.25	19.85	18.84	17.57	5.52	19.16	20.49	21.13	25.83
85.71	32.31	54.85	73.99	48.56	124.06	73.93	93.18	149.76	46.22	443.70	375.18	515.58	506.85
4.12	1.58	2.25	2.85	2.35	6.78	1.23	4.76	8.60	2.47	2.93	0.40	1.34	4.30
0.74	9.71	9.71	43.86	16.63	6.05	45.24	20.50	33.59	1.87	3.80	4.21	0.62	0.99
0.61	0.32	0.51	0.38	0.39	1.21	0.04	0.75	1.39	0.32	0.22	0.04	0.10	0.08
0.66	0.60	0.50	0.82	0.55	3.91	3.06	3.35	4.40	0.69	0.18	0.10	0.18	0.33
1.54	0.64	0.95	1.06	1.07	2.94	1.27	1.68	3.63	0.91	0.76	1.25	0.55	1.03
107.96	55.76	69.91	115.01	149.80	152.30	113.80	137.01	637.31	166.12	261.55	210.94	174.69	729.31
10.21	9.27	7.54	7.06	6.62	19.70	13.05	14.73	21.87	6.00	15.97	18.49	16.63	20.74
2.17	0.87	1.31	1.72	1.14	3.25	1.78	2.39	3.94	1.18	10.01	5.31	10.27	12.00
0.26	0.11	0.15	0.18	0.15	0.51	0.02	0.35	0.64	0.18	0.19	0.02	0.08	0.10
0.57	0.30	0.70	0.69	0.67	2.29	1.69	2.94	3.74	0.94	0.56	0.42	0.37	0.82
0.15	0.13	0.22	1.52	0.89	0.90	5.81	2.02	7.38	0.12	0.23	0.51	0.15	0.21
3.66	3.65	3.22	1.91	2.63	10.09	3.69	3.92	9.87	2.01	4.11	4.71	3.59	6.22
2.82	1.21	1.76	1.95	1.77	4.96	2.32	3.23	6.27	1.50	4.20	4.63	4.72	5.97
4.22	15.52	8.02	5.26	3.35	5.33	6.14	14.45	5.02	2.00	3.55	9.18	4.78	4.45
2.35	4.45	3.11	2.70	2.39	2.71	3.35	3.04	2.47	2.29	4.51	3.87	5.59	4.30
0.65	0.58	0.72	0.75	0.64	0.68	0.60	0.67	0.71	0.57	1.19	0.97	1.59	1.24
19.82	43.76	34.73	16.94	26.02	28.10	64.24	43.93	13.97	19.59	11.02	16.30	8.82	7.77
1.28	1.12	0.91	0.68	0.60	0.86	0.71	0.91	0.67	0.72	1.95	2.57	4.34	2.71
39.43	37.29	41.93	42.97	42.42	38.12	41.51	39.03	38.03	39.30	44.33	70.65	50.21	42.25
0.95	0.74	0.93	0.92	0.97	1.02	0.66	0.78	1.24	1.09	0.83	0.90	0.79	0.80
0.08	0.04	0.04	0.08	0.06	0.05	0.03	0.03	0.10	0.09	0.08	0.06	0.07	0.10
3.33	0.50	1.28	0.79	1.04	1.87	1.89	1.90	0.95	2.32	3.71	3.59	6.64	4.87
0.17	0.25	0.37	0.54	0.27	0.11	0.23	0.32	0.07	0.28	1.53	1.90	2.01	1.15
0.64	0.12	0.17	0.18	0.15	0.26	0.25	0.25	0.19	0.43	1.53	0.97	3.37	2.71
19.73	15.52	22.60	28.33	17.49	17.06	18.96	19.22	16.92	17.64	125.35	78.55	173.32	105.10
4.61	8.62	3.91	2.46	2.26	3.42	3.99	4.13	2.33	2.89	7.41	10.24	15.29	9.44

Mio-Pliocene SW part of basin							Mio-Pliocene NE part of basin						
Sebkha Aridal		Sebkha El Farma		Oued El Khatt			Sebkha Tah E	Sebkha Tah W		Sebkha Tisfourine	Onhym Quarry		Amma
S	S	S	S	S	S	S	S	S	S	S	S	S	S
16--18	16--21	17--32	17--37	19--06	19--10	19--12	20--07	20--23	20--28	23--13	24--09	24--16	26--30
38.60	43.09	65.84	40.21	42.84	40.81	21.72	35.21	73.86	50.72	32.37	40.23	42.26	32.29
1.97	2.42	4.32	2.43	1.86	2.34	1.28	3.24	2.57	1.60	1.32	3.68	2.85	2.88
0.08	0.10	0.28	0.09	0.09	0.13	0.08	0.15	0.18	0.14	0.19	0.30	0.11	0.18
0.93	0.57	1.51	1.55	0.53	0.62	0.72	0.81	4.29	9.13	11.32	0.72	0.64	1.08
0.34	0.53	1.29	0.60	0.60	0.76	0.47	0.98	0.47	0.40	0.34	1.58	0.87	1.24
32.80	28.02	12.74	29.52	30.49	31.15	44.51	34.76	7.56	16.60	22.08	28.53	29.02	33.83
0.07	0.04	0.10	0.06	0.11	0.02	0.03	0.03	0.86	0.72	0.45	0.04	0.07	0.09
0.83	0.62	0.84	0.92	0.40	0.42	0.19	0.93	0.51	0.44	0.67	1.01	0.64	0.84
0.53	0.87	1.52	1.21	0.85	0.89	0.50	0.95	1.03	0.70	0.56	1.18	1.35	1.08
UD	0.10	0.02	UD	UD	UD	UD	0.01	UD	0.01	UD	0.01	0.01	0.02
23.15	24.50	13.00	22.00	22.89	22.84	29.56	23.38	10.05	21.50	31.82	22.00	24.00	26.63
99.33	100.99	101.52	98.66	100.70	100.03	99.10	100.49	101.44	102.01	101.19	99.35	101.95	100.26
19.59	17.81	15.24	16.55	23.03	17.44	16.97	10.87	28.74	31.70	24.52	10.93	14.83	11.21
0.64	1.40	1.81	1.32	2.13	2.12	2.63	1.02	2.02	1.59	0.84	1.17	2.11	1.29
6.93	6.24	16.13	50.22	4.72	4.46	3.03	8.90	6.04	4.92	3.00	12.89	6.32	4.24
1.34	1.64	4.09	1.29	1.85	1.45	1.30	2.57	2.52	1.27	0.77	3.92	1.56	1.46
16.91	34.35	72.63	37.35	21.29	25.58	13.34	21.93	23.36	23.96	19.75	48.81	16.90	25.72
15.83	15.81	31.33	18.35	23.58	10.08	17.25	24.39	27.78	11.89	13.27	25.31	10.20	10.66
2.18	3.72	3.12	1.55	1.60	2.24	2.28	2.83	1.96	2.22	0.39	4.65	2.31	2.26
6.52	6.91	8.44	6.53	6.55	6.46	7.48	7.17	6.66	7.90	4.50	9.25	8.51	6.36
2.47	2.86	4.82	2.33	2.72	5.71	2.24	3.03	3.86	2.67	2.02	4.54	3.60	2.22
7.67	7.90	29.30	8.25	13.75	29.75	6.66	14.63	17.92	15.49	21.70	21.78	15.89	11.13
2.18	3.16	5.17	2.72	2.67	2.64	1.65	3.37	3.05	1.66	0.97	4.52	3.04	2.64
12.57	22.01	38.84	28.92	23.41	21.95	12.69	22.39	27.41	16.60	8.28	29.56	31.44	21.98
144.24	188.15	161.80	336.93	73.31	67.09	103.49	114.54	114.17	118.19	87.48	154.18	831.61	66.67
10.74	6.26	12.36	3.50	5.32	5.60	4.40	16.85	15.99	12.41	4.49	10.19	6.34	5.41
43.09	79.51	165.37	48.15	79.78	31.07	41.25	46.03	117.78	21.64	35.23	93.54	30.30	27.63
1.22	1.77	5.49	1.82	2.72	2.89	1.76	2.40	2.97	1.44	1.58	5.78	2.48	2.85
0.21	0.86	0.73	0.30	0.27	0.76	0.27	0.76	1.51	3.08	0.68	0.61	0.52	0.48
0.17	0.18	0.58	0.20	0.27	0.25	0.19	0.32	0.42	0.12	0.14	0.56	0.31	0.24
0.09	0.24	1.79	0.78	0.25	0.24	0.19	0.33	0.27	0.25	0.11	0.44	0.44	0.22
0.29	0.36	1.00	0.39	0.54	0.51	0.33	0.58	0.73	0.41	0.31	0.98	0.59	0.51
125.16	871.61	289.70	274.67	173.33	146.30	137.15	151.92	188.15	131.16	43.67	176.12	221.73	148.11
6.70	8.40	13.32	5.22	5.85	7.53	5.13	14.81	13.79	9.70	4.91	12.30	6.48	8.06
1.09	2.02	4.08	1.22	1.94	0.92	1.03	1.23	2.89	0.66	1.00	2.48	0.91	0.82
0.09	0.13	0.41	0.14	0.20	0.18	0.13	0.19	0.24	0.08	0.11	0.50	0.17	0.18
0.62	0.93	0.87	0.81	0.51	0.82	0.70	0.91	0.70	0.62	0.23	0.59	0.37	0.71
0.09	0.16	0.26	0.19	0.13	0.12	0.09	0.18	0.19	0.15	0.07	0.17	0.18	0.12
2.20	5.36	5.29	3.24	2.71	3.07	2.30	2.62	3.95	3.48	2.49	4.07	3.73	2.89
1.06	2.03	3.22	1.46	1.44	1.35	0.85	1.61	2.53	1.48	1.05	3.12	1.74	1.46
0.61	1.04	2.44	0.76	0.66	0.60	0.39	0.61	2.47	2.23	1.93	0.94	0.90	0.60
5.00	5.13	3.26	4.06	3.16	5.20	3.94	5.76	5.46	7.67	6.35	3.14	4.16	5.54
0.79	1.24	0.79	1.14	0.78	0.93	0.65	0.63	1.00	1.17	1.35	0.80	1.12	1.00
15.00	7.80	9.72	12.53	16.36	7.44	20.35	15.11	10.98	8.05	12.69	8.11	5.88	7.32
0.49	0.55	1.03	0.94	0.90	0.60	0.37	0.57	1.29	0.67	2.71	0.67	0.75	0.64
39.40	39.34	40.52	39.42	41.19	33.71	40.07	37.55	40.78	33.02	35.40	37.69	33.19	33.62
0.62	1.34	1.08	1.49	1.10	1.35	1.17	0.88	0.86	0.78	1.09	1.21	1.02	1.49
0.08	0.10	0.13	0.07	0.08	0.14	0.08	0.11	0.09	0.11	0.06	0.15	0.15	0.14
2.43	2.29	3.71	2.81	3.60	1.56	2.31	3.40	4.17	1.50	2.95	2.74	1.20	1.68
0.94	0.46	0.43	0.49	1.11	0.39	1.29	1.11	1.19	0.50	0.67	0.52	0.60	0.41
1.65	0.91	1.46	0.54	0.81	0.87	0.59	2.35	2.40	1.57	1.00	1.10	0.75	0.85
32.19	48.59	40.46	37.45	43.17	21.44	31.64	17.89	46.65	17.10	45.58	23.88	19.47	18.98
3.08	2.26	4.27	3.36	3.65	3.36	2.25	5.23	7.05	4.37	12.73	2.65	2.81	3.57

Mio-Pliocene NE part of basin															
fatma	Core-1					Core-2		Core-3		Core-4					
S	S	S	S	S	S	S	S	S	S	S	S	S	S	S	S
26--34	C1--01	C1--03	C1--04	C1--05	C1--08	C2--01	C2--02	C3--01	C3--03	C4--01	C4--03	C4--05	C4--07	C4--08	C4--13
17.70	37.81	48.07	39.78	53.29	52.49	54.23	57.79	49.96	37.81	29.50	37.26	40.50	52.42	48.72	59.69
1.44	1.33	1.60	1.53	1.80	1.78	4.65	5.05	4.09	4.41	1.67	3.11	3.14	3.48	3.86	5.91
0.46	0.11	0.13	0.12	0.14	0.15	0.43	0.46	0.58	0.19	0.17	0.21	0.57	0.55	0.46	0.38
1.55	0.38	9.80	10.57	7.99	8.56	1.33	1.62	1.00	1.11	0.85	0.75	0.79	1.09	1.14	1.68
1.86	0.50	0.46	0.43	0.47	0.47	1.93	2.30	1.90	1.70	0.88	0.96	2.25	1.97	1.94	2.51
42.80	35.06	17.22	19.91	14.59	14.94	20.43	17.23	24.12	32.30	37.94	32.02	29.25	20.63	23.01	14.71
0.07	0.45	0.23	0.27	0.68	0.69	0.12	0.24	0.21	0.11	0.05	0.14	0.21	0.14	0.16	0.26
0.50	0.34	0.45	0.43	0.52	0.52	2.47	1.15	1.08	1.09	0.53	0.93	0.84	0.88	0.89	1.01
0.50	0.64	0.75	0.69	0.82	0.77	1.48	1.50	1.13	1.49	0.72	1.15	1.05	1.13	1.21	1.79
0.02	0.01	0.01	0.01	0.01	0.02	0.03	0.03	0.03	0.02	0.01	0.02	0.03	0.03	0.03	0.03
32.83	26.32	24.05	27.59	20.26	21.05	14.30	14.90	17.10	20.30	29.98	25.15	22.95	18.04	18.96	13.11
99.86	102.98	102.81	101.38	100.60	101.49	101.51	102.38	101.35	100.62	102.41	101.82	101.75	100.48	100.48	101.16
12.29	28.43	30.04	26.00	29.61	29.49	11.66	11.44	12.22	8.57	17.66	11.98	12.90	15.06	12.62	10.10
1.00	1.88	1.67	1.60	1.58	1.48	0.60	1.30	1.05	1.37	1.36	1.24	1.25	1.28	1.36	1.77
7.65	3.11	7.81	6.98	6.73	5.04	13.29	15.03	10.95	11.89	4.04	6.79	8.26	11.81	12.18	21.08
2.45	1.24	0.99	1.57	1.53	1.54	4.62	5.27	5.45	4.44	1.37	2.27	4.49	4.85	4.63	5.37
51.37	32.51	21.82	29.35	18.71	36.29	38.27	49.47	47.03	40.22	23.08	20.64	51.36	43.04	42.02	47.62
25.39	32.10	21.71	11.43	21.03	10.42	15.77	22.12	19.85	16.66	21.24	17.27	29.50	30.38	27.80	33.92
4.77	1.13	1.51	1.28	2.15	1.42	3.78	4.34	3.19	3.01	4.38	8.26	7.17	5.31	6.56	7.88
11.61	7.00	6.04	4.18	5.36	3.44	6.63	8.07	4.46	5.35	7.16	5.84	8.58	9.27	9.72	12.87
5.98	2.87	2.64	-0.89	4.06	-0.69	3.72	8.40	2.56	2.33	3.83	7.54	9.38	7.90	8.91	10.09
16.94	9.05	9.45	9.68	15.55	13.98	21.94	25.07	20.99	19.20	9.92	13.19	24.57	22.01	23.13	31.16
2.48	1.73	2.03	2.08	2.10	2.14	5.60	6.04	5.34	5.05	1.97	3.59	4.22	4.60	5.03	7.01
11.81	15.22	18.07	17.32	19.76	19.05	35.45	37.65	28.67	28.86	15.61	26.19	25.03	27.55	30.28	45.73
541.67	104.30	154.26	155.97	116.06	112.18	218.13	216.33	322.87	341.99	685.13	854.82	645.81	210.31	253.31	202.92
6.63	11.37	8.96	10.04	13.13	12.85	13.35	14.78	16.34	12.13	7.92	7.68	15.70	15.60	14.25	13.31
103.28	59.33	94.44	66.28	98.68	88.50	468.26	486.28	811.01	344.35	117.27	138.50	661.44	671.76	527.72	115.59
7.93	1.98	3.29	3.15	2.21	2.44	8.53	9.38	11.99	7.55	3.43	3.85	9.45	9.36	7.67	6.85
0.69	1.95	1.26	2.77	1.62	17.77	0.32	0.45	0.72	0.47	0.26	0.28	0.54	0.50	0.60	0.44
0.51	0.21	0.28	0.30	0.35	0.26	0.74	0.83	0.75	0.64	0.35	0.79	1.26	0.85	0.86	0.95
0.61	0.42	0.22	0.36	0.24	0.39	0.61	0.68	0.65	0.59	0.47	0.43	0.69	0.56	0.62	0.62
0.39	0.47	0.53	0.55	0.52	0.54	1.03	1.21	0.75	0.92	0.29	0.51	0.59	0.86	0.94	1.67
131.71	128.31	120.83	109.68	145.71	132.18	231.66	237.39	207.84	180.94	130.61	198.85	174.25	183.04	189.70	260.39
9.63	10.35	9.13	9.51	11.30	12.10	15.76	18.60	22.45	14.20	5.84	8.72	18.16	21.41	17.85	14.59
2.48	1.31	2.04	1.60	2.17	2.06	10.26	10.70	17.28	7.41	2.34	3.03	14.12	15.32	11.51	2.75
0.40	0.12	0.20	0.19	0.14	0.18	0.56	0.57	0.74	0.47	0.21	0.24	0.56	0.62	0.49	0.42
0.73	0.54	0.74	0.43	1.02	0.54	1.28	10.85	0.78	1.41	1.34	1.02	2.68	3.23	4.95	1.39
0.12	0.15	0.16	0.15	0.19	0.18	0.21	0.23	0.18	0.18	0.17	0.18	0.18	0.17	0.18	0.31
2.73	3.16	2.94	3.54	3.89	3.47	5.47	5.93	4.02	4.02	2.27	3.20	4.90	5.03	5.39	7.41
2.09	1.40	1.51	1.54	1.78	1.85	3.91	4.41	4.90	3.25	1.19	1.99	3.98	5.41	4.55	3.74
1.24	1.32	1.35	2.70	2.94	2.64	1.48	2.97	2.35	1.87	0.80	1.01	1.87	2.02	1.81	2.99
3.93	8.37	9.27	6.05	7.39	7.85	3.41	3.53	4.12	3.20	4.25	3.85	4.04	4.41	3.86	2.72
0.85	1.14	1.53	0.98	1.17	1.20	0.85	0.84	0.90	0.73	0.86	0.88	0.89	1.11	0.98	0.70
12.13	22.86	14.36	7.41	11.80	5.65	4.03	5.02	4.05	5.13	17.91	8.68	7.41	5.62	6.11	9.06
0.44	1.25	1.00	1.21	0.83	1.30	1.04	1.02	1.54	1.08	0.27	0.24	0.56	1.02	0.69	0.48
41.61	45.20	46.22	41.55	45.56	42.93	45.63	45.45	46.93	46.47	50.18	45.78	46.85	43.86	45.83	42.06
1.45	0.91	1.02	0.95	0.86	0.94	1.18	1.26	1.37	1.17	0.74	1.14	1.16	1.37	1.25	1.10
0.10	0.04	0.05	0.14	0.07	0.15	0.29	0.24	0.27	0.27	0.06	0.13	0.15	0.16	0.17	0.16
2.19	4.59	3.60	2.74	3.93	3.03	2.38	2.74	4.45	3.11	2.97	2.96	3.44	3.28	2.86	2.64
0.49	0.99	0.99	0.39	1.12	0.29	0.41	0.45	0.42	0.41	0.92	0.84	0.57	0.71	0.66	0.71
0.57	1.62	1.49	2.40	2.45	3.74	2.01	1.83	3.66	2.27	1.11	1.31	1.83	1.68	1.47	1.03
42.10	47.97	95.80	42.20	64.59	57.39	101.42	92.27	148.91	77.54	85.47	61.07	147.20	138.44	113.99	21.54
2.02	9.18	6.05	7.43	5.26	8.50	4.17	4.28	7.03	4.71	1.33	1.06	2.53	4.03	2.72	1.85

Mio-Pliocene NE part of basin											Pleistocene	Recent Sediments		
	Core-1										Seguit El Hamra	Oued Draa		
S	SM	SM	SM	SM	SM	SM	SM	SM	SM	SM	sand	sand+silt	silt	silt+sand
C4--14	C1--11	C1--16	C1--19	C1--20	C1--21	C1--22	C1--23	C1--24	C1--25	C1--26	07--04	06--01	06--02	06--03
44.66	20.48	34.96	48.40	52.15	64.35	63.49	84.46	27.47	42.61	23.56	85.69	67.59	61.65	61.53
4.02	1.77	3.88	6.63	7.65	7.09	6.92	2.64	5.60	9.23	5.49	UD	11.21	11.71	12.66
0.45	0.15	0.31	0.50	0.60	0.64	0.64	0.31	0.38	0.59	0.36	0.14	0.67	0.77	0.69
1.08	15.30	12.44	8.33	7.02	4.67	5.11	0.93	11.77	8.16	11.45	0.25	2.06	2.59	2.55
2.11	0.68	1.44	2.85	3.20	2.17	1.74	0.67	2.05	1.87	2.32	0.28	4.42	5.00	4.98
25.36	25.35	19.06	12.01	9.78	6.25	7.26	3.29	22.16	14.08	22.72	6.77	4.22	5.59	5.74
0.11	0.18	0.33	0.38	0.38	0.38	0.34	1.55	0.86	0.66	0.51	0.05	0.12	0.13	0.14
0.88	0.44	0.67	1.07	1.28	1.25	1.31	0.60	0.69	1.00	0.63	0.16	0.63	1.48	0.74
1.24	0.56	1.11	1.82	2.04	2.04	1.99	0.94	1.83	2.94	1.85	0.23	2.70	2.70	2.76
0.03	0.04	0.02	0.02	0.02	0.01	0.01	UD	0.02	0.02	0.02	0.01	0.05	0.06	0.07
20.80	36.96	28.76	19.27	16.58	11.02	12.29	2.87	29.80	20.80	31.33	5.63	6.91	9.11	8.67
100.86	101.94	103.04	101.36	100.80	99.96	101.22	98.32	102.74	102.09	100.37	100.04	100.72	100.95	100.67
11.11	11.57	9.01	7.30	6.82	9.08	9.17	31.99	4.91	4.62	4.29		6.03	5.26	4.86
1.41	1.27	1.66	1.70	1.59	1.63	1.52	1.57	2.65	2.94	2.94	1.44	4.29	1.82	3.73
13.65	4.72	8.55	15.01	15.95	14.58	15.60	7.59	12.85	22.00	14.44	10.30	44.76	51.80	55.39
4.81	2.19	3.87	6.52	7.90	7.33	7.42	2.45	6.59	9.22	6.30	3.73	10.44	11.44	11.66
38.83	25.32	61.49	54.56	68.09	67.68	76.94	37.17	198.89	124.50	61.16	52.28	79.35	88.12	86.18
31.50	10.56	51.17	65.43	81.89	74.39	75.88	44.21	127.39	138.66	87.83	23.48	44.91	66.66	50.52
6.00	2.74	2.25	3.32	3.98	3.15	2.59	1.92	3.35	3.16	5.41	2.79	11.77	14.05	12.29
9.25	8.09	12.99	21.42	24.07	19.36	18.58	10.58	35.70	24.58	77.18	10.54	25.00	27.67	28.12
7.37	-1.03	4.12	7.55	5.54	9.00	7.23	6.39	19.99	10.77	23.39	5.70	21.35	22.21	21.92
24.14	20.75	31.67	65.50	74.86	56.96	57.23	29.05	89.68	71.46	214.04	28.56	69.17	83.17	63.32
5.18	2.40	4.94	7.47	9.74	9.16	8.98	3.57	7.57	11.83	7.50	5.28	14.18	15.29	16.25
30.93	15.97	33.56	57.99	63.69	62.75	61.72	26.29	47.73	82.23	48.18	35.56	87.42	71.36	93.02
238.96	89.01	95.10	113.07	122.24	113.04	117.64	131.89	230.25	240.67	257.70	336.78	129.16	150.30	174.55
17.75	7.44	12.33	19.03	21.59	24.93	23.30	22.74	25.71	32.03	19.56	10.33	24.61	27.15	24.03
622.73	55.28	126.75	189.60	226.58	335.27	359.90	77.83	134.69	211.46	114.94	285.71	294.69	564.12	243.88
7.97	2.74	5.24	8.54	10.70	12.14	12.26	3.93	6.38	9.82	5.92	6.36	11.83	13.97	12.44
0.42	2.19	1.96	0.79	0.94	1.56	2.54	3.40	63.45	6.42	112.60	0.95	0.59	0.79	0.81
0.80	0.37	0.72	1.09	1.33	1.26	1.22	0.26	0.92	1.41	0.91	0.69	1.81	2.10	2.09
0.48	0.20	0.29	0.27	0.43	0.42	0.52	0.26	1.46	0.59	1.70	0.69	0.54	0.68	0.67
1.00	0.75	1.61	2.89	3.25	2.83	2.83	1.06	2.33	4.11	2.27	0.98	5.08	4.97	5.14
191.66	62.87	122.56	198.71	211.10	252.32	256.59	139.83	125.54	243.55	147.68	432.16	436.92	427.00	489.16
23.90	6.74	12.10	19.62	22.66	25.25	23.82	19.87	19.97	28.77	16.94	12.57	31.14	32.64	32.82
14.04	1.41	2.94	4.53	5.61	8.02	8.58	1.52	3.28	5.12	2.86	6.41	7.35	13.49	6.12
0.49	0.17	0.32	0.51	0.69	0.76	0.77	0.08	0.41	0.64	0.39	0.42	0.84	0.98	0.89
1.31	0.46	1.00	1.04	1.23	1.05	1.11	0.80	0.83	1.25	0.74	0.63	1.30	1.49	1.33
0.21	0.13	0.28	0.50	0.52	0.48	0.48	0.19	0.31	0.92	0.30	0.23	0.46	0.47	0.50
5.05	5.53	4.29	5.70	6.19	6.30	6.71	3.77	3.80	6.57	3.72	5.42	14.01	13.75	20.29
6.49	1.52	3.17	5.16	6.14	6.81	6.61	3.92	4.53	7.35	4.25	2.81	8.89	9.59	9.31
1.76	1.58	2.55	4.38	4.36	3.69	3.77	15.48	16.07	110.42	21.10	1.96	2.87	3.35	2.32
4.97	3.07	3.13	3.01	2.87	3.45	3.21	8.10	3.03	3.12	2.69	3.37	2.98	2.85	2.81
1.35	0.69	0.82	0.79	0.78	0.93	0.89	1.60	0.69	0.80	0.68	0.75	0.85	0.84	0.80
4.85	6.95	16.15	12.67	13.33	10.92	11.47	11.26	28.14	18.85	20.66	8.35	5.05	6.95	5.43
1.08	0.56	1.41	1.55	1.54	2.16	2.55	2.04	1.35	2.33	0.79	1.01	0.76	0.68	0.76
44.35	39.13	43.14	41.86	40.42	41.83	41.93	51.37	41.04	41.34	40.17	44.59	40.08	41.83	39.84
1.35	0.91	0.98	1.03	1.05	1.01	1.02	0.87	0.78	0.90	0.87	1.22	1.27	1.20	1.37
0.15	0.21	0.08	0.10	0.10	0.10	0.10	0.06	0.05	0.07	0.07	0.16	0.23	0.17	0.23
3.41	1.30	3.94	3.05	3.40	3.84	4.08	4.18	3.57	5.64	1.14	2.23	1.80	2.41	1.80
0.81	0.42	0.83	1.20	1.20	1.10	0.99	1.19	0.64	1.11	1.44	0.45	0.57	0.76	0.59
1.92	0.92	0.95	0.89	0.90	1.29	1.25	2.15	0.72	1.30	0.25	0.98	0.98	0.98	0.85
129.58	25.19	32.78	29.09	28.69	45.75	48.52	31.74	20.44	22.93	18.25	76.59	28.24	49.32	20.91
3.98	2.46	5.38	5.90	5.69	8.02	9.19	10.35	5.97	9.10	3.13	4.50	2.65	2.32	2.67

Recent Sediments													
Tan-Tan River		Oued Chebeika		Seguit El Hamra				Cap Jubi	Oued Akhfennir		Ouel El Craa	Laayoune Plage	Tarfaya
sand	sand+silt	sand	mud	mud	mud	silt+sand	mud	sand	sand	sand	sand	sand	sand
06--04	06--05	06--06	06--07	07--01	07--02	07--03	07--05	08--02	09--01	09--02	14--01	15--10	18--03a
82.23	65.15	81.88	45.19	52.07	46.49	51.98	47.81	42.88	49.12	47.74	56.83	47.17	44.12
5.03	9.47	5.11	13.37	12.68	20.93	13.04	19.54	2.69	3.01	3.06	4.51	5.16	4.57
0.56	0.64	0.12	0.66	0.69	0.77	0.70	0.86	0.08	0.33	0.28	0.40	0.12	0.07
0.94	2.21	0.44	3.61	3.10	3.34	2.71	3.54	1.05	1.16	1.11	1.20	1.12	0.72
2.48	3.84	0.61	5.25	4.86	7.52	4.95	7.27	0.79	1.82	1.66	2.03	1.04	0.71
3.04	6.98	3.86	12.53	10.56	3.66	10.27	5.62	28.82	24.28	24.80	18.49	23.46	26.34
0.06	0.13	0.05	0.23	0.43	0.25	0.39	0.26	0.13	0.09	0.10	0.14	0.11	0.10
0.70	0.89	0.23	1.13	1.17	2.37	1.57	0.99	1.03	1.23	1.12	0.82	1.91	1.75
1.49	2.27	3.67	3.35	2.42	3.51	2.40	3.34	1.26	1.18	1.19	1.36	1.84	1.88
0.03	0.05	0.01	0.07	0.07	0.09	0.06	0.08	0.01	0.02	0.02	0.02	0.01	0.01
3.41	9.36	3.63	16.10	13.10	11.73	11.86	11.56	23.47	20.05	20.59	15.48	19.38	20.95
100.09	101.13	99.71	101.61	101.28	100.80	100.08	101.03	102.37	102.43	101.79	101.41	101.48	101.38
16.35	6.88	16.02	3.38	4.11	2.22	3.99	2.45	15.94	16.32	15.60	12.60	9.14	9.65
2.13	2.55	15.96	2.96	2.07	2.56	1.53	3.37	1.22	0.96	1.06	1.66	0.96	1.07
13.75	32.59	6.24	43.82	56.26	100.90	56.96	98.90	5.15	6.94	7.81	4.41	9.18	6.13
5.07	8.54	1.29	12.29	11.65	16.46	11.57	17.76	1.20	3.02	2.84	1.07	1.87	1.25
41.98	64.12	11.61	104.59	106.16	147.40	107.52	152.30	10.39	42.87	40.26	7.97	13.56	8.51
16.41	33.07	3.31	59.06	65.25	86.86	72.49	88.30	2.64	14.12	11.99	3.70	13.74	3.94
3.33	8.51	0.63	12.28	12.95	17.69	11.63	18.77	-	1.51	1.51		0.45	
8.15	21.02	2.02	36.03	37.00	48.20	35.91	49.32	1.96	7.59	8.07	0.10	2.47	1.41
6.67	17.59	1.63	21.60	20.79	26.52	19.11	27.13	3.18	3.29	3.09	0.82	1.91	1.57
62.05	52.56	16.91	80.25	89.58	99.92	102.85	114.44	12.23	22.48	23.49	5.14	14.89	16.97
6.14	11.61	4.72	17.14	16.30	26.32	16.49	25.85	2.68	3.44	3.54	1.18	4.87	4.23
40.57	67.96	89.92	100.70	86.74	84.17	87.02	132.74	27.37	26.43	28.11	6.23	42.25	43.14
116.12	159.78	107.43	252.65	256.48	180.67	266.36	202.21	1064.02	718.77	761.15	125.35	972.81	1020.10
18.98	23.78	5.18	20.65	24.88	24.97	23.80	27.81	6.44	8.90	10.33	3.68	7.73	5.82
668.74	314.19	85.51	231.22	203.76	135.06	195.59	133.48	28.10	68.28	51.56	207.06	45.35	32.28
8.83	11.62	2.19	11.20	12.25	14.82	12.29	16.11	1.53	4.11	3.98	2.11	2.55	1.88
0.39	0.68	0.23	1.71	2.59	1.77	3.00	2.54	0.26	0.73	0.93	0.20	0.28	0.25
0.91	1.59	0.31	2.07	2.10	3.50	2.09	3.33	0.23	0.48	0.46	0.17	0.36	0.32
0.45	0.56	0.10	0.52	0.69	0.65	0.71	0.70	0.35	0.67	0.64	0.08	0.41	0.39
1.39	3.25	1.27	5.11	4.78	7.64	4.83	8.29	0.49	0.57	0.66	0.17	0.74	0.61
373.23	432.26	686.95	301.75	439.22	363.15	481.82	410.91	213.75	275.48	316.42	118.38	330.52	329.48
22.56	27.98	8.02	30.81	35.00	43.93	35.00	51.30	5.73	9.75	9.28	4.98	7.58	6.01
15.59	7.75	2.17	5.79	5.18	3.70	4.85	3.66	0.81	1.71	1.44	4.84	1.28	0.98
0.44	0.86	0.16	0.81	0.87	1.06	0.88	1.16	0.12	0.28	0.27	0.13	0.19	0.15
0.85	1.14	0.21	1.40	1.33	1.86	1.29	1.87	0.24	0.47	0.46	0.26	0.40	0.29
0.22	0.39	0.44	0.56	0.53	0.79	0.52	0.80	0.15	0.21	0.23	0.04	0.22	0.23
9.34	15.49	7.44	16.54	17.20	21.26	15.86	24.02	3.33	5.08	5.01	2.16	5.02	3.88
6.17	8.20	1.75	8.84	9.78	12.27	9.38	14.02	1.45	2.04	2.07	1.43	1.93	1.64
1.82	1.99	0.62	2.78	4.30	2.40	4.40	3.22	1.00	1.36	1.72	0.76	0.95	0.90
4.45	3.28	6.22	2.51	3.01	2.67	3.03	2.89	4.76	3.23	3.27	4.65	4.04	4.82
1.22	0.96	1.36	0.72	0.84	0.75	0.81	0.79	1.20	0.68	0.73	1.34	1.03	1.31
2.66	4.03	1.89	6.68	6.67	7.08	7.73	6.30	1.82	6.92	5.80	2.58	7.13	2.41
1.85	0.96	2.77	0.72	0.76	0.69	0.81	0.75	-	1.35	1.37		4.27	
42.91	40.56	39.34	39.94	39.30	36.48	40.37	36.43	34.68	39.87	35.78	42.75	35.36	32.99
1.19	1.18	1.55	1.49	1.41	1.76	1.47	1.84	0.89	1.09	0.90	1.36	0.98	1.03
0.31	0.26	0.39	0.21	0.18	0.19	0.16	0.20	0.46	0.21	0.24	0.29	0.14	0.32
2.01	1.57	1.64	1.64	1.76	1.80	2.02	1.79	1.34	1.86	1.49	36.96	5.55	2.80
0.39	0.52	0.28	0.56	0.61	0.59	0.67	0.58	0.25	0.33	0.30	0.46	1.01	0.46
2.33	1.13	2.56	0.57	0.67	0.52	0.66	0.56	3.29	1.17	1.28	36.73	3.13	4.13
131.83	36.80	66.32	18.82	17.50	8.20	16.91	7.51	23.35	22.64	18.14	193.10	24.21	25.92
6.76	3.29	12.69	2.51	2.70	2.48	3.01	2.73	-	6.48	6.15		16.80	

	Upper Cretaceous							Mio-Pliocene						
E beach	Sebkha Tisfurine	Onhym Quarry				Akhfennir		Core-1				Core-2		Core-3
sand	WM	WM	WM	WM	WM	WM	WM	WM	WM	WM	WM	WM	WM	WM
18--04a	23--01	24--03	24--04	24--05	24--06	24--18	26--25	C1--06	C1--07	C1--09	C1--10	C2--03	C2--04	C3--02
50.23	24.93	42.53	36.82	34.91	41.08	13.89	50.31	45.77	58.43	80.95	82.44	8.86	13.11	42.04
5.25	5.15	5.35	4.74	4.73	4.22	3.11	4.60	1.45	1.92	4.22	4.44	2.27	3.19	3.97
0.09	0.39	0.41	0.39	0.34	0.34	0.18	0.70	0.12	0.17	0.31	0.31	0.17	0.21	0.39
0.66	10.45	2.62	2.13	2.70	2.59	13.57	1.90	9.68	6.96	2.75	1.58	16.52	14.68	1.12
0.82	2.25	2.44	1.95	2.10	2.11	3.16	5.25	0.37	0.49	1.56	1.97	5.16	6.43	1.71
22.45	22.73	21.64	26.32	26.45	23.54	25.02	18.50	17.34	12.02	3.34	1.60	33.36	30.48	29.57
0.10	0.36	0.17	0.15	0.12	0.14	0.42	0.06	0.52	0.78	0.77	0.84	0.27	0.27	0.17
1.77	2.22	2.62	2.34	2.45	2.52	2.55	1.25	0.43	0.59	0.97	1.14	0.52	0.40	1.12
1.84	1.79	1.61	1.42	1.42	1.33	0.79	1.29	0.69	0.85	1.40	1.45	0.61	0.95	1.11
0.01	0.02	0.03	0.03	0.03	0.03	0.01	0.09	0.01	0.01	UD	UD	0.04	0.03	0.02
18.33	30.58	23.33	23.88	26.00	22.61	39.13	66.14	24.50	17.21	5.58	3.24	34.30	32.30	20.80
101.68	101.08	102.86	100.26	101.34	100.60	101.96	100.15	100.91	99.46	101.91	99.08	102.14	102.16	102.13
	0.25	0.28	0.24	0.24	0.24	0.28	0.10							
9.57	4.84	7.95	7.77	7.38	9.73	4.47	10.94	31.57	30.43	19.18	18.57	3.90	4.11	10.59
1.04	0.91	0.69	0.68	0.64	0.58	0.35	1.12	1.60	1.44	1.44	1.27	1.17	2.38	0.99
7.42	15.84	22.18	21.38	20.50	18.13	10.93	16.64	5.66	5.39	10.09	10.56	10.92	14.04	13.56
1.56	5.47	5.14	5.15	4.68	4.63	3.64	4.29	1.42	1.66	3.32	3.72	2.93	3.40	3.65
10.06	183.24	41.57	43.33	41.80	41.06	30.18	57.64	21.04	48.21	60.25	72.06	71.66	76.59	24.96
9.38	126.79	24.85	37.70	34.51	34.78	51.07	31.29	6.70	26.02	39.22	52.04	49.98	47.03	15.41
0.18	6.25	3.74	4.69	5.60	4.16	2.16	5.76	0.84	1.35	1.48	1.70	2.93	2.99	3.62
1.70	83.06	10.59	12.88	12.15	11.46	12.42	22.03	2.67	6.82	10.68	12.60	7.79	10.68	7.45
1.78	50.80	7.01	7.50	7.35	6.71	5.40	7.55	-0.09	3.51	4.43	4.78	1.15	2.56	2.97
14.91	134.73	35.55	29.84	35.01	35.55	33.65	41.96	13.27	15.63	23.26	27.21	34.52	37.98	22.98
4.91	6.33	6.63	5.96	5.76	5.39	4.32	5.08	1.76	2.38	5.01	5.52	3.02	4.22	5.24
43.41	44.06	40.91	37.14	35.80	34.38	24.87	32.43	16.74	21.25	39.43	42.37	17.06	26.57	37.75
865.86	311.88	317.03	352.72	337.14	335.12	318.63	264.50	126.52	103.72	90.75	95.92	238.51	213.14	380.53
6.78	18.84	12.74	12.36	10.46	11.46	16.15	11.16	10.12	14.27	18.63	20.48	6.43	6.90	9.35
36.58	86.52	220.68	109.81	82.44	82.26	466.66	94.21	84.37	127.62	113.89	98.49	72.54	93.96	52.72
2.16	5.85	7.07	6.96	6.03	6.30	3.19	5.93	2.11	3.00	1.10	1.66	6.20	5.77	4.71
0.25	27.54	0.92	1.11	1.27	1.41	3.78	2.02	2.51	9.42	8.37	6.15	1.03	1.71	0.35
0.37	0.71	0.83	0.74	0.71	0.63	0.13	0.61	0.22	0.27	0.11	0.01	0.43	0.52	0.56
0.47	1.94	0.48	0.49	0.40	0.47	0.20	0.44	0.34	0.31	0.15	0.50	1.53	1.82	0.50
0.65	2.08	1.78	1.66	1.62	1.34	0.75	1.31	0.46	0.59	1.53	1.56	0.88	1.40	1.16
343.32	716.34	200.41	169.27	161.47	178.29	257.36	164.70	121.96	151.99	213.83	227.32	51.46	76.14	221.23
6.99	16.57	15.71	17.28	13.12	14.92	15.20	12.92	9.00	12.37	17.44	18.96	8.33	9.20	10.51
1.09	2.42	5.44	2.93	2.26	2.23	10.98	2.54	1.90	2.78	1.39	2.02	1.77	2.30	1.39
0.16	0.39	0.53	0.46	0.41	0.42	0.10	0.39	0.13	0.19	0.07	0.00	0.28	0.29	0.29
0.41	1.01	0.94	0.70	0.83	0.56	0.55	0.83	1.19	1.65	0.45	0.76	0.63	0.69	2.42
0.22	0.33	0.22	0.20	0.19	0.19	0.22	0.26	0.17	0.25	0.33	0.36	0.08	0.13	0.21
4.38	3.50	7.33	6.68	6.31	5.65	4.03	5.71	3.89	3.47	3.57	3.84	7.62	7.73	5.45
1.76	4.37	4.57	4.32	3.66	3.90	4.05	3.93	1.44	2.07	3.74	4.21	2.28	2.67	3.07
0.96	16.60	2.87	2.53	2.88	2.00	3.55	3.26	2.85	3.06	3.34	3.86	1.58	1.94	1.35
4.49	3.03	3.06	3.36	2.80	3.22	4.17	3.01	6.35	7.44	5.25	5.09	2.84	2.71	2.88
1.13	0.80	0.89	0.84	0.78	0.84	1.11	0.91	1.01	1.24	1.12	1.13	0.78	0.79	0.84
5.32	29.02	5.44	8.72	9.44	8.92	12.62	7.97	4.66	12.58	10.49	12.36	21.92	17.59	5.03
9.64	0.70	1.22	0.92	0.65	0.94	1.88	0.68	1.70	1.53	2.52	2.47	0.78	0.89	0.85
33.49	35.77	40.55	37.42	36.47	36.95	42.49	37.09	44.37	45.86	81.99	48.85	41.03	40.92	37.86
1.03	0.88	1.23	1.40	1.25	1.30	0.94	1.16	0.89	0.87	0.94	0.93	1.30	1.33	1.12
0.17	0.04	0.21	0.14	0.14	0.13	0.07	0.14	0.21	0.06	0.08	0.07	0.06	0.07	0.24
5.50	1.53	2.35	2.93	2.84	3.03	4.11	1.42	2.51	3.82	3.67	4.13	6.41	4.40	2.07
0.93	0.69	0.60	0.87	0.83	0.85	1.69	0.54	0.32	0.54	0.65	0.72	0.70	0.61	0.62
3.98	0.23	1.20	0.96	0.86	1.00	1.30	0.51	3.79	2.09	1.74	1.63	0.83	0.65	1.25
23.49	15.80	42.93	21.33	17.61	17.78	128.11	21.94	59.51	76.77	34.26	26.46	24.72	27.64	14.46
38.23	2.65	4.20	3.68	2.34	3.59	7.05	2.24	10.67	9.17	11.78	11.14	2.84	3.08	2.90

Mio-Pliocene						
Core-3			Core-4			
WM	WM	WM	WM	WM	WM	WM
C3--04	C3--05	C3--06	C4--09	C4--10	C4--15	C4--16
48.47	33.77	5.89	52.75	40.75	20.72	21.93
5.30	3.46	1.93	3.67	3.25	3.57	3.13
0.34	0.30	0.08	0.60	0.32	0.23	0.30
1.55	1.17	1.31	1.12	0.85	1.30	1.19
2.72	2.24	1.82	2.18	1.45	2.66	3.42
21.34	33.73	59.71	20.55	28.27	40.05	39.11
0.12	0.51	0.07	0.17	0.29	0.58	0.58
0.85	0.67	0.13	0.78	0.69	0.54	0.54
1.67	1.13	0.22	1.15	1.09	1.05	0.91
0.02	0.02	0.02	0.03	0.02	0.02	0.03
17.30	24.20	28.50	17.09	23.18	31.46	30.78
99.79	101.31	99.87	100.22	100.25	102.28	102.00
9.15	9.76	3.05	14.37	12.54	5.80	7.01
1.96	1.69	1.69	1.47	1.58	1.94	1.69
19.52	12.40	2.83	12.48	11.29	15.46	14.30
5.49	3.82	1.39	5.86	3.52	4.45	3.70
48.51	37.84	133.20	52.23	32.68	56.09	69.43
31.09	23.55	31.14	20.68	28.27	40.52	34.15
4.66	4.25	2.67	4.41	3.19	4.04	4.94
12.67	10.27	22.02	7.60	7.91	9.38	15.47
5.04	2.79	4.11	7.30	6.99	3.95	6.68
43.66	37.54	81.64	25.20	19.80	27.85	36.36
7.04	4.52	1.56	5.28	4.17	5.04	4.19
45.44	28.98	7.23	29.75	28.94	30.04	25.15
244.68	339.19	949.84	247.79	305.03	474.51	378.84
11.68	10.26	3.89	18.04	10.82	9.10	10.07
158.55	222.94	24.35	764.17	344.38	74.51	157.86
6.95	5.74	1.20	12.28	5.63	5.39	6.20
0.41	0.62	2.10	0.69	0.83	0.58	1.10
0.82	0.46	0.19	0.85	0.63	0.88	0.62
0.65	0.64	1.20	0.69	0.46	0.85	1.27
1.69	1.07	0.40	0.95	0.89	1.46	1.22
244.28	161.69	108.63	187.17	190.42	118.29	109.16
14.60	11.61	2.80	22.10	13.62	10.86	12.24
3.65	5.07	0.68	17.02	7.67	1.84	3.58
0.42	0.31	0.08	0.71	0.35	0.30	0.32
0.92	0.87	0.25	9.97	5.70	0.74	0.94
0.25	0.18	0.06	0.17	0.17	0.18	0.21
6.73	5.92	1.92	5.30	4.87	7.57	9.52
4.05	3.05	0.78	5.41	3.42	2.77	2.96
1.73	7.07	1.48	2.30	2.89	8.28	5.23
2.66	3.04	2.02	3.77	3.87	2.44	3.30
0.74	0.80	0.56	0.92	0.97	0.62	0.80
7.68	7.73	40.10	3.82	8.27	14.65	11.55
0.87	0.72	0.29	1.23	1.07	0.68	0.60
43.41	43.98	35.81	44.89	44.88	40.39	44.06
1.25	1.13	0.72	1.23	1.26	1.19	1.22
0.18	0.16	0.04	0.28	0.12	0.11	0.11
2.46	2.29	1.41	2.72	3.57	4.32	2.21
0.64	0.62	0.23	0.40	0.86	0.72	0.49
0.92	1.00	0.18	2.37	1.37	0.97	0.65
28.88	58.29	17.54	130.32	97.86	16.73	42.62
3.13	2.73	1.05	5.02	4.27	2.69	2.47

S=sandsone
SM=sandy marl
BS=black shale
WM=weathered marl
LOI=loss on ignition
Na2O*%= Cl- bound Na2O from seawater or brine salt
UD= under detection limit

Table 3.2.2 Rare earth element (REE) compositions of the Tarfaya basin sediments from Lower Cretaceous to recent

tratigraphic ag	Lower cretaceous					Upper Cretaceous														
Sections	Boukhchebat					Sebkha Tah E		Sebkha Tah W		Sebkha Tisfourine		Amma fatma		Core-1		Core-3	Core-4			
Rock type	S	S	S	S	S	SM	SM	SM	SM	SM	SM	arbonat	BS	BS	BS	BS	BS	BS	BS	BS
Sa. no.	27--02	27--12	27--21	27--26	27--28	20--02	20--05	20--13	20-19	23--04	23-11	26-14	26--23	C1--27	C1--28	C3--07	C4--17	C4--18	C4--20	C4--25
La	8.60	6.63	14.89	15.32	7.91	32.35	13.13	20.45	25.48	13.04	10.69	1.15	9.19	14.87	23.30	10.21	9.27	7.54	7.06	6.62
Ce	20.83	13.39	30.02	33.11	17.33	64.71	28.07	35.63	49.71	19.09	15.92	1.58	16.88	26.66	36.93	19.71	14.15	12.53	12.66	12.23
Pr	2.48	1.80	3.99	4.10	2.04	7.70	3.25	4.68	6.06	2.72	2.25	0.19	2.12	3.41	5.11	2.36	1.81	1.57	1.61	1.50
Nd	9.75	7.17	15.70	15.76	8.09	28.87	12.74	18.04	23.17	10.69	8.89	0.72	8.18	13.01	19.74	8.89	7.04	6.08	6.17	5.66
Sm	1.97	1.38	2.91	3.06	1.57	5.56	2.49	3.51	4.43	2.06	1.75	0.13	1.61	2.53	3.82	1.73	1.36	1.17	1.20	1.13
Eu	0.47	0.32	0.65	0.57	0.46	1.18	0.56	0.76	0.90	0.46	0.38	0.03	0.35	0.53	0.83	0.38	0.30	0.25	0.26	0.25
Gd	1.82	1.23	2.82	2.60	1.51	5.20	2.27	3.44	4.29	2.10	1.75	0.14	1.51	2.35	3.86	1.67	1.48	1.13	1.16	1.06
Tb	0.28	0.16	0.41	0.38	0.21	0.79	0.34	0.52	0.69	0.33	0.27	0.02	0.24	0.36	0.60	0.27	0.22	0.17	0.18	0.16
Dy	1.57	0.82	2.34	2.04	1.12	4.62	1.92	3.15	4.22	2.00	1.65	0.14	1.38	2.19	3.71	1.60	1.40	1.07	1.09	1.00
Ho	0.30	0.15	0.46	0.41	0.22	0.91	0.37	0.65	0.87	0.43	0.36	0.03	0.28	0.45	0.79	0.33	0.30	0.23	0.23	0.20
Er	0.82	0.41	1.28	1.17	0.57	2.55	1.02	1.85	2.54	1.25	1.03	0.09	0.81	1.29	2.30	0.95	0.85	0.64	0.64	0.59
Tm	0.12	0.06	0.19	0.18	0.08	0.38	0.14	0.28	0.39	0.18	0.15	0.01	0.12	0.19	0.34	0.15	0.12	0.10	0.10	0.09
Yb	0.82	0.42	1.30	1.29	0.53	2.57	0.98	1.84	2.67	1.23	1.02	0.09	0.81	1.29	2.27	0.95	0.81	0.65	0.64	0.60
Lu	0.12	0.07	0.20	0.21	0.08	0.38	0.15	0.28	0.40	0.19	0.16	0.01	0.12	0.20	0.36	0.15	0.12	0.10	0.10	0.09
Y	8.62	4.35	14.96	12.34	6.27	25.91	10.64	22.05	26.47	17.60	1.12	1.12	9.73	15.13	30.29	10.77	12.53	8.11	7.64	6.84
∑REE	49.94	34.03	77.17	80.19	41.74	157.76	67.42	95.07	125.81	55.75	46.26	4.33	43.59	69.32	103.96	49.34	39.22	33.23	33.09	31.18
LREE/HREE	7.45	9.11	7.50	8.63	8.54	8.00	8.31	6.86	6.78	6.18	6.20	7.06	7.20	7.27	6.25	7.09	6.34	7.07	6.95	7.15
Eu/Eu*	0.76	0.76	0.69	0.62	0.92	0.67	0.72	0.67	0.63	0.67	0.66	0.66	0.69	0.66	0.66	0.69	0.65	0.67	0.68	0.69
Ce/Ce*	1.11	0.95	0.95	1.02	1.06	1.01	1.05	0.89	0.98	0.79	0.80	0.84	0.94	0.92	0.83	0.98	0.85	0.89	0.92	0.95
La/Sm	4.36	4.78	5.11	5.01	5.03	5.81	5.27	5.82	5.75	6.34	6.12	8.58	5.72	5.89	6.09	5.89	6.82	6.47	5.86	5.86
Gd/Yb	2.23	2.92	2.18	2.02	2.85	2.02	2.33	1.87	1.61	1.72	1.72	1.55	1.86	1.82	1.70	1.77	1.83	1.73	1.81	1.77
La/Yb	10.55	15.67	11.50	11.89	14.97	12.57	13.44	11.12	9.56	10.63	10.51	12.73	11.30	11.51	10.27	10.80	11.50	11.58	11.08	11.05
Y/Ho	28.34	28.47	32.41	30.36	28.67	28.40	29.08	34.04	30.45	41.17	3.15	37.86	34.26	33.76	38.10	32.31	41.60	35.72	33.53	33.78
Gd_N/Yb_N	1.85	2.42	1.80	1.67	2.36	1.67	1.92	1.55	1.33	1.42	1.42	1.28	1.54	1.50	1.41	1.46	1.51	1.43	1.50	1.47

Early Eocene					Oligo-Early Miocene				Mio-Pliocene SW part of basin						
Sebkha El Farma					Sebkha Aridal				Sebkha Aridal		Sebkha El Farma		Oued El Khatt		
BS	BS	BS	BS	SM	SM	SM	SM	SM	S	S	S	S	S	S	S
17--01	17--07	17--16	17--20	17--24	16--02	16--07	16--10	16--14	16--18	16--21	17--32	17--37	19--06	19--10	19--12
19.70	13.05	14.73	21.87	6.00	15.97	18.49	16.63	20.74	6.70	8.40	13.32	5.22	5.85	7.53	5.13
35.69	17.98	22.47	41.69	11.39	30.15	33.82	31.70	39.96	8.27	17.26	28.78	9.95	12.17	12.96	7.97
4.64	2.69	3.15	5.14	1.43	3.68	4.14	3.88	4.86	1.42	1.86	3.31	1.20	1.46	1.68	1.18
17.76	10.57	12.19	19.57	5.53	14.14	15.64	15.07	18.80	5.45	6.96	12.97	4.55	5.60	6.38	4.59
3.46	2.08	2.33	3.76	1.11	2.67	2.94	2.92	3.62	0.98	1.30	2.56	0.89	1.12	1.23	0.94
0.75	0.48	0.52	0.80	0.25	0.54	0.62	0.60	0.78	0.26	0.33	0.59	0.23	0.26	0.29	0.22
3.36	2.28	2.48	3.51	1.08	2.67	2.88	2.93	3.64	1.15	1.24	2.44	0.79	1.07	1.15	0.92
0.52	0.36	0.38	0.53	0.16	0.43	0.46	0.47	0.59	0.19	0.18	0.38	0.12	0.16	0.17	0.13
3.02	2.27	2.39	3.05	0.95	2.64	2.82	2.92	3.69	1.34	1.00	2.19	0.64	0.91	0.96	0.72
0.61	0.50	0.52	0.61	0.19	0.57	0.61	0.62	0.79	0.30	0.20	0.44	0.12	0.18	0.19	0.14
1.73	1.48	1.52	1.69	0.52	1.68	1.79	1.86	2.33	0.84	0.55	1.20	0.34	0.51	0.52	0.39
0.26	0.22	0.23	0.25	0.08	0.26	0.29	0.29	0.36	0.12	0.08	0.18	0.05	0.08	0.07	0.06
1.66	1.48	1.49	1.69	0.53	1.81	2.03	2.06	2.53	0.73	0.55	1.15	0.35	0.50	0.48	0.38
0.24	0.23	0.23	0.25	0.08	0.28	0.32	0.33	0.39	0.11	0.09	0.17	0.05	0.08	0.07	0.06
19.25	19.85	18.84	17.57	5.52	19.16	20.49	21.13	25.83	10.74	6.26	12.36	3.50	5.32	5.60	4.40
93.41	55.67	64.62	104.41	29.29	77.50	86.86	82.29	103.09	27.86	40.00	69.68	24.51	29.94	33.68	22.85
7.12	5.25	5.94	7.95	7.11	6.44	6.70	6.11	6.14	4.76	9.20	7.48	8.83	7.53	8.26	7.05
0.67	0.67	0.66	0.67	0.70	0.62	0.65	0.62	0.65	0.76	0.80	0.73	0.84	0.72	0.74	0.73
0.92	0.74	0.81	0.96	0.95	0.96	0.95	0.97	0.98	0.66	1.07	1.06	0.98	1.02	0.89	0.79
5.69	6.27	6.31	5.82	5.43	5.97	6.28	5.70	5.73	6.87	6.44	5.19	5.85	5.21	6.11	5.44
2.02	1.54	1.67	2.08	2.04	1.48	1.42	1.42	1.44	1.57	2.28	2.12	2.28	2.13	2.41	2.44
11.84	8.83	9.92	12.96	11.36	8.83	9.09	8.06	8.21	9.12	15.40	11.57	14.98	11.65	15.81	13.59
31.49	39.49	36.28	28.87	29.42	33.67	33.72	33.82	32.50	35.55	31.35	28.39	28.18	29.74	30.16	30.35
1.67	1.27	1.38	1.72	1.68	1.22	1.17	1.18	1.19	1.30	1.88	1.75	1.88	1.76	1.99	2.02

Mio-Pliocene NE part of basin						Mio-Pliocene NE part of basin													
Sebkha Tah E	Sebkha Tah W		Sebkha Tisfourine	Onhym Quarry		Amma fatma		Core-1					Core-2		Core-3			
S	S	S	S	S	S	S	S	S	S	S	S	S	S	S	S	S	S	S
20--07	20--23	20--28	23--13	24--09	24--16	26--30	26--34	C1--01	C1--03	C1--04	C1--05	C1--08	C2--01	C2--02	C3--01	C3--03	C4--01	C4--03
14.81	13.79	9.70	4.91	12.30	6.48	8.06	9.63	10.35	9.13	9.51	11.30	12.10	15.76	18.60	22.45	14.20	5.84	8.72
15.13	28.44	18.42	9.70	25.88	13.49	14.31	20.19	18.55	19.62	20.19	22.05	24.65	34.01	40.35	48.34	30.69	12.21	18.62
3.91	3.30	2.22	1.15	3.08	1.59	1.85	2.40	2.42	2.18	2.31	2.55	2.78	3.85	4.55	5.59	3.53	1.49	2.17
16.40	13.35	8.95	4.56	11.81	6.25	6.96	9.20	9.63	8.56	9.09	10.19	10.90	14.71	17.28	21.53	13.48	5.89	8.55
3.51	2.74	1.84	0.87	2.35	1.25	1.31	1.76	1.90	1.70	1.83	2.08	2.18	2.88	3.34	4.15	2.68	1.20	1.73
0.85	0.62	0.43	0.18	0.52	0.29	0.29	0.32	0.44	0.39	0.42	0.48	0.49	0.62	0.69	0.80	0.57	0.28	0.38
3.71	2.77	1.86	0.81	2.09	1.19	1.18	1.51	1.92	1.63	1.75	2.08	2.15	2.56	2.93	3.42	2.37	1.21	1.53
0.53	0.41	0.28	0.12	0.32	0.19	0.17	0.22	0.28	0.24	0.26	0.31	0.32	0.39	0.44	0.48	0.35	0.19	0.23
2.84	2.34	1.60	0.67	1.79	1.08	0.94	1.19	1.66	1.37	1.50	1.83	1.84	2.31	2.54	2.73	2.07	1.21	1.30
0.54	0.47	0.33	0.13	0.35	0.21	0.18	0.23	0.33	0.27	0.30	0.37	0.37	0.47	0.51	0.55	0.41	0.25	0.26
1.39	1.27	0.92	0.36	0.97	0.58	0.50	0.64	0.90	0.71	0.80	1.02	1.02	1.32	1.44	1.59	1.15	0.73	0.72
0.18	0.19	0.13	0.05	0.14	0.09	0.07	0.09	0.13	0.10	0.12	0.15	0.15	0.20	0.22	0.25	0.17	0.11	0.11
1.15	1.19	0.87	0.36	0.96	0.57	0.48	0.65	0.80	0.61	0.76	0.95	0.96	1.39	1.53	1.78	1.19	0.69	0.73
0.17	0.18	0.13	0.05	0.14	0.08	0.07	0.10	0.12	0.09	0.11	0.14	0.14	0.22	0.24	0.29	0.18	0.10	0.11
16.85	15.99	12.41	4.49	10.19	6.34	5.41	6.63	11.37	8.96	10.04	13.13	12.85	13.35	14.78	16.34	12.13	7.92	7.68
65.14	71.06	47.67	23.94	62.72	33.35	36.38	48.13	49.42	46.59	48.96	55.48	60.05	80.69	94.66	113.93	73.07	31.40	45.16
5.11	6.99	6.73	8.26	8.18	7.28	9.05	9.33	6.99	8.22	7.65	7.04	7.57	8.04	8.54	9.21	8.18	5.92	7.99
0.72	0.69	0.72	0.67	0.71	0.73	0.72	0.60	0.70	0.71	0.73	0.70	0.69	0.70	0.68	0.65	0.70	0.70	0.71
0.49	1.03	0.97	1.00	1.03	1.03	0.91	1.03	0.91	1.08	1.06	1.01	1.04	1.07	1.08	1.06	1.06	1.02	1.05
4.22	5.04	5.27	5.64	5.24	5.17	6.16	5.46	5.45	5.37	5.20	5.42	5.56	5.47	5.57	5.41	5.29	4.85	5.04
3.23	2.33	2.13	2.23	2.17	2.09	2.47	2.32	2.40	2.70	2.29	2.19	2.24	1.84	1.91	1.92	1.99	1.74	2.10
12.89	11.57	11.14	13.57	12.76	11.37	16.90	14.82	12.94	15.07	12.45	11.88	12.61	11.31	12.15	12.63	11.93	8.40	12.01
31.20	34.16	37.51	34.35	29.14	29.51	29.85	28.68	34.34	33.68	33.56	35.37	34.50	28.67	29.04	29.77	29.41	31.31	29.47
2.67	1.93	1.76	1.85	1.79	1.73	2.04	1.92	1.98	2.23	1.90	1.81	1.86	1.52	1.58	1.59	1.64	1.44	1.74

Mio-Pliocene NE part of basin					Mio-Pliocene NE part of basin										Pleistocene	Recent Sediments				
Core-4					Core-1										Seguit El Hamra	Oued Draa			Tan-Tan River	
S	S	S	S	S	SM	SM	SM	SM	SM	SM	SM	SM	SM	SM	sand	sand+silt	silt	silt+sand	sand	sand+sil
C4--05	C4--07	C4--08	C4--13	C4--14	C1--11	C1--16	C1--19	C1--20	C1--21	C1--22	C1--23	C1--24	C1--25	C1--26	07--04	06--01	06--02	06--03	06--04	06--05
18.16	21.41	17.85	14.59	23.90	6.74	12.10	19.62	22.66	25.25	23.82	19.87	19.97	28.77	16.94	12.57	31.14	32.64	32.82	22.56	27.98
39.59	45.85	38.54	31.07	51.41	14.00	22.85	37.72	42.23	49.16	45.59	37.06	31.05	49.68	29.34	24.57	65.93	70.69	68.66	48.18	57.89
4.62	5.28	4.43	3.61	5.96	1.52	2.89	4.65	5.19	5.83	5.47	4.58	4.26	6.54	3.79	3.01	7.66	8.19	7.98	5.64	6.86
17.69	19.85	16.94	14.02	22.80	5.87	11.09	17.67	19.68	21.90	20.74	18.01	16.48	24.93	14.50	11.54	29.16	31.25	30.32	21.28	26.57
3.36	3.72	3.28	2.84	4.22	1.16	2.13	3.43	3.84	4.24	4.01	3.53	3.22	4.76	2.84	2.19	5.72	6.16	5.81	3.95	5.15
0.68	0.73	0.65	0.67	0.80	0.26	0.47	0.72	0.83	0.89	0.86	0.75	0.70	1.01	0.60	0.49	1.18	1.26	1.22	0.76	1.06
2.96	3.19	2.85	2.63	3.56	1.14	2.04	3.23	3.58	3.99	3.74	3.45	3.19	4.63	2.72	1.99	5.21	5.62	5.22	3.54	4.75
0.45	0.47	0.42	0.41	0.52	0.18	0.32	0.50	0.57	0.63	0.59	0.53	0.50	0.71	0.42	0.29	0.80	0.86	0.79	0.55	0.74
2.58	2.74	2.42	2.37	3.04	1.09	1.90	3.04	3.44	3.92	3.69	3.14	3.09	4.39	2.62	1.73	4.64	5.03	4.54	3.31	4.40
0.53	0.56	0.48	0.47	0.61	0.24	0.39	0.62	0.71	0.81	0.76	0.65	0.66	0.92	0.55	0.35	0.91	1.01	0.90	0.68	0.88
1.51	1.60	1.40	1.30	1.76	0.69	1.09	1.77	1.99	2.31	2.17	1.83	1.93	2.63	1.57	1.00	2.53	2.83	2.49	1.97	2.46
0.23	0.25	0.21	0.19	0.28	0.11	0.17	0.27	0.30	0.36	0.33	0.27	0.29	0.39	0.24	0.15	0.38	0.43	0.37	0.31	0.37
1.62	1.76	1.48	1.29	1.91	0.82	1.12	1.78	2.06	2.41	2.29	1.77	1.93	2.59	1.58	1.06	2.55	2.95	2.47	2.14	2.49
0.26	0.28	0.23	0.19	0.30	0.13	0.17	0.27	0.31	0.36	0.35	0.26	0.30	0.40	0.24	0.16	0.38	0.45	0.37	0.33	0.37
15.70	15.60	14.25	13.31	17.75	7.44	12.33	19.03	21.59	24.93	23.30	22.74	25.71	32.03	19.56	10.33	24.61	27.15	24.03	18.98	23.78
94.24	107.69	91.19	75.65	121.06	33.95	58.70	95.29	107.38	122.07	114.42	95.70	87.60	132.35	77.96	61.11	158.18	169.36	163.94	115.18	141.98
8.23	8.86	8.53	7.47	9.04	6.65	7.11	7.24	7.22	7.19	7.16	6.98	6.30	6.89	6.78	7.98	8.03	7.77	8.50	7.93	7.56
0.66	0.65	0.65	0.75	0.63	0.69	0.69	0.66	0.68	0.66	0.68	0.65	0.67	0.66	0.66	0.72	0.66	0.65	0.68	0.63	0.65
1.06	1.06	1.06	1.05	1.06	1.07	0.95	0.97	0.95	0.99	0.98	0.95	0.83	0.89	0.90	0.98	1.05	1.06	1.04	1.05	1.02
5.40	5.76	5.45	5.13	5.67	5.80	5.68	5.71	5.91	5.95	5.93	5.63	6.20	6.04	5.97	5.75	5.44	5.30	5.65	5.72	5.43
1.83	1.81	1.92	2.03	1.86	1.40	1.82	1.81	1.74	1.66	1.63	1.95	1.65	1.79	1.72	1.88	2.05	1.91	2.11	1.65	1.90
11.24	12.18	12.04	11.29	12.51	8.23	10.81	10.99	11.01	10.49	10.38	11.22	10.33	11.10	10.71	11.83	12.23	11.06	13.28	10.55	11.21
29.77	28.05	29.39	28.05	29.20	31.60	31.88	30.51	30.61	30.72	30.50	35.07	38.74	34.90	35.71	29.30	26.98	26.97	26.85	28.03	27.09
1.52	1.50	1.59	1.68	1.54	1.15	1.51	1.50	1.44	1.37	1.35	1.61	1.37	1.48	1.42	1.55	1.69	1.58	1.75	1.37	1.58

Recent Sediments												
Oued Chebeika		Seguit El Hamra				Cap Jubi	Oued Akhfennir		Ouel El Craa	Laayoune Plage	Tarfaya E beach	
sand	mud	mud	mud	silt+sand	mud	sand	sand	sand	sand	sand	sand	sand
06--06	06--07	07--01	07--02	07--03	07--05	08--02	09--01	09--02	14--01	15--10	18--03a	18--04a
8.02	30.81	35.00	43.93	35.00	51.30	5.73	9.75	9.28	4.98	7.58	6.01	6.99
16.67	64.01	72.84	84.81	71.68	106.47	11.24	19.91	19.12	10.13	15.11	11.76	13.55
1.99	7.42	8.44	10.80	8.29	12.10	1.40	2.45	2.41	1.29	1.83	1.43	1.67
7.57	28.19	32.03	40.85	31.49	45.31	5.56	9.70	9.48	5.12	7.26	5.61	6.51
1.42	5.36	6.07	7.61	5.88	8.32	1.12	1.91	1.93	1.00	1.46	1.09	1.27
0.39	1.15	1.27	1.54	1.21	1.68	0.26	0.44	0.44	0.20	0.38	0.28	0.33
1.22	4.79	5.44	6.35	5.18	6.92	1.11	1.76	1.85	0.85	1.41	1.04	1.23
0.17	0.69	0.80	0.90	0.76	0.98	0.17	0.26	0.28	0.12	0.22	0.16	0.18
0.95	3.92	4.57	5.01	4.36	5.47	1.01	1.52	1.68	0.66	1.27	0.94	1.08
0.19	0.76	0.90	0.97	0.86	1.05	0.21	0.30	0.34	0.13	0.26	0.19	0.22
0.52	2.10	2.48	2.67	2.38	2.88	0.58	0.84	0.94	0.39	0.73	0.54	0.64
0.08	0.31	0.36	0.40	0.35	0.42	0.09	0.12	0.13	0.06	0.10	0.08	0.10
0.52	2.09	2.43	2.66	2.35	2.81	0.57	0.79	0.87	0.45	0.68	0.55	0.63
0.08	0.31	0.36	0.39	0.35	0.42	0.09	0.12	0.13	0.07	0.10	0.08	0.09
5.18	20.65	24.88	24.97	23.80	27.81	6.44	8.90	10.33	3.68	7.73	5.82	6.78
39.78	151.92	172.97	208.88	170.15	246.12	29.13	49.88	48.89	25.47	38.39	29.76	34.51
9.58	9.08	8.91	9.72	9.18	10.67	6.55	7.65	6.78	8.22	6.98	7.25	7.18
0.91	0.70	0.67	0.68	0.67	0.68	0.70	0.73	0.72	0.67	0.81	0.81	0.80
1.02	1.04	1.04	0.95	1.03	1.05	0.97	1.00	0.99	0.98	0.99	0.98	0.97
5.65	5.74	5.76	5.78	5.95	6.17	5.12	5.10	4.82	4.98	5.18	5.53	5.50
2.33	2.29	2.24	2.38	2.20	2.46	1.95	2.22	2.13	1.89	2.07	1.89	1.93
15.34	14.76	14.43	16.51	14.89	18.24	10.07	12.30	10.69	11.08	11.11	10.94	11.03
27.79	27.04	27.69	25.85	27.74	26.39	30.87	29.35	30.25	27.43	30.22	30.50	30.31
1.93	1.90	1.86	1.97	1.82	2.03	1.61	1.84	1.76	1.56	1.72	1.56	1.60

Upper Cretaceous							Mio-Pliocene										Mio-Pliocene			
Sebkha Tisfurine	Onhym Quarry				Akhfennir		Core-1				Core-2		Core-3		Core-3		Core-4			
WM	WM	WM	WM	WM	WM	WM	WM	WM	WM	WM	WM	WM	WM	WM	WM	WM	WM	WM	WM	WM
23--01	24--03	24--04	24--05	24--06	24--18	26--25	C1--06	C1--07	C1--09	C1--10	C2--03	C2--04	C3--02	C3--04	C3--05	C3--06	C4--09	C4--10	C4--15	C4--16
16.57	15.71	17.28	13.12	14.92	15.20	12.92	9.00	12.37	17.44	18.96	8.33	9.20	10.51	14.60	11.61	2.80	22.10	13.62	10.86	12.24
28.00	33.32	36.77	28.20	31.71	28.90	27.54	18.60	26.33	35.28	40.04	21.30	20.79	25.40	31.48	25.45	5.57	47.04	29.00	24.37	27.04
3.69	3.83	4.23	3.24	3.64	3.55	3.18	2.19	3.04	4.23	4.72	2.30	2.32	2.70	3.57	2.87	0.72	5.31	3.32	2.68	2.99
14.24	14.59	16.22	12.57	13.96	13.71	12.35	8.71	12.17	16.77	18.75	9.27	9.06	10.78	13.73	11.07	2.74	20.12	12.75	10.33	11.39
2.79	2.82	3.05	2.46	2.70	2.64	2.43	1.75	2.50	3.37	3.78	1.71	1.71	2.24	2.71	2.17	0.55	3.87	2.42	2.01	2.23
0.59	0.61	0.62	0.53	0.57	0.56	0.53	0.41	0.57	0.76	0.83	0.36	0.35	0.53	0.59	0.48	0.12	0.77	0.51	0.44	0.46
2.66	2.60	2.66	2.20	2.40	2.50	2.26	1.73	2.44	3.24	3.61	1.44	1.50	2.07	2.40	1.97	0.55	3.44	2.16	1.84	2.01
0.41	0.39	0.40	0.33	0.36	0.37	0.34	0.25	0.36	0.49	0.55	0.21	0.22	0.31	0.36	0.30	0.09	0.52	0.32	0.28	0.30
2.40	2.26	2.18	1.89	2.01	2.25	1.93	1.47	2.12	2.88	3.20	1.16	1.24	1.69	2.06	1.75	0.53	3.03	1.88	1.58	1.74
0.50	0.45	0.43	0.37	0.39	0.48	0.38	0.29	0.42	0.58	0.63	0.22	0.24	0.32	0.40	0.35	0.11	0.62	0.38	0.31	0.34
1.45	1.26	1.20	1.01	1.09	1.42	1.04	0.78	1.15	1.58	1.72	0.59	0.67	0.85	1.11	0.97	0.32	1.79	1.09	0.84	0.96
0.21	0.19	0.18	0.15	0.16	0.23	0.16	0.11	0.16	0.23	0.24	0.09	0.10	0.12	0.17	0.15	0.05	0.28	0.17	0.13	0.14
1.43	1.30	1.20	1.00	1.06	1.58	1.06	0.72	1.06	1.49	1.61	0.59	0.68	0.82	1.11	0.98	0.33	1.94	1.14	0.81	0.93
0.22	0.19	0.18	0.15	0.15	0.25	0.16	0.11	0.16	0.22	0.23	0.09	0.10	0.12	0.17	0.15	0.05	0.31	0.18	0.12	0.14
18.84	12.74	12.36	10.46	11.46	16.15	11.16	10.12	14.27	18.63	20.48	6.43	6.90	9.35	11.68	10.26	3.89	18.04	10.82	9.10	10.07
75.15	79.51	86.59	67.24	75.12	73.63	66.26	46.12	64.87	88.56	98.88	47.65	48.20	58.46	74.45	60.28	14.54	111.13	68.94	56.60	62.91
7.04	8.13	9.22	8.39	8.78	7.04	7.99	7.37	7.16	7.20	7.32	9.78	9.04	8.20	8.50	8.03	6.09	8.26	8.35	8.51	8.50
0.66	0.69	0.67	0.70	0.68	0.66	0.69	0.71	0.71	0.70	0.69	0.69	0.67	0.75	0.71	0.71	0.68	0.64	0.68	0.70	0.67
0.88	1.05	1.05	1.06	1.05	0.97	1.05	1.03	1.05	1.01	1.04	1.19	1.10	1.17	1.07	1.08	0.96	1.06	1.06	1.11	1.10
5.94	5.57	5.67	5.33	5.52	5.76	5.32	5.13	4.95	5.17	5.01	4.89	5.36	4.69	5.39	5.34	5.06	5.71	5.62	5.41	5.49
1.86	2.00	2.22	2.20	2.26	1.58	2.13	2.39	2.31	2.18	2.24	2.46	2.22	2.53	2.16	2.01	1.69	1.77	1.90	2.28	2.15
11.63	12.10	14.44	13.14	14.06	9.60	12.20	12.47	11.71	11.72	11.77	14.22	13.57	12.85	13.16	11.84	8.53	11.40	11.98	13.44	13.10
37.35	28.28	28.74	28.50	29.22	33.97	29.69	34.72	34.18	32.12	32.40	29.22	28.28	29.15	29.06	29.63	34.63	29.19	28.76	29.23	29.29
1.54	1.66	1.84	1.82	1.87	1.31	1.76	1.98	1.91	1.80	1.85	2.04	1.83	2.09	1.79	1.66	1.40	1.47	1.58	1.88	1.78

Table 3.2.3 Range of elemental ratios of the Tarfaya basin sediments in this study compared to the ratios in similar fractions derived from felsic rocks, mafic rocks and upper continental crust.

Elememtal Ratio	Lower Cretaceous	Upper Cretaceous	Early Eocene	Oligo-Early Miocene	Mio-Pliocene SW part of the basin	Mio-Pliocene NE part of the basin	Mio-Pliocene NE part (sandy marls)	Pleistocene Recent sediments	Upper Cretaceous and Mio-Pliocene weathered marls	Range of sediments from felsic sources[1]	Range of sediments from mafic sources[1]	UCC[2]
La/Sc	3.94-8.15	2.35-4.45	2.29-3.35	3.87-5.59	3.14-5.20	2.72-9.27	2.69-8.10	2.51-6.22	2.02-7.44	2.50-16.3	0.43-0.86	2.21
Th/Sc	1.00-1.74	0.58-1.03	0.57-0.71	0.97-1.59	0.65-1.24	0.63-1.53	0.68-1.60	0.68-1.36	0.56-1.24	0.84-20.5	0.05-0.22	0.79
Cr/Th	3.45-10.15	8.10-43.76	13.97-64.24	7.77-16.30	7.44-20.35	4.03-22.86	6.95-28.14	1.82-8.35	3.82-40.10	4.00-15.00	25-500	7.76
Th/Co	0.20-1.05	0.43-1.96	0.67-0.91	1.95-4.34	0.37-1.03	0.24-2.71	0.56-2.55	0.68-9.64	0.29-2.52	0.67-19.4	0.04-1.40	0.63
La/Co	1.31-5.39	1.62-8.99	2.33-4.13	7.41-15.29	2.25-4.27	1.06-12.73	2.46-10.35	2.30-38.23	1.05-11.78	1.80-13.8	0.14-0.38	1.76
Eu/Eu*	0.62-0.92	0.63-0.72	0.66-0.70	0.62-0.65	0.72-0.84	0.60-0.75	0.65-0.69	0.63-0.91	0.64-0.75	0.40-0.94	0.71-0.95	0.63

[1] Cullers (1994, 2000); Cullers and Podkovyrov (2000); Cullers et al. (1988).

[2] McLennan (2011); Taylor and Mclennan (1985).

Table 3.2.4 Nd isotopic data for sediments samples of the Tarfaya basin.

Sections	Stratigraphy	Rock type	Sa.no.	T_{strat} (Ma)	Sm (ppm)	Nd (ppm)	$^{147}Sm/^{144}Nd$	$f^{Sm/Nd}$	$^{143}Nd/^{144}Nd$	±2σ	$\epsilon_{Nd}(0)$	$\epsilon_{Nd}(T)$	T_{DM} (Ga)*	T_{CHUR} (Ga)*
Boukhchebat	Lower cretaceous	sandstone	27--02	120	1.97	9.75	0.12	-0.3786	0.511835	±12	-15.7	-14.5	2.0	1.6
"	"	sandstone	27--12	120	1.38	7.17	0.12	-0.4065	0.511791	±07	-16.5	-15.3	2.0	1.6
"	"	sandstone	27--26	120	3.06	15.76	0.12	-0.4041	0.511654	±12	-19.2	-18.0	2.2	1.9
"	"	sandstone	27--28	120	1.57	8.09	0.12	-0.4022	0.511792	±07	-16.5	-15.3	2.0	1.6
Tisfourine	Upper cretaceous	sandy marl	23--04	80	2.06	10.69	0.12	-0.4089	0.511880	±12	-14.8	-14.0	1.8	1.4
"	"	sandy marl	23--11	80	1.75	8.89	0.12	-0.3957	0.511870	±07	-15.0	-14.2	1.8	1.5
Amma Fatma	"	carbonate	26--14	80	0.13	0.72	0.11	-0.4450	0.512023	±12	-12.0	-11.1	1.5	1.1
"	"	black shale	26--23	80	1.61	8.18	0.12	-0.3959	0.511893	±12	-14.5	-13.7	1.8	1.5
core-1	"	black shale	C1--27	80	2.53	13.01	0.12	-0.4030	0.511913	±12	-14.1	-13.3	1.8	1.4
"	"	black shale	C1--28	80	3.82	19.74	0.12	-0.4049	0.511898	±12	-14.4	-13.6	1.8	1.4
core-4	"	black shale	C4--18	80	1.17	6.08	0.12	-0.4100	0.511882	±12	-14.7	-13.9	1.8	1.4
"	"	black shale	C4--25	80	1.13	5.66	0.12	-0.3861	0.511871	±12	-15.0	-14.2	1.9	1.5
Sebkha El Farma	Early Eocene	black shale	17--01	40	3.46	17.76	0.12	-0.4004	0.511882	±12	-14.7	-14.3	1.8	1.5
"	"	black shale	17--16	40	2.33	12.19	0.12	-0.4117	0.511898	±12	-14.4	-14.0	1.8	1.4
"	"	sandy marl	17--24	40	1.11	5.53	0.12	-0.3854	0.511907	±12	-14.3	-13.9	1.9	1.5
Sebkha Aridal	Oligo-Early Miocene	sandy marl	16--02	25	2.67	14.14	0.11	-0.4187	0.511453	±12	-23.1	-22.9	2.5	2.2
"	"	sandy marl	16-10	25	2.92	15.07	0.12	-0.4049	0.511433	±12	-23.5	-23.3	2.6	2.3
Sebkha Aridal	Mio-Pliocene	sandstone	16--18	10	0.98	5.45	0.11	-0.4503	0.511326	±07	-25.6	-25.5	2.5	2.2
Sebkha El Farma	SW Part of the basin	sandstone	17--32	10	2.56	12.97	0.12	-0.3922	0.512017	±12	-12.1	-12.0	1.7	1.2
Oued El Khatt	"	sandstone	19--06	10	1.12	5.60	0.12	-0.3841	0.511971	±12	-13.0	-12.9	1.8	1.3
"	"	sandstone	19--12	10	0.94	4.59	0.12	-0.3678	0.511989	±12	-12.7	-12.6	1.8	1.4
Tisfourine	Mio-Pliocene	sandstone	23--13	10	0.87	4.56	0.12	-0.4140	0.511761	±12	-17.1	-17.0	2.0	1.6
Onhymm quarry	NE Part of the basin	sandstone	24-09	10	2.35	11.81	0.12	-0.3889	0.511983	±12	-12.8	-12.7	1.7	1.3
"	"	sandstone	24-16	10	1.25	6.25	0.12	-0.3839	0.511919	±12	-14.0	-13.9	1.8	1.5
Amma Fatma	"	sandstone	26--34	10	1.76	9.20	0.12	-0.4106	0.511982	±12	-12.8	-12.7	1.7	1.2
core-1	"	sandstone	C1--01	10	1.90	9.63	0.12	-0.3935	0.511930	±12	-13.8	-13.7	1.8	1.4
"	"	sandstone	C1--05	10	2.08	10.19	0.12	-0.3714	0.511916	±07	-14.1	-14.0	1.8	1.5
"	"	sandy marl	C1--16	10	2.13	11.09	0.12	-0.4100	0.511926	±12	-13.9	-13.8	1.7	1.3
"	"	sandy marl	C1--25	10	4.76	24.93	0.12	-0.4127	0.511885	±12	-14.7	-14.6	1.8	1.4
Core-4	"	sandstone	C4-03	10	1.73	8.55	0.12	-0.3781	0.512134	±12	-9.8	-9.7	1.5	1.0
"	"	sandstone	C4--07	10	3.72	19.85	0.11	-0.4243	0.511927	±12	-13.9	-13.8	1.7	1.3
"	"	sandstone	C4--13	10	2.84	14.02	0.12	-0.3767	0.511995	±12	-12.6	-12.5	1.8	1.3
Seguit el hamra	Pleistocene	sand	07---04	1	2.19	11.54	0.11	-0.4175	0.512094	±12	-10.6	-10.6	1.5	1.0
Oued draa	recent sediments	silt+sand	06--03	0	5.81	30.32	0.12	-0.4108	0.511926	±12	-13.9	-13.9	1.7	1.3
Oued Cheibeika	"	mud	06--07	0	5.36	28.19	0.12	-0.4151	0.511789	±12	-16.6	-16.6	1.9	1.6
Seguit el hamra	"	mud	07--05	0	8.32	45.31	0.11	-0.4358	0.511886	±12	-14.7	-14.7	1.7	1.3
Oued El craa	"	sand	14--01	0	1.00	5.12	0.12	-0.3991	0.511649	±07	-19.3	-19.3	2.2	1.9
Amma Fatma	Upper cretaceous	WM	24-03	80	2.82	14.59	0.12	-0.4059	0.511936	±25	-13.7	-12.9	1.8	1.3
Core-1	Mio-Pliocene	WM	C1--09	10	3.37	16.77	0.12	-0.3814	0.511947	±12	-13.5	-12.7	1.8	1.4
Core-4	"	WM	C4--16	10	2.23	11.39	0.12	-0.3990	0.511970	±12	-13.0	-12.2	1.7	1.3

Tstrat= stratigraphic age estimated from fossil record and Morocco Geogolical map; [a] The model ages T_{DM} were calculated following the model of DePaolo (1981)

Table 3.2.5 Sr isotopic data for sediments samples of the Tarfaya basin.

Sections	Stratigraphy	Rock type	Sa.no.	T_{strat}	Rb (ppm)	Sr (ppm)	$^{87}Rb/^{86}Sr$	$^{87}Sr/^{86}Sr$	±2σ	I sr (T)	ϵ_{Sr} 0	ϵ_{Sr} (T)
Boukhchebat	Lower cretaceous	sandstone	27--02	120	51.08	50.33	2.96	0.802673	±20	0.797619	1393.5	1324.1
"	"	sandstone	27--12	120	46.27	37.20	3.65	0.846050	±20	0.839830	2009.2	1923.4
"	"	sandstone	27--26	120	42.13	56.63	2.18	0.840446	±20	0.836727	1929.7	1879.3
"	"	sandstone	27--28	120	48.08	78.87	1.78	0.828855	±20	0.825811	1765.2	1724.3
Tisfourine	Upper cretaceous	sandy marl	23--04	80	23.39	826.89	0.08	0.734558	±20	0.734464	426.7	426.7
"	"	sandy marl	23--11	80	23.28	205.87	0.33	0.739028	±20	0.738655	490.1	486.2
Amma Fatma	"	carbonate	26--14	80	1.51	424.76	0.01	0.714019	±20	0.714007	135.1	136.3
"	"	black shale	26--23	80	25.81	398.80	0.19	0.729871	±20	0.729658	360.1	358.5
core-1	"	black shale	C1--27	80	45.17	265.41	0.49	0.732798	±20	0.732236	401.7	395.1
"	"	black shale	C1--28	80	59.13	274.89	0.62	0.737295	±20	0.736585	465.5	456.8
core-4	"	black shale	C4--18	80	15.88	499.29	0.09	0.723076	±20	0.722972	263.7	263.6
"	"	black shale	C4--25	80	16.79	907.06	0.05	0.721284	±20	0.721223	238.2	238.8
Sebkha El Farma	Early Eocene	black shale	17--01	40	50.11	376.67	0.39	0.717516	±20	0.717297	184.8	182.3
"	"	black shale	17--16	40	31.75	683.56	0.13	0.722039	±20	0.721962	249.0	248.6
"	"	sandy marl	17--24	40	17.07	339.52	0.15	0.725936	±20	0.725854	304.3	303.8
Sebkha Aridal	Oligo-Early Miocene	sandy marl	16--02	25	24.93	317.50	0.23	0.731301	±20	0.731221	380.4	379.7
"	"	sandy marl	16-10	25	19.66	244.77	0.23	0.730462	±20	0.730379	368.5	367.8
Sebkha Aridal	Mio-Pliocene	sandstone	16--18	10	12.57	144.24	0.25	0.726188	±20	0.726152	307.8	307.5
Sebkha El Farma	SW Part of the basin	sandstone	17--32	10	38.84	161.80	0.70	0.721137	±20	0.721039	236.2	234.9
Oued El Khatt	"	sandstone	19--06	10	23.41	73.31	0.93	0.748414	±20	0.748283	623.3	621.7
"	"	sandstone	19--12	10	12.69	103.49	0.36	0.752345	±20	0.752295	679.1	678.6
Tisfourine	Mio-Pliocene	sandstone	23--13	10	8.28	87.48	0.27	0.742575	±20	0.742536	540.4	540.1
Onhymm quarry	NE Part of the basin	sandstone	24-09	10	29.56	154.18	0.56	0.724488	±20	0.724409	283.7	282.8
"	"	sandstone	24-16	10	31.44	831.61	0.11	0.739709	±20	0.739693	499.8	499.7
Amma Fatma	"	sandstone	26--34	10	11.81	541.67	0.06	0.720118	±20	0.720109	221.7	221.7
core-1	"	sandstone	C1--01	10	15.22	104.30	0.42	0.739994	±20	0.739934	503.8	503.1
"	"	sandstone	C1--05	10	19.76	116.06	0.49	0.735976	±20	0.735906	446.8	446.0
"	"	sandy marl	C1--16	10	33.56	95.10	1.02	0.741814	±20	0.741668	529.6	527.8
"	"	sandy marl	C1--25	10	82.23	240.67	0.99	0.732708	±20	0.732567	400.4	398.6
Core-4	"	sandstone	C4-03	10	26.19	854.82	0.09	0.722332	±20	0.722320	253.1	253.1
"	"	sandstone	C4--07	10	27.55	210.31	0.38	0.721780	±20	0.721726	245.3	244.7
"	"	sandstone	C4--13	10	45.73	202.92	0.65	0.726323	±20	0.726230	309.8	308.6
Seguit el hamra	Pleistocene	sand	07---04	1	35.56	336.78	0.31	0.726487	±20	0.726482	312.1	312.0
Oued draa	recent sediments	silt+sand	06--03	0	93.02	174.55	1.55	0.729867	±20	0.729867	360.1	360.1
Oued Cheibeika	"	mud	06--07	0	100.70	252.65	1.16	0.739094	±20	0.739094	491.0	491.0
Seguit el hamra	"	mud	07--05	0	132.74	202.21	1.90	0.727649	±20	0.727649	328.6	328.6
Oued El craa	"	sand	14--01	0	6.23	125.35	0.14	0.720207	±20	0.720207	223.0	223.0
Amma Fatma	Upper cretaceous	WM	24-03	80	40.91	317.03	0.37	0.728087	±20	0.727662	334.8	330.2
Core-1	Mio-Pliocene	WM	C1--09	10	39.43	90.75	1.26	0.740953	±20	0.739520	517.4	498.5
Core-4	"	WM	C4--16	10	25.15	378.84	0.19	0.727168	±20	0.726949	321.8	320.0

Tstrat= stratigraphic age estimated from fossil record and Morocco Geogolical map

Table 3.3.1 Clay mineral data for the sediments samples of the Tarfaya basin. The major and trace elements ratios are taken as reference

Sections	Stratigraphic age	Rock type	Sa. no.	Smectite	Illite	Kaolinite	Chlorite	Palygorskite	Corrensite	Sepiolite	Illite chemistry	Illite	Kaolinite/Illite	Al_2O_3/Na_2O	TiO_2/Na_2O	K_2O/Na_2O	Th/Sc	Zr/Sc	Zr/Hf
				%	%	%	%	%	%	%	index	Crystallinity							
Amma Fatma	Upper Cretaceous	black shale	26--17	10	47	34	6	1	0	0	0.28	0.42	0.72	6.55	0.43	2.31			
"	(Turonian)	black shale	26--23	37	35	10	11	7	0	0	0.43	0.23	0.29	7.78	0.49	2.61	0.70	15.31	35.87
Core-4	"	black shale	C4--17	13	32	51	0	5	0	0	0.23	0.32	1.59	4.26	0.35	1.1	0.58	15.52	37.29
"	"	black shale	C4--18	3	36	51	6	5	0	0	0.26	0.29	1.42	6.34	0.5	1.56	0.72	22.60	41.93
"	"	black shale	C4--25	1	39	48	7	5	0	0	0.21	0.26	1.23	14.63	1	2.88	0.64	17.49	42.42
Sebkha Tah	Upper Cretaceous	sandy marl	20--02	20	50	14	9	4	0	0	0.39	0.32	0.28	4.97	0.31	1.28	0.70	20.14	38.75
"	(Santonian)	sandy marl	20--05	30	35	18	10	7	0	0	0.40	0.39	0.51	3.05	0.21	0.95	0.85	17.25	36.04
"	"	black shale	20--13	20	61	17	2	0	0	0	0.44	0.44	0.28	6.93	0.43	1.95	0.70	18.07	37.76
"	"	sandy marl	20--19	74	13	10	0	3	0	0	0.43	0.20	0.77	3.94	0.4	1.22	1.03	71.89	40.50
Sebkha Tisfourine	Upper Cretaceous	sandy marl	23--03	0	15	0	0	0	84	0	0.50	0.69	0.00	1.36	0.08	0.33			
"	(Campanian)	sandy marl	23--04	0	38	1	0	0	61	0	0.46	0.58	0.03	1.11	0.1	0.45	0.76	13.71	34.57
"	"	sandy marl	23--07	0	42	0	0	0	58	0	0.46	0.60	0.00	1.12	0.07	0.26			
Core-1	"	black shale	C1--27	38	52	5	1	3	0	0	0.35	0.34	0.10	1.09	0.08	0.42	0.72	18.46	40.60
"	"	black shale	C1--28	36	55	5	1	3	0	0	0.32	0.33	0.09	1.28	0.1	0.4	0.76	24.23	41.65
Sebkha El Farma	Early Eocene	black shale	17--01	0	13	0	5	53	20	9	0.33	0.26	0.00	1.81	0.1	0.56	0.68	17.06	38.12
"	"	black shale	17--07	37	33	5	1	22	0	2	0.35	0.43	0.15	0.47	0.04	0.19	0.60	18.96	41.51
"	"	black shale	17--16	0	33	0	3	58	2	4	0.32	0.27	0.00	0.64	0.05	0.22	0.67	19.22	39.03
"	"	black shale	17--20	42	27	5	1	24	0	2	0.24	0.37	0.19	2.35	0.14	0.6	0.71	16.92	38.03
"	"	sandy marl	17--24	11	31	1	0	38	0	19	0.40	0.27	0.03	3.46	0.26	0.98	0.57	17.64	39.30
"	"	sandy marl	17--28	17	9	0	0	71	0	3	0.24	0.22	0.00	1.32	0.12	0.45			
Sebkha Aridal	Oligo- Early	sandy marl	16--02	0	1	6	1	2	90	0	0.27	0.15	6.00	3.52	0.35	0.95	1.19	125.35	44.33
"	Miocene	sandy marl	16--07	0	4	7	1	6	82	0	0.30	0.27	1.75	0.63	0.06	0.14	0.97	78.55	70.65
"	"	sandy marl	16--10	0	10	0	0	16	73	0	0.24	0.35	0.00	3.95	0.58	1.35	1.59	173.32	50.21
"	"	sandy marl	16--14	0	4	0	0	4	92	0	0.76	0.28	0.00	5.05	0.6	1.72	1.24	105.10	42.25
Sebkha Aridal	Mio-Pliocene	sandstone	16--21	69	16	2	2	11	0	0	0.32	0.27	0.13	3.9	0.16	1.4	1.24	48.59	39.34
Sebkha El Farma	SW part of the basin	sandstone	17--32	50	8	1	4	7	29	0	0.45	0.34	0.13	5.14	0.33	1.81	0.79	40.46	40.52
Oued El Khatt	"	sandstone	19--06	91	2	6	1	1	0	0	0.29	0.33	3.00	4.65	0.23	2.13	0.78	43.17	41.19
"	"	sandstone	19--10	80	5	0	0	15	0	0	0.22	0.23	0.00	5.57	0.31	2.12	0.93	21.44	33.71
"	"	sandstone	19--12	73	20	2	1	3	0	0	0.39	0.32	0.10	6.74	0.42	2.63	0.65	31.64	40.07
Sebkha Tah	Mio-Pliocene	sandstone	20--27	24	19	0	0	58	0	0	0.24	0.25	0.00	1.66	0.14	0.71			
Sebkha Tisfourine	SW part of the basin	sandstone	23--13	59	40	0	0	0	0	0	0.44	0.42	0.00	1.97	0.28	0.84	1.35	45.58	35.40
Onhym Quarry	"	sandstone	24--09	73	13	3	5	6	0	0	0.41	0.25	0.23	3.64	0.3	1.17	0.80	23.88	37.69
"	"	sandstone	24--16	10	28	8	10	44	0	0	0.23	0.19	0.29	4.45	0.17	2.11	1.12	19.47	33.19
Amma Fatma	"	sandstone	26--34	2	24	5	6	34	0	29	0.27	0.32	0.21	2.88	0.92	1	0.85	42.10	41.61
Core-1	"	sandstone	C1--03	78	13	0	0	9	0	0	0.33	0.42	0.00	3.56	0.29	1.67	1.53	95.80	46.22
"	"	sandstone	C1--05	88	8	0	0	4	0	0	0.31	0.14	0.00	3.46	0.27	1.58	1.17	64.59	45.56
"	"	sandstone	C1--08	53	22	0	0	25	0	0	0.35	0.14	0.00	3.42	0.29	1.48	1.20	57.39	42.93
Core-4	"	sandstone	C4--03	36	36	4	22	3	0	0	0.24	0.13	0.11	3.34	0.23	1.24	0.88	61.07	45.78
"	"	sandstone	C4--07	58	19	6	10	7	0	0	0.32	0.16	0.32	3.95	0.63	1.28	1.11	138.44	43.86
"	"	sandstone	C4--13	49	24	5	8	15	0	0	0.37	0.42	0.21	5.85	0.38	1.77	0.70	21.54	42.06
"	"	sandstone	C4--14	52	25	5	11	6	0	0	0.40	0.23	0.20	4.57	0.51	1.41	1.35	129.58	44.35
"	Recent sediments	sand+silt	06--01	8	44	30	10	8	0	0	0.42	0.26	0.68	17.79	1.06	4.29	0.85	28.24	40.08

"	"	sand+silt	06--02	7	46	25	11	10	0	0	0.38	0.23	0.54	7.91	0.52	1.82	0.84	49.32	41.83
"	"	sand+silt	06--07	11	50	19	6	14	0	0	0.31	0.49	0.38	11.83	0.58	2.96	0.72	18.82	39.94
"	"	muddy sand	07--01	2	39	37	7	15	0	0	0.32	0.63	0.95	10.84	0.59	2.07	0.84	17.50	39.30
"	"	mudstone	07--02	22	32	31	7	7	0	0	0.42	0.41	0.97	15.28	0.56	2.56	0.75	8.20	36.48
"	"	sand+silt	07--05	6	38	38	7	10	0	0	0.37	0.34	1.00	19.74	0.87	3.37	0.79	7.51	36.43
Sebkha Tisfourine	Upper Cretaceous	WM	23--01	53	25	6	9	7	0	0	0.35	0.23	0.24	2.61	0.2	0.91	0.80	15.80	35.77
Onhym Quarry	"	WM	24--02	3	55	16	15	11	0	0	0.39	0.29	0.29	4.57	0.32	1.3			
"	"	WM	24--03	39	38	9	10	4	0	0	0.38	0.25	0.24	2.29	0.18	0.69	0.89	42.93	40.55
"	"	WM	24--04	15	51	13	12	9	0	0	0.34	0.25	0.25	2.26	0.19	0.68	0.84	21.33	37.42
"	"	WM	24--05	45	34	8	11	3	0	0	0.42	0.24	0.24	2.14	0.15	0.64	0.78	17.61	36.47
"	"	WM	24--06	55	27	5	10	4	0	0	0.37	0.23	0.19	1.85	0.15	0.58	0.84	17.78	36.95
"	"	WM	24--07	54	26	8	7	5	0	0	0.43	0.19	0.31	1.98	0.17	0.65			
Akhfenner	"	WM	24--18	53	25	6	9	7	0	0	0.35	0.23	0.24	1.37	0.08	0.35	1.11	73.21	24.28
Chebeika	"	WM	26--04	67	18	10	0	4	0	0	0.35	0.24	0.56	5.08	0.95	2.8			
"	"	WM	26--08	45	42	11	0	1	0	0	0.30	0.31	0.26	2.34	0.5	1.07			
"	"	WM	26--09	32	31	10	14	12	0	0	0.40	0.18	0.32	4.64	0.27	1.47			
Amma Fatma	"	WM	26--25	45	25	13	9	8	0	0	0.37	0.17	0.36	4	0.61	1.12	0.91	21.94	37.09
Core-1	Mio-Pliocene	WM	C1--06	72	13	0	0	15	0	0	0.30	0.14	0.00	3.37	0.28	1.6	1.01	59.51	44.37
"	"	WM	C1--07	63	17	0	0	20	0	0	0.22	0.15	0.00	3.25	0.29	1.44	1.24	76.77	45.86
"	"	WM	C1--09	29	24	0	0	47	0	0	0.17	0.30	0.00	4.35	0.32	1.44	1.12	34.26	81.99
"	"	WM	C1--10	17	15	0	0	68	0	0	0.22	0.24	0.00	3.89	0.27	1.27	1.13	26.46	48.85
Core-2	"	WM	C2--03	11	44	13	12	21	0	0	0.40	0.26	0.30	4.37	0.33	1.17	0.78	24.72	41.03
"	"	WM	C2--04	7	52	13	15	13	0	0	0.35	0.27	0.25	7.98	0.53	2.38	0.79	27.64	40.92
Core-3	"	WM	C3--02	46	23	13	11	7	0	0	0.40	0.20	0.57	3.54	0.35	0.99	0.84	14.46	37.86
"	"	WM	C3--04	38	30	11	12	9	0	0	0.39	0.25	0.37	6.24	0.4	1.96	0.74	28.88	43.41
"	"	WM	C3--05	0	55	42	4	0	0	0	0.26	0.40	0.76	5.16	0.45	1.69	0.80	58.29	43.98
"	"	WM	C3--06	0	61	33	6	0	0	0	0.38	0.50	0.54	14.85	0.62	1.69	0.56	17.54	35.81
Core-4	"	WM	C4--09	39	31	10	11	8	0	0	0.32	0.20	0.32	4.71	0.77	1.47	0.92	130.32	44.89
"	"	WM	C4--10	28	38	10	14	10	0	0	0.34	0.25	0.26	4.71	0.46	1.58	0.97	97.86	44.88
"	"	WM	C4--15	19	45	12	14	10	0	0	0.39	0.25	0.27	6.61	0.43	1.94	0.62	16.73	40.39
"	"	WM	C4--16	11	48	16	14	11	0	0	0.36	0.24	0.33	5.8	0.56	1.69	0.80	42.62	44.06

WM=weathered marl